

Insights into the metabolic regulation of insulin secretion using a metabolomics approach

by

Mei Huang

A thesis
presented to the University of Waterloo
in fulfillment of the
thesis requirement for the degree of
Doctor of Philosophy
In
Chemistry

Waterloo, Ontario, Canada, 2014

© Mei Huang 2014

AUTHOR'S DECLARATION

I hereby declare that I am the sole author of this thesis. This is a true copy of the thesis, including any required final revisions, as accepted by my examiners.

I understand that my thesis may be made electronically available to the public.

Abstract

In the post genomic era, metabolomics, as an integrated part of system biology, offers a promising approach to identify biomarkers associated with diseases and hence has been widely used in disease diagnosis, toxicology, plant science, and pharmaceutical and environmental research. Based on the specific study goals, metabolomics involves two major categories: targeted and untargeted. Unlike targeted metabolomics with well-established analysis method, untargeted metabolomics still needs to overcome some technical challenges. This dissertation attempts to address these challenges and to establish a feasible untargeted metabolomics platform from sample preparation to data interpretation and biologically meaningful validation. In this dissertation, gas chromatography-mass spectrometry (GC-MS) was used as the analytical instrument to detect and identify metabolites. This GC-MS based untargeted metabolomics was successfully applied to study four different aspects of glucose-stimulated insulin secretion (GSIS), including the biochemical mechanism underlying insulin secretion, biphasic insulin secretion, time-dependent effects (TDE) of glucose on insulin secretion, as well as the role of alpha-ketoglutarate dependent hydroxylation in regulation of insulin secretion. GSIS was identified by orthogonal partial least squares (OPLS) to be associated with not only glycolysis and tricarboxylic acid cycle (TCA cycle), but also the pentose phosphate pathway (PPP), the sorbitol-aldose reductase pathway as well as aspartate. The characterization of the kinetics of insulin secretion revealed that alpha-ketoglutarate, succinate and hydroxyproline were the metabolites strongly associated with the second phase of biphasic insulin secretion. Study of TDE by using a metabolomics approach showed that the time-dependent inhibition (TDI) of glucose on insulin secretion is mainly regulated by redox state in pancreatic beta cells, since it was suggested to be correlated to the decreased ratio between dihydroxyacetone phosphate (DHAP) and alpha-glycerolphosphate (alpha-GP). This was probably the result of the reduced malate-aspartate shuttle activity and lower lactate output in beta cells. On the other hand, time-dependent potentiation (TDP) might be mediated by succinate-regulated pro-insulin biosynthesis. Finally, alpha-ketoglutarate dependent hydroxylation was found to be a master regulator that controls glucose metabolism as well as glucose derived anaplerosis, a finding which, if true, provides a positive feedback loop for the secretion function of pancreatic beta cells. Overall, this GC-MS based untargeted metabolomics approach was established and then was used to study the mechanism of GSIS. Alpha-ketoglutarate was revealed to be critical to kinetically coupling glucose metabolism to (especially the second phase of) insulin secretion probably via an alpha-ketoglutarate dependent hydroxylation mechanism.

Acknowledgements

This thesis represents not only my work at the keyboard, it is an outcome resulting from collaborative efforts of many people that I would like to take this opportunity to acknowledge.

Foremost, I would like to express my sincere gratitude to my supervisory committee Dr. Jamie Joseph, Dr. John Honek (co-supervisor from 2008 to 2013), Dr. Brendan J. McConkey, Dr. J. Guy Guillemette, and Dr. Wojciech Gabryelski for their insightful instruction, timely help, and invaluable guidance over the past five years. I am deeply grateful to my supervisor, Dr. Jamie Joseph, for giving me an opportunity to pursue my PhD degree under his supervision, providing me with a special atmosphere for doing research, and offering me the excellent guidance and strict training on research. I have been given unique opportunities in his group... and took advantage of them. His professional guidance will certainly make my future career path easier to navigate. I would also like to give my special thanks to Dr. Jonathan Blay, the associate director of the School of Pharmacy, for his strong support, warm encouragement, and his sustained attention evident from the first day he joined us. His unique and impressive style of dealing with research and management has positive influence on my career as well as my life.

Thanks should also go to our team members for their support and encouragement over the years. Tanya Sheinin, the greatest lab manager I have ever met, was the first person who helped me with my first lab experiment. Renjitha Pillai, the colleague I was longest associated with, understood my situation thoroughly. Thanks for her excellent help both inside and outside of the lab! Stephanie Schaefer inspired me when I wanted to give up. Julia Guan kindly helped me with islets isolation and brought good fortune into my life. Julia May-Kay Wong worked side by side with me for the generation of glucose utilization data in my last project. Also, thanks to Iulia Dude for her editorial help.

My deepest gratitude goes to my family, my parents, my sister and my son for their warmest and unequivocal support throughout my life! It is them who made me who I am today. Thanks in particular to my son for being considerate and patient while I was spending time and effort on my research and thesis that I could have been spending with him!

Table of Contents

AUTHOR'S DECLARATION	ii
Abstract	iii
Acknowledgements	iv
Table of Contents	v
List of Figures	ix
List of Abbreviations	xi
Chapter 1 Introduction.....	1
1.1 Insulin secretion	1
1.1.1 Diabetes mellitus	1
1.1.2 Structures producing and secreting insulin.....	2
1.1.3 Mechanistic control of insulin secretion.....	2
1.1.4 Biphasic insulin secretion.....	8
1.1.5 Concluding remarks.....	10
1.2 Metabolomics	11
1.2.1 Introduction of metabolomics.....	11
1.2.2 Target and untargeted metabolomics.....	12
1.2.3 Metabolite extraction.....	14
1.2.4 Instruments used for metabolomics.....	16
1.2.5 Data analysis and data mining	18
1.2.6 Future outlook	22
1.3 Hypothesis	22
1.4 Overall objectives.....	22
1.4.1 Aim 1	22
1.4.2 Aim 2.....	22
1.4.3 Aim 3.....	23
1.4.4 Aim 4.....	23
Chapter 2 Materials and Methods.....	24
2.1 Materials.....	24
2.1.1 Cell lines	24
2.1.2 Animals	24
2.1.3 RT-PCR primers	24

2.1.4 siRNA duplex construction and transfection.....	25
2.1.5 Reagents	26
2.2 Methods	26
2.2.1 Insulin secretion assay	26
2.2.2 Pancreatic islet isolation	26
2.2.3 Cell viability assay	26
2.2.4 Glucose utilization assay	27
2.2.5 <i>In situ</i> mitochondrial bioenergetics	27
2.2.6 Real time PCR	28
2.2.7 Western blot.....	28
2.2.8 Transfection of siRNA duplex.....	29
2.2.9 Metabolites extraction and sample preparation	29
2.2.10 Metabolites measurement	29
2.2.11 Metabolomic data analysis	30
Chapter 3 Metabolomic Analysis of Pancreatic Beta Cell Insulin Release in Response to Glucose ...	31
3.1 Overview	32
3.2 Introduction	32
3.3 Results	34
3.3.1 Insulin secretion.....	34
3.3.2 Metabolite analysis by GC-MS	35
3.3.3 Metabolites identification.....	37
3.3.4 Orthogonal projection to latent structures (OPLS) analysis	37
3.3.5 Metabolic pathway analysis	40
3.3.6 Role of the PPP and sorbitol-aldose reductase pathway in regulation of insulin secretion .	47
3.4 Discussion	49
3.5 Conclusion.....	54
Chapter 4 Assessment of the Metabolic Pathways Associated with the Second Phase Glucose-Stimulated Insulin Secretion.....	55
4.1 Overview	56
4.2 Introduction	56
4.3 Results	58
4.3.1 Dynamic insulin secretion in INS-1 832/13 cells.....	58

4.3.2 Dynamic metabolome response to glucose challenge	60
4.3.3 Metabolome alteration associated with the second phase insulin secretion	60
4.3.4 Metabolic pathway analysis	63
4.3.5 Block of pyruvate influx selectively affects second phase insulin secretion.....	68
4.4 Discussion	70
4.5 Conclusion.....	73
Chapter 5 Mechanistic Study of Time-Dependent Effects of Glucose on Insulin Secretion	75
5.1 Overview	76
5.2 Introduction	76
5.3 Results	78
5.3.1 Glucose stimulated insulin secretion (GSIS) showing time dependent effects	78
5.3.2 Metabolite detection and identification	79
5.3.3 Multivariate analysis	81
5.3.4 Coupling factors of time-dependent effect	85
5.4 Discussion	91
5.5 Conclusion.....	95
Chapter 6 Hydroxylation, an Important Mechanism in Regulation of Glucose Metabolism	96
6.1 Overview	96
6.2 Introduction	96
6.3 Results	98
6.3.1 EDHB affects insulin secretion in INS-1 832/13 cells	98
6.3.2 EDHB affects insulin secretion in primary rat and human islets.....	100
6.3.3 EDHB affects glucose utilization and oxygen consumption	101
6.3.4 EDHB has no effects on HIF-1alpha expression or function	103
6.3.5 Prolyl hydroxylases suppression has no effect on GSIS	105
6.3.6 High dosage of EDHB affects glucose metabolism	107
6.4 Discussion	109
6.5 Conclusion.....	111
Chapter 7 Discussion and Conclusion.....	112
7.1 Discussion	113
7.1.1 Technique aspects of untargeted metabolomics	113
7.1.2 Multivariate analysis in metabolomics	114

7.1.3 Significance of untargeted metabolomics.....	115
7.1.4 Insight into metabolic regulation of insulin secretion	116
7.2 Conclusion.....	117
7.3 Future outlook	118
Appendix A Publications and Manuscripts in Preparation.....	120
Bibliography	121

List of Figures

Figure 1-1 Pyruvate cycling pathways in pancreatic beta cells	6
Figure 1-2 Schematic summary of MS-based targeted and untargeted metabolomics.....	13
Figure 2-1 Schematic summary of oxygen consumption rate measurement	28
Figure 3-1 Glucose stimulated insulin secretion in INS-1 832/13 beta cells.	34
Figure 3-2 Representative total ion current chromatogram (TIC) of metabolites	36
Figure 3-3 Score and loading plots generated by OPLS on identified metabolites.....	38
Figure 3-4 Regression coefficient plots of metabolites potentially coupling glucose metabolism to insulin secretion.....	39
Figure 3-5 Glycolytic metabolite levels are up-regulated by glucose	41
Figure 3-6 TCA metabolite levels are up-regulated by glucose	42
Figure 3-7 Aldose reductase and pentose phosphate pathway metabolites are up-regulated by glucose	43
Figure 3-8 Fatty acids are up-regulated by high glucose.....	44
Figure 3-9 Amino acid metabolite levels are changed by high glucose	45
Figure 3-10 Metabolic signals identified by MVA to be correlated to insulin secretion	46
Figure 3-11 Role of the pentose phosphate and sorbitol-aldose reductase pathway in GSIS.	48
Figure 4-1 Time course glucose-stimulated insulin secretion and metabolome of 832/13 cells	59
Figure 4-2 Multivariate analysis of metabolome responsible for second phase insulin secretion	62
Figure 4-3 Time course responses of glycolytic metabolite levels.....	64
Figure 4-4 Time course responses of TCA metabolite levels.....	65
Figure 4-5 Time course responses of other metabolites positively associated to second phase insulin secretion.....	66
Figure 4-6 Time course responses of amino acids	67
Figure 4-7 Effect of pyruvate inhibitors on biphasic insulin secretion in rat islets	69
Figure 5-1 Glucose-stimulated insulin secretion showing time-dependent effects	79
Figure 5-2 Representative total ion current chromatogram (TIC) of metabolome in INS-1 832/13 beta cells showing time-dependent effects.....	80
Figure 5-3 Orthogonal projection to latent Structures (OPLS) analysis on metabolome showing time-dependent effects	83
Figure 5-4 Time-dependent effects revealed by glycolytic intermediates.....	86
Figure 5-5 Time-dependent effects revealed by TCA intermediates.....	88

Figure 5-6 Time-dependent effects revealed by pentose phosphate pathway intermediates.....	89
Figure 5-7 Time-dependent effects revealed by amino acids.....	90
Figure 6-1 Effects of EDHB on insulin secretion and cell viability.....	100
Figure 6-2 Effects of EDHB on glucose metabolism.....	102
Figure 6-3 Effects of EDHB on hypoxia-inducible factor 1-alpha (HIF-1alpha) gene and protein...	104
Figure 6-4 Effects of EDHB on HIF-1alpha target genes	105
Figure 6-5 Effects of siRNA-mediated suppression of prolyl hydroxylases GSIS	106
Figure 6-6 Effects of EDHB on glycolysis metabolites	107
Figure 6-7 Effects of EDHB on TCA metabolites	108
Figure 6-8 Effects of EDHB on aspartate.....	109

List of Abbreviations

alpha-GP	alpha-glycerolphosphate
AMDIS	automated mass spectral deconvolution and identification system
ARNT	aryl hydrocarbon receptor nuclear translocator
ATP	adenosine triphosphate
cAMP	cyclic adenosine monophosphate
CE	capillary electrophoresis
CIC	isocitrate carrier
CL	ATP citrate lyase
CPT-I	carnitine palmitoyl transferase I
cyclophilin E	PPIE peptidylprolyl isomerase E
DHAP	dihydroxyacetone phosphate
EBPC	2,5-dihydro-4-hydroxy-5-oxo-1-(phenylmethyl)-1H-pyrrole-3-carboxylic acid ethyl ester
EDHB	ethyl-3,4-dihydroxybenzoate
FFA	free fatty acid
FT-ICR	fourier transform ion cyclotron resonance
FT-IR	fourier transform infrared spectroscopy
G6P	glucose-6-phosphate
G6PDH	glucose-6-phosphate dehydrogenase
GABA	gamma-aminobutyric acid
GADP	glyceraldehyde 3-phosphate
GAPDH	glyceraldehyde 3-phosphate dehydrogenase
GC	gas chromatography
GC-MS	gas chromatography–mass spectrometry
GDH	glutamate dehydrogenase
GK	glucokinase
GLP-1	glucagon-like peptide 1
GLUT1	glucose transporter 1
GLUT2	glucose transporter 2
GSIS	glucose-stimulated insulin secretion

GTP	guanosine triphosphate
HG	high glucose
HIF-1alpha	hypoxia-inducible factor 1 alpha
HILIC	hydrophilic interaction liquid chromatography
IAPP	islet amyloid polypeptide
ICDc	isocitrate dehydrogenase
IP	inositol phosphate
IVGTT	intravenous glucose tolerance test
K _{ATP} channel	ATP-sensitive K ⁺ channels
Kir6.2	inward-rectifier potassium ion channel subunit
KOH	potassium hydroxide
KRB	Krebs Ringer bicarbonate buffer
LC	liquid chromatography
LC-CoA	long-chain acyl-CoA
LDH	lactate dehydrogenase
LG	low glucose
MCFs	metabolic coupling factors
MDH	malate dehydrogenase
ME	malic enzyme
MEc	cytosolic malic enzyme
MS	mass spectrometry
MSTFA	N-methyl-N-(trimethylsilyl)-trifluoroacetamide
MVA	multivariate analysis
NADP	nicotinamide adenine dinucleotide phosphate
NADPH	nicotinamide adenine dinucleotide phosphate - reduced
NaOH	sodium hydroxide
NMR	nuclear magnetic resonance
OAA	oxaloacetate
OGTT	oral glucose tolerance test
OPLS	orthogonal projection to latent structures
PC	pyruvate carboxylase
PCA	principal component analysis

PDH	pyruvate dehydrogenase
PEP	phosphoenolpyruvate
PEPCKm	mitochondrial phosphoenolpyruvate carboxykinase isoenzyme
PHD1	prolyl hydroxylase 1
PHD2	prolyl hydroxylase 2
PHD3	prolyl hydroxylase 3
PKC	protein kinase C
PKM1	pyruvate kinase muscle isozyme 1
PKM2	pyruvate kinase muscle isozyme 2
PLC	phospholipase C
PLS	projections to latent structures
PLS-DA	projections to latent structures discriminant analysis
PP cells	pancreatic polypeptide cells
PPP	pentose phosphate pathway
RPLC	reversed phase liquid chromatography
SSA	succinic semialdehyde
SUR1	sulphonylurea receptor
TCA cycle	tricarboxylic acid cycle
TDE	time-dependent effect
TDI	time-dependent inhibition
TDP	time-dependent potentiation
TIC	total ion chromatogram
TPA	tetradecanoyl phorbol acetate
UPLC	ultra-performance liquid chromatography
UV	unit variance
VDCC	voltage-dependent calcium channels

Chapter 1

Introduction

1.1 Insulin secretion

1.1.1 Diabetes mellitus

382 million people worldwide are suffering from diabetes mellitus [1]. This degree of prevalence is close to what had been predicted not to happen until 2030 [2], which indicates that the incidence has climbed rapidly in the last decade. Due to the complications caused by long-term hyperglycemia and the growth of the epidemic, diabetes is predicted to become one of main killers in the near future. Even worse, diabetes currently can only be treated but not cured. In addition, the life-long management plan of this disease makes it a large economic burden for both individuals and health care authorities of many countries. Therefore, it is imperative to reveal the mechanisms of diabetes and introduce a new treatment strategy in order to meet both cost and health challenges this disease presents.

Diabetes is a group of metabolic disorders characterized by hyperglycemia, where the disruption of carbohydrate metabolism causes excessive glucose in the circulatory system [3]. As the primary energy source for the human body, blood glucose levels are subject to a tight control regulated by an astonishingly complex mechanism, which generates a perfect balance between glucose production and glucose utilization. Ideally, glucose concentration should be maintained in a relatively narrow range (4.0 ~ 6.1 mM) despite the fluctuation caused by glucose release and glucose removal [3]. If plasma glucose levels are elevated, for example, after a meal, insulin will be released into the circulatory system in a glucose dependent manner to suppress endogenous glucose release [4] and to encourage glucose uptake by insulin-sensitive tissues, such as the liver, skeletal muscle and adipose tissue [5-7], so that the rate of glucose removal from the plasma parallels that of glucose release [8, 9]. As the major acute glucose regulatory hormone, insulin is able to change the plasma glucose level in a matter of minutes and is central to maintaining glucose homeostasis. Disturbance of glucose homeostasis due to an insufficiency of insulin secretion or defect of insulin action, or both, will cause diabetes mellitus [3]. As a consequence, external insulin is absolutely required for treatment of type 1 diabetes and may also be included in type 2 diabetes management plans.

1.1.2 Structures producing and secreting insulin

Insulin is produced by beta cells in the islets of Langerhans of the pancreas. The mass of islets constitutes around 1~2% of the mean pancreas weight in healthy adults; the number of islets in the adult human pancreas ranges from several hundred thousand to several million [10]. Islets are aggregates of endocrine cells and contain five different endocrine cell types [11]: alpha cells, beta cells [12], delta cells [13], pancreatic polypeptide (PP) cells [14], and epsilon cells [15]. As the main population within islets of Langerhans, beta cells account for 50~80 % of the total number of endocrine cells in islets [11, 16-19]. The second most abundant cell type in the islets of Langerhans is alpha cells (15 ~ 20 %), which secrete glucagon, a hormone coordinately working with insulin and reciprocally regulating glycaemia [19, 20].

With the exception of pathological conditions, beta cells can adapt to physiological demand and secrete the appropriate amount of insulin in the correct proportion to plasma glucose levels to guarantee the removal of excessive glucose from the circulatory system and to achieve the tight control of glucose homeostasis. For example, obese subjects or pregnant women normally release more insulin than individuals who are not in either of these conditions [21-23] to match the increased demand from glucose. Altered performance of pancreatic beta cells is linked to various types of disorders in diabetes. In type 1 diabetes, genetically susceptible individuals experience a significant loss of beta cells as a result of T-cell-mediated autoimmune reaction [24-26]. On the other hand, the dysfunction of pancreatic beta cells, such as loss of adaptive capacity to physiological stimuli, increased apoptosis, and deposition of amyloid (its precursor, islet amyloid polypeptide (IAPP), is a peptide co-secreted with insulin) [27, 28], contributes to the development of type 2 diabetes [10].

1.1.3 Mechanistic control of insulin secretion

1.1.3.1 K_{ATP} channel dependent pathway

Because insulin is the prime regulator of glucose homeostasis, understanding and improving endogenous insulin secretion is important for devising a successful diabetes management plan [29]. Despite years of intensive research efforts from scientists dedicated to revealing the biochemical mechanism underlying insulin secretion, only one well-established glucose metabolism and insulin secretion coupling pathway has been widely accepted by the diabetes research community.

When the extracellular concentration of glucose increases, glucose is conveyed into pancreatic beta cells by glucose transporter 1 (GLUT1) in humans and glucose transporter 2 (GLUT2) in rodents [30,

31]. An instant equilibration of glucose between extra- and intracellular space is reached rapidly [32]. Hence glucose metabolism in beta cells is primarily driven by substrate availability, not the transport of glucose across cellular membrane. It is generally believed that, instead of glucose, it is the second messengers generated by glucose metabolism that are required to elicit exocytosis of insulin secretory granules. Because of the low activity of glycogen synthesis and the pentose phosphate pathway (PPP) [33], most glucose fluxes into aerobic glycolysis, a glucose metabolic process initiated and controlled by glucokinase [34]. The conversion of glucose to glucose-6-phosphate (G6P) by glucokinase likely constitutes the rate-determining step in glycolysis happening in pancreatic beta cells [35, 36]. As the end product of glycolysis, pyruvate establishes the tight link between glucose metabolism in cytosol and in mitochondria by feeding glucose-derived carbon into the tricarboxylic acid cycle (TCA cycle) via pyruvate dehydrogenase (PDH). Acetyl-CoA, the product of pyruvate decarboxylation, is turned into adenosine triphosphate (ATP) by a series of biochemical reactions in the TCA cycle and oxidative phosphorylation pathway (electron transport chain). Hence, the increase of extracellular glucose in the circulatory system eventually leads to an increase of oxidative ATP production at the expense of Mg-adenosine diphosphate (ADP) within pancreatic beta cells.

ATP will bind and close ATP-sensitive K^+ channels (K_{ATP} channels) present on the plasma membrane of pancreatic beta cells [37-39]. The K_{ATP} channel is a hetero-octameric complex [40, 41] composed of four inward-rectifier potassium ion channel (Kir6.2) subunits and four sulphonylurea receptor (SUR1) subunits [42, 43]. The former is the target of ATP, which can close Kir6.2 [44], while ADP binds to SUR1 and holds the K_{ATP} channel open. The closure of K_{ATP} channels will decrease K^+ conductance and cause depolarization of the cell membrane until the threshold is reached to open voltage-sensitive Ca^{2+} -channels [45-47]. The opening of Ca^{2+} -channels causes an influx of extracellular Ca^{2+} into beta cells along the electrochemical gradient and an increase of intracellular Ca^{2+} concentration, which directly triggers exocytosis of insulin secretory granules [48, 49]. Because ATP/ADP ratio plays a crucial role in physiological control of insulin secretion through modulating K_{ATP} channels, this stimulus-secretion coupling pathway is called the K_{ATP} channel-dependent pathway or triggering pathway [50].

K_{ATP} channels play a central role in maintaining glucose homeostasis, and thus is the target of current anti-diabetic or anti-hypoglycemia medicine aiming to either mimic or antagonize the triggering effects of glucose on insulin secretion [51, 52]. Sulphonylureas (e.g. tolbutamide, glipizide) are widely used for treatment of type 2 diabetes, because they stimulate endogenous insulin secretion by binding

to SUR1 and closing the K_{ATP} channel in a glucose-independent manner [53, 54]. Meglitinides (glinides) inhibit the K_{ATP} channel in a way similar to sulfonylureas by binding to a different site of SUR1 [55]. Diazoxide and other K_{ATP} channel activators, used for hypoglycemia and/or hyperinsulinemia, have an opposite effect of sulfonylureas by opening the K_{ATP} channel and hence stopping glucose and other insulin secretagogues from inducing insulin secretion [38, 51]. These drugs are widely used in anti-diabetic clinical treatment as well as research.

1.1.3.2 K_{ATP} channel independent pathway

Experiments using these K_{ATP} channel-targeted drugs provide evidence that the K_{ATP} -dependent pathway may not be the only avenue for nutrient-induced insulin secretion in beta cells. Even when K_{ATP} channels were bypassed by treating islets with a combination of high concentration of K^+ and a K_{ATP} channel opener diazoxide, the glucose challenge in a physiological range can still elicit a K_{ATP} channel independent insulin response [56, 57]. In addition to pharmacological evidence, genetic data from models lacking the K_{ATP} channel is even more compelling. K_{ATP} channel knock-out islets unexpectedly retain glucose responsiveness and the K_{ATP} channel knock-out animals still remain euglycemic [58, 59]. Heterozygous knock-out ($Kir6.2^{+/-}$ and $SUR1^{+/-}$) mice can maintain a good control of glucose homeostasis and demonstrate improved ability to release insulin in response to elevated glucose [60, 61]. Even in homozygous knockout ($Kir6.2^{-/-}$ and $SUR1^{-/-}$) mice, the ability of islets to respond to glycemic stimuli is impaired but not abolished [62]. What supplements this discovery and makes it even more interesting is the effect of glucagon-like peptide 1 (GLP-1) and acetylcholine (Ach) on K_{ATP} channel knock-out beta cells. These two stimulatory elements augmenting beta cell insulin secretion in a glucose-dependent mechanism still retain their incretin effects on islets isolated from SUR1 knock-out mice [63, 64]. These findings together suggest the existence of some other second messenger(s), in addition to ATP/ADP ratio, derived from glucose metabolism but working independently of the K_{ATP} channel in pancreatic beta cells. This is therefore called the K_{ATP} channel independent pathway or amplifying pathway [64, 65].

1.1.3.3 Pyruvate carboxylase mediated anaplerosis

One of the proposed mechanisms for the amplifying pathway under active investigation is pyruvate carboxylase (PC) mediated anaplerosis (the replenishment and increase of TCA cycle intermediates) for enhanced TCA cycle activity [66]. Key evidence for its involvement in the coupling of glucose stimulation and insulin secretion includes at least three facts. First, PC is highly expressed in

pancreatic beta cells [33, 67]. Second, the elevated carboxylation of pyruvate occurs in concert with insulin secretion [68, 69]. Third, pharmacological [69] and biological [70] inhibition of PC activity clearly decrease glucose stimulated insulin secretion (GSIS) in both INS-1 cells [70] and rat islets [71]. In agreement with all the above-mentioned data, physiologically reduced PC expression is found in various type 2 diabetes models [72, 73].

1.1.3.4 Pyruvate cycling

Because PC is highly expressed in pancreatic beta cells [33, 67], approximately 50 percent of cytosolic pyruvate enters the anaplerotic branch of the TCA cycle via PC as oxaloacetate (OAA) [33, 74-77]. The physiological significance of glucose-derived anaplerosis lies not only on their role in TCA cycle, but also on their involvement in other pathways. Different metabolic pathways and/or cycles other than just TCA are formed by the efflux of TCA cycle intermediates from mitochondria to cytoplasm (cataplerosis, the depletion and the reduction of TCA cycle intermediates) [78] via different transporters, such as di- and tri-carboxylic carriers, and their conversion back to pyruvate or TCA cycle intermediates [79]. Some of these cycles are the pyruvate cycles, which include pyruvate-malate cycle [80], pyruvate-citrate cycle [69, 81] and pyruvate-isocitrate cycle [49, 82], and pyruvate-phosphoenolpyruvate (PEP) cycle [83]. The first three pyruvate cycling pathways have been proved to be quantitatively correlated with dose-dependent GSIS by ^{13}C NMR analysis [76]. The detailed pyruvate cycling pathways are summarized in Figure 1-1.

The biological significance of pyruvate cycling pathways might lie in the byproducts generated during cycling, as well as the exchange of metabolic intermediates between cytoplasmic and mitochondrial compartments. The reason is simple: signals carried by mitochondrial oxidative metabolism need to be transported to the cytoplasm and used to activate the downstream exocytotic effectors acting on insulin granule exocytosis machinery. Reduced nicotinamide adenine dinucleotide phosphate (NADPH) generated from all three pyruvate cycling pathways might be one of these cytosolic effectors [49, 81, 84]. NADPH can be produced by either pyruvate cycling pathways or the PPP. However, due to its low activity, the PPP, on its own, unlikely accounts for the rise in NADPH content [85] occurring prior to cell membrane depolarization and Ca^{2+} elevation [86] in beta cells.

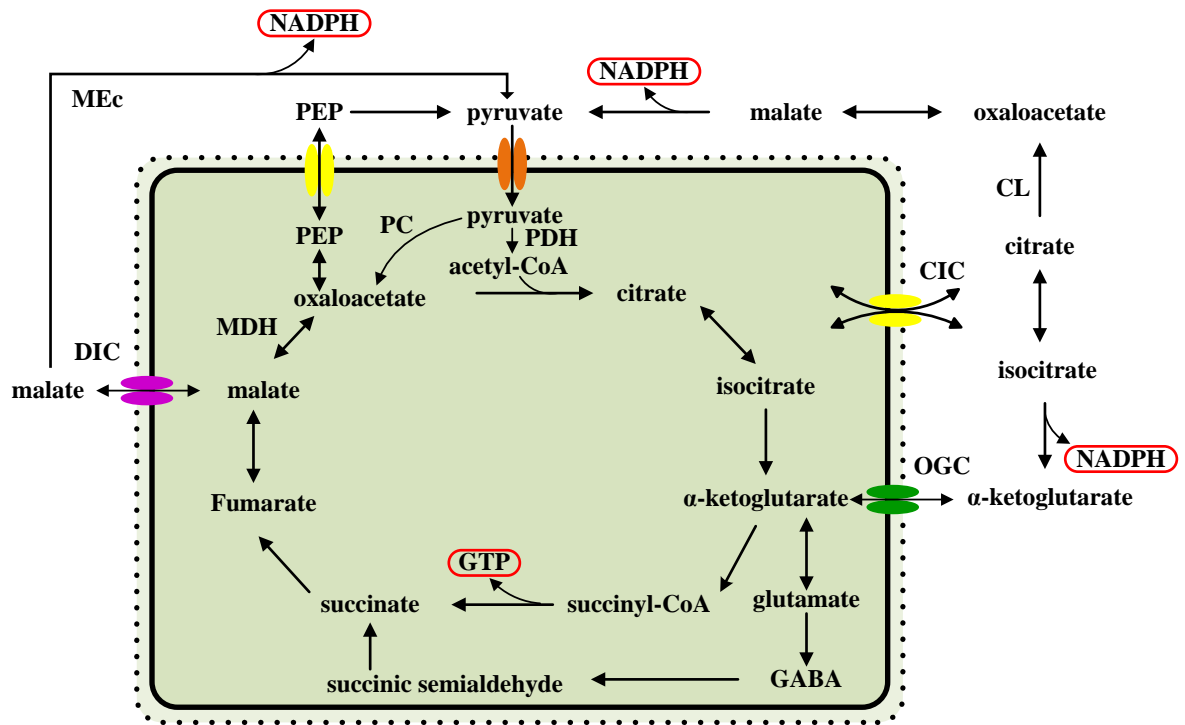


Figure 1-1 Pyruvate cycling pathways in pancreatic beta cells

Glucose-derived pyruvate enters mitochondria through a pyruvate carrier in roughly equal proportion via oxidative and anaplerotic pathways. Approximately half of pyruvate is oxidized to acetyl-CoA by pyruvate dehydrogenase (PDH), and the other half is converted to oxaloacetic acid (OAA) by pyruvate carboxylase (PC). These two products condense to form citrate, which starts tricarboxylic acid cycle (TCA cycle). In addition, glucose-derived carbon is also a driving force for other signaling pathways, which are formed by the efficient exchange of metabolites between the cytoplasmic and mitochondrial matrix via a set of mitochondrial carriers, to generate metabolic coupling factors. These pathways are: pyruvate-citrate, pyruvate-isocitrate, pyruvate-malate, and pyruvate-phosphoenolpyruvate (PEP) cycles, and GABA shunt. In pyruvate-malate cycle, mitochondrial OAA is reduced to malate by mitochondrial malate dehydrogenase (MDH) and then carboxylated back to pyruvate, either by a cytoplasmic or a mitochondrial form of malic enzyme (ME). In pyruvate-citrate cycle, citrate is exported from mitochondria to cytoplasm via the citrate-isocitrate carrier (CIC), and cleaved by ATP citrate lyase (CL) to OAA and acetyl-CoA. The former is converted to malate by cytosolic malic enzyme (MEc) and then recycled back to pyruvate via a cytosolic MDH. The latter is converted to malonyl-CoA and then long-chain acyl-CoA (LC-CoA), which are the key components of

malonyl-CoA /LC-CoA hypothesis of GSIS. In pyruvate-isocitrate or isocitrate-alpha-ketoglutarate cycle, isocitrate exits mitochondria and is then converted to alpha-ketoglutarate by a cytosolic NADP-dependent isocitrate dehydrogenase (ICDc). Alpha-ketoglutarate can flux back to mitochondria via alpha-ketoglutarate carrier (OGC). In the pyruvate-phosphoenolpyruvate (PEP) cycle, PEP is the precursor of pyruvate and can be used to produce pyruvate and then OAA. OAA is converted back to PEP, which can exit mitochondria and translocate to cytoplasm, via a guanosine triphosphate (GTP) dependent mitochondrial phosphoenolpyruvate carboxykinase isoenzyme (PEPCKm). In GABA shunt, alpha-ketoglutarate is converted to glutamate by glutamate dehydrogenase (GDH) and then used to generate GABA through oxidative decarboxylation catalyzed by glutamate decarboxylase. GABA can either leave the mitochondria for further generation of gamma-hydroxybutyrate or can be further metabolized to succinic semialdehyde (SSA) and then metabolized to succinate, which fluxes back to TCA cycle. (Adapted from [35, 87]).

In addition to NADPH, each pyruvate cycle produces other specific products unique to stimulus-secretion coupling, such as cytosolic acetyl-CoA and malonyl-CoA generated in the pyruvate-citrate cycle. It is speculated that acetyl-CoA probably exerts its effect on insulin secretion by providing the acetyl group needed for acetylation of many enzymes and signaling molecules, which are actively involved in beta cell secretion function [88, 89]. Malonyl-CoA links the TCA cycle to lipid signaling pathways by providing a precursor for de novo lipogenesis and altering beta oxidation via inhibition of carnitine palmitoyl transferase I (CPT-I) [90, 91]. Alpha-ketoglutarate, which can be transported to cytoplasm through the pyruvate-isocitrate cycling pathway, is implicated in fuel-induced secretion coupling by either mediating the cross-talk between glucose and amino acid stimulated insulin secretion [92-94] or controlling Fe(II)-alpha-ketoglutarate dependent hydroxylase activity through substrate availability [95, 96].

The fourth pyruvate cycling is pyruvate-phosphoenolpyruvate cycle [83], which might serve to generate guanosine triphosphate (GTP) for insulin secretion. PEP itself acts as an insulinotropic metabolite by suppressing okadaic acid-sensitive Ser/Thr protein phosphatase activity [97], an event that has been shown to augment Ca^{2+} influx in RINm5F cells [98].

1.1.3.5 Gamma-aminobutyric acid (GABA) shunt

Another pathway between TCA cycle intermediates is gamma-aminobutyric acid (GABA) shunt, which works independently of alpha-ketoglutarate dehydrogenase to link succinate to alpha-

ketoglutarate and produces GABA and gamma-hydroxybutyrate [99, 100]. The former serves as a positive feedback loop to GSIS via GABA_A receptor [101, 102] and the latter helps with glucose suppression of glucagon secretion [103]. Like pyruvate cycling, glucose-derived anaplerosis is also the driving force for this pathway.

1.1.4 Biphasic insulin secretion

As a response to a sustained stimulation of insulin secretagogues, dynamic insulin secretion is characterized by the biphasic feature, a phenomenon first reported by Grodsky in rat pancreas [104-106] and by Cerasi [107] in humans in the 1960s. These observations showed that the dynamics of insulin secretion had a biphasic effect upon stimulation induced by an abrupt and sustained increase in the concentration of glucose. The first phase is relatively transient (0-10 min) and is predominantly characterized by a high insulin secretion peaking in the first 10 min of stimulation. This first phase is followed by the longer-lasting second phase initiated with lower insulin secretion rate that either remains stable or slowly rises as long as the glucose concentration remains high [104].

The characteristics of biphasic insulin secretion vary somewhat with species [108]. The insulin secretion of the second phase observed in rat pancreases and isolated rat islets often rise quickly and will eventually be well above the peak of the first phase [109-113]. However, in freshly isolated mouse islets or perfused mouse pancreases, the second phase has been demonstrated to be flat and lower than the peak of the first phase [114-117]. Consequently, the rising phase has been believed to be slight [118] or non-existent [114, 115, 119-121]. This difference in the magnitude of second phase between rat and mouse was originally attributed to a great production of cyclic adenosine monophosphate (cAMP) [122] and/or expression of distinct isoforms of protein kinase C [121] in rat beta cells. Recently, it was proved that the difference in the second phase between species was actually caused by the pre-culture conditions prior to the perfusion experiment, in which pre-stimulatory glucose level can indeed play a crucial role in either decreasing or increasing the pattern of second phase depending on the species being studied [123].

Whether the biphasicity of insulin secretion is of any physiological significance or just an experimental phenomenon has been under debate for years. The latter position is supported mainly by the fact that the abrupt change of glucose concentration almost never happens in nature. Indeed, in real physiological conditions, plasma glucose level is elevated gradually and insulin secretion stimulated by oral glucose ingestion never bears any clear sign of biphasicity. However, this can be

easily refuted since *in vivo* biphasic insulin secretion elicited by hyperglycemic clamp or intravenous glucose administration was observed from both mouse [113] and human (six healthy volunteers aged 16-28 with no diabetes in the family history as well four diabetic patients) [107] almost as early as *in vitro* [104-106]. Coupling data also reveal the existence of early rapid insulin response, an analogue of the *in vitro* first phase insulin secretion of beta cells, to physiological plasma glucose level. This early rapid insulin response can be further enhanced by gastrointestinal hormones acting as incretins [124]. This evidence at least demonstrates that biphasicity of insulin secretion is not an artificial observation due to stress from experimental conditions. The physiological significance of biphasic insulin secretion was revealed by further evidence showing that early insulin response serves to regulate postprandial glucose homeostasis in both dog [125, 126] and human [110] by acting as a rapid inhibitor of hepatic glucose production [127]. In contrast, the second phase insulin release was confirmed to exert its effects on both glucose production and utilization [127], since it takes longer for insulin to cross the endothelial barrier of muscle cells and activate glucose uptake and utilization in muscle. Moreover, data from clinical studies demonstrate that alteration of acute insulin release is an early sign of beta cell dysfunction in impaired glucose tolerant and type 2 diabetic patients [48, 128-130]. Taken together, this evidence indicates that biphasic time course insulin secretion is a real characteristic of beta cell function rather than an artificial experimental phenomenon, and is likely used to dynamically optimize the insulin action on target tissues based on their different structures and specific functions [108]. Therefore, the study of biphasic insulin secretion mechanism will be helpful for both early screening and identification of pre-diabetes as well as treatment of type 2 diabetes.

To date, several major and non-exclusive models have been proposed to explain the mechanism of biphasic insulin secretion. The first model is the pool model [105, 106, 131, 132], which assumes that cells contain two distinct pools of insulin granules with different releasability: a small pool docked to the plasma membrane and ready for immediate release, the depletion of which corresponds to the nadir in biphasic insulin secretion, and a large pool located away from cellular membrane requiring translocation of insulin granule from cytosol to membrane upon stimulation [111]. However, this model faces some challenges, both in the timing of the first phase insulin secretion and the origin of released granules. Biochemical evidence observed that the first phase lasted about 10 min, while electrophysiological data defined it as only 100 ms [133]. Moreover, evidence generated by imaging techniques used to monitor exocytosis concluded that granules released during both phases of glucose stimulation have a similar origin, distinct from the docked pool [134, 135].

The second model is the signal model, which proposes that two phases of insulin secretion are governed by different signaling pathways. This hypothesis was mainly based on an observation that only fuel secretagogues are capable of inducing the second phase, and non-metabolizable stimuli can only elicit the first phase [133, 136-138]. This, at least, suggests that second phase insulin secretion depends on beta cell metabolism.

The third hypothesis, which does not contradict either of the above-mentioned models, proposes that the actual insulin secretion at any moment is determined by the current glycemic challenge as well as previous stimulus, because glucose can elicit both an acute stimulatory effect and a time-dependent effect (TDE) on pancreatic beta cells [106, 107, 139-142]. TDE refers to the observation that if the pancreatic beta cells are challenged repeatedly, beta cell responsiveness to subsequent stimulations can be either enhanced (time-dependent potentiation or TDP) [104, 106, 119, 131, 140, 143-146] or impaired (time-dependent inhibition or TDI) [119, 143, 144, 146] by previous exposure to stimuli. The type and magnitude of the subsequent insulin responses depend on the type of secretagogues, as well as condition of exposure, including secretagogues' concentration (dose dependency) and duration (time dimension) of stimulation applied: high concentrations and long durations generate amplification of subsequent insulin responses, while low concentrations and short pulses of stimulation tend to induce a refractory state [104-107, 119, 131, 139-145]. Hence, the biphasic insulin release might reflect the net balance between TDP and TDI on the acute stimulation [147]. One important piece of supportive evidence is that a tight correlation was discovered between the magnitude of TDP and the slope of second-phase insulin response [144]. In this model, biphasic insulin release is a function of the combined regulation of acute GSIS by both TDP and TDI events initiated by glucose, each of them having its own kinetics and dose dependence.

Based on current available literature, it is very hard to conclude which model accurately describes the actual mechanism underlying the biphasic insulin secretion.

1.1.5 Concluding remarks

Compared to all above-mentioned intensive research efforts being applied to diabetes during the last several decades, our knowledge about the true biochemical mechanism underlying nutrient-induced insulin secretion remains limited. Although a large amount of data has been collected, many new questions have been simultaneously created. It is not at all unusual to see contradictory results coming from similar studies with different approaches. A good example is the study examining whether the

PPP [33, 148-150] or malic enzyme (ME) [49, 151-159] is involved in regulation of GSIS. Data as well as conclusions from different studies clearly oppose each other.

Admittedly, in some cases the problems are caused by differences between the experimental conditions used in different studies. For example, the species difference of second phase insulin secretion was proved to result from pre-culture conditions as well as pre-stimulatory glucose levels [123]. Disagreement about the exact role of malonyl-CoA decarboxylase in GSIS is due to the presence or absence of exogenous free fatty acid (FFA) in the stimulation buffer [160, 161].

More importantly, it is an inherent feature of the traditional research strategy, in which observation is normally focused on the change of one or several effectors caused by manipulation (decrease or increase) of up-stream factor(s). However, it is almost never this case in nature. In fact, most signaling molecules, including both metabolic factors and proteins, lie at the crossroads of several metabolic (or signal transduction) pathways and are involved in multiple biological processes. So, any manipulation of even one up-stream signaling molecule will most likely cause significant changes in the activity of several downstream metabolic pathways, including hundreds of metabolites through signal transduction cascades. Missing some parts of the whole signal transduction network is common, because classical biochemical approaches only allow the determination of one molecule at a time and hence are prone to cause misinterpretation of observations under investigation. The best example is ATP. No manipulation of ATP will alter the activity of the K_{ATP} channel dependent pathway without affecting countless other metabolic and signal pathways.

Therefore, a different and powerful approach is needed for detection of global biochemical events to overcome this intrinsic drawback in traditional research strategies. This requires that relevant research should aim at studying and understanding the metabolic network as whole and this should be done at the metabolome level.

1.2 Metabolomics

1.2.1 Introduction of metabolomics

Generally speaking, metabolomics refers to the systematic determination of either a few metabolites, or the profile of the whole metabolome, the total set of all native metabolites presented in and required for maintaining the normal function of a particular biological system [162], e.g. cell, tissue, organ or organism [163].

Metabolites are low molecular weight molecules produced by metabolism, which is composed of a series of life-sustaining enzymatic chemical reactions supplying the carbon and energy resources needed for cells. Enzymes coordinately organized to serve a certain function within a living system are called metabolic pathways. Unlike genes, mRNA transcripts, or proteins, which have different variants, isoforms or even post-translational modifications, metabolites (especially those produced by primary metabolism) preserve similar or even exactly the same chemical structure irrespective of their location or species and are usually well-connected to other metabolites to form a whole metabolic network. It is very difficult to estimate the exact number of endogenous metabolites in different species. The present number of metabolites in humans is predicted to be 40,000 by the Human Metabolome Database (HMDB) [164], which is much less than what has been reported for genes or proteins. Although the plant and fungal kingdom is predicted to have 200,000 and 400,000 metabolites, approximately 5000 of them might be actually present in the well-studied plant model *Arabidopsis Thaliana* [165]. This is definitely an advantage of metabolomics over other functional genomics studies. These two features, especially conserved chemical structures spanning the species barrier, strongly indicate that metabolites are central to maintaining cells viability and function.

Since they are the end products of a cellular process in living systems, metabolites can directly link phenotype to their underlying genetic source and the dynamic changes of metabolites reflect the integrative activity resulting from all previous levels of regulation and control mechanisms in an entire biochemical cascade. Actually, an interference of a biological system at any level (genes, mRNA, proteins) will be amplified, accumulated and eventually manifested by either quantitative or chemical change of metabolites both spatially and temporally. In other words, the metabolome is the net function of an integrated system formed by multiple levels of cellular process, including genome, transcriptome, and proteome, and is further influenced by environmental stimuli, healthy behavior and pharmaceutical interventions. Hence, metabolomics is different and complementary to other functional genomics studies and can provide a unique advantage for mechanistic studies. To date, metabolomics has been widely used in studying environment stress [166], toxicology [167], pathophysiology [168, 169], pharmaceuticals [170], nutrition [171-174], and phenotypic characterization as well as clinical diagnosis [175-177].

1.2.2 Target and untargeted metabolomics

Depending on the objective of studies, metabolomics can be divided into two major groups: targeted and untargeted [163, 178] metabolomics.

Targeted metabolomics, which requires the known chemical structures of metabolites and the establishment of a standard curve built upon proper internal and/or external standards analysis, is a selective identification and an absolute quantification of a few number of pre-defined compounds precisely from crude extract [163]. The major disadvantage of this approach is that it is not helpful for the discovery of biomarkers or the survey of problems with unknown mechanisms.

Different from targeted metabolomics, untargeted metabolomics focuses on a comprehensive determination of the whole metabolome and comparison of relative abundance of various metabolites in different experimental conditions. The aim is to discover biomarkers, some metabolites used to indicate a certain biological function. Because of this particular purpose, untargeted metabolomics poses both theoretical and practical challenges on unbiased analysis at each level ranging from sample preparation, data acquisition to data analysis and data mining.

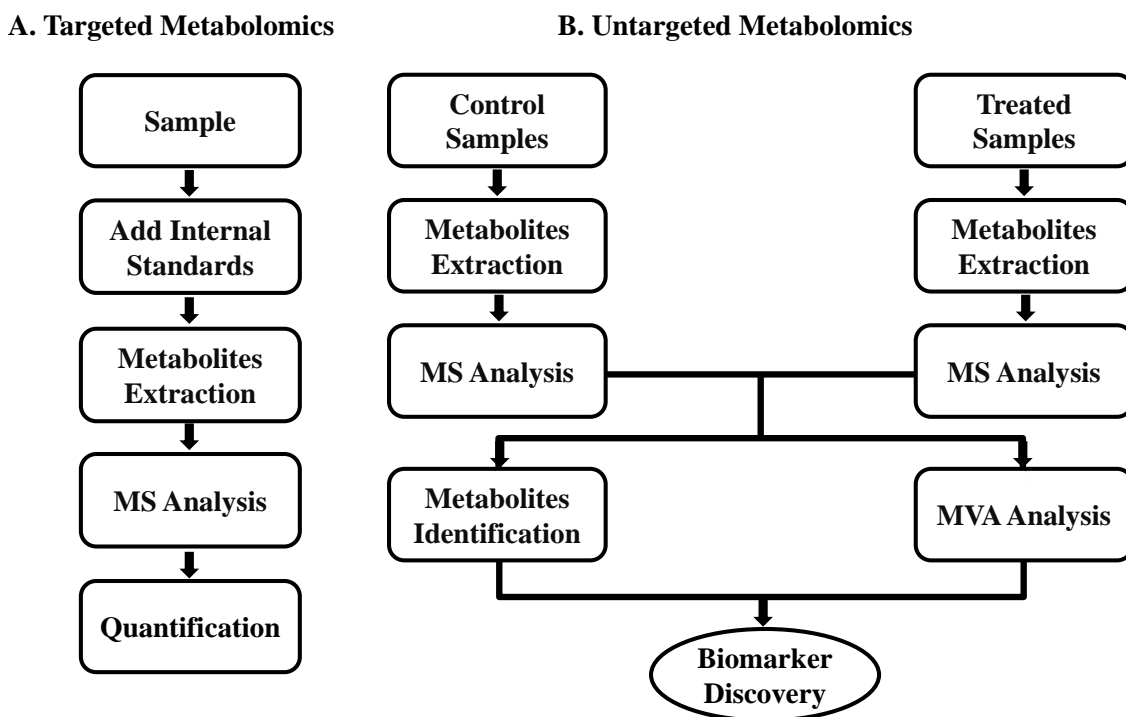


Figure 1-2 Schematic summary of MS-based targeted and untargeted metabolomics

(A). Targeted metabolomics. Stable isotope-labeled standards are added to the sample prior to sample extraction and derivatization. The MS signal intensity of stable isotope-labeled standards is then used to establish a standard curve for absolute quantification of metabolites concentration determined by analytical instrument. **(B). Untargeted metabolomics.** Samples

with different replicates are collected from two different conditions (perturbed vs. unperturbed) designed to characterize a certain function, then processed and analyzed by analytical instruments, which will generate two independent data sets. These data sets will be searched against currently available spectral libraries for metabolites identification. In the meantime, a global comparison of two data sets by multivariate statistical analysis can identify significant biomarkers responsible for the differentiation of these two different experimental conditions. However, the absolute concentration of analytes is unknown. (Adapted from [169])

1.2.3 Metabolite extraction

As the product of enzyme-catalyzed reactions, metabolites are constantly produced, consumed, degraded, and excreted by cells and their half-lives are at the scale of seconds or even milliseconds [179-181]. Therefore, the rapid turnover of metabolites resulting from the high activity of metabolic enzymes defines the necessity of the immediate inactivation of metabolic enzyme activities, which is the first and utmost step in metabolites extraction to avoid further biochemical conversions or chemical degradation. An effective quenching of the metabolic enzymes is normally achieved through rapid changes in temperature ($< -40\text{ }^{\circ}\text{C}$ or $> 80\text{ }^{\circ}\text{C}$) or pH (pH < 2.0 or pH > 10). Normally, perchloric acid, trichloroacetic acid (TCA), potassium hydroxide (KOH), and sodium hydroxide (NaOH) are used for the creation of an extreme pH environment [182-186], but this method generally requires pH neutralization in the next few steps and is limited when extracting pH-sensitive metabolites. Liquid nitrogen or ethanol/dry ice bath inactivates cellular metabolism by generating an extremely low temperature. Other cold organic solvent-based solutions, e.g. methanol, ethanol, are also effective in quenching metabolism by destabilizing enzymes [165].

The second step usually includes the disruption of the cell membrane and separation of metabolites from the complex biological matrix. Many different methods can be used to disturb the cell membrane and to release intracellular metabolites. Mechanical-based cell disruption, including ultrasonics [187-190], microwave [191], or even manual grinding, breaks the cell envelopes down mainly through the mechanical force applied to cells. Non-mechanical disruption methods release intracellular contents from cells by using traditional enzymatic (e.g. glycosidases, lysozyme [192, 193]), chemical (e.g. organic, acidic, alkaline solvent) or physical (freeze-thawing cycle, or heating) agents to increase permeability of cells. Non-mechanical disruption methods normally have restrictions on temperature, pH or specificity. For example, heating most likely will cause loss of

temperature-sensitive metabolites. Lytic enzymes generally require an aqueous medium and mild temperature, which is incompatible with conditions used for inactivation of metabolism.

Unlike other functional genomics, which contain structurally conserved molecules (four nucleotides for genomics and transcriptomics, twenty one amino acids for proteomics), metabolomics aims at analyzing a group of molecules with various chemical properties and structures ranging from ionic inorganic species to hydrophilic carbohydrates, hydrophobic lipids, acidic carboxylic acids, polar and non-polar amino acids as well as vitamins. Therefore, although the number of metabolites is much less than that of proteins or genes, the chemical complexity makes it virtually impossible to establish a simple and absolutely unbiased extraction method for a whole metabolome. Up to date, almost no such comprehensive extraction techniques have been published showing acceptable reproducibility, robustness, and recovery for all classes of metabolites [194, 195]. One general practice is to adapt a sampling method for as many classes of metabolites as possible by incorporating a multi-step purification procedure needed for isolation of metabolites with different polarity and molecular weight to gain a broader perspective of the metabolome. However, it will be a time-consuming, laborious process and can easily add artifacts to extracted metabolite pools. An alternative and widely used approach is to sacrifice several classes of compounds for a good and stable yield of other types of metabolic intermediates favored by the extraction method, in which comprehensiveness is traded off for reproducibility. For example, a method based on a nonpolar organic solvent, which is incompatible with water soluble and polar metabolites, can be safely used for selective extraction of insoluble or nonpolar metabolites. Practically, a multiple solvent mixture is generally used for the purpose of increased coverage of different classes of metabolites. For example, cold methanol/chloroform/water mixture, stepwise [196] or mixed simultaneously, was successfully applied to the extraction of both polar- and non-polar metabolites [194, 195, 197-201]. However, it was proven to be not efficient for nucleotides even when chloroform's toxic and carcinogenic effects are not taken into consideration. Cold methanol and water mixture (< 20 °C) is a simple and efficient method for extraction of polar and mid-polar metabolites from animal cells [182, 186, 194, 202-204]. The concentration of steady-state metabolites may range widely from 10^{-1} to 10^{-7} M [205, 206]. In addition to sampling of a wide range of compound classes, the extraction process must also preserve the concentrations of metabolites. It is important that these intracellular metabolites are released in a quantitative manner and the ratio of metabolites concentration in their original state remains unaffected. Otherwise, the extraction process will add even more complexity to metabolomics analysis. The wide range of chemical properties and concentrations of intracellular metabolites as

well as the dynamic regulation by enzymes involved in metabolic pathways makes the sample preparation process for untargeted metabolomics a very challenging task.

1.2.4 Instruments used for metabolomics

The significant improvements in modern analytical chemistry instrumentation over the last several decades have made the study of metabolomics much more accessible. A wide range of analytical platforms, such as ultraviolet–visible spectroscopy [207], fourier transform infrared spectroscopy (FT-IR) [208-210] or raman spectroscopies, mass spectrometry (MS) [163, 211, 212], and nuclear magnetic resonance (NMR) [213-217], have been applied to analyze metabolites. Because each technology is unique and provides different information, the research objective and the sample under analysis should be considered when choosing an instrument to work with.

Generally speaking, MS is the most widely used analytical technique for metabolomics research because it is superior to other instruments in terms of simplicity and sensitivity. So, MS is widely used for identification of low-abundant metabolites. Newly developed mass spectrometers with improved sensitivity and/or resolution can even capture samples with concentration at fmol level and can support identification of metabolites without the need to search a MS spectral library. Even though MS spectra only display masses of the ionized molecule and its fragments, the abundance of structural information contained in MS spectra is much more than what has been interpreted and utilized.

The matrix effect from crude extract is a notorious part of analytical technique so an efficient chromatographic (gas- or liquid-) or electrophoretic separation prior to MS is necessary for metabolomics analysis. The coupling of metabolites analytical technology to chromatographic or electrophoretic separation, e.g. gas chromatography (GC) [203, 212], liquid chromatography (LC) or capillary electrophoresis (CE), can remarkably expand the capacity of MS-based metabolomics technologies by enhancing their resolution, sensitivity and selectivity, because the well-known co-elution and ion suppression effects due to complex biological background are minimized [218, 219].

For the last thirty five years, GC coupled with MS has been commonly used in the field of metabolomics [220-222] and can detect different metabolites with various chemical properties, as long as they were volatile. Metabolites with low thermal stability, high polarity and low volatility are hard to measure and need to be derivatized and converted to GC-measurable molecules [223, 224]. Although its application is limited by molecular weight, thermal stability, polarity and volatility of

metabolites, GC-MS is still one of the most popular technologies for metabolomics studies due to the superior separation power of GC column, the well-developed deconvolution algorithms [225, 226] as well as the comprehensive and searchable MS spectral databases [223] generated from globally standardized operations in GC-MS labs. Additionally, GC-MS data has some well-described algorithms for automated raw data processing. AMDIS (automated mass spectral deconvolution and identification system) offers a variety of enhanced functions, such as noise reduction, spectra deconvolution, peak detection, and compound identification, while LC-MS or CE-MS lacks the equivalence of the same competency. Moreover, GC-MS has some well-established, comprehensive libraries to aid users with metabolite identification, while LC-MS and CE-MS require additional implementation of vendor independent and metabolites specific libraries. Examples of such libraries include NIST11/2011/EPA/NIH Mass Spectral Library containing 243,893 EI spectra, and 10th edition of Wiley Registry of Mass Spectral Data containing 719,000 spectra. These are two commercially available libraries for small chemical molecules, natural products as well as drugs. FiehnLib is a library containing both retention index and mass spectra from quadrupole and time-of-flight only for metabolites below 550 Da [227].

On the contrary, LC-MS offers its own set of unique advantages, because it is capable of covering different classes of metabolites with a broad range of polarity, molecular weight and chemical structure [228-230]. Reverse-phase liquid chromatography (RPLC) has been a well-established method for separation of metabolites prior to MS detection without requirement of any pre-treatment of metabolites samples. Recently, a newly developed method called hydrophilic interaction liquid chromatography (HILIC) was shown to be more friendly and efficient for separation of ionic or highly polar metabolites [231]. Ultra-performance liquid chromatography (UPLC) [232] displays better resolution, retention time reproducibility, and signal-to-noise ratio than HPLC [229, 230, 233-235]. Following current trends, substantial improvement of metabolomics data acquisition techniques can be predicted to happen in the near future especially for liquid chromatography based methods.

An even more promising separation technique is CE-MS. CE-MS separates analytes in submillimeter capillaries according to their ionic mobility under the influence of an electric field and hence allows both charged and uncharged metabolites to be separated in one single run so that multiple metabolites classes can be potentially analyzed simultaneously [236-241]. CE-MS is therefore especially attractive for researchers doing high-throughput untargeted metabolomics study. Other advantages of CE, such as low sample volume and relatively short analysis time, give CE the upper hand over GC

and LC, and also contribute to its bright future of CE serving as the major analytical technique for metabolomics.

NMR is another widely used analytical technique in the field of metabolomics. NMR is particularly useful for characterization of structurally unknown compounds and also has the ability to distinguish between isomers [242], e.g. citrate vs. isocitrate. Additionally, NMR-based metabolomics is characterized by its non-destructive data collection and minimum sample preparation process so that samples in different conditions can be saved for further analysis [243]. NMR is also well-known for being highly quantitative, reproducible and non-selective [213] and hence can be promisingly applied to unbiased measurement of all classes of metabolites and even metabolic fluxes [244, 245]. However, its inherently low sensitivity (compared to MS) resulting from natural abundance of chemical atoms prevents it from being as popular as MS in detecting low-abundant metabolites at the current stage. The sensitivity of NMR can be improved by the extension of analysis time, application of high magnetic fields and the proper use of cryogenic probes. For example, ^{13}C NMR spectroscopy can only detect samples in μmol to mmol concentration range, or nmol at high fields with new cryoprobes [246]. Due to the low sensitivity of NMR and the prevalence of ^1H , most NMR-based metabolomics data has been generated by ^1H NMR spectroscopic investigations of biofluids, such as urine and plasma. The application of robotic flow injection methods further enables the high-throughput analysis of biofluids samples--as many as 100 samples per day [247]. NMR can also be expanded to analyze the intact tissue samples by using a technique known as ^1H MAS NMR spectroscopy [248-250].

Overall, MS and NMR are two major analytical techniques used in metabolomics. They have their own pros and cons and the combination of these two complementary spectroscopies will be helpful to generate comprehensive and integrated metabolomics data.

1.2.5 Data analysis and data mining

Data analysis of targeted metabolomics simply quantifies predefined metabolites by using the information provided by internal or external standards, which is a traditional and mature analytical technique. However, untargeted metabolomic data is rich in information, and data analysis must follow a different approach.

The first goal of untargeted metabolomics data analysis is to define the unknown compounds based on their chemical structures (size, molecular weight, retention time, element composition, isotope

ratio, mass spectral fragmentation patterns), which are revealed by structure analysis. For this purpose, one strategy is searching spectra against (metabolite-specific) spectral libraries, such as The Human Metabolome Database (HMDB) [164, 251, 252], Golm Metabolome Database (GMD) [253], METLIN [254-256], Fiehn [227], and National Institute of Standards and Technology (<http://www.nist.gov/>). A well-organized and information-rich database normally allows the automatic and high-throughput metabolite identification based on their unique physical and chemical properties revealed by raw data collected from analytical techniques. Such chemical identification converting raw spectroscopic data to corresponding metabolites is the utmost important step in a successful metabolomics study. Unfortunately, compared to the well-developed genes and proteins databases, these libraries need further improvement. Currently, there are still no public spectral libraries specifically devoted to endogenous metabolites. An equivalent strategy for metabolites identification without the requirement of databases is fourier transform ion cyclotron resonance (FT-ICR) MS, which has a high enough resolution to directly generate the empirical formulae of metabolites.

The second objective of data analysis for untargeted metabolomics is the quantitative comparison of metabolite levels between parallel experimental conditions with a goal to link the relative change of metabolites abundance to the functional assignment which is supposed to be unraveled by an appropriate design of comparative experiments. Due to the inherent complexity of metabolomic data sets, classical statistical tools, e.g. student's t-test, cannot fulfill this task and hence a special data handling and analysis tool, multivariate analysis (MVA), is needed to handle and understand the multidimensional metabolomics data set.

The goal of MVA is to provide an easily interpretable data set for ongoing research with a proper mathematical approach to facilitate the correct identification of metabolites responsible for the classification of samples. For this purpose, MVA simplifies the complex metabolic data table by reducing the dimensionality of original complex data sets to much fewer variables with minimal loss of information contained in original data matrix. The advantage of MVA versus traditional statistics methods lies in the fact that MVA can identify the underlying data structure between observations, variables, and between both observations and variables that might be obscured in raw data sets. MVA can also compare the relative importance between all predicted factors since the metabolomics data set, including the whole metabolic network rather than one or several metabolic pathways, is analyzed as a whole.

Two major MVA classes can be used for metabolomics data analysis, unsupervised and supervised. Unsupervised MVA, such as hierarchical clustering analysis [257-260], principal component analysis (PCA) [261], self-organizing maps [257, 262], and independent component analysis [263], is a powerful analysis tool when nothing is known about the class information of samples and hence this is normally used for an overview of metabolomics data profiles. For example, it can be used to identify the grouping, trends, and outliers of a data set. In contrast, supervised MVA only deals with the data set when the information regarding classes is already clear and can reveal the quantitative relationship between observations and variables, which are grouped into two different data tables (X and Y). X normally contains spectral data and Y is commonly reserved for experiment conditions, like treatment of samples, duration of treatment, study objectives, etc. Hence, supervised MVA is commonly used as the typical data handling tool for correct identification of biomarkers. Many algorithms are used for supervised MVA [264], such as discriminant analysis [265], partial least squares (projection to latent structures) (PLS) [266-269], ANNs [270], rule induction [271, 272], inductive logic programming [273], and evolutionary computation [274, 275]. If a data table contains qualitative value, such as treatment information of samples, partial least squares discriminant analysis (PLS-DA) [266, 276-280] can be used to replace PLS. But system variations in the X matrix that are unrelated to the Y matrix will negatively affect PLS models, the interpretation of data as well as the identification of biomarkers. To overcome this inherent limitation, orthogonal projection to latent structures (OPLS) [281, 282] is created as a modification of PLS. OPLS is able to separate system variations into two parts: Y-relative (predictive) and Y-irrelative (orthogonal). So, the interpretation of data will not be affected by Y-orthogonal variations since only the variations relevant to Y matrix are used for modeling. Analogously, PLS-DA also has its equivalence, called OPLS-DA [283]. Another advantage of OPLS is it is a cross-validated method, which provides more reliable modeling than simple correlation analysis of variables against class [284].

Projection-based MVA, e.g. PCA, PLS and OPLS, assumes that existence of latent variables [285], which are not necessarily measurable as observable variables (metabolites). Latent variables can represent the aggregation of many relevant observable variables so that they help to reduce the dimensionality of data sets. Latent variables are weighted. That means the most important latent variable, which is called the first principal component in PCA or the first predictive/orthogonal component in PLS and OPLS, describes the largest variations of the original metabolite data matrix. The second latent variable has the second largest discriminating power and so on [286]. The plot of observations (samples) along the first few latent variables provides a visualized summary of all

samples in the original metabolic data table, which is called score plot. Score plot can not only find clusters, but also reveal the strong outliers, which is the observation outside the Hotelling's T² ellipse (95% confidence interval) plot [287]. The closer the data points representing samples are in score plot, the more similar they are to each other. DModX (distance to model) can also be used to detect the outliers based on the distance of observations to the model plane [288, 289]. Likewise, a loading plot is able to show the relationship between all variables in a way similar to the score plot. Normally, all variables are equally important regardless of their actual concentration for MVA analysis, because they are first centered by subtracting the mean value, dividing their standard deviation and then unit variance (UV) scaled. This scaling is good to rescue the false negative results due to the low intensity of metabolites. These plots are basic but powerful tools to qualitatively understand metabolomics data.

One risk with MVA is data overfitting. Hence, validation is necessary to avoid issues such as the bias against certain variables, or a high false discovery-rate. A common validation method requires two data sets: one is training and another is predictive. The former will generate a R², which indicates the goodness of fit and the latter will have a Q² parameter, which reflects the goodness of prediction. The high value of both parameters indicates a good fit, but a high R² with decreasing Q² generally suggests a problem of overfitting.

In order to do MVA, data need to be arranged into a proper table, where each row is a sample (it is referred to as "observation" in MVA) and each column represents a metabolite or a putative metabolite (called "variable" in MVA) measured by spectroscopies. Due to the two dimensional nature of hyphenated instruments (e.g. GC-MS, UPLC-NMR), generation of such a data table requires the pre-processing of raw data by proper deconvolution algorithms [225, 258, 290-293], such as AMDIS [225, 291], LECO ChromaTOF (Leco Corporation, St. Joseph, MI) [294], AnalyzerPro (SpectralWorks, Runcorn, United Kingdom). On top of that, appropriate peak alignment methods [295, 296] are needed to overcome the variability of chemical shift or retention time, such as MZmine [297, 298], MetAlign [299, 300], MathDAMP [301], XCMS [302, 303], metaXCMS [304, 305], XCMS online [306, 307], and SpectConnect [308].

Overall, as an integrated part of untargeted metabolomics, MVA is a powerful and robust chemometric tool for data analysis.

1.2.6 Future outlook

Metabolomics is a relatively new discipline and is rapidly expanding. Its further progress needs the support from improved analytical instruments, bioinformatics as well as the establishment of data regulation standards within this community. To meet the growing challenge of metabolomics research, multidimensional chromatography [309-313] has been tested aiming at improving the sensitivity, resolution, comprehensiveness, and throughput of this method. Similarly, efforts to improve the NMR spectroscopy sensitivity will be likewise continued. Like other functional genomics, metabolomics will ultimately require the development of agreed standards of data generation, analysis, management, publication, and sharing within the community, which was recently initiated by NIH in 2005 [314-317], but still needs further support.

1.3 Hypothesis

Metabolic pathways play an imperative role in coupling glucose metabolism to insulin secretion. However, the complete understanding of the mechanism underlying GSIS remain unresolved. We hypothesize that, in addition to ATP, glucose metabolism must generate other metabolic coupling factors to control pancreatic beta cell secretion function. In this dissertation, a GC-MS based untargeted metabolomics approach will be established and be used to investigate different aspects of GSIS and to reveal the underlying mechanisms.

1.4 Overall objectives

The purpose of my thesis is to establish a GC-MS based untargeted metabolomics approach to reveal the unknown mechanisms in regulation of GSIS. It will be comprised of four parts:

1.4.1 Aim 1

To establish a feasible untargeted metabolomics platform from sample preparation to data analysis. Our GC-MS based untargeted metabolomics will be applied to study the mechanism underlying GSIS and any discovery will be verified in both INS-1 832/13 cell line and islets of Langerhans models.

1.4.2 Aim 2

Glucose induces biphasic insulin secretion in islets beta cells. To study the kinetic aspects of GSIS, a time-resolved metabolome analysis was performed to investigate the mechanism controlling the second phase of insulin secretion in INS-1 832/13 cells.

1.4.3 Aim 3

Pancreatic beta cells have a memory, which is called time-dependent effects (TDEs), of previous applied insulin secretagogues. So, their secretion activity is determined by the stimuli that cells are currently exposed and previously challenged. In this part, a TDEs model was created on INS-1 832/13 cells and was studied by using a metabolomics approach.

1.4.4 Aim 4

Alpha-ketoglutarate was proved to be an important metabolic factor coupling glucose metabolism to insulin secretion. A metabolomics approach was used to discover the downstream effectors of alpha-ketoglutarate and study alpha-ketoglutarate-mediated hydroxylation in regulation of insulin secretion and its underlying mechanisms.

Chapter 2

Materials and Methods

2.1 Materials

2.1.1 Cell lines

The clonal beta cell line 832/13, derived from the parental INS-1 rat insulinoma cells, was kindly provided by Christopher Newgard [318]. INS-1 832/13 cells were cultured at 37 °C and 5% CO₂ in RPMI-1640 supplemented with 10% fetal bovine serum, 100 U/ml penicillin, 100 µg/ml streptomycin, 10 mmol/l HEPES, 2 mmol/l L-glutamine, 1 mmol/l sodium pyruvate, and 50 µmol/l beta-mercaptoethanol.

2.1.2 Animals

Islets were isolated from Sprague-Dawley rats. All animal experiments were approved by local Animal Care Committees at the University of Waterloo and handled according to the guidelines of the Canadian Council on Animal Care.

2.1.3 RT-PCR primers

Primer sequences for target genes are:

Prolyl hydroxylase 1 (PHD1):

PHD1 forward (AGC AAC AGC ACT ACC CAT AGC AGT),

PHD1 reverse (AGG CAC AAT ATA GTC CAA GGC CAG),

Prolyl hydroxylase 2 (PHD2):

PHD2 forward (AAG ATC ACC TGG ATC GAG GGC AAA),

PHD2 reverse (CATG GCT TTC GTT CGG CCG TTT AT),

Prolyl hydroxylase 3 (PHD3):

PHD3 forward (ATGA AGT TCA GCC CTC CTA TGC CA)

PHD3 reverse (TCA CAC CAC CGT CAG TCT TTA GCA),

Hypoxia-inducible factor 1-alpha inhibitor (FIH-1)

FIH-1 forward (TGC AGC AAA CAC TCA ATG ACA CCG),

FIH-1 reverse (TCA CAT TCC CTT CCA TGC CGA TGA).

Aryl hydrocarbon receptor nuclear translocator (ARNT)

ARNT forward (GCG GCG ACG GAA CAA GAT GAC A)
ARNT reverse (ACA CCA CTC GGC CAG TCT CAC A)
Glucose transporter 2 (Glut2)
Glut2 forward (CCT GGC CGG GAT GAT TGG CA)
Glut2 reverse (AGG CCC GAG GAA GTC CGC AA)
Glucokinase (GK)
GK forward (ATG CTG GAT GAC AGA GCC AGG AT)
GK reverse (TCG GGG ATG GAG TAC ATC TGG TG)
Glyceraldehyde 3-phosphate dehydrogenase (GAPDH)
GAPDH forward (GGC TCT CTG CTC CTC CCT GTT)
GAPDH reverse (GTG AGA CCC AGA CTT CTC CAT G)
Pyruvate kinase muscle isozyme 1 (PKM1)
PKM1 forward (TGG AGG CCA GCG ATG GAA TCA)
PKM1 reverse (GCT CTT CAA ACA GCA GGC GGT)
pyruvate kinase muscle isozyme (PKM2)
PKM2 forward (TGG AGG CCA GCG ATG GAA TCA)
PKM2 reverse (GCG GCG GAG TTC CTC GAA TAA)
PPIE peptidylprolyl isomerase E (cyclophilin E)
Cyclophilin E forward (AGA TGG CAC AGG AGG AAA GAG CAT)
Cyclophilin E reverse (AGG GTT TCT CCA CTT CGA TCT TGC)

2.1.4 siRNA duplex construction and transfection

Two siRNA duplexes were constructed against each target gene. Relative to the start codon, the 5' end of the siRNA target sequence corresponded to the following nucleotide in:

Prolyl hydroxylase 1 (PHD1/EGLN2, GenBank™ accession number NM_053046.3):

siPHD1-1, nucleotide 506 (CAA GUU CUA GGC UGA GGG AGG AAG C),

siPHD1-2, nucleotide 292 (GCG UUG GUU ACC AAG GAG UGC CAG C).

Prolyl hydroxylase 2 (PHD2/EGLN1, GenBank™ accession number: NM_022051.2):

siPHD2-1, nucleotide 513 (CCC UCA UGA AGU ACA GCC UGC AUA C),

siPHD2-2, nucleotide 112 (CAA CUG GUC AGC CAG AAG AGU GAC T).

Prolyl hydroxylase 3 (PHD3/EGLN3, GenBank™ accession number: NM_019371.1):

siPHD3-1, nucleotide 914 (CCA GGA AAU GGA ACA GGU UAU GUT C),

siPHD3-2, nucleotide 1716 (GGA CGA UUA CGG ACA ACC UGA UGA C).

A previously described siRNA sequence (5'-GAGACCCUAUCCGUGAUUA-3') with no known gene homology was used as a control (siControl) [81, 84, 319].

2.1.5 Reagents

All reagents were purchased from SIGMA unless otherwise specified. Anti-HIF1alpha antibody was purchased from Santa Cruz. Pierce™ ECL Western Blotting Substrate (32106) was purchased from Thermo Scientific.

2.2 Methods

2.2.1 Insulin secretion assay

Insulin secretion and protein content assays were performed as previously described [318, 320, 321]. Briefly, cells (or islets) were incubated twice in experimental media containing low glucose concentration for 1 hour (0.5 hr for islets) and then incubated for 2 hours at the indicated glucose concentration unless otherwise specified. The experimental medium was a Krebs-Ringer-bicarbonate-Hepes (KRB) solution consisting of 118 mM NaCl, 5.4 mM KCl, 2.4 mM CaCl₂, 1.2 mM KH₂PO₄, 5mM NaHCO₃, 10mM HEPES, 1.2 mM MgSO₄ and 0.2% BSA at pH 7.4. The supernatant was taken and insulin was measured by RIA using the Coat-a-Count kit (SIEMENS, Los Angeles, CA).

2.2.2 Pancreatic islet isolation

Islets were harvested from adult male Sprague-Dawley rats weighing 250–300 g and cultured as described previously [322-324]. Briefly, animals were anesthetized with 60 mg/kg sodium pentobarbital. Islets were isolated by collagenase (SIGMA) digestion and cultured in RPMI 1640 growth medium supplemented with 10% fetal bovine serum, 10 mM HEPES (Sigma), 1% antibiotic-antimycotic solution (Hyclone), and 11 mM glucose.

2.2.3 Cell viability assay

Cells were cultured for the desired test exposure period. At the end of experiment, the exposure buffer was replaced with 500 µL/well of RPMI 1640 and CellTiter-Blue® (Promega G8080) reagent mixture. Cells were incubated in the mixture at a standard cell culture condition for 2 hours. At the end of incubation, the plate was shaken for 10 seconds and 100 µL of RPMI and the CellTiter-Blue®

reagent mixture was transferred to 96-well plate for the measurement of fluorescence at 560 and 590 nm.

2.2.4 Glucose utilization assay

Cells were cultured with the radiotracer [$5\text{-}^3\text{H}$] glucose at 0.08 Ci/mol, and samples were processed for measurement of glucose utilization as previously described [325]. Briefly, cells were incubated with [$5\text{-}^3\text{H}$] glucose containing KRB solution for the specified time and then the supernatant containing [$5\text{-}^3\text{H}$] water was mixed with 10% perchloric acid. The mixture was equilibrated with 0.5 ml of water sealed in scintillation vial at 50 °C for 18-24 h. Following this vapor-phase equilibration step, sample tubes were removed from the vial cooled to room temperature, and mixed with scintillation mixture (Bio-Safe, Research Products International). $^3\text{H}_2\text{O}$ content was determined by counting over a 5-min period on a PerkinElmer liquid scintillation spectrometer and used as indicator of glucose utilization.

2.2.5 *In situ* mitochondrial bioenergetics

INS-1 832/13 cells (2×10^4 cells/well) were plated on a Seahorse Bioscience XF24 cell culture microplates and kept at 37 °C cell culture incubator until confluent. Similarly, islets (50 islets/well) were seeded onto Seahorse Bioscience XF24 islets culture microplates and kept at 37 °C incubator the day before experiment. A disposable sensor cartridge, embedded with 24 pairs of fluorescent biosensors (oxygen and pH), in Seahorse Bioscience XF assay kit was pre-calibrated the day before experiment. On the experiment day, cells at 100% confluence were incubated with KRB buffer containing low concentration glucose for 2×60 min at 37 °C before loading into a Seahorse Bioscience XF24 respiratory machine. Cells were then treated sequentially with low glucose (2 mM glucose), high glucose (16.7 mM final concentration), oligomycin (5 μM), 2,4-dinitrophenol (50 μM) and pyruvate (25 mM), and rotenone (5 μM) and myxothiazol (5 μM). Oxygen consumption within a transient micro chamber in each of the 24 wells created by the sensor cartridge was determined by a XF24 Extracellular Flux Analyzer (Seahorse Bioscience, Billerica, MA) as previously described [326, 327] to test the oxygen consumption rate of cells at rest level, glucose-stimulated oxygen consumption, maximum respiratory capacity, and proton leak-dependent respectively as Figure 2-1 shows. Mitochondrial respiration was calculated by subtracting extra-mitochondrial respiration values. Changes in respiration rates relative to resting respiration values were determined by

expressing the percent change in oxygen consumption rate relative to resting oxygen consumption rate.

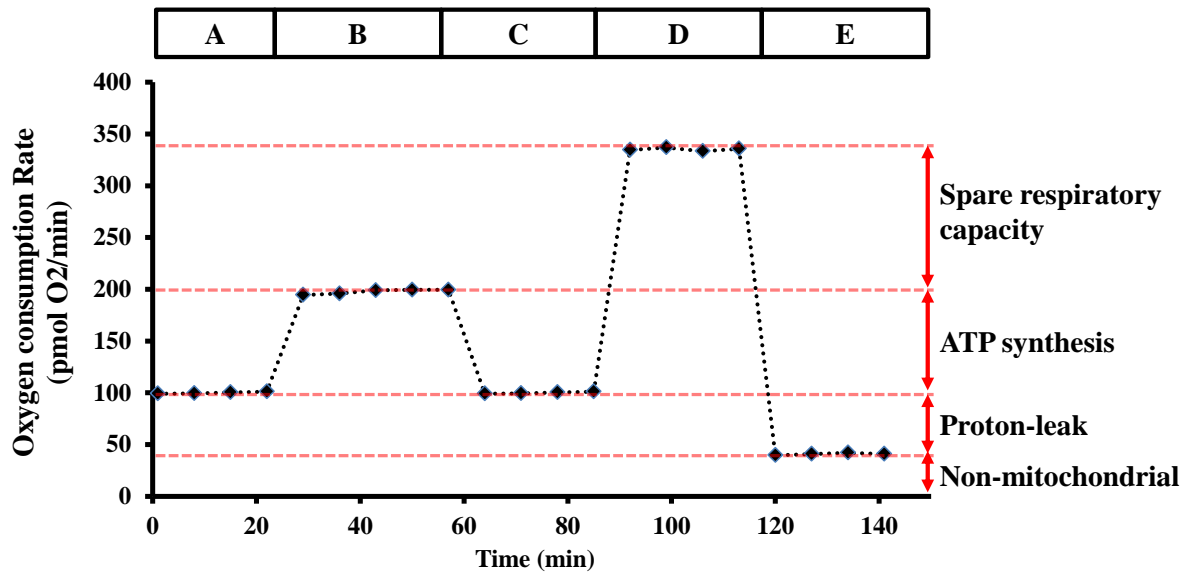


Figure 2-1 Schematic summary of oxygen consumption rate measurement

Cells pre-treated with low glucose for 2 hours were incubated sequentially with (A): low glucose (2 mM glucose), (B) high glucose (16.7 mM final concentration), (C) 5 μ M oligomycin, (D) 50 μ M 2,4-dinitrophenol and 25 mM pyruvate, and (E) 5 μ M rotenone and 5 μ M myxothiazol. Oxygen consumption rates were calculated for each period. Data used to indicate the activity of either spare respiratory capacity, or ATP synthesis, or proton-leak or non-mitochondrial oxygen consumption were derived from the difference of oxygen consumption rate between different periods as shown in figure.

2.2.6 Real time PCR

RNA isolation (Bio-Rad # 732-6820: AurumTM Total RNA mini kit), reverse transcription (Bio-Rad # 170-8891: iScript cDNA synthesis kit), and real time PCR (Bio-Rad #172-5200: SsoFastTM EvaGreen® Supermix) analysis were performed on cell extracts from 832/13 cells to determine the mRNA levels of target. Gene expression levels were corrected by cyclophilin E (Cyp) expression.

2.2.7 Western blot

Cellular proteins were extracted with cell lysis buffer (Cell Signaling #9803) containing 100 \times Protease Inhibitor Cocktail (Cell Signaling #5871). Extracts (40 μ g) were resolved on pre-cast

INVITROGEN NuPAGE® Novex® 10% Bis-Tris polyacrylamide gels (Invitrogen #NP0301BOX) and electro-transferred to INVITROGEN Invitrolon™ 0.45 µm PVDF Membrane (INVITROGEN #LC2005). A polyclonal antibody against HIF-1alpha (Santa Cruz) was used as the primary antibody followed by horseradish peroxidase-conjugated anti-rabbit antibody (SIGMA A6154) to detect HIF-1alpha. Similarly, γ -tubulin was detected by immunoblotting by a mouse antibody against γ -tubulin (SIGMA T6557) followed by horseradish peroxidase-conjugated anti-mouse antibody (Sigma A9917). Protein bands were detected with the Pierce™ ECL Western Blotting Substrate (Thermo Scientific 32106).

2.2.8 Transfection of siRNA duplex

siRNA duplexes were introduced into 832/13 cells at 50% confluence using Lipofectamine RNAiMax in compliance with the manufacturer's instructions (Invitrogen). Experiments were performed 72 h after duplex transfection.

2.2.9 Metabolites extraction and sample preparation

Metabolite levels were assessed by gas chromatography-mass spectrometry (GC-MS) as previously described [319, 320]. After the insulin secretion assay, the cells were washed once with ice-cold PBS, scraped off the plates followed by centrifugation at 3,500 rpm for 1 minute at 4 °C. The supernatant was discarded and the cell pellet was re-suspended in 100 µL water followed by sonicating for 60 seconds (~40 KHz, ~140 W). 1 mL of cold methanol was added and followed by another 5 minutes centrifugation at 13,300 rpm. The supernatant was mixed with 5 µL of 0.25 mg/ml myristic acid-d27 as an internal standard (IS; for retention time locking) followed by drying with nitrogen. Derivatization was then carried out in two steps: first, carbonyls were protected by methoximation using methoxyamine hydrochloride in pyridine at 50 °C for 30 minutes. Second, acidic groups were silylated with 90 µL N-methyl-N-(trimethylsilyl)-trifluoroacetamide (MSTFA) with 1% trimethylchlorosilane (TMCS) at 50 °C for 30 minutes. Both chemicals used for derivatization were from Sigma (St. Louis, MO).

2.2.10 Metabolites measurement

GC-MS was performed on an Agilent 7890A gas chromatograph coupled with a quadrupole mass spectrometer (5895C Agilent USA). 1 µL samples were injected in splitless mode using an Agilent auto sampler. The injector temperature was set at 250 °C. Chromatography was performed on a two of

15 m × 250 μm × 0.25 μm DB5-MS column with a phase thickness of 0.25 μm (J&W Scientific). The temperature program started isothermally at 50 °C for 5 min, followed by a temperature ramp of 10 °C/min to 300 °C where it was held for 10 min and run in backflush mode for another 15 min. The transfer line and ion source were both maintained at 250 °C. The ionization energy of electron ionization (EI) was set to 70 eV and the data acquisition rate was 20 Hz with a scanning range of 50–800 m/z. All samples were analyzed in a randomized order.

2.2.11 Metabolomic data analysis

Raw data files were exported to the Automated Mass Spectral Deconvolution and Identification System (AMDIS, Version 2.65) for smoothing, alignment and deconvolution of mass spectra. SpectConnect (<http://spectconnect.mit.edu/>) was used for spectra alignment. Target compounds were identified by matching both retention time and mass spectra in Fiehn GC-MS Metabolomics Retention Time Locking (RTL) Library (Version 2.0) or by only matching mass spectra in NIST library (2008). The GC/MS peak area is used as the abundance of metabolites and for further data analysis. Spectral data were normalized by the signal of internal standards (myristic acid d-27) and were exported to SIMCA P+ 12.0 software from Umetrics (San Jose, California). All metabolites variables were mean-centered, and UV-scaled. PCA was used to obtain an overview of the data and OPLS was used to relate the metabolic alterations to either the insulin secretion or other functions. In figures of metabolites profile, statistical significance was assessed by Student's t test or by one-way or two-way analysis of variance for repeated.

Chapter 3
Metabolomic Analysis of Pancreatic Beta Cell Insulin Release in
Response to Glucose

3.1 Overview

Defining the key metabolic pathways that are important for fuel-regulated insulin secretion is critical to providing a complete picture of how nutrients regulate insulin secretion. We have performed a detailed metabolomics study of the clonal beta cell line INS-1 832/13 using a gas chromatography-mass spectrometer (GC-MS) to investigate potential coupling factors that link metabolic pathways to insulin secretion. Mid-polar and polar metabolites, extracted from the INS-1 832/13 beta cells, were derivatized and then run on a GC-MS. 355 out of 527 chromatographic peaks were identified as metabolites by our metabolomic platform. These identified metabolites allowed us to perform a systematic analysis of key pathways involved in glucose-stimulated insulin secretion (GSIS). Of these metabolites, 41 were consistently identified as biomarkers for GSIS by orthogonal partial least-squares (OPLS). Most of the identified metabolites are from common metabolic pathways, including glycolysis, the sorbitol-aldose reductase pathway, the PPP, and the tricarboxylic acid cycle (TCA cycle), which suggests these pathways play an important role in GSIS. Lipids and related products were also shown to contribute to the clustering of high glucose sample groups. Amino acids lysine, tyrosine, alanine and serine were up-regulated by glucose whereas aspartate was down-regulated by glucose suggesting these amino acids might play a key role in GSIS. In summary, a coordinated signaling cascade elicited by glucose metabolism in pancreatic beta cells is revealed by our metabolomics platform providing a new conceptual framework for future research and/or drug discovery.

3.2 Introduction

As a key regulator of whole body metabolism, the hormone insulin is secreted by pancreatic beta cells as a response to an elevation in nutrients. Defective insulin secretion resulting from dysfunctional beta cells is a major determinant leading to the development of type 2 diabetes [328, 329]. Understanding how the beta cell secretes insulin is critical to developing novel therapies to treat type 2 diabetes.

A key metabolic pathway regulating insulin release involves an increase in the ATP/ADP ratio leading to an inhibition of ATP-sensitive K^+ (K_{ATP}) channels, plasma membrane depolarization, activation of voltage-gated Ca^{2+} channels, and influx of extracellular Ca^{2+} that leads to insulin granule exocytosis [109]. This pathway, often referred to as the K_{ATP} channel-dependent pathway or triggering pathway, is unable to fully explain the mechanism of GSIS. Studies over the last several

decades have suggested that there is an unknown coupling mechanism that may act independently of K_{ATP} channels (referred to as the K_{ATP} channel-independent pathway or amplifying pathway) [109, 330]. Strong evidence for the K_{ATP} channel-independent pathway(s) of GSIS has been provided by studies showing that glucose can still augment insulin secretion in islets from mice that lack functional K_{ATP} channels [60] or in conditions where the K_{ATP} channels are held open using diazoxide followed by membrane depolarization with high K^+ [56]. Some potential coupling factors that may act in a K_{ATP} channel-independent fashion include GTP [331-333], glutamate [94, 334, 335], malonylCoA/ long-chain acyl-CoA (LC-CoA) [336, 337], and NADPH [49, 80, 81, 338].

Most of these candidate coupling factors were discovered using enzyme based reactions that can only measure one metabolite at a time. However, metabolism itself is a complex network of interdependent chemical reactions catalyzed by highly regulated enzymes. Since beta cells rely on metabolism to regulate insulin secretion, it is likely that multiple interconnected metabolic pathways are involved in this process. The discovery of the currently proposed candidate coupling factors was mainly based on manipulation of one single gene or enzyme, which could lead to false-positive or false negative observations. In some instances this has been demonstrated with the publication of contradictory results for some of these proposed coupling factors [151, 157, 158, 161, 334, 337, 339].

Thus, the intrinsic disadvantage of the current traditional methods used to study beta cell metabolism requires a more comprehensive and powerful method for reliable reconstruction of the metabolic networks in beta cells in response to experimental perturbations. This goal was, at least partially, fulfilled by the appearance of metabolomic platforms that simultaneously profiles (identify and quantify) a large array of metabolites [340].

GC-MS based metabolomics is one of the most efficient metabolomics platforms because of the high separation efficiency to resolve the complex biological mixtures, comprehensive databases and the good reproducibility [340-342]. As an integrated part of systems biology, metabolomics has certain advantages over other “omics” technologies, since metabolites are the end products of cellular biological process and their level ultimately reflects the most integrated response of a biological system. The net effect of genomic (~25,000 genes), transcriptomic (~100,000 transcripts) and proteomics (~1,000,000 proteins) is reflected in the net changes in metabolite levels in cells [169]. Although the concept of metabolomics has been successfully applied in a number of studies including diabetes research [343], the analytical techniques used in untargeted metabolomics still require further development. There is still a need for improved metabolite extraction methods that gives a better

yield of the diverse chemicals found in cells, improved handling of the wide-ranging concentration of analytes, and improved data mining software to assess the “information-rich” data sets [344].

In our study, a robust GC-MS based metabolomics strategy was applied to a clonal beta cell line INS-1 832/13. An untargeted metabolomic analysis was performed to reveal critical metabolic pathways that could play a key role in beta cell stimulus secretion coupling. We show that glucose initiates a series of signaling cascades in beta cells and provide evidence for key up- and down-regulated pathways in beta cell metabolism.

3.3 Results

3.3.1 Insulin secretion

Insulin secretion was assessed after incubating cells with low glucose (LG, 2 mM) or high glucose (HG, 16.7 mM) for 2 hours. As Figure 3-1 shows, LG treated cells had an insulin output of 129 ± 5 μ U insulin/mL/mg protein and HG treated cells had an insulin output of 793 ± 80 μ U insulin/mL/mg protein. The fold increase in insulin output was 6.1 ± 0.6 .

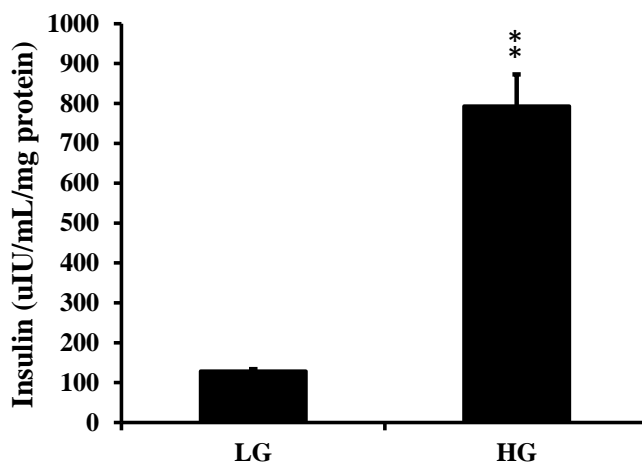


Figure 3-1 Glucose stimulated insulin secretion in INS-1 832/13 beta cells.

High glucose induced a six fold increase in insulin secretion. Cells were pre-incubated with 2 mM glucose for 2×1 hour followed by 2 hour incubation with either 2 mM or 16.7 mM glucose before KRB medium was removed for insulin assay. Insulin concentration was normalized by protein amount. Results represent mean \pm S.E. of three (n = 3) independent experiments for each condition. LG, low glucose (2 mM); HG, high glucose (16.7 mM). **, p<0.01 LG versus HG

3.3.2 Metabolite analysis by GC-MS

Cells treated with either LG or HG were harvested followed by metabolite extraction and then assessed using GC-MS (GC-Quadrupole MS in EI scan mode). A typical total ion chromatogram (TIC) from 832/13 beta cells is shown in Figure 3-2A for LG and Figure 3-2B for HG. Figure 3-2C shows the net difference of chromatogram between LG and HG samples (LG chromatogram subtracted from the HG chromatogram). Figure 3-2C demonstrates that some chromatographic peaks were positive (increased in abundance) and others were negative (decreased in abundance). For example, peaks for pyruvate, succinate, fumarate, malate, alpha-ketoglutarate, dihydroxyacetone phosphate (DHAP), (iso)citrate, palmitate, glucose-6-phosphate (G6P) and 6-phosphogluconate were all up regulated whereas aspartate was down-regulated in response to glucose.

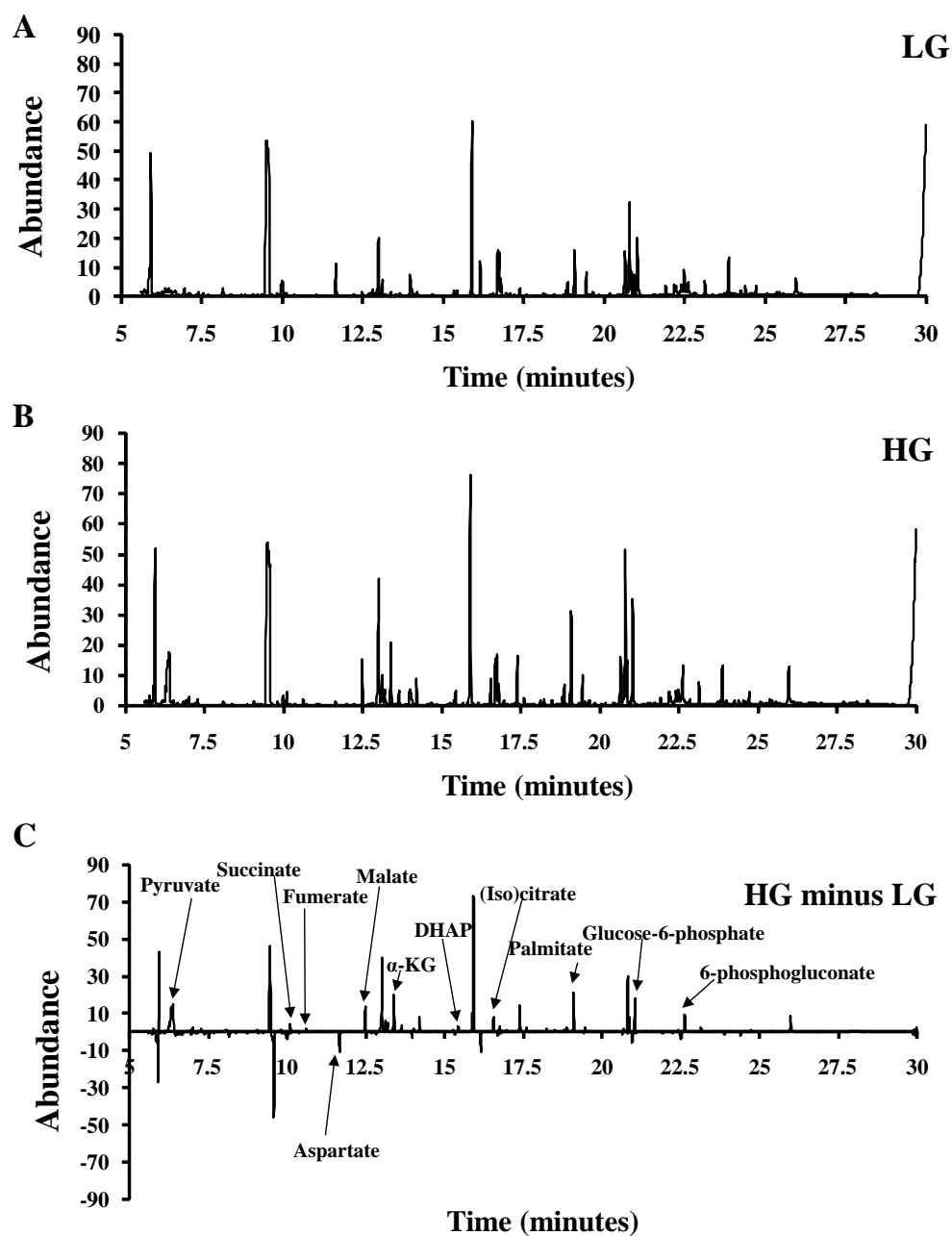


Figure 3-2 Representative total ion current chromatogram (TIC) of metabolites

The representative total ion current chromatogram (TIC) of metabolites isolated from (A) low glucose (LG) treated cells, (B) high glucose (HG) treated cells. (C) is (B)-(A) showing many metabolite levels are up-regulated by high glucose. Peaks showing metabolites of interested are

labeled in (C). Samples were run on GC/MS. GC gradient is running up to 30 min and retention time is depicted in minute.

3.3.3 Metabolites identification

Deconvolution of the data set by AMDIS identified 527 unique chromatographic peaks (putative metabolites) across all data sets. The Fiehn library identified 152 of the 527 peaks using retention time and mass spectra, and of these identified metabolites 101 were unique (51 of the identified peaks were from metabolites that had multiple derivatization products). The remaining 375 peaks were assessed using the NIST library resulting in the identification of an additional 302 metabolites. Of the 302 identified metabolites 254 were unique metabolites (48 of the identified peaks by NIST were from metabolites that had multiple derivatization products). The remaining 73 peaks could not be identified using either the Fiehn or NIST libraries.

3.3.4 Orthogonal projection to latent structures (OPLS) analysis

We constructed an OPLS model that accounts for metabolic variations related to high glucose treatment of our cells. The model generated only one predictive component (PC1) that describes 92% of the variations in the X and Y matrixes ($R^2X = 0.92$ and $R^2Y = 0.995$). The R^2X and R^2Y values are a measure of fit, i.e. how well the model fits the X data set. The model also had three orthogonal components ($R^2X_0 = 0.678$). A large R^2 (close to 1) indicates a good modeling, but it is not sufficient. The Q^2 value indicates how well the model (X) predicts new data (Y). A large Q^2 ($Q^2 > 0.5$) indicates a good predictability. The model had an acceptable predictability of 93.5% ($Q^2 = 0.935$). The orthogonal variation is likely composed of technical and biological variation not related to treating cells with either LG or HG.

The score plot (Figure 3-3A) and the loading plot (Figure 3-3B) provide an overview of the OPLS model. For our single-Y OPLS model (a model that contains only one predictive component), the score plot shows the first predictive component (PC1) vs. the first orthogonal component in X (Figure 3-2A, t_1 vs. t_0). The score plot shows clustering of the LG datasets and clustering of the HG datasets along $t[1]$. The loading plot (Figure 3-3B) illustrates which metabolites mainly account for the clustering seen in the score plot. In the loading plot, the metabolites positively (negative) furthest away from the origin of the coordinates along the first PC (X-axis) are considered biomarkers contributing most either positively (negatively) to GSIS.

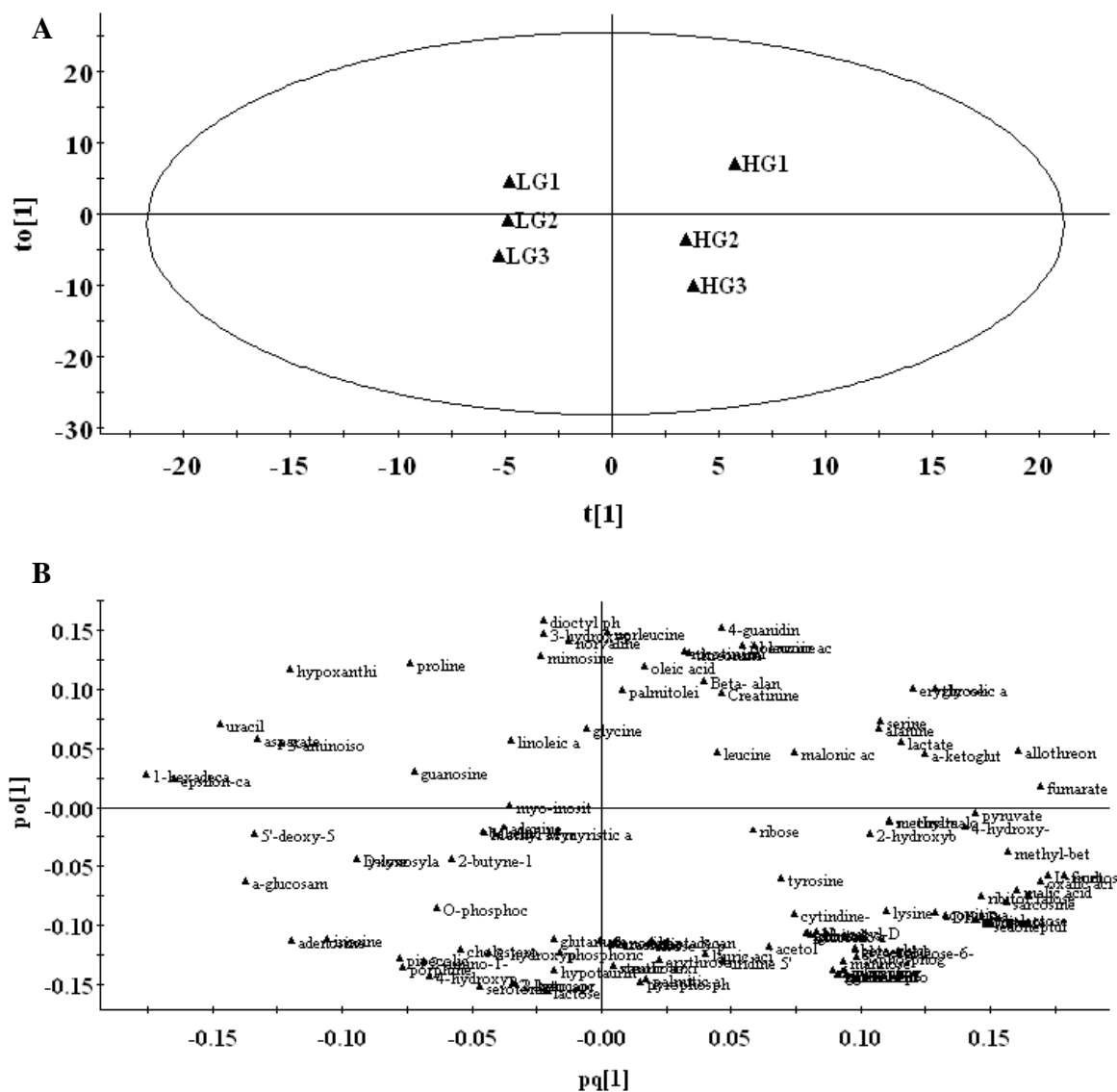


Figure 3-3 Score and loading plots generated by OPLS on identified metabolites.

(A) Score plot, ellipse is Hotelling T² (95% confidence interval). (B) Loading plot. One Y-predictive component and three orthogonal components were generated in this model. In score plot, samples were plotted against the score vector $t[1]$ and $to[1]$, and separated into two groups by $t[1]$, which are corresponding low glucose and high glucose treated cells. No outliers were identified. Likewise, loading plot showed the individual influence of all variables on new latent variables.

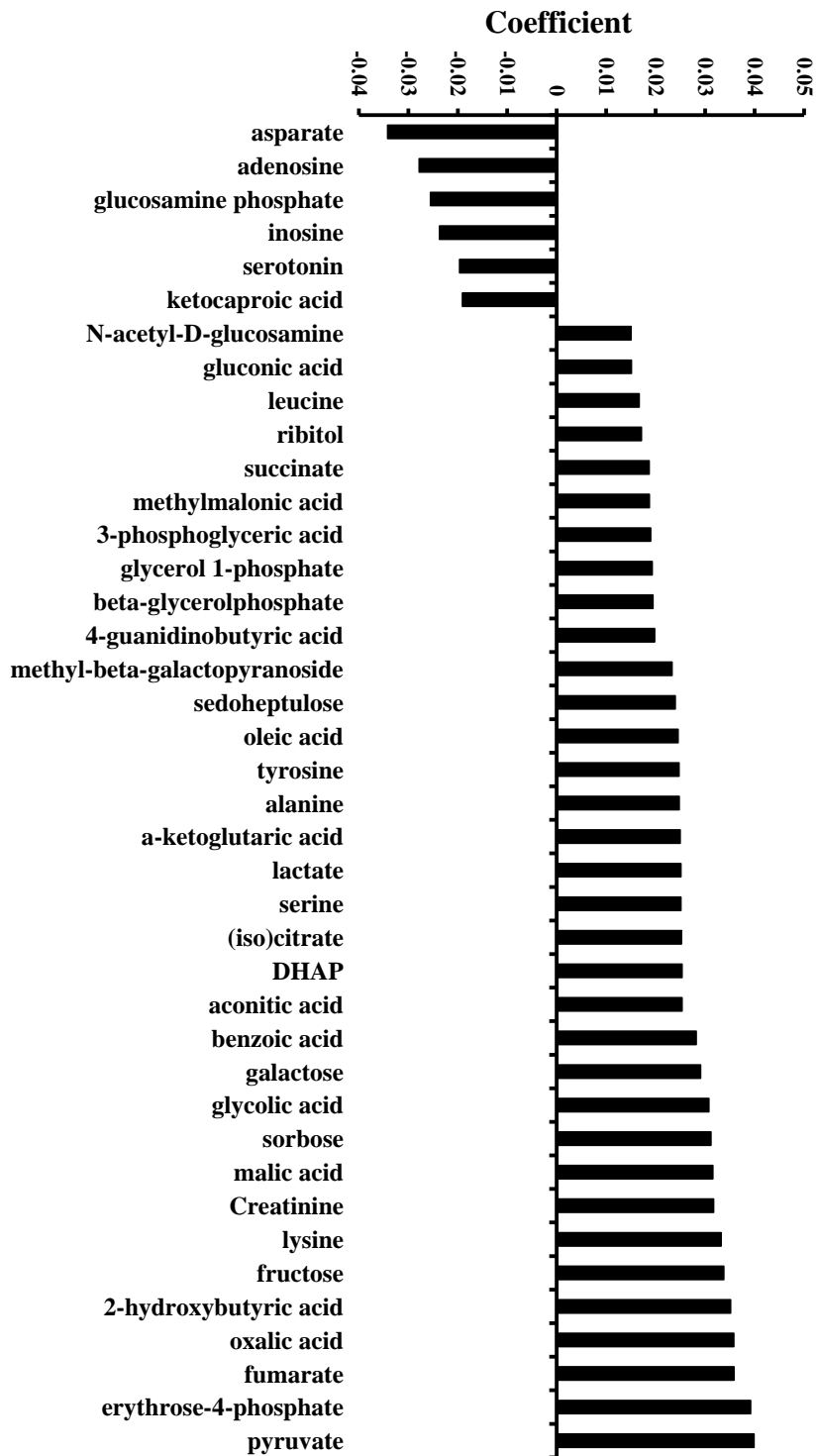


Figure 3-4 Regression coefficient plots of metabolites potentially coupling glucose metabolism to insulin secretion

The regression coefficients are used for interpreting the influence of the variables in the X-matrix (metabolites) on Y-matrix (insulin secretion) (n = 3). Metabolites that have high positive coefficient value are positively correlated to modeling. Analogous relationships hold for the items have significant negative coefficient value. Included are metabolites with coefficients that are either less than -0.015 or greater than 0.015.

Figures 3-4 showed the coefficient value of 41 metabolites suggested to probably play a significant role in differentiating the 832/13 cells cultured at 2.0 mM glucose from those in 16.7 mM glucose. Among them, 6 were negatively associated with GSIS and included aspartate, adenosine, alpha-D-glucosamine phosphate, inosine, serotonin and ketocaproic acid. The remaining 34 were positively associated with GSIS.

3.3.5 Metabolic pathway analysis

41 metabolites differentiated the response of the 832/13 cells cultured at LG from those cultured at HG (Figure 3-4). These metabolites belong to a number of metabolic pathways including glycolysis, TCA cycle, amino acid, fatty acid, PPP and sorbitol-aldose reductase pathway. The coefficient plot confirms that glycolytic intermediates play a critical role in the insulin secretion response of beta cells to glucose. Key glycolytic metabolites identified in the current set of data include G6P, DHAP, 3-phosphoglycerate and pyruvate (Figure 3-5).

Anaplerosis, which is a net increase in TCA cycle intermediates, has also been suggested to play a key role in the metabolic regulation of insulin secretion [80, 81, 345]. Key TCA cycle metabolites, including (iso)citrate, alpha-ketoglutarate, succinate, fumarate, malate and trans-aconitic acid, were identified in our OPLS model (Figure 3-6). Oxaloacetate and succinyl-CoA were not detected in our experiments. These TCA metabolites also contributed significantly to the clustering seen in INS-1 832/13 cells cultured at 16.7 mM glucose (Figure 3-3B).

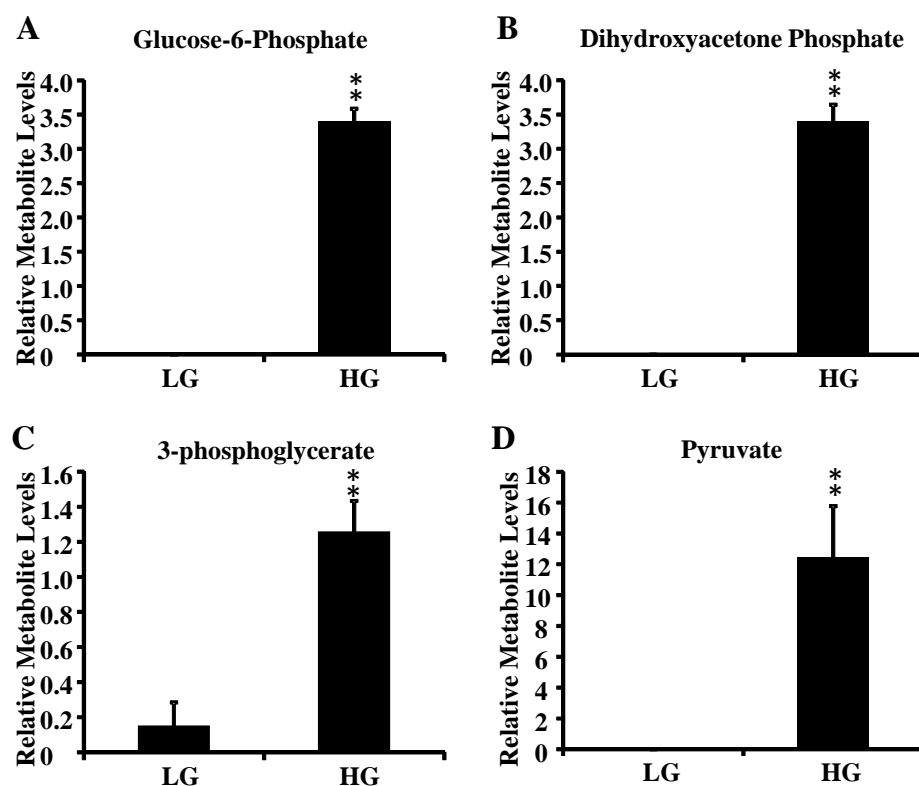


Figure 3-5 Glycolytic metabolite levels are up-regulated by glucose

Each biological sample has been pre-incubated with 2 mM glucose for 2×1 hr and then incubated with either 2 mM glucose (labeled as LG) or 16.7 mM glucose (labeled as HG). The metabolites levels were normalized by internal standards (Myristic acid D-27). Peak identification and retention time in minutes: A) Glucose-6-phosphate at 21.598 min B) Dihydroxyacetone phosphate at 15.6729 min C) 3-phosphoglycerate at 16.3969 min D) Pyruvate at 6.2946 min. Results represent mean ± S.E. of three (n = 3) independent experiments for each condition. **, $p < 0.01$ LG versus HG

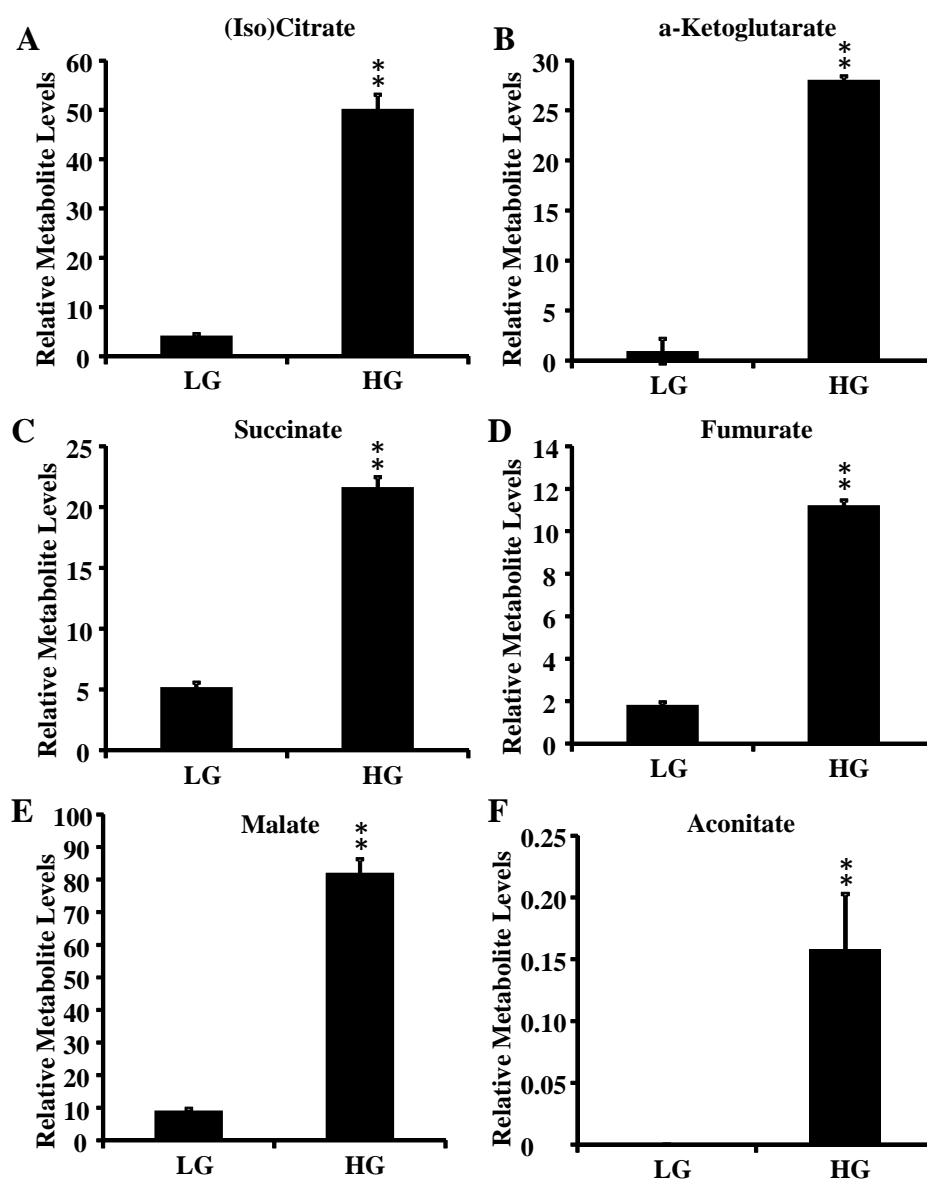


Figure 3-6 TCA metabolite levels are up-regulated by glucose

Each biological sample has been pre-incubated with 2 mM glucose for 2×1 hr and then incubated with either 2 mM glucose (labeled as LG) or 16.7 mM glucose (labeled as HG). The metabolites levels were normalized by internal standards (Myristic acid D-27). Peak identification and retention time in minutes: A) (Iso)citrate at 16.5566 min B) Alpha-ketoglutarate at 13.6546 min C) Succinate at 10.1176 min D) Fumurate at 10.6339 min E)

Malate at 12.4841 min F) Aconitate at 15.7555 min. Results represent mean \pm S.E. of three (n = 3) independent experiments for each condition. **, p<0.01 LG versus HG

Interestingly, other metabolites were also strongly associated with insulin secretion as seen in our OPLS model coefficient plot (Figure 3-4), such as, the sorbitol-aldose reductase pathway intermediates sorbitol, fructose, and the PPP intermediates 6-phosphogluconate, ribulose 5-phosphate, ribose-5-phosphate (Figure 3-7).

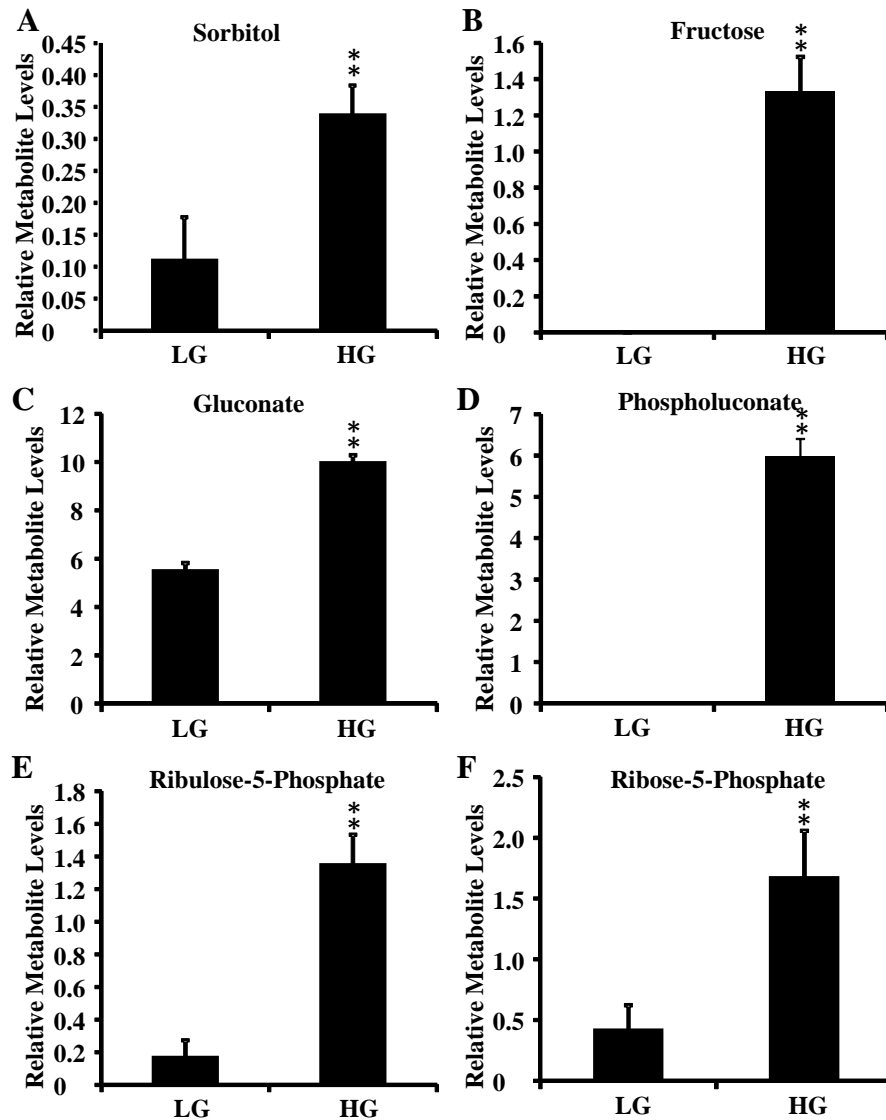


Figure 3-7 Aldose reductase and pentose phosphate pathway metabolites are up-regulated by glucose

Each biological sample has been pre-incubated with 2 mM glucose for 2×1 hr and then incubated with either 2 mM glucose (labeled as LG) or 16.7 mM glucose (labeled as HG). The metabolites levels were normalized by internal standards (Myristic acid D-27). Peak identification and retention time in minutes: A) Sorbitol at 17.8669 min B) Fructose at 17.2064 min C) Gluconate at 18.1216 min D) Phospholuconate at 22.5526 min E) Ribulose-5-phosphate at 19.6844 min F) Ribose-5-phosphate at 19.5758 min. Results represent mean ± S.E. of three (n = 3) independent experiments for each condition. **, p<0.01 LG versus HG

Intermediates associated with fatty acid metabolism were also identified in our coefficient plot including palmitic acid, oleic acid, palmitoleic acid, glycerol-1-phosphate (Figure 3-8).

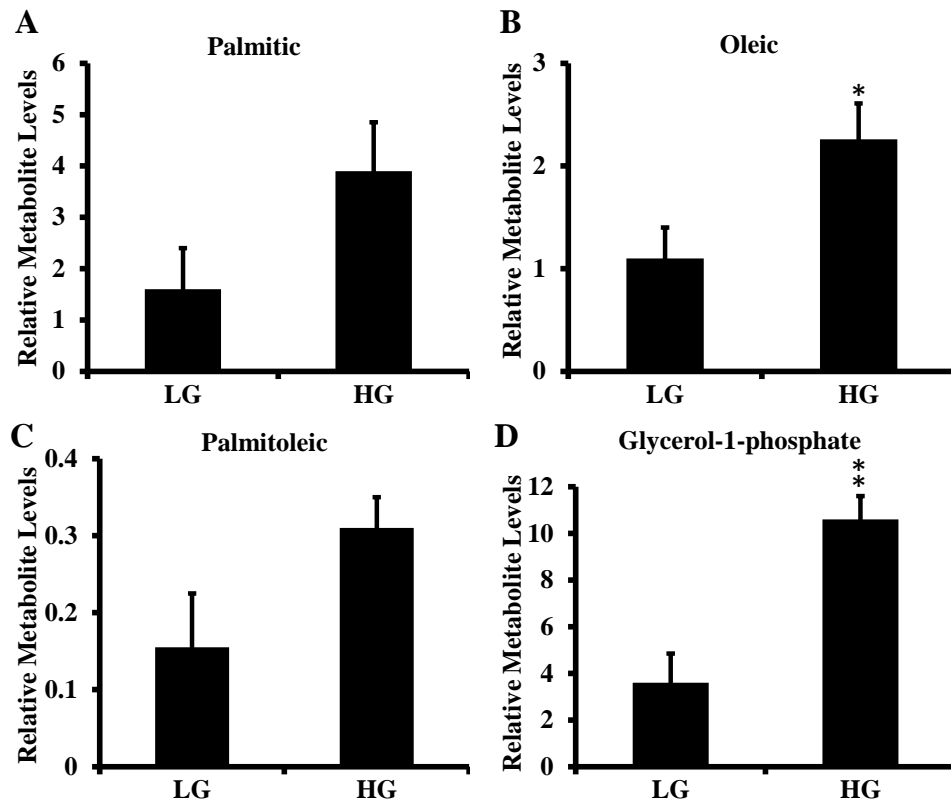


Figure 3-8 Fatty acids are up-regulated by high glucose

Each biological sample has been pre-incubated with 2 mM glucose for 2×1 hr and then incubated with either 2 mM glucose (labeled as LG) or 16.7 mM glucose (labeled as HG). The metabolites levels were normalized by internal standards (Myristic acid D-27). Peak identification and retention time in minutes: A) Palmitic acid at 19.08 min B) Oleic at 20.771

min C) Palmitoleic acid at 18.867 min D) Glycerol-1-phosphate at 15.431 min. Results represent mean \pm S.E. of three (n = 3) independent experiments for each condition. *, p<0.05; **, p<0.01 LG versus HG

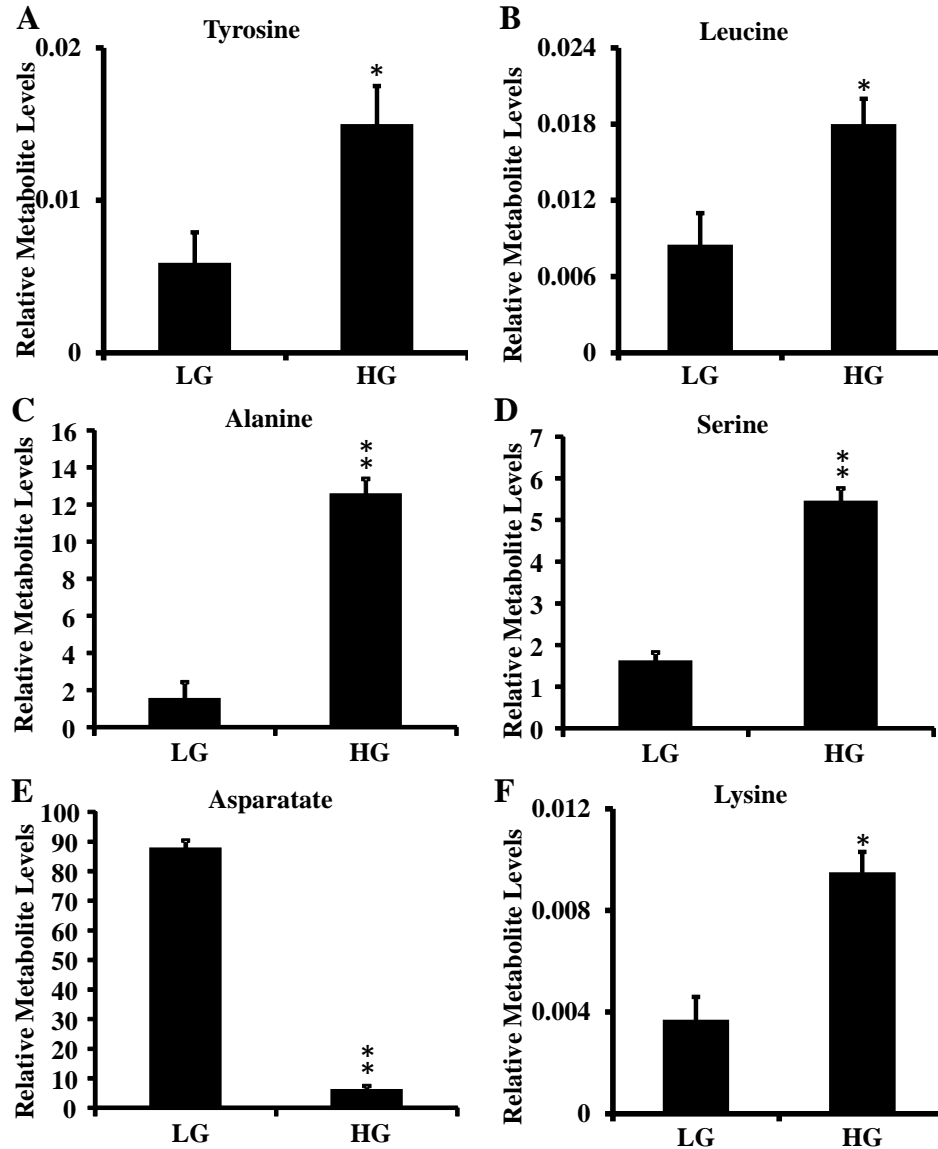


Figure 3-9 Amino acid metabolite levels are changed by high glucose

Each biological sample has been pre-incubated with 2 mM glucose for 2 \times 1 hr and then incubated with either 2 mM glucose (labeled as LG) or 16.7 mM glucose (labeled as HG). The metabolites levels were normalized by internal standards (Myristic acid D-27). Peak

identification and retention time in minutes: A) Tyrosine at 17.908 min B) Leucine at 7.81 min C) Alanine at 6.928 min D) Serine at 9.278 min E) Aspartate at 11.643 min F) Lysine at 17.712 min. Results represent mean \pm S.E. of three (n = 3) independent experiments for each condition. *, p<0.05; **, p<0.01 LG versus HG

Amino acids leucine, lysine, tyrosine, alanine and serine were positively associated with clustering the INS-1 832/13 cell response to 16.7 mM glucose (Figure 3-9). On other hand, aspartate was the most negatively associated metabolite contributing to clustering of the response of INS-1 832/13 cells to 16.7 mM glucose (Figure 3-9). The metabolic pathways that has been shown to be associated with GSIS as our OPLS model suggested was summarized in Figure 3-10.

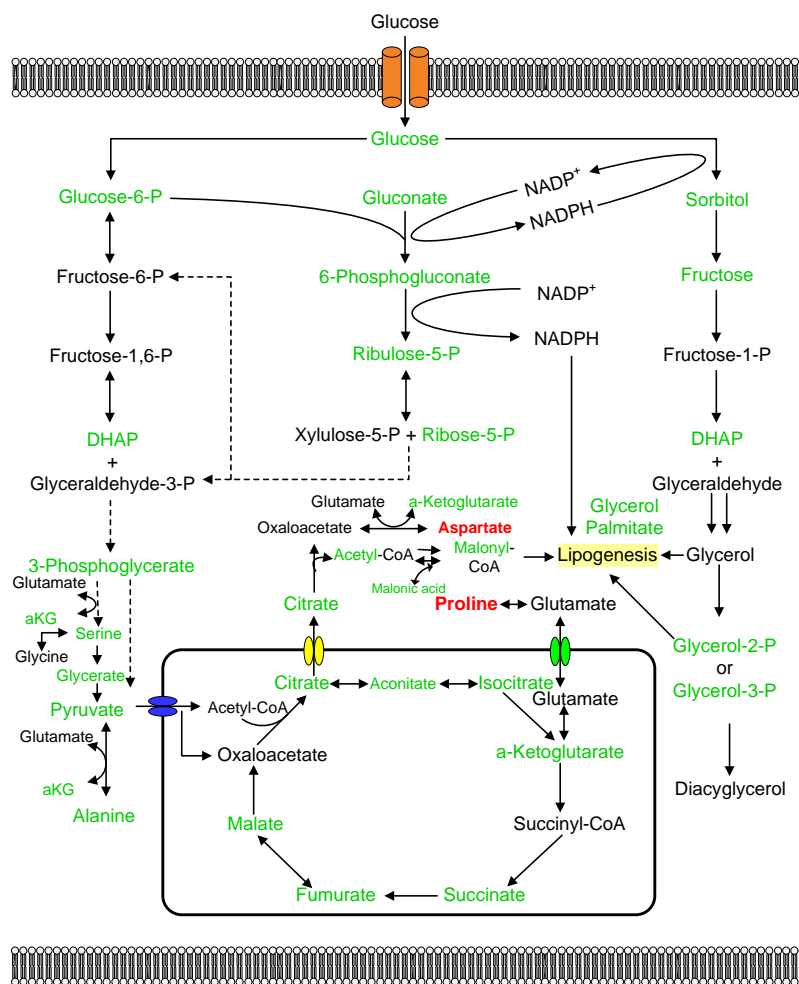


Figure 3-10 Metabolic signals identified by MVA to be correlated to insulin secretion

Metabolites with coefficient value (> 0.015) are highlighted in green and are suggested by OPLS model to be positively correlated with glucose-stimulated insulin secretion. Metabolites with

coefficient value (< 0.015) are highlighted in red and are suggested by OPLS model to be negatively correlated with glucose-stimulated insulin secretion. DHAP: dihydroxyacetone phosphate. Glycerol-2-P: glycerol-2-phosphate

3.3.6 Role of the PPP and sorbitol-aldose reductase pathway in regulation of insulin secretion

Although the role of the PPP and sorbitol-aldose reductase pathway in insulin secretion is controversial [150, 346-349], metabolites involved in these two pathways are suggested to be positively associated to GSIS by our data. In order to assess the significance of flux through the PPP, the effects of pharmaceutical inhibitors and siRNA mediated knock-down are further tested.

Two siRNAs against glucose-6-phosphate dehydrogenase (G6PDH), the first enzyme believed to be the rate-limiting step in the PPP, were used to assess the role of this enzyme in GSIS. The first siRNA (siG6PDH-1) and second siRNA (siG6PDH-2) both knockdown G6PDH mRNA by $60 \pm 5\%$ and $62 \pm 6\%$ respectively (Figure 3-11A), however neither siRNA affected GSIS (Figure 3-11B).

It is possible that blocking flux to both of these pathways may also affect insulin secretion so we next tried pharmaceutical inhibitors. 6-aminonicotinamide (6-AN), an inhibitor of the NADP⁺-dependent enzyme, 6-phosphogluconate dehydrogenase [350], and 2,5-Dihydro-4-hydroxy-5-oxo-1-(phenylmethyl)-1H-pyrrole-3-carboxylic acid ethyl ester (EBPC), a specific inhibitor of the sorbitol-aldose reductase pathway enzyme aldose reductase, were also used to inhibit the PPP. As compared to no treatment control or DMSO vehicle control, neither 6-AN, nor EBPC or even their combination had effect on GSIS in INS-1 832/13 cell line (Figure 3-11C). Different dosage and their combination had no effect on GSIS (data not shown). However, both 6-AN and EBPC increase insulin secretion in human (Figure 3-11D) and rat (Figure 3-11E) islets by more than 20 percent. More interestingly, insulin stimulated by the combination of 6-AN and EBPC was enhanced by one fold in human islets (Figure 3-11D) and 50 percent in rat islets (Figure 3-11E).

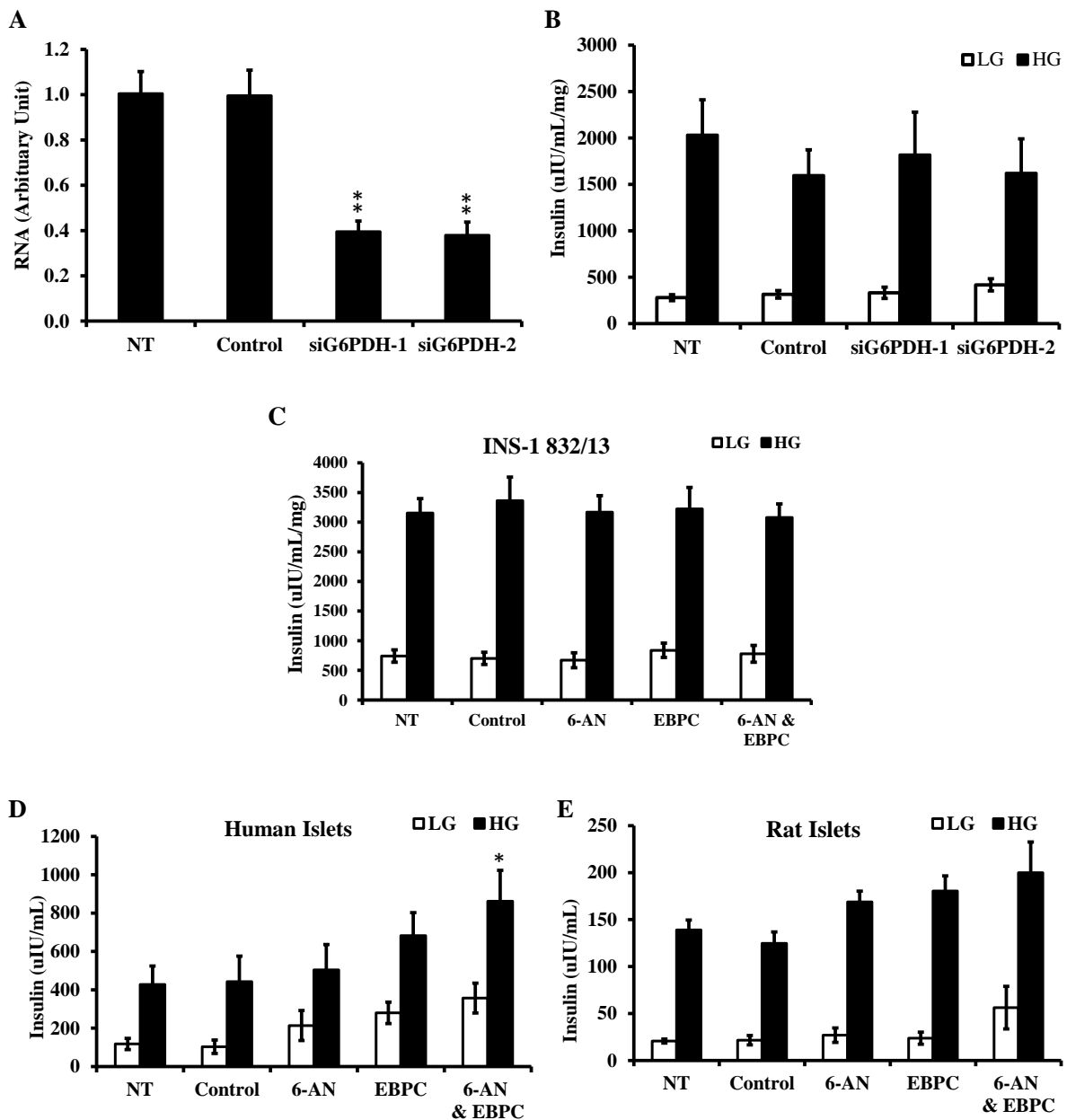


Figure 3-11 Role of the pentose phosphate and sorbitol-aldose reductase pathway in GSIS.

(A) Gene expression of cells treated with two siRNAs (siG6PDH-1 and siG6PDH-2) directed against G6PDH (n = 5) for 72 hr. Both siRNAs duplexes decrease G6PDH RNA by 60 percent. (B) Effects of the two siRNAs against G6PDH on GSIS (n = 5). Neither siRNA duplex affects GSIS. (C) Effects of pentose phosphate inhibitor 6-AN (500 μ M), aldose reductase inhibitor EBPC (50 μ M), or a combination of 6-AN and EBPC on GSIS in INS-1 832/13 cell line (n = 5).

Neither of inhibitors nor their combination affects GSIS in INS-1 832/13 cells. Effects of pentose phosphate inhibitor 6-AN (500 μ M), aldose reductase inhibitor EBPC (50 μ M), or a combination of 6-AN and EBPC on GSIS in (D) human islets (n = 8) and (E) rat islets (n = 7). Both inhibitors and their combination increase GSIS in human and rat islets. Cells were treated with 6-AN and EBPC during the insulin secretion assay. Low glucose (LG), High glucose (HG). *, p<0.05; **, p<0.01 non-treated versus treated.

3.4 Discussion

Although GSIS has been extensively studied, the biochemical pathways linked to insulin secretion have not been completely defined. In our study, an unbiased GC-MS based untargeted metabolomics approach was applied to INS-1 832/13 cells in order to gain insight into the metabolic regulation of insulin secretion. Overall, 527 chromatographic peaks (or potential metabolites) were detected of which 355 were identified as unique metabolites. Limiting the identification of unique metabolites from the 527 chromatographic peaks was partly due to the fact that some metabolites had multiple active functional groups that could be modified during the derivatization process. Using a combination of two libraries, the Fiehn library which identifies endogenous metabolites and the NIST library which identifies endogenous and exogenous metabolites, led to the identification of 355 unique metabolites. The number of identified metabolites is larger than other studies of beta cells using similar techniques [333, 343, 351]. The most significant metabolites that differentiated low glucose treated cells from those treated with 16.7 mM glucose were identified by supervised pattern recognition using OPLS. Less than 8% of the information is lost during the analysis and there was only one principal component. Our OPLS model forms a good summary of the data set and has good predictability. Among all the metabolites detected by our system, 41 metabolites were found to be strongly associated with the metabolic response of cells to high glucose using our OPLS model.

The unique metabolic phenotype of beta cells allows these cells to sense blood glucose levels. This is formed partly from the expression of a combination of glucose transporter 2 (high K_m glucose transporter) and glucose phosphorylating enzyme glucokinase (hexokinase IV, GK) [352]. Glucose transporter 2 and glucokinase allow for a continuous flux of glucose carbon to enter glycolysis in a dose dependent manner. Glycolysis is the first key step in glucose sensing and it has been suggested that signals derived from glycolysis play a role in insulin secretion [49, 353]. As expected glycolytic intermediates, including G6P, dihydroxyacetone phosphate, 3-phosphoglycerate and pyruvate, were

elevated in response to treating cells with 16.7 mM glucose and these glycolytic metabolites were strongly associated with GSIS in our OPLS model.

In addition to increased glycolytic flux, several other cytosolic pathways were also shown to be associated with GSIS in our OPLS model. These pathways include the PPP, represented by 6-phosphogluconate, ribulose-5-phosphate, ribose-5-phosphate, and the sorbitol-aldose reductase pathway (also known as the polyol pathway), represented by sorbitol and fructose in our metabolomics study. A key role for NADPH in regulating insulin release has been suggested (reviewed in refs [35, 49]) and the PPP is one pathway that may produce NADPH for modulating insulin secretion. The PPP plays a role in providing NADPH, ribose-5-phosphate for synthesis of nucleotides and nucleic acids, and erythrose-4-phosphate for synthesis of aromatic amino acids. The role of the PPP in insulin release is still being debated [150, 346-349]. The contribution of the PPP to total glucose utilization has been shown to be low in beta cells [33, 76, 354]. Also, the oxidative portion of the PPP contributes a relatively small amount of the total glucose oxidation rate [33]. It has been suggested that part of the reason for the low PPP activity in beta cells may be because of the glucose-stimulated increase in the cytosolic NADPH/NADP⁺ ratio [80, 84] which is thought to inhibit G6PDH (the flux-generating enzyme of the PPP) [355]. Since the activity of the PPP is low, it has been suggested that it contributes very little to the overall generation of NADPH [67] as compared to other NADPH producing pathways such as the pyruvate cycling pathways [35, 49]. However, the overall contribution of this pathway to NADPH production has not yet been directly studied. Interestingly, other studies have suggested that the PPP activity is dependent on glucose concentration and its enzyme transaldolase might be activated by glucose [286]. A recent paper has performed metabolomic studies on first phase insulin secretion in the INS-1 832/13 cells [148]. They focused on metabolites that changed in the first 15 minutes after the addition of high glucose. They also found that PPP intermediates were associated with insulin secretion.

Intravenous (IVGTT) and oral glucose tolerance tests (OGTT) in patients with G6PDH deficiency showed that first phase insulin release was defective in these individuals [356]. Also more recently it has been shown that inhibition of G6PDH with siRNAs led to increased ROS, apoptosis, decreased proliferation, and impaired insulin secretion [349]. The impaired GSIS associated with long-term high glucose treatment of cells could be improved by overexpressing G6PDH [349]. G6PDH deficient mice had smaller islets and impaired glucose tolerance which suggests an important role for the PPP in beta cells [349]. Since our OPLS model also suggests that metabolites involved in PPP were

associated with GSIS and this is consistent with previously published studies [343], we performed further studies on the role of this pathway. Although the pharmaceutical inhibitor 6-AN affects GSIS in human islets, neither 6-AN changes insulin secretion in rat islets nor siRNAs against G6PDH alters the secretion function of INS-1 832/13 cells. Several reasons might contribute to this seemingly contradictory result. First, it could result from either the different permeability that different biological structures possess, or the physiological difference between species. The PPP activity in human islets was observed to be different from that in rat islets [149]. Second, it might be caused by the presence and absence of insulin in medium. The PPP seems to contribute to secretory activity only if insulin is not accumulated in medium [348]. Last, the way how inhibitors were applied to cells might also play a certain role, because 6-AN was reported to disturb insulin secretion in pancreatic rat islets if they are pre-treated with this pharmaceutical inhibitor for six hours [150]. But in our experiment, 6-AN was not included for pre-treatment. Overall, the exact role of PPP in regulation of insulin secretion still needs further investigation.

The sorbitol-aldose reductase pathway contributes only a small fraction to the total glucose utilization (both PPP and sorbitol-aldose reductase pathways do not exceed 10% of the overall glucose utilization [33]). Interestingly, the sorbitol-aldose reductase pathway enzyme, aldose reductase, which has a high K_m value for glucose (20-200 mM) [357, 358] can be stimulated by ATP and inhibited by ADP by about $\pm 20\%$ over the physiological concentration range of these nucleotides [358]. Another sorbitol-aldose reductase pathway enzyme, sorbitol dehydrogenase activity is also favored by high glucose usually accompanied by lower NADH levels [169, 359]. Treating cells with high glucose likely stimulates the sorbitol-aldose reductase pathway since glucose stimulates an increase in the $NAD^+/NADH$ ratio in beta cells. The sorbitol-aldose reductase pathway has been shown to play a role in GSIS in some studies [360] and not in others [361, 362]. In one study, inhibitors of aldehyde and aldose reductases were shown not to inhibit GSIS or glucose metabolism in islets [361]. Overexpression of aldose reductase lead to a reduction of the $NADPH/NADP^+$ ratio and this was associated with beta cell apoptosis [363]. In line with the above discussed evidence, our studies also suggest that this pathway is up-regulated in response to glucose in beta cells. However, it is unlikely this increase is relevant to insulin secretion since a specific inhibitor of aldose reductase does not inhibit GSIS.

To date, the PPP and sorbitol-aldose reductase pathways have only been studied individually, even though there may be potential for cross-talk between these two pathways. The sorbitol-aldose

reductase pathway oxidizes NADPH whereas the PPP reduces NADPH which may allow both pathways to facilitate each other's activity through the cyclic use of NADPH. In addition, increased sorbitol-aldose reductase pathway activity could provide fructose for glycosylation and glycerol production which has been suggested to be important for GSIS [345, 364]. On one hand, if PPP supports GSIS by generating reducing equivalents, in the form of NADPH, or providing other precursor, like ribose-5-phosphate (R5P), for the synthesis of nucleotides and nucleic acids, inhibition of PPP could potentially lead to the decrease of GSIS. On the other hand, since there is significant glucose flux into these pathways, inhibition of both the PPP and the sorbitol-aldose reductase pathway may promote greater glucose flux through glycolysis and increase insulin secretion. Interestingly, we show that using inhibitors of both pathways does not inhibit insulin secretion in INS-1 832/13 cells, but did improve GSIS in both human and rat islets. The discrepancy between cell line and islets, as well as the exact role of PPP and sorbitol-aldose reductase pathways in regulation of GSIS remains to be elucidated.

The role of lipids in GSIS is controversial. Numerous studies suggesting that glucose-stimulated lipid synthesis plays a role in insulin secretion [336, 365, 366] whereas other studies provide evidence against this hypothesis [160, 161, 321, 367, 368]. Most researchers in the area agree that intracellular levels of citrate, malonyl-CoA, palmitate and LC-CoA's rise rapidly in beta cells exposed to elevated glucose concentrations. This evidence led to the proposed malonyl-CoA/LC-CoA hypothesis that states that PC mediated replenishment of oxaloacetate in the TCA cycle facilitates the accumulation and escape of citrate from the mitochondrial matrix into the cytosol for lipid synthesis. The role of lipids in GSIS is supported by our data showing that the levels of palmitic acid, oleic acid, palmitoleic acid and lauric acid are elevated by treating cells with 16.7 mM glucose and were also identified by our OPLS model as significant metabolites contributing to the clustering of high glucose treated cells.

Amino acids, leucine, lysine, tyrosine, alanine and serine were also shown to contribute significantly to the clustering of high glucose treated cells in our OPLS model of insulin secretion. The significance of these amino acids in insulin secretion may be only to provide sufficient resources for insulin biosynthesis. However, it is also possible that they could be directly involved in regulating insulin release. Leucine is a known activator of glutamate dehydrogenase (GDH) [369] and an increased GDH activity has been suggested to play a key role in GSIS [370]. The elevated leucine levels seen in our studies provide further support for this role. One commonly mentioned amino acid associated with GSIS is glutamate. Glutamate was originally proposed as a potential coupling factor

linking glucose metabolism to insulin secretion [334]; however, this effect is controversial [339]. In our study glutamate was not a significant player in our OPLS model and in fact was negatively associated with insulin release. Less is known about the roles that alanine and serine play in GSIS. But our OPLS model suggests there may be a link. Interestingly, a role of these amino acids is supported by in vivo studies showing that alanine and serine induced a strong enhancement of insulin secretion as compared to other amino acids [371].

The most significantly reduced metabolite by high glucose treatment was the amino acid aspartate, which is consistent with previous studies [343, 347, 372]. Aspartate can be transaminated to glutamate by aspartate aminotransaminase. Aspartate aminotransferase plays a role in the malate-aspartate shuttle which shuttles NADH from the cytosol into the mitochondrial matrix and is a key player in the regeneration NAD⁺ for maintaining flux through glycolysis. High glucose treatment of beta cells may reduce aspartate levels in part due to the higher demand on the malate-aspartate shuttle enzyme aspartate transaminase. Interestingly, the glycerol-phosphate shuttle metabolite dihydroxyacetone phosphate was also positively associated with GSIS in our OPLS model.

Glycolysis-derived pyruvate enters the TCA cycle via one of two pathways, one involving pyruvate dehydrogenase (PDH) and the other involving PC. Pyruvate entering via PDH is oxidized to CO₂ generating NADH and FADH₂ for ATP synthesis and pyruvate entering via PC is involved in net accumulation of TCA intermediates (anaplerosis) [33, 74, 75, 77]. All TCA intermediates were positively associated with insulin secretion in our OPLS model. Citrate/isocitrate, alpha-ketoglutarate, succinate, fumarate and malate were elevated by high glucose treatment of cells. The replenishment of TCA intermediates (PC mediated anaplerosis) appears to be of critical importance for beta cell glucose competence as ¹³C-NMR isotopomer analysis revealed that glucose responsiveness was more stringently associated to anaplerotic substrate flow as opposed to oxidative substrate flux [76]. Efficient knockdown of PC activity (by 50% or more) renders clonal beta cells and primary rat islets in a glucose unresponsive state without any changes in the glucose oxidation rate. Interestingly, PC activity was also reported to be reduced by at least 70% in human islets obtained from type 2 diabetics [72].

The intrinsic disadvantage of the current traditional methods used to study beta cell metabolism requires a more comprehensive and powerful technology for reliable reconstruction of the metabolic networks in beta cells in response to experimental perturbations. In our metabolomics study, a potential limitation is the work uses the clonal cell line, 832/13 cells, in contrast to isolated islets. As

an insulinoma cell line, INS 832/13 should have some specific metabolic activity like any other immortalized tumor cell does, such as cellular replication, which might mislead researchers by obscuring the real metabolic pathways involved in GSIS. To address this issue, further efforts will be made to upgrade our metabolomics study to animal or human pancreatic islets and results observed here will be compared to those seen in primary islets. However, the advantage of using the 832/13 cells is that it is a homogenous preparation of beta cells as compared to islet preparations and obtaining sufficient number of cells is relatively easy. One of the key limitations of the metabolic platforms is the detection of low abundance metabolites and we feel that the current methodology presented here improves upon this and provides an important step towards making it easier to use isolated islets in metabolomics studies. However, there is still a need for improved metabolite extraction methods that gives a better yield of the diverse chemicals found in cells, improved handling of the wide-ranging concentration of analytes, and improved data mining software to assess the “information-rich” data sets [344].

3.5 Conclusion

Glucose metabolism plays multiple roles in the regulation of insulin secretion from beta cells. Most of the literature focuses on the role of glycolysis, ATP/ADP ratio, TCA cycle and anaplerosis in insulin secretion. However, other pathways may also be critical. For example, although it has been previously under-estimated in the past, our study suggests that the sorbitol-aldose reductase pathway and PPP might play an important role in beta cell stimulus-secretion coupling. There appears to be a coordinated effort in beta cells to increase the activity of a number of metabolic pathways in response to glucose; however, which pathways are critical for insulin secretion still needs to be investigated. The current metabolomics approach presented in this study allows one to assess the effects of perturbations to beta cell metabolism on most of the key metabolic pathways in a single assay. It is important to have broad assessment of these pathways in response to manipulating metabolic enzymes because of the complex metabolic interconnectivity seen in these cells. This integrating paradigm will provide a new conceptual framework for future research and drug discovery.

Chapter 4

Assessment of the Metabolic Pathways Associated with the Second Phase Glucose-Stimulated Insulin Secretion

4.1 Overview

Biphasic glucose-stimulated insulin secretion (GSIS) involves a rapid first phase followed by a prolonged second phase of insulin secretion. The biochemical signaling pathways that control these two phases of insulin secretion are poorly defined. In this study, we used a gas chromatography mass spectroscopy (GC-MS) based metabolomics approach to perform a global analysis of cellular metabolism during biphasic insulin secretion. A time course metabolomic analysis of the clonal beta cell line INS-1 832/13 cells showed that the second phase insulin secretion was negatively associated with hydroxyproline, proline, aspartate, glycine and lactate, and positively with both glycolysis (glucose-6-phosphate and dihydroxyacetone phosphate) and TCA cycle intermediates. Inhibition of TCA activity by UK5099, an inhibitor of the pyruvate carrier, selectively decreased second phase insulin secretion by 50 percent without altering the first phase insulin secretion in freshly isolated rat pancreatic islets. Our data suggest glycolysis derived anaplerosis via pyruvate carboxylase (PC) plays a central role in modulating the second phase insulin secretion. Overall, the insights provided by our study create a framework for planning future studies in the assessment of the metabolic regulation of biphasic insulin secretion.

4.2 Introduction

In vivo insulin secretion is biphasic, with a first-phase burst in insulin secretion occurring within the first 10 minutes after a glucose load and a subsequent second phase. The second-phase of insulin secretion may either reach plateau very quickly, as seen in mice, or show a progressively slow increase in insulin release reaching a plateau in next 2-3 hours, as seen in rats and humans [373]. Healthy human subjects have a biphasic insulin secretory response *in vivo* similar to that observed in perfused rat pancreas [374, 375], whereas isolated perfused human islets have a similar biphasic insulin response similar to that of perfused mouse islets [376-378].

The biphasic nature of insulin secretion seems to be critical for the regulation of postprandial glucose homeostasis. A role for the first phase insulin secretion is supported by studies from both dogs [125, 126] and humans [110] showing that it likely plays a role in the regulation of postprandial glucose homeostasis by acting on the liver to inhibit endogenous glucose production [127]. In contrast, the second phase insulin release may play a role in inhibiting liver glucose production as well as promoting muscle glucose uptake and utilization [127]. Of these two functions of the second phase

insulin secretion, it has been suggested that the role in promoting muscle glucose uptake is more critical.

Defects in both phases of insulin secretion, especially the first phase, may be the earliest detectable sign in individuals destined to develop type 2 diabetes [373]. Pre-type 2 diabetics have selective impaired first phase insulin secretion and this has been suggested to be an early warning of beta cell dysfunction [127, 128, 373]. However, how this defect occurs is unknown and in fact the biochemical mechanisms that control biphasic insulin secretion are still incompletely understood.

The critical metabolic pathways that regulate biphasic insulin secretion are not known. One key glucose-derived signal in beta cells is a rise in the ATP:ADP ratio, which stimulates closure of ATP-sensitive K^+ (K_{ATP}) channels, resulting in plasma membrane depolarization, activation of voltage-gated Ca^{2+} channels (VDCC) and Ca^{2+} -mediated stimulation of insulin granule exocytosis [379, 380]. This so-called “ K_{ATP} channel-dependent” mechanism appears to be particularly important in triggering exocytosis of a small number of granules from a plasma membrane-docked “readily releasable pool (RRP)” responsible for the first, acute phase of insulin release [65]. The RRP might also be implicated in control of the first phase insulin secretion as a recent study showed [148].

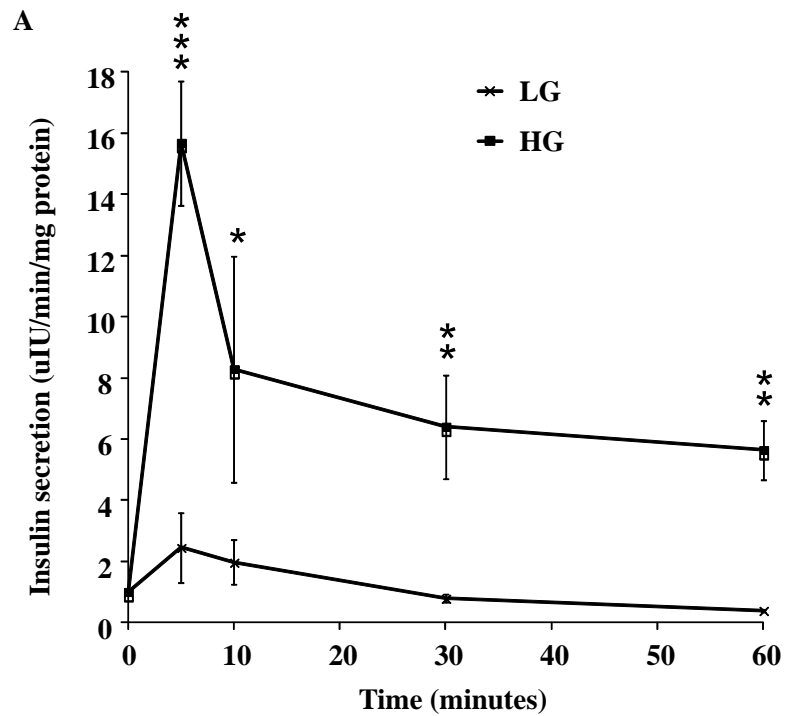
In contrast, in the second and sustained phase of insulin secretion, ATP and Ca^{2+} may play only limited or permissive roles, allowing other glucose-derived second messengers to come to the forefront [49]. Support for the “ K_{ATP} channel-independent pathway” of beta cell glucose signaling comes from studies showing that glucose causes a significant increase in insulin secretion even when K_{ATP} channels are held open by application of diazoxide followed by membrane depolarization with high K^+ , or in animals in which the sulfonylurea receptor-1 (SUR1) K^+ channel (a subunit of the K_{ATP} channel) was knocked out [58, 60, 64]. These and more recent studies suggest that mitochondrial metabolism of glucose generates signals, in addition to the changes in ATP:ADP ratio, that are important for the control of insulin secretion [49, 76, 81, 84, 321, 337, 381].

Since there is a lack of comprehensive data sets describing the metabolic activity of beta cells during the second phase insulin secretion, we used a metabolomics approach to gain more insight into how metabolic pathways integrate with the second phase insulin secretion. We developed an OPLS model [282, 286] to identify that key metabolites are strongly associated with the second phase insulin secretion. Our study shows that TCA intermediates seem to be the dominant modulator of the second phase insulin release.

4.3 Results

4.3.1 Dynamic insulin secretion in INS-1 832/13 cells

Dynamic insulin secretion was assessed after incubating the insulin secreting INS-1 832/13 cells with low glucose (LG, 2 mM) or high glucose (HG, 16.7 mM) for 0, 5, 10, 30 and 60 minutes. Insulin secretion in Figure 4-1 was expressed as the rate of insulin release, which was first normalized for protein concentration followed by subtracting the amount of insulin released at the previous time point and finally corrected for time. LG treated cells had a small peak at 5 minutes but overall had a minimal insulin response over the 60 minute time period (Figure 4-1A). HG treated cells had a biphasic insulin secretion with a peak reaching around 8 fold at 5 minutes followed by a sustained insulin response as long as glucose challenge stays (Figure 4-1A). This confirms that INS-1 832/13 does possess biphasic characteristic in insulin release.



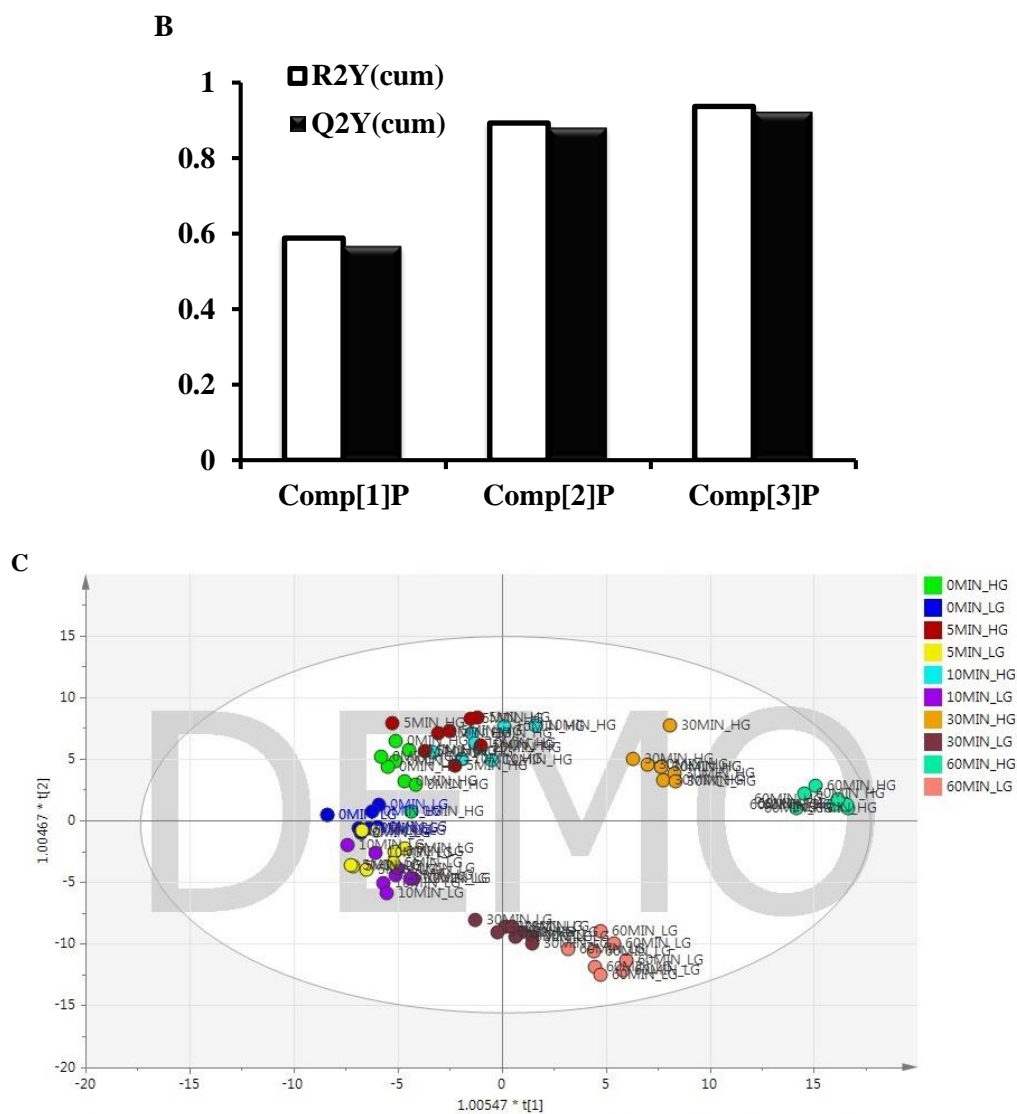


Figure 4-1 Time course glucose-stimulated insulin secretion and metabolome of 832/13 cells

(A) Time-resolved insulin secretion in INS-1 832/13 cells. Insulin secretion rate was corrected for protein concentration and time in response to low glucose (2 mM) and high glucose (16.7 mM). **(B) OPLS model summary of metabolome from INS-1 832/13 cells collected at different times in first hour after glucose challenge** **(C) Metabolome profile recognized by OPLS score plot along the first and second components.** Cells were first pre-cultured for 2 hours at 2 mM glucose followed by incubating cells at either 2 mM glucose or 16.7 mM glucose for 0, 5, 10, 30, or 60 minutes. Results represent mean \pm S.E. of four ($n = 4$) biologically independent

experiments for each condition. Each sample was running twice on GC/MS. *, $p < 0.05$; **, $p < 0.01$; ***, $p < 0.001$, LG versus HG

4.3.2 Dynamic metabolome response to glucose challenge

Following the insulin secretion assay, cell metabolites were extracted for analysis by GC-MS. Deconvolution of the mass spectra by AMDIS identified 325 unique peaks (potential metabolites) across the whole data set. The Fiehn library identified 102 of the 325 peaks and of these identified metabolites 73 were unique (29 of the identified peaks were from metabolites that had multiple derivatization products). The remaining 223 peaks were assessed using the NIST library resulting in the identification of additional 124 metabolites. Of the 124 identified metabolites 47 were unique. The remaining peaks could not be identified using either the Fiehn or NIST library.

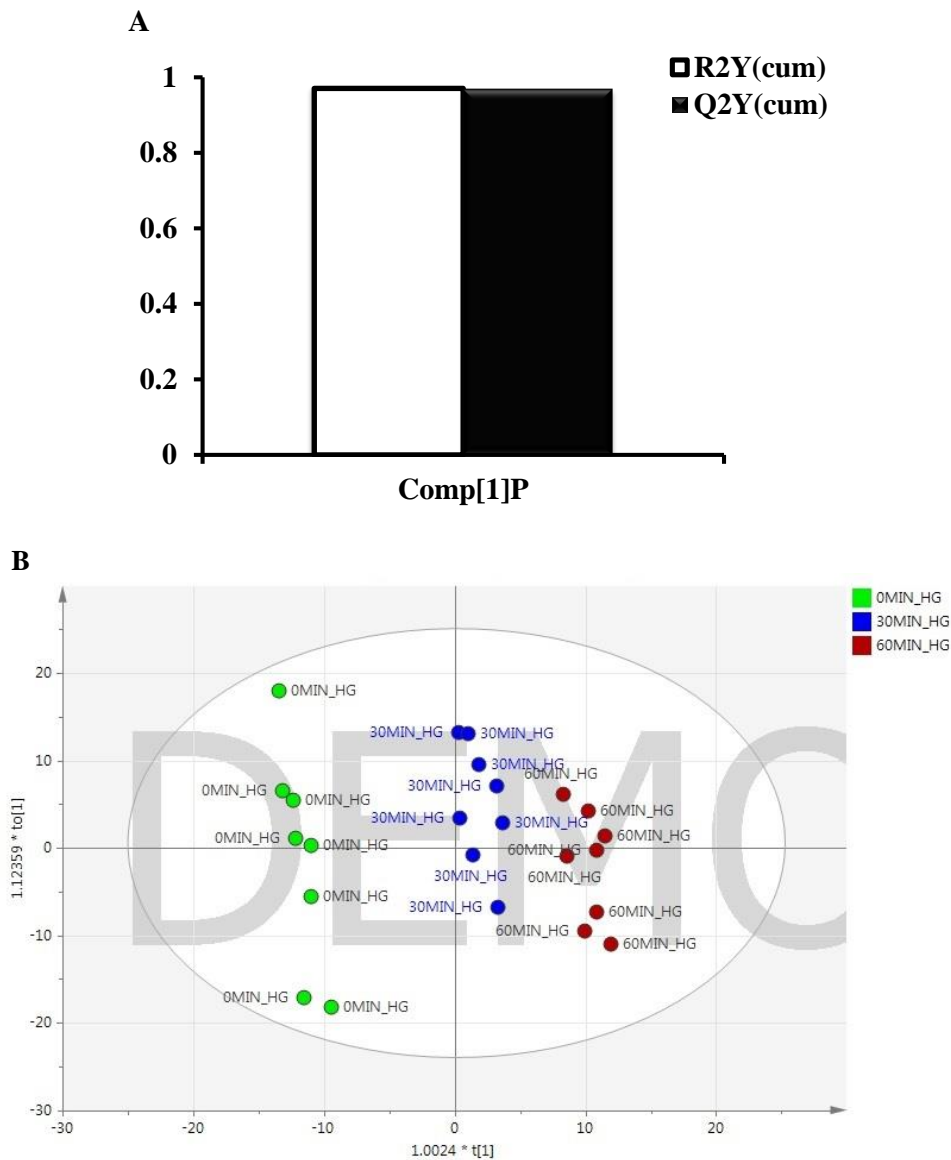
OPLS was constructed to overview the metabolome change in the first one hour after cells are challenged with glucose. As shown in Figure 4-1B, the model yielded three predictive (relevant to glucose challenge) and three orthogonal (unrelevant to glucose challenge) components, which can explain 93.7% ($R^2Y_{(cum)}=0.937$) information contained in original mass spectra data set and has a predictive power of 92.2% ($Q^2Y_{(cum)}=0.922$). The samples were proved to cluster according to first the time and then the concentration of glucose challenge. The scores loading (Figure 4-1C) shows samples quenched at 30 and 60 min are closer to each other, compared to those quenched at 5 and 10 min. This reveals that metabolome change paralleled GSIS observed in INS-1 832/13 cells as shown in Figure 4-1A.

4.3.3 Metabolome alteration associated with the second phase insulin secretion

To understand the metabolic change of the second phase insulin secretion, an OPLS model was generated for data collected from samples quenched at 30 and 60 min, which corresponds to the second phase insulin secretion. As shown in Figure 4-2A, this model produced one predictive and one orthogonal components with 16.7% of the variation in the metabolome related to the time of quenching ($R^2X=0.216$), which describe 97% ($R^2Y_{(cum)}=0.97$) variation and has a predictive power of 96.8% ($Q^2Y_{(cum)}=0.968$). Samples collected from different time points are separated by the predictive component as shown in Figure 4-2B, which suggests that a distinct change of metabolome in second phase is likely anticipated.

As the coefficient plot revealed (Figure 4-2C), all detected TCA intermediates, including alpha-ketoglutarate, succinate, malate, fumarate, and (iso)citrate, were identified as positive biomarkers for

the second phase insulin secretion. Whereas, dihydroxyacetone phosphate (DHAP) and pyruvate had lower coefficient value, which suggests that they are less important to the second phase insulin secretion. The level of G6P almost did not change from 30 min to 60 min. That is probably why the coefficient value of G6P for the second phase is negligible (Figure 4-2C). Alanine, capric acid, palmitic acid and sedoheptulose anhydride monohydrate (Sedoheptulose AM) were also positively associated with the second phase insulin secretion as coefficient plot revealed. Hydroxyproline, proline, glycine, aspartate and lactate retained the negative effects on the second phase insulin secretion.



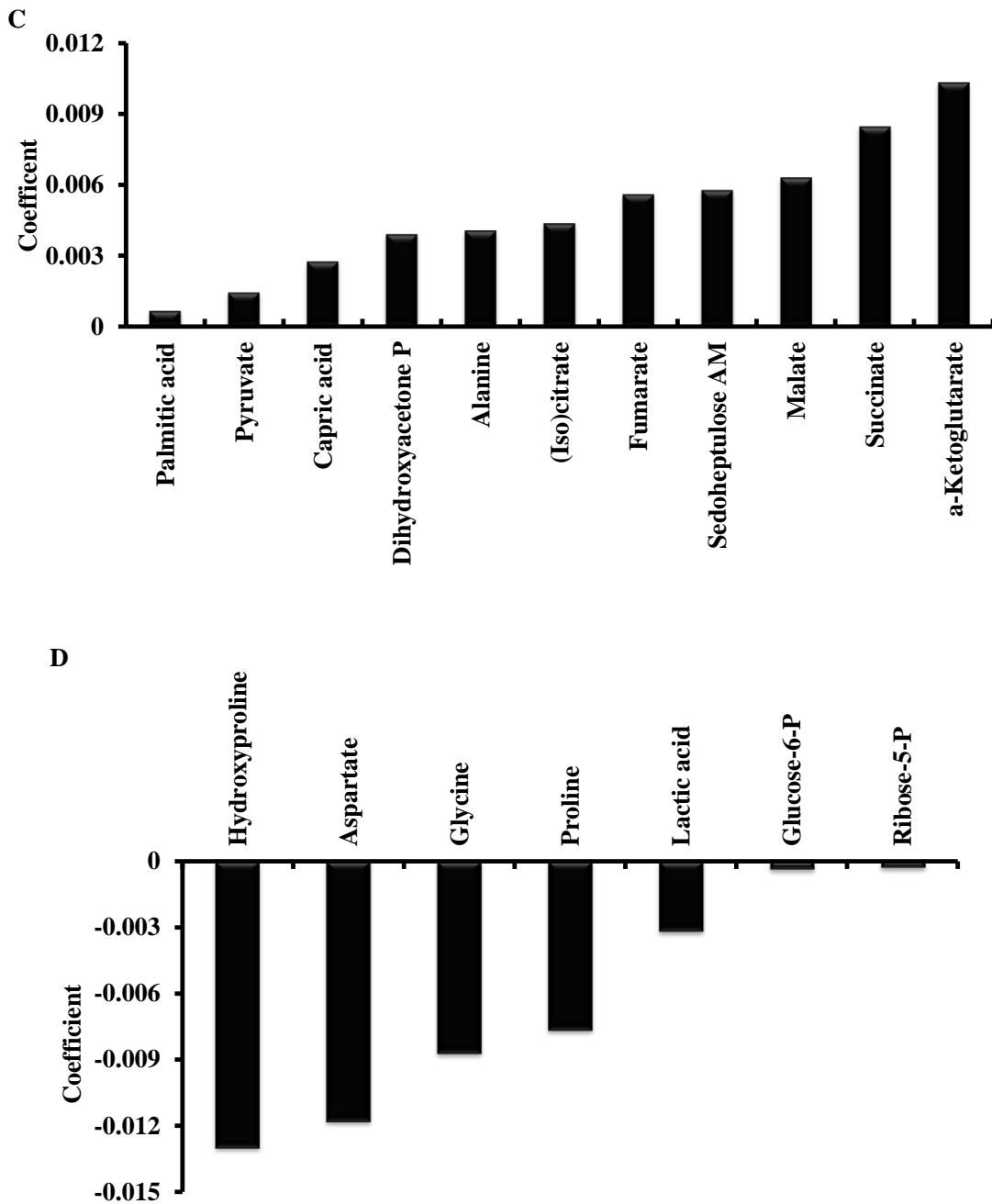


Figure 4-2 Multivariate analysis of metabolome responsible for second phase insulin secretion
(A) OPLS model summary of the metabolomics data from INS-1 832/13 cells collected at 0, 30 and 60 min. Only one predictive component was identified in new model. **(B)** OPLS score plot showing the grouping of samples collected at 0, 30 and 60 min along the first predictive and orthogonal component of an OPLS model. Cells were distributed along the first predictive

component and grouped into three clusters. (C) Coefficient plot showing the key metabolites positively associated with the second phase insulin secretion identified from Fiehn database. (D) Coefficient plot showing the key metabolites negatively associated with the second phase insulin secretion identified from Fiehn database. Results represent mean \pm S.E. of four ($n = 4$) biologically independent experiments for each condition. Each sample was running twice on GC/MS.

4.3.4 Metabolic pathway analysis

Our study suggests that a number of key metabolites differentiated the metabolic response in the second phase insulin secretion to glucose in the INS-1 832/13 cells. These metabolites belong to a number of metabolic pathways.

The coefficient plots confirm that glycolytic intermediates play a critical role in biphasic insulin secretion. Key glycolytic metabolites associated with the second phase insulin secretion include G6P, dihydroxyacetone phosphate, lactate and pyruvate (Figure 4-3). Treating cells with high glucose led to a rapid accumulation of G6P peaking at 30 minutes (Figure 4-3A). Interestingly, dihydroxyacetone phosphate showed a delayed accumulation taking 10 minutes before a difference could be seen as compared to control cells (Figure 4-3B). Pyruvate levels exhibited a time based linear accumulation with no peak up to 60 minutes (Figure 4-3C). Surprisingly, lactate levels showed a strong biphasic response to high glucose (Figure 4-3D).

Key TCA cycle metabolites, including (iso)citrate, alpha-ketoglutarate, succinate, fumarate and malate, were identified to be associated with the second phase insulin secretion by our OPLS model (Figure 4-2). Oxaloacetate and succinyl-CoA were not detected in our experiments. (Iso)citrate, fumarate and malate showed a rapid rise in metabolite levels beginning at 5 minutes (the earliest measurement in these studies) (Figure 4-4A, B and C). (Iso)citrate and fumarate levels peaked at around 10 minutes whereas malate levels peaked at 30 minutes in response to treating cells with high glucose. Alpha-ketoglutarate and succinate levels showed a delayed response to high glucose that did not begin to rise until 10 minutes after treating cells with high glucose and a progressive rise for the duration of the experiment (Figure 4-4D and E). All of these TCA metabolites, particularly alpha-ketoglutarate and succinate, showed a strong association to the second phase insulin release (Figure 4-2C).

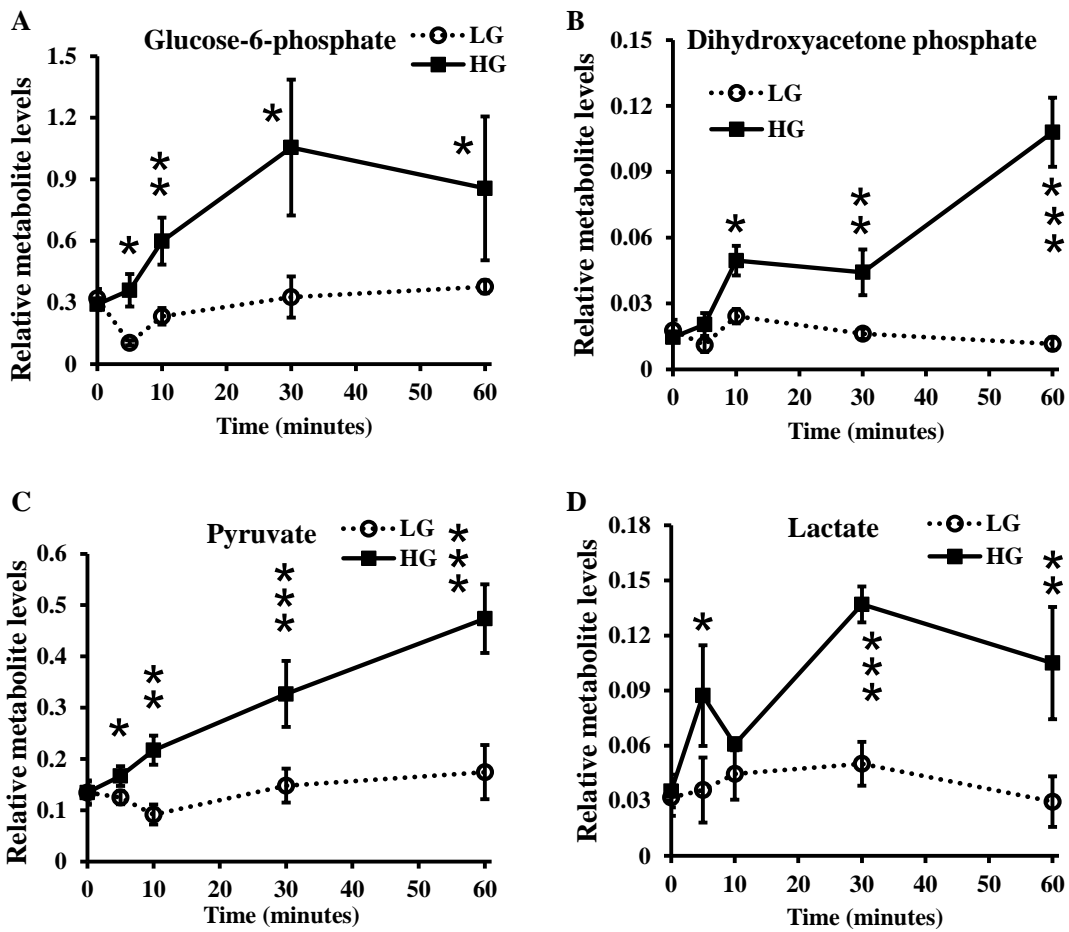


Figure 4-3 Time course responses of glycolytic metabolite levels

Metabolites were isolated from INS-1 832/13 beta cells and run on GC/MS. Metabolites are identified by searching MS spectra against Fiehn library. The metabolites levels were normalized by internal standards (Myristic acid D-27). A) glucose-6-phosphate, B) dihydroxyacetone phosphate, C) pyruvate, D) lactate. (LG = 2 mM glucose; HG = 16.7 mM glucose) (n=4) *, p<0.05; **, p<0.01; ***, p < 0.001, LG versus HG

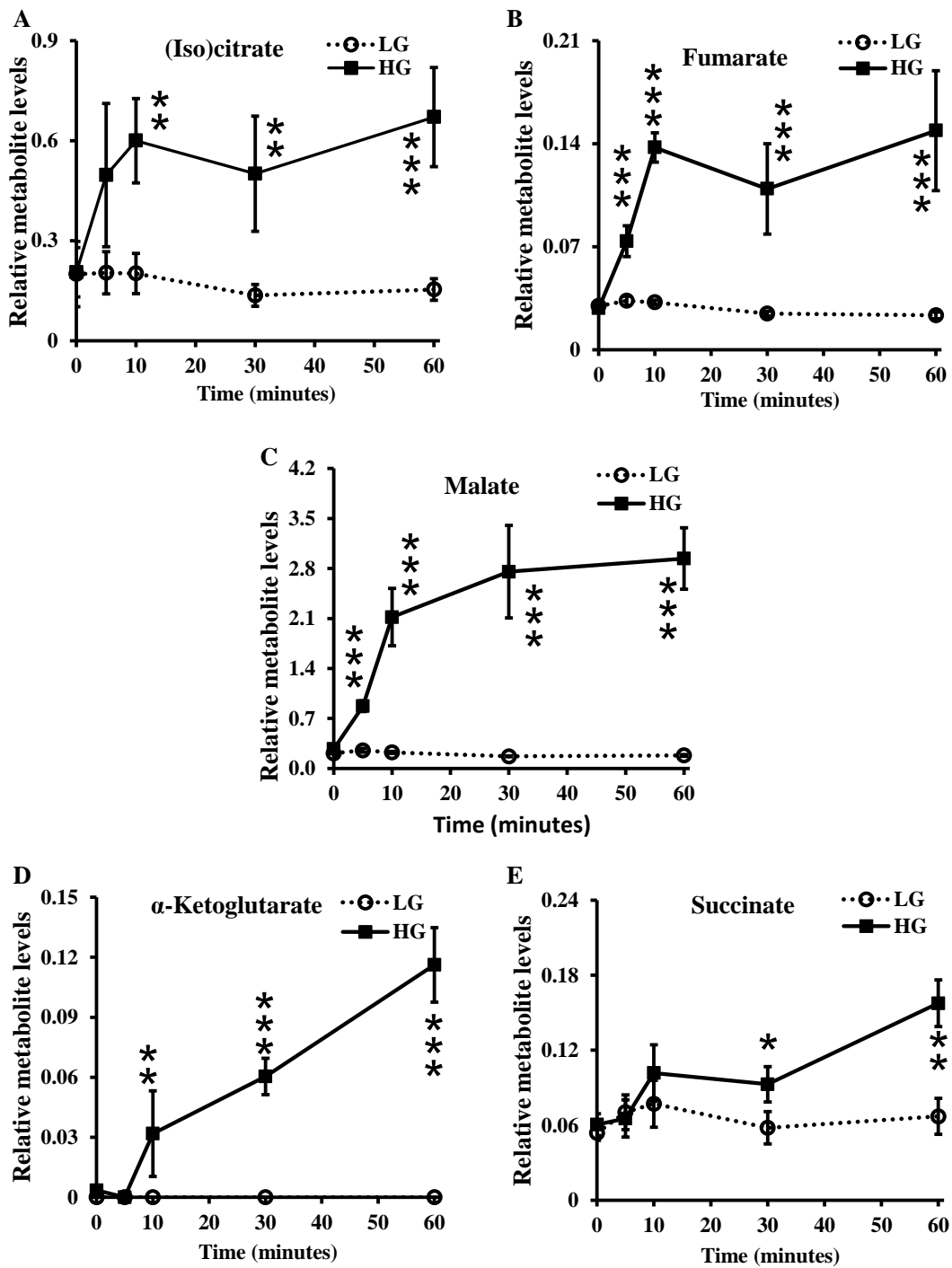


Figure 4-4 Time course responses of TCA metabolite levels

Metabolites were isolated from INS-1 832/13 beta cells and run on GC/MS. Metabolites are identified by searching MS spectra against Fiehn library. The metabolites levels were

normalized by internal standards (Myristic acid D-27). A) citrate/isocitrate (in our GC-MS system citrate and isocitrate are indistinguishable from each other), B) fumarate, C) malate, D) alpha-ketoglutarate, E) succinate. (LG = 2 mM glucose; HG = 16.7 mM glucose) (n=4). *, p<0.05; **, p<0.01; ***, p < 0.001, LG versus HG

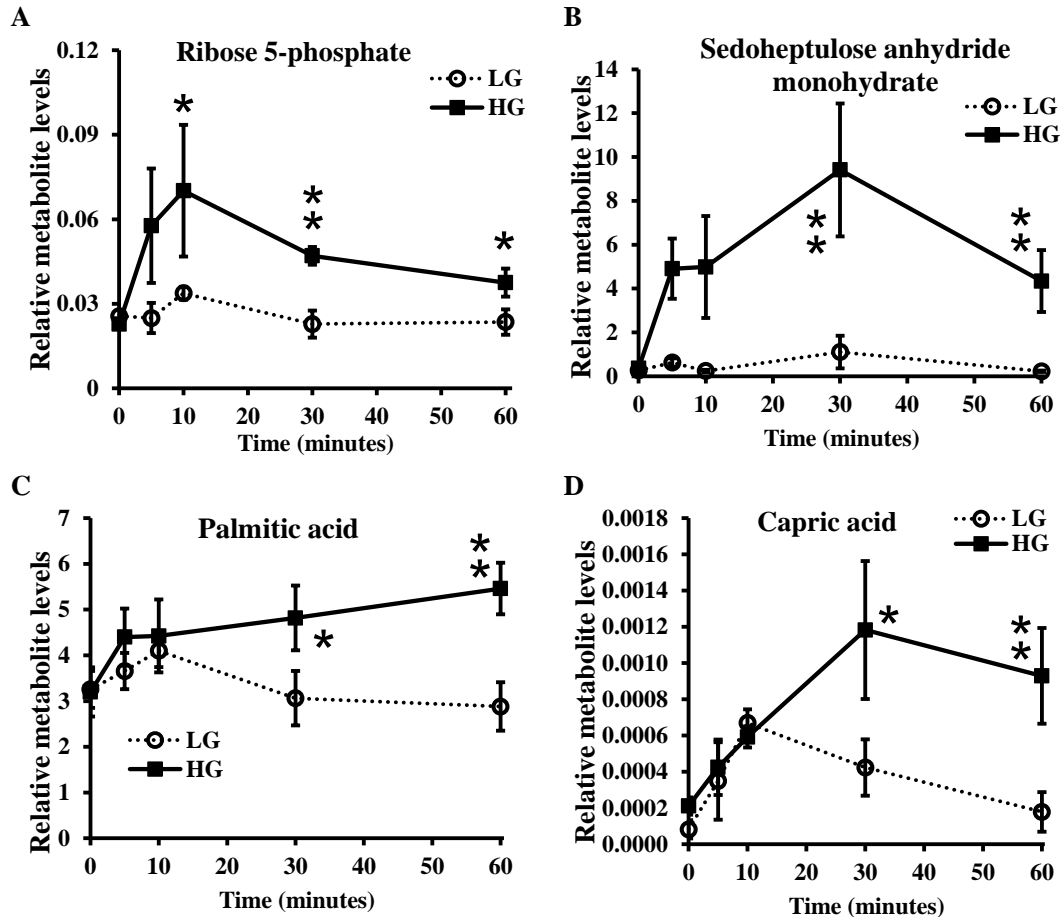


Figure 4-5 Time course responses of other metabolites positively associated to second phase insulin secretion

Metabolites were isolated from INS-1 832/13 beta cells and run on GC/MS. Metabolites are identified by searching MS spectra against Fiehn library. The metabolites levels were normalized by internal standards (Myristic acid D-27). A) Ribose 5-phosphate, B) Sedoheptulose anhydride monohydrate, C) Palmitic acid, D) Capric acid (LG = 2 mM glucose; HG = 16.7 mM glucose) (n=4). *, p<0.05; **, p<0.01 LG versus HG

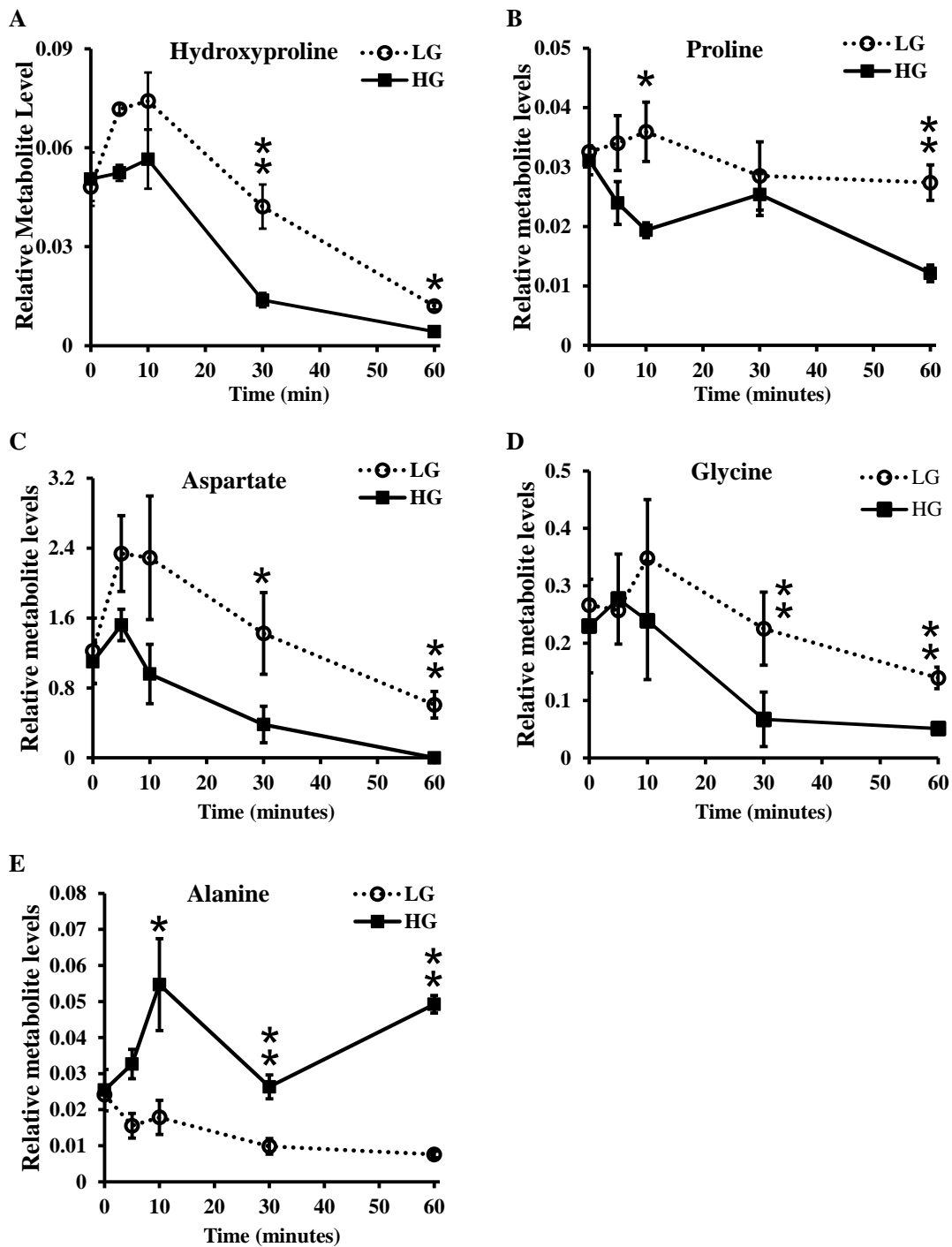


Figure 4-6 Time course responses of amino acids

Metabolites were isolated from INS-1 832/13 beta cells and run on GC/MS. Metabolites are identified by searching MS spectra against Fiehn library. The metabolites levels were

normalized by internal standards (Myristic acid D-27). A) Hydroxyproline, B) Proline, C) Aspartate, D) Glycine, E) Alanine (LG = 2 mM glucose; HG = 16.7 mM glucose) (n=4). *, p<0.05; **, p<0.01 LG versus HG

Other metabolites were also associated with biphasic insulin secretion as our coefficient plot suggested (Figure 4-5). Ribose-5-phosphate, an intermediate in the PPP, increased in response to high glucose and peaked at 10 minutes (Figure 4-5A). Other PPP metabolites were found not to change during the treatment of cells with high glucose (6-phosphogluconate, ribulose-5-phosphate and erythrose-4-phosphate, data not shown). Sedoheptulose anhydride monohydrate (Figure 4-5B) and capric acid (Figure 4-5D) had a rapid rise in metabolite levels peaking at 30 minutes. Palmitic acid (Figure 4-5C) showed no significant difference in the response to high glucose until the 30 minute time point.

Alanine was the only amino acid positively associated with biphasic insulin secretion from INS-1 832/13 cell (Figure 4-6E). On the other hand, hydroxyproline, proline (Figure 4-6A and B), aspartate (Figure 4-6C) and glycine showed a time based decrease and were revealed to be negatively associated with the second phase insulin secretion.

4.3.5 Block of pyruvate influx selectively affects second phase insulin secretion

Since TCA intermediates were identified as the most potent factors involved in the second phase insulin secretion by the metabolomics analysis, studies were done to further investigate the importance of glycolysis derived anaplerosis in biphasic insulin secretion. Mitochondrial pyruvate carrier sits at a critical junction between cytosolic generation of pyruvate in glycolysis and mitochondrial metabolism of pyruvate, which supplies anaplerosis with glucose-derived carbon. Using the specific inhibitor of mitochondrial pyruvate transport, UK5099, we found that both 100 μ M and 150 μ M UK5099 decreased the level of insulin secretion in the second phase by 50 percent ($45 \pm 7\%$ for 100 μ M, $48 \pm 0.3\%$ for 150 μ M) without altering the first phase insulin secreted from freshly isolated rat islets or the subsequent insulin secretion triggered by the combination of high glucose and KCl as shown in Figure 4-7. UK5099 also resulted in a reduction in mitochondrial pyruvate transport and metabolism (data not shown).

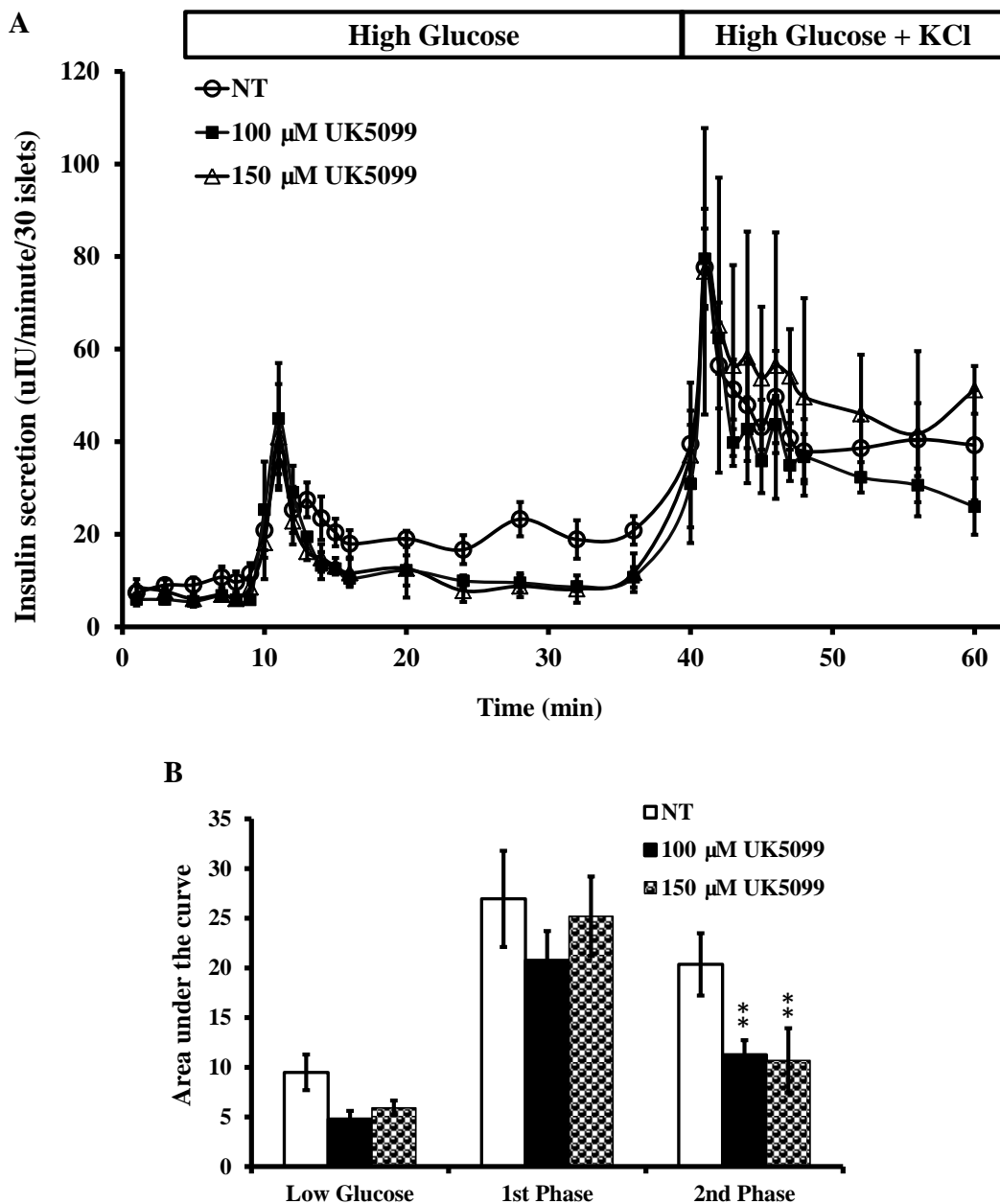


Figure 4-7 Effect of pyruvate inhibitors on biphasic insulin secretion in rat islets

(A). Insulin secreted by perfused rat islets. Rat islets were perfused from 1 to 8 min with 2.8 mM low glucose (LG) followed by 16.7 mM high glucose (time points from 9 – 40 min) and finally with 16.7 mM high glucose with 40 mM KCl (time points from 41– 60 min). (B). Area under the curve of the insulin secretion responses in A (basal, 1– 8 min; 1st phase, 9 –18 min;

2nd phase, 19 – 40 min; HG and KCl, 41– 60 min). Results represent mean \pm S.E. of four (n > 3) independent experiments for each condition. **, p<0.01 non-treated versus UK5099 treated

4.4 Discussion

Although the biphasicity of insulin secretion in perfused pancreas and perifused islets has been a well-established physiological phenomenon [104-107] for the last two decades, the dynamic secretory response of pancreatic beta cell lines has received less attention than freshly isolated primary pancreatic beta cells. In fact, a clear biphasic feature in INS-1 832/13 cells [133, 382], but not in betaHC-9, HIT-T15 or INS-1 beta cells, was observed as a response to sustained elevated glucose stimulation. This biphasicity phenomenon in INS-1 832/13 cells was confirmed by our data (Figure 4-1) since cell activity in the first ten minutes was distinctly different from what happens afterwards (up to 60 min) at both GSIS and metabolome levels. Hence, INS-1 832/13 cells were used in our study to investigate the coupling mechanism underlying dynamic insulin secretion.

The profound difference of glucose responsiveness between different cell lines might be caused by a certain mechanism working independently of K_{ATP} channel, as the combination of 250 μ M diazoxide and 40 mM KCl can evoke a biphasic response in INS-1 832/13 cells but not in HIT-T15 or INS-1 [133]. The presence of K_{ATP} channel-independent (or amplifying) pathway probably involves the coupling of glycolytic and TCA cycle metabolic pathways paralleled by hypoxia-inducible factor 1 alpha (HIF-1alpha)-mediated regulation of distal mechanism in insulin secretion signaling pathways [333]. Some other studies suggest that phospholipase C (PLC) / protein kinase C (PKC) pathway [121, 383-385] and/or cAMP [122] might be particularly important to the second phase insulin secretion, because the difference of nutrient-activated PLC isozyme expression [383] and inositol phosphate (IP) accumulation seem to be associated with species difference of the second phase insulin level between rat and mouse islets [386]. On the other hand, PKC activator tetradecanoyl phorbol acetate (TPA) [387], and phorbol 12-myristate 13-acetate [388] are strong inducers of the sustained second phase insulin secretory response and can markedly increase the second phase response of mouse islets to glucose. However, islets isolation procedure [112], pre-stimulatory glucose level [113] as well as the length of pre-culture period [123] were later proved to contribute to the second phase of insulin secretion. The change of these experimental conditions could significantly improve the second phase response of mouse islets to insulin secretagogues.

Up to now, no study has been done to investigate the mechanism specifically contributing to the second phase [383] or the relative importance of these potential pathways to different phases of

insulin secretion [148]. Our study attempted to fill this void by using untargeted metabolomics approach to obtain a broad profile of what happens metabolically in INS 832/13 beta cells during time course based stimulation. Since beta cells rely on metabolism to regulate insulin secretion it is likely that multiple interconnected metabolic pathways are involved in this process. The most significant metabolites that differentiated biphasic insulin secretion in response to high glucose were identified by OPLS. Among all the metabolites detected, some were found to be strongly associated with the metabolic response of cells to time course based stimulation as well as insulin secretion.

All glycolytic intermediates were up-regulated by high glucose stimulation, but exhibited different kinetic characteristics. Glucose challenge led to a rapid accumulation of G6P peaking at 30 minutes. Pyruvate showed a time based linear accumulation with no peak up to 60 minutes. Pyruvate and NADH can be converted to NAD^+ and lactate by lactate dehydrogenase (LDH). In this process, NAD^+ is regenerated to maintain flux through glycolysis. Lactate was shown to accumulate with time in our studies and its response appeared to be biphasic suggesting that some of the glycolysis derived pyruvate in beta cells is diverted away from mitochondrial entry. This is consistent with previously published studies using the INS-1 832/13 cells [148, 382].

Pyruvate links upstream glucose metabolism in glycolysis to the downstream generation of metabolic signaling molecules involved in regulating insulin release. Most of the pyruvate generated by glycolysis is directed towards metabolism in the mitochondrial TCA cycle. Islet beta cells have two key mitochondrial enzymes involved in pyruvate metabolism, PC and pyruvate dehydrogenase (PDH) [33, 75-77]. Pyruvate entering the TCA cycle through the PDH reaction leads to the generation of ATP that modulates K_{ATP} channels whereas pyruvate metabolism through the PC reaction leads to an increase in TCA intermediates (called anaplerosis). TCA cycle intermediates detected by our GC-MS, including (iso)citrate, alpha-ketoglutarate, succinate, fumarate and malate, were identified by our OPLS model as key components strongly associated with the second phase insulin secretion (Figure 4-2C). The levels of these metabolites were noticeably raised during the second phase of insulin secretion (Figure 4-4). Interestingly, alpha-ketoglutarate and succinate levels did not begin to rise until around 10 minutes after stimulating the cells, followed by a progressive rise with time. That's probably why both alpha-ketoglutarate and succinate showed the strongest association with the second phase insulin secretion. Our data suggests anaplerosis is likely involved in regulating the second phase insulin secretion.

In order to investigate the importance of anaplerosis to biphasic insulin secretion, UK5099 [389] was used to inhibit the influx of pyruvate from cytoplasm to mitochondria in rat islets. UK5099 is an

inhibitor of mitochondrial pyruvate carrier which specifically modifies a thiol group on the carrier. It is able to cause a reduction in mitochondrial pyruvate transport and metabolism (data not published yet). Figure 4-7 showed that UK5099 had a preference to decrease the second phase of insulin secretion in rat islets and this inhibition effect was reversible. Additionally, the ability of rat islets to respond to insulin secretagogues was not affected once UK5099 was eliminated from the perfusion buffer. The selective inhibition of the second phase insulin secretion by UK5099 suggests that if glucose-derived carbon supply is limited, the proportion of pyruvate flux into TCA as acetyl-coA through pyruvate dehydrogenase takes precedence over anaplerosis through pyruvate carboxylases to maintain the basal level of insulin secretion as well as other basic ATP-dependent activity critical for cell survival. This phenomenon indicates that anaplerosis as part of the K_{ATP} independent pathway, rather than ATP generation, might be the dominant factor underlying the second phase insulin secretion, which is in agreement with the previous study done by Straub [133].

Among all TCA cycle intermediates, alpha-ketoglutarate deserves our special attention for two reasons. First, alpha-ketoglutarate links pyruvate metabolic fate to insulin secretion through pyruvate-isocitrate cycling [49, 82]. Second, alpha-ketoglutarate functions as an essential component of reactions catalyzed by alpha-ketoglutarate dependent hydroxylases [390], which facilitates oxidative decomposition of alpha-ketoglutarate leading to generation of CO_2 , succinate, active oxygen species and hydroxylated substrate. One of the first identified substrates is proline. The hydroxylation of proline by prolyl hydroxylase might be involved in regulation of insulin secretion through both hypoxia inducible factors 1 alpha (HIF-1alpha) -dependent [96] and -independent [95] mechanisms. The latter is also confirmed by data from our group (data not published yet). Hydroxyproline, the hydroxylation product of proline, is negatively associated with the second phase insulin secretion. An increase of alpha-ketoglutarate occurs simultaneously with a decrease in hydroxyproline which may indicate alpha-ketoglutarate mediated proline hydroxylation is one important coupling pathway modulating the second phase insulin secretion. Since the selective inhibition of UK5099 on the second phase insulin secretion in rat islets perfusion is acute and reversible, its effect on biphasicity of insulin release is most likely through an HIF-1alpha-independent mechanism (data not published yet).

Glucose increased ribose-5-phosphate peaking at 10 minutes, which is in a good agreement with another study showing that PPP potentially plays a role in the first phase insulin secretion [148]. Interestingly, other PPP metabolites were found not to change in response to high glucose (ribulose-5-phosphate and erythrose-4-phosphate, data not shown). Our data suggests that the upstream oxidative

arm of the PPP (specifically the activity of glucose-6-phosphate dehydrogenase (G6PDH)) was up-regulated in response to glucose, however, downstream products were generally not altered. The significance of selective up-regulation of the G6PDH activity, but not other parts of the PPP, has not been shown before, possibly because the PPP serves to provide ribose-5-phosphate for the synthesis of nucleotides and nucleic acids.

In addition, the hexosamine biosynthesis pathway metabolite N-acetylglucosamine (data not shown) identified from NIST library was also shown to rise rapidly with glucose treatment (data not shown), which is consistent with its potential role in regulating insulin secretion [391]. The reason why alanine, sedoheptulose anhydride monohydrate, palmitic acid and capric acid are indicative of second phase insulin secretion remains unresolved. Another interesting aspect of the current set of studies is that a number of metabolites were consistently down-regulated during the second phase insulin secretion. These include proline, aspartate, and glycine. In many organisms, proline is believed to act as a stress protectant by serving multiple functions: protein and membrane stabilization, lowering the T_m of DNA, and scavenging of reactive oxygen species [392]. Although its function as a universal antioxidant in mammalian systems is relatively unexplored, proline is suggested to scavenge intracellular ROS in mammalian cells [393] and thereby inhibit ROS-elicited apoptosis in various cancer cell lines [394, 395]. If that endogenous proline is, in fact, a ROS scavenger and the inverse relationship between proline content and ROS levels also exists in pancreatic beta cells, our data imply that anti-oxidative defense mechanisms of pancreatic beta cells are particularly weak (the expression levels of antioxidant enzymes such as superoxide dismutase, catalase, and glutathione peroxidase are known to be very low in islets compared with other tissues [396]) and can be easily overwhelmed by the redox imbalance arising from overproduction of reactive oxygen and nitrogen species [397, 398]. The significance of the reduction of these metabolites as it relates to biphasic insulin secretion is unknown and is currently under investigation in our laboratory.

4.5 Conclusion

In the current study we showed that a number of metabolites were associated with second phase insulin secretion. Of all candidates, alpha-ketoglutarate, succinate and other TCA cycle intermediates were the metabolites strongly associated with second phase insulin secretion. Hydroxyproline, proline and aspartate were negatively correlated with second phase insulin secretion. This evidence indicates that alpha-ketoglutarate mediated proline hydroxylation is probably central for the second phase insulin secretion. In conclusion, our study provides a good overview of the metabolic changes that

occur during second phase insulin secretion and offers valuable insights into the understanding of the metabolic effects of glucose in beta cells.

Chapter 5
Mechanistic Study of Time-Dependent Effects of Glucose on
Insulin Secretion

5.1 Overview

Glucose-stimulated insulin secretion (GSIS) of primary pancreatic beta cells is determined by the net balance between the acute stimulation-secretion coupling generated by the concomitant stimuli that cells are currently exposed to, and time-dependent effects (TDEs) elicited by previously applied insulin secretagogues. TDEs can be either inhibitory or potentiating. Their interaction is believed to form the biphasic slope of insulin release. In this study, the regulatory process governing the dynamics of insulin release was investigated using a gas chromatography mass spectroscopy (GC-MS)-based metabolomics approach. Our data reveal that time-dependent inhibition (TDI) at the insulin secretion level probably exists, but is neutralized by an opposing effect in our INS-1 832/13 cell line, and the secretory activity of pancreatic beta cells actually results from the integrated reaction between acute stimulation-secretion coupling and its memory of previously applied stimuli. Multivariate analysis (MVA) identified statistically significant alterations in the levels of 19 metabolites, which are involved in both glucose cytosolic and mitochondrial metabolism. Our data showed that the TDI effect is probably mediated by the redox state of beta cells, represented by the NAD^+/NADH ratio generated by glycerol-phosphate shuttle and malate-aspartate shuttle activity as well as lactate output and proline level. In fact, the level of these intermediates is strongly affected by the duration of the pre-culture period. On the other hand, time-dependent potentiation (TDP) might be mediated by 3-phosphoglycerate and citrate-induced hyper phosphorylation of regulatory proteins involved in insulin exocytosis of pancreatic beta cells. Overall, our data suggest that the upstream glycolytic pathway can mediate the TDI effect observed in the INS-1 832/13 cell line and that the proximal part of stimulation-secretion coupling might be responsible for time-dependent potentiation.

5.2 Introduction

As a major insulin secretagogue, glucose can not only promote the acute insulin secretion, but also induce a memory of pancreatic beta cells for previous glucose challenge. A major difference between the acute glucose stimulatory effect and beta cell memory is that the latter does not require the continuous presence of insulin secretagogue and will last for a certain period of time even after insulin secretagogue is removed from medium. This phenomenon, which is also called time-dependent effects (TDEs), was first reported by Grodsky, G.M. [105-107] and Neshier and Cerasi [139-142]. TDEs refer to the observation that repeatedly challenged pancreatic beta cells can develop either an enhanced (time-dependent potentiation or TDP) [104, 106, 119, 131, 140, 143-146] or

impaired (time-dependent inhibition or TDI) [119, 143, 144, 146] response to subsequent stimulation. The type and magnitude of subsequent insulin responses depend on the type of secretagogues and the condition of exposure, including the concentration (dose dependent) of secretagogues and the duration (time dependent) of the stimulation applied: high concentrations and long durations generate amplification of the subsequent insulin responses, while low concentrations and short pulses of stimulation tend to induce a refractory state [104-107, 119, 131, 139-145].

TDEs offer a flexible mechanism to modulate GSIS and adapt pancreatic beta cells to environmental changes by promptly sensing the energy status and by altering the insulin secretion rate in a timely manner. The signaling cascade of TDEs is, hence, an ideal pharmaceutical target of type 2 diabetes therapy. In addition, TDEs were suggested to be the underlying mechanism for biphasic insulin secretion, because a tight correlation was discovered between the magnitude of TDP and the slope of second-phase insulin response [144]. The biphasic insulin release was believed to reflect the effect of the net balance between TDP and TDI on the acute stimulation [147]. TDEs hypothesis does not contradict either the pool-model [105, 106, 131, 132] or the signal-modulation hypothesis. Indeed, the TDEs hypothesis perfectly fits into both models [111].

Currently, it is known that both TDP and TDI effects are determined by glucose metabolism, and neither cyclic AMP [399] nor polymerization of tubulin [400] is involved in this process. However, significant differences seem to exist between the characteristic of TDP and TDI. First, TDP generation is calcium dependent [146], while TDI is not [401]. Second, duration of the TDI effect has been observed to last longer than TDP [120]. Third and last, they affect insulin secretion in different ways. TDP augments insulin release by acting on velocity [401], while TDI appears to change K_m (enzyme substrate concentration at which the reaction rate is half of V_{max}) of the response [402]. Although anaplerotic input [403] and involvement of nitric oxide synthase [404] have been suggested to be sufficient to elicit glucose-induced TDP, not much has been discovered about TDI, and its mechanism remains to be further investigated.

Here, a robust GC-MS based untargeted metabolomic analysis was applied to study the mechanism of glucose-induced time-dependent effects and their potential roles in biphasic insulin release of INS-1 832/13 cell line.

5.3 Results

5.3.1 Glucose stimulated insulin secretion (GSIS) showing time dependent effects

GSIS was done by pre-culturing INS-1 832/13 cells in KRB medium with 2 mM glucose for different periods of time as indicated in figure legend before exposure to non-stimulating and stimulating glucose. As Figure 5-1A shows, although a 70 percent decrease of insulin secreted by cells cultured in basal level glucose was observed as pre-culture time extended from one hour to three hours, the insulin released in the first hour remained the same for cells incubated with stimulatory levels of glucose. The discrepancy between two different conditions indicates either a lack of TDI or an opposite effect elicited by stimulatory level glucose, which can neutralize the TDI effect observed in low glucose treated cells. If TDI is completely absent at stimulatory glucose levels, a steady and stable insulin secretion rate should always be observed, despite pre-treatment duration. On the contrary, the presence of an opposing effect should be characterized by a time-dependent secretion pattern. To distinguish between these two possibilities, insulin secreted in the first 10 minutes was collected and plotted. As shown in Figure 5-1B, with longer pre-culture time, more insulin was released by beta cells, which clearly suggests that a TDI effect existed, but was overcome quickly by a potentiation mechanism in stimulating glucose treated beta cells. Although TDI was also reported to last longer than TDP [111], this potentiation effect is predicted to last equally long in order to neutralize the TDI effect, which should be reflected at the metabolome level if they retain different mechanisms. As TDP possesses different characteristics from TDI [120, 146, 401-404], distinctive coupling factors might be anticipated, enabling us to perform a metabolomic study of beta cells.

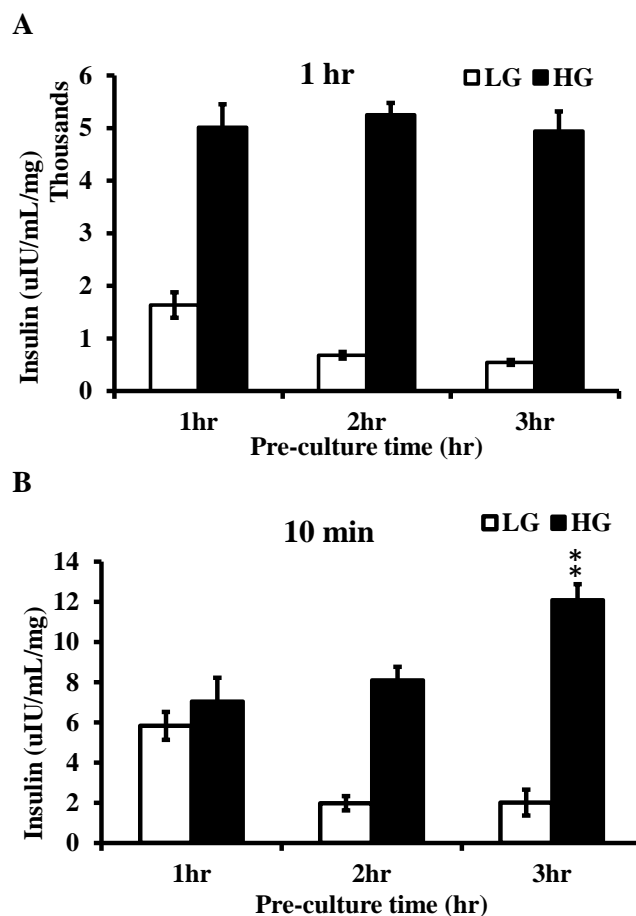


Figure 5-1 Glucose-stimulated insulin secretion showing time-dependent effects

INS-1 832/13 beta cells was pre-cultured with 2 mM glucose for different periods of time and exposed to either 2 or 10 mM glucose for (A) 1hr or (B) 10 minutes before insulin was measured by radioimmunoassay. Insulin secretion corrected for protein concentration. Results represent mean \pm S.E. of four (n = 8) independent experiments for each condition. **, p<0.01; ***, p < 0.001, cells pre-treated for 1hr versus either 2hr or 3hr

5.3.2 Metabolite detection and identification

Following a one hour culture period with KRB and subsequent insulin assay, cells were harvested and metabolites were extracted and assessed using GC-MS (GC-Quadrupole MS in EI scan mode). The representative total ion chromatogram (TIC) of metabolism from INS-1 832/13 beta cells is shown in Figure 5-2(A-D). Figure 5-2(E-F) shows the net difference of TIC generated by cells pre-cultured in non-stimulating glucose for 1 or 3 hour, but incubated in either non-stimulating (Figure 5-2E) or

stimulating (Figure 5-2F) glucose. These data suggest that a longer pre-culture period will reduce the quantity of a few metabolites (Figure 5-2E), which agrees with the observation of insulin secretion in Figure 5-1A and further confirms that the metabolism activity cultured in non-stimulating glucose conditions decreases along pre-stimulatory time. Additionally, despite the seemingly unaffected insulin response in high glucose treated cells, many metabolites are, in fact, up-regulated by glucose as pre-culture time persists (Figure 5-2F). This strongly suggests that the failure to observe TDI at the insulin secretion level in high glucose condition is probably due to the neutralization of TDI by its opposite effect, rather than being caused by an actual deficiency of TDI.

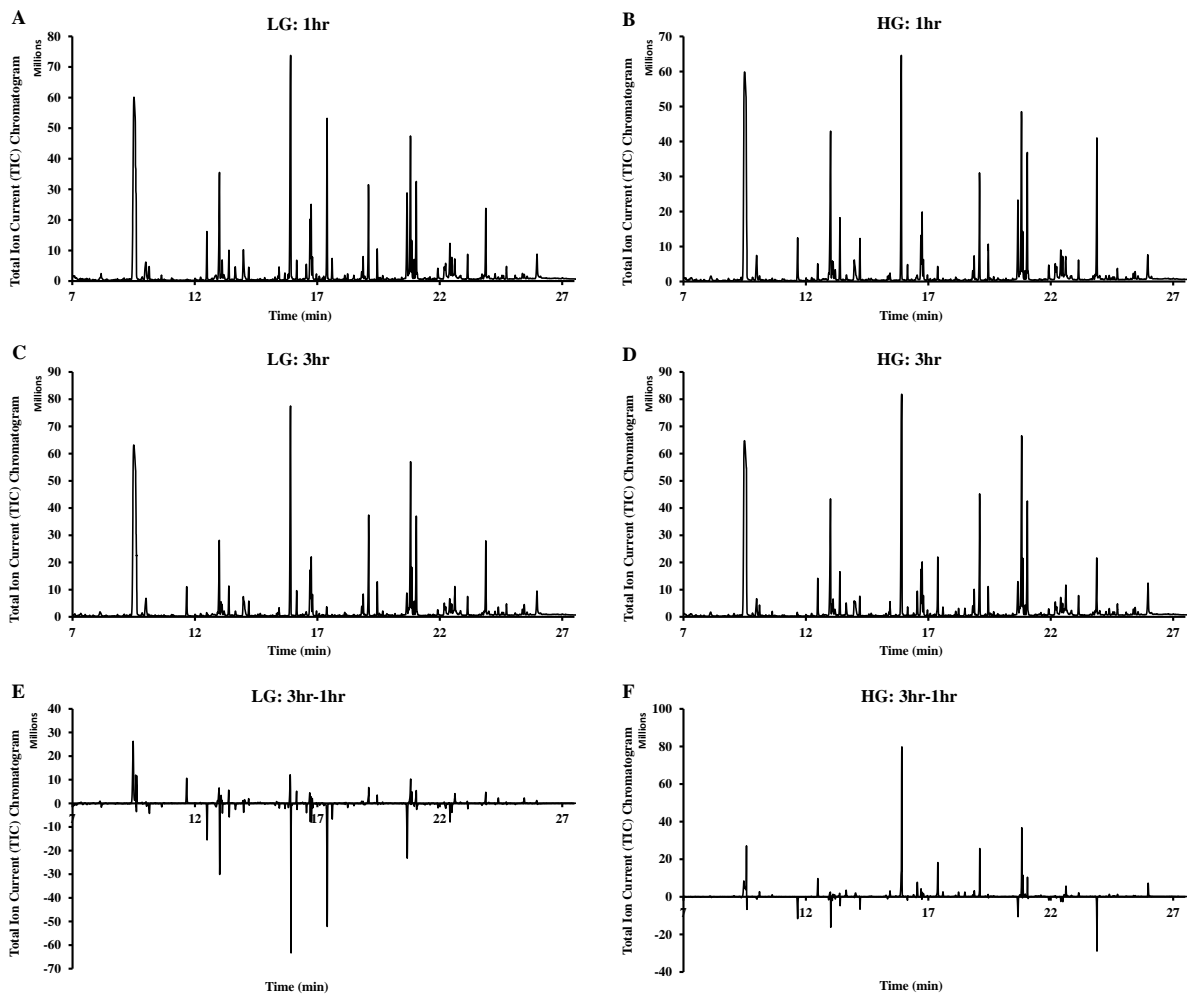


Figure 5-2 Representative total ion current chromatogram (TIC) of metabolome in INS-1 832/13 beta cells showing time-dependent effects.

(A) Representative TIC for the metabolome isolated from INS-1 832/13 beta cells pre-cultured for 1 hr in low (2mM) glucose (LG). (B) Representative TIC for the metabolome isolated from INS-1 832/13 beta cells pre-cultured for 1 hr high (10mM) glucose. (C) Representative TIC for the metabolome isolated from INS-1 832/13 beta cells pre-cultured for 3 hr in low (2mM) glucose (LG). (D) Representative TIC for the metabolome isolated from INS-1 832/13 beta cells pre-cultured for 3 hr in high (10mM) glucose. (E) 1 hr LG TIC subtracted from 3 hr LG TIC. (F) 1 hr HG TIC subtracted from 3 hr HG TIC.

Deconvolution of the mass spectra by AMDIS identified 459 unique chromatographic peaks (potential metabolites) across all data sets. The Fiehn library identified 86 unique metabolites using retention time and mass spectra. The remaining 304 peaks were assessed using the NIST library (based only on mass spectra) resulting in the identification of an additional 292 compounds. The remaining 81 peaks could not be identified in either the Fiehn or NIST libraries.

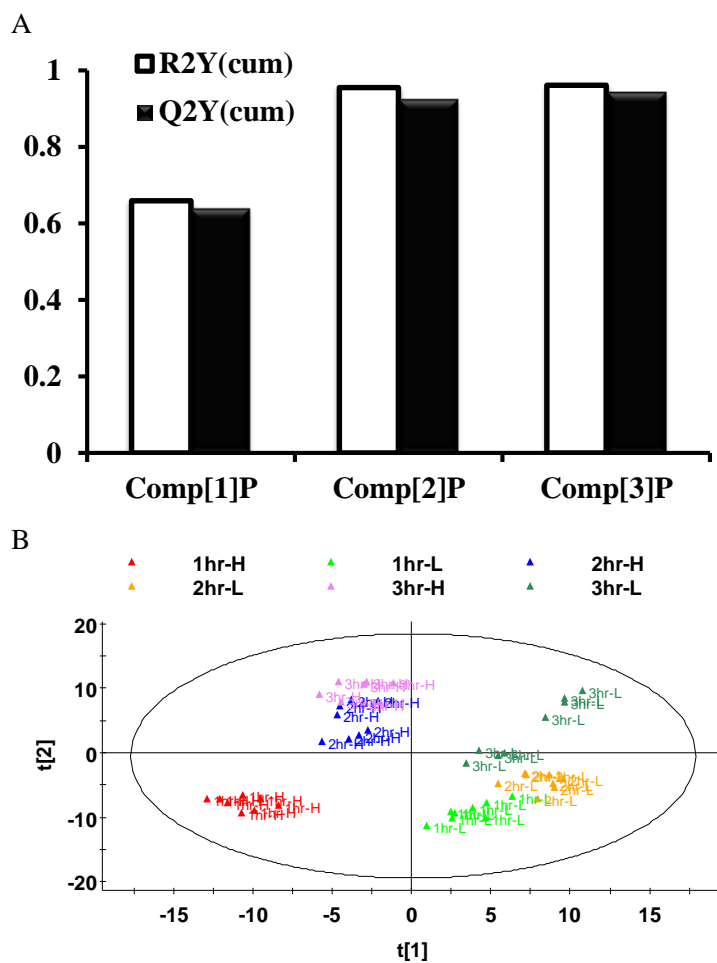
5.3.3 Multivariate analysis

An OPLS model was created to analyze our mass spectra (MS)-based metabolomics data and to identify the significant metabolites or metabolic pathways that might play an important role in mediating glucose-induced TDE. As Figure 5-3A suggests, three predictive components and two orthogonal components were generated in our model. This model can describe 96.1% ($R_2Y_{(cum)}=96.1\%$) of variations in our data set and have almost equally good predictability ($Q_2Y_{(cum)}=94.4\%$). The remaining variations are likely composed of technical and biological variations, which are possibly not relevant to our model.

In the score plot (Figure 5-3B), which shows new variables computed as linear combinations of original variables to provide a summary of our data set, cells are grouped according to the concentration of second stimuli (low or high glucose) and the duration of the first pulse (Figure 5-3C). The group of non-stimulating glucose treated cells distributed evenly along the second component. However, the group of stimulatory glucose treated cells further clustered into two different sub-groups along PC2, where the 1hr group was much farther away from both 2hr and 3hr groups. Again, this phenomenon doesn't match their corresponding insulin secretion observed in Figure 5-1, but supports the idea that a potentiation mechanism exists and acts to oppose and neutralize the TDI effect.

The loadings are the weights with which the X-variables are combined to form the X-scores. Figure 5-3C represents the importance of the metabolites in the selected component and hence reveals which

metabolites show the correlation structure or describe the similarity and dissimilarity between our samples. As Figure 5-3C shows, insulin secretion dominates the first principal component and pre-culture duration nearly dominates the second principal component. The pre-cultured time period is negatively correlated to insulin secretion in component 1. The loading plot (Figure 5-3C) illustrates which metabolites mainly account for this clustering along the corresponding principal component. Thus, those metabolites farthest away from the origin of the coordinates along the first PC could be considered as biomarkers for GSIS and, similarly, those along the second PC could be considered to contribute to TDE.



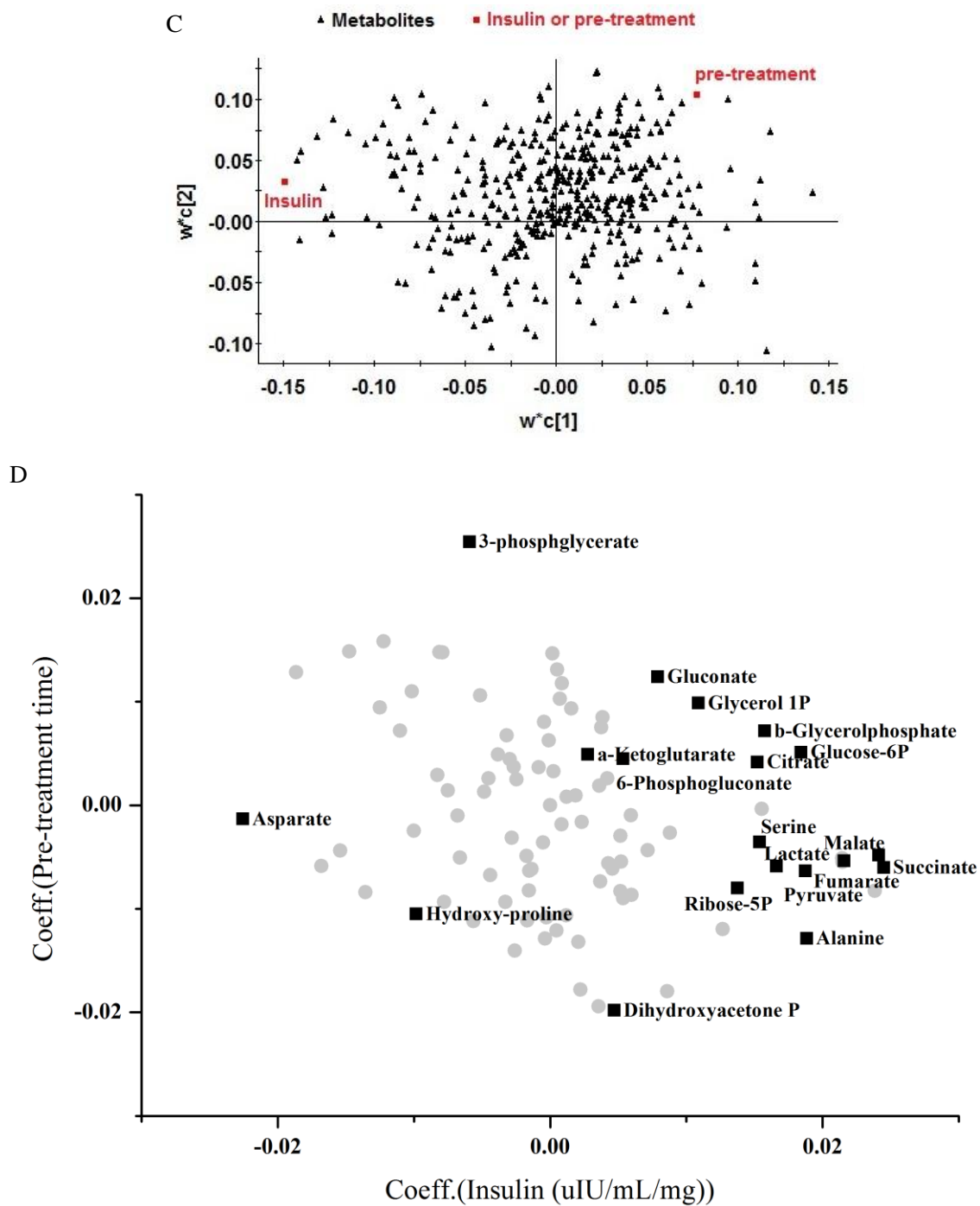


Figure 5-3 Orthogonal projection to latent Structures (OPLS) analysis on metabolome showing time-dependent effects

(A) Model overview to show the summary of the fit of the model. The figure displays cumulative $R^2Y_{(cum)}$ (fraction of the variation of the data explained by each component) and cumulative $Q^2Y_{(cum)}$ (fraction of the information of the data predicted by each component in new model). The two Y (insulin and pre-treatment) are correlated and are summarized by three new predictive variables, the scores t1 to t3, explaining 96% of the variation. (B) Score plot of t1 vs. t2 to show the observations cluster in different groups. Each group represents a setting of the experimental design. The ellipse represents the Hotelling T2 with 95% confidence. The scores t1 and t2, one vector for components 1 and 2, are new variables computed as linear combinations of all the original variables to provide a good summary of our samples. No obvious outliers are present in our data. The score plot shows that low glucose (LG)-treated samples are separated from high glucose (HG)-treated samples by t1 and then they are further separated into 3 different sub-groups by t2 based on the pre-treatment time. 2hr, 3hr and high glucose treated group diffuses from 1 hr and high glucose treated group. (C) Loading plot of component 1 vs. component 2 used to show which variables describe the similarity and dissimilarity between groups. Metabolites close to insulin secretion (one Y variable) are positive correlated to insulin secretion and those far away from insulin secretion are negatively correlated to insulin secretion. Our data set shows that some metabolite with both high weight on component 1 and component 2 are correlated to both insulin secretion and pre-treatment (another Y variable). Some other metabolites only with high weight value on component 1 are more correlated to pre-treatment than insulin. (D) Coefficient plot summarizes the relationship between the Y variables (insulin secretion and pre-treatment) and the X variables (metabolites). X-axis represents coefficient over insulin secretion and Y-axis represents coefficient over pre-treatment. The metabolites with the highest or lowest X values are either positive or negatively correlated to insulin, and vice versa. Metabolites with the highest or lowest Y values are either positive or negatively correlated to pre-treatment.

The loading plot shown in Figure 5-3C, however, only reveals the correlation structure between metabolites and samples along the first two PCs. In order to get a complete picture of the metabolomic data, a coefficient plot is generated in Figure 5-3D, in which the coefficient over insulin secretion is plotted as the x-axis and the coefficient over pre-culture duration is plotted as the y-axis. The coefficient summarizes the relationship between our samples and metabolites over all principal components. The metabolites farther away from the origin of the coordinates along the axis could be considered as the biomarkers contributing more to that factor. Our coefficient plot (Figure 5-3D)

shows that, almost all TCA cycle intermediates and most glycolytic metabolites are more correlated to insulin secretion, since they have high positive x-values and low y-values. Likewise, 3-phosphoglycerate and dihydroxyacetone phosphate are metabolites which are suggested (either positively or negatively) to correlate to TDE as shown in Figure 5-3D. Ribose-5-phosphate and alanine might also negatively correlate to the TDE. There are still some other potential coupling factors, however, they are not listed in our figure because either their function or their names are unknown.

5.3.4 Coupling factors of time-dependent effect

The metabolites identified in our study are involved in almost 30 metabolic pathways, such as glycolysis, TCA cycle, PPP, amino acid, fatty acid and nucleotides metabolism.

As shown in Figures 5-4, glucose-6-phosphate, dihydroxyacetone phosphate (DHAP), 3-phosphoglycerate and lactate are all correlated with both GSIS and the TDE. The level of some metabolites increased with a longer pre-culture duration, approximately by 67.9% ($\pm 9.5\%$) for glucose 6-phosphate and 156% ($\pm 12.1\%$) for 3-phosphoglycerate. The level of others decreased as pre-culture time persisted, approximately by 80.8% ($\pm 5.3\%$) for DHAP and 51.5% ($\pm 10.6\%$) for lactate. As multivariate analysis (MVA) suggested, DHAP and 3-phosphoglycerate, either negatively or positively associated with TDE, were actually the most significant metabolic intermediates.

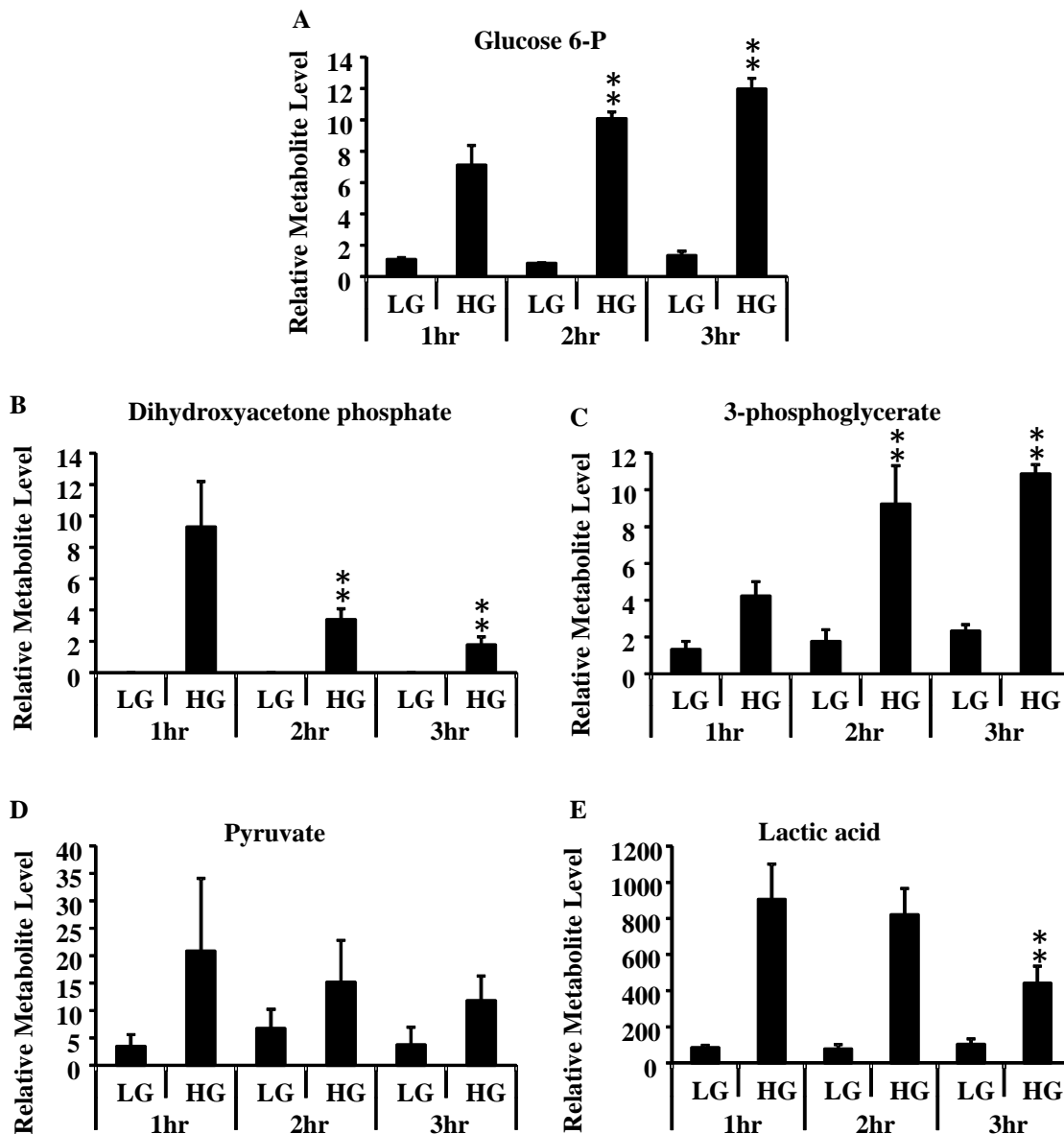


Figure 5-4 Time-dependent effects revealed by glycolytic intermediates

Metabolites are isolated from INS-1 832/13 beta cells, run on GC/MS and identified by searching spectra against Fiehn library. The metabolites levels are normalized by internal standards (Myristic acid D-27). A) Glucose-6-phosphate, B) dihydroxyacetone phosphate, C) 3-phosphoglycerate, D) Pyruvate, E) Lactic acid. (LG = 2 mM glucose; HG = 10 mM glucose) (n=4). 1 hr LG versus 2hr or 3hr LG #, $p < 0.05$; ##, $p < 0.01$; 1 hr HG versus 2hr or 3hr HG *, $p < 0.05$; **, $p < 0.01$.

All TCA cycle intermediates also positively contributed to the clustering of samples along insulin secretion, a finding which was in line with all previous studies [319, 320, 343]. However, in terms of their relationship to TDE, the TCA cycle seems to be split into two mini-cycles. The first half cycle, represented by citrate and alpha-ketoglutarate, was positively correlated with TDE, since metabolite levels were up-regulated (40 percent for alpha-ketoglutarate and 140 percent for citrate) in cells treated with stimulatory glucose as pre-stimulatory period extended. The second half cycle, represented by succinate, fumarate and malate, was negatively correlated with TDE, since the intermediates' levels were down-regulated by 54 percent for succinate, 57 percent for fumarate and 75 percent for malate along pre-stimulatory duration in cells treated with non-stimulatory glucose. In addition to glycolysis, another glucose cytosolic metabolism pathway---the PPP---represented by gluconate, 6-phosphogluconate and ribose-5-phosphate in our study, was correlated with both insulin secretion and the pre-stimulatory period. The metabolite intermediate levels were increased 167 percent for gluconate, 250 percent for 6-phosphogluconate and 50 percent for ribose-5-phosphate by stimulation of glucose as pre-culture time extended. Similarly, glycerol 1-phosphate, another glucose cytosolic metabolite involved in the polyol pathway, was increased by 118 percent by stimulation of glucose as pre-culture time extended. Another similar product, glycerol-2-phosphate, was up-regulated by 94 percent in the same condition.

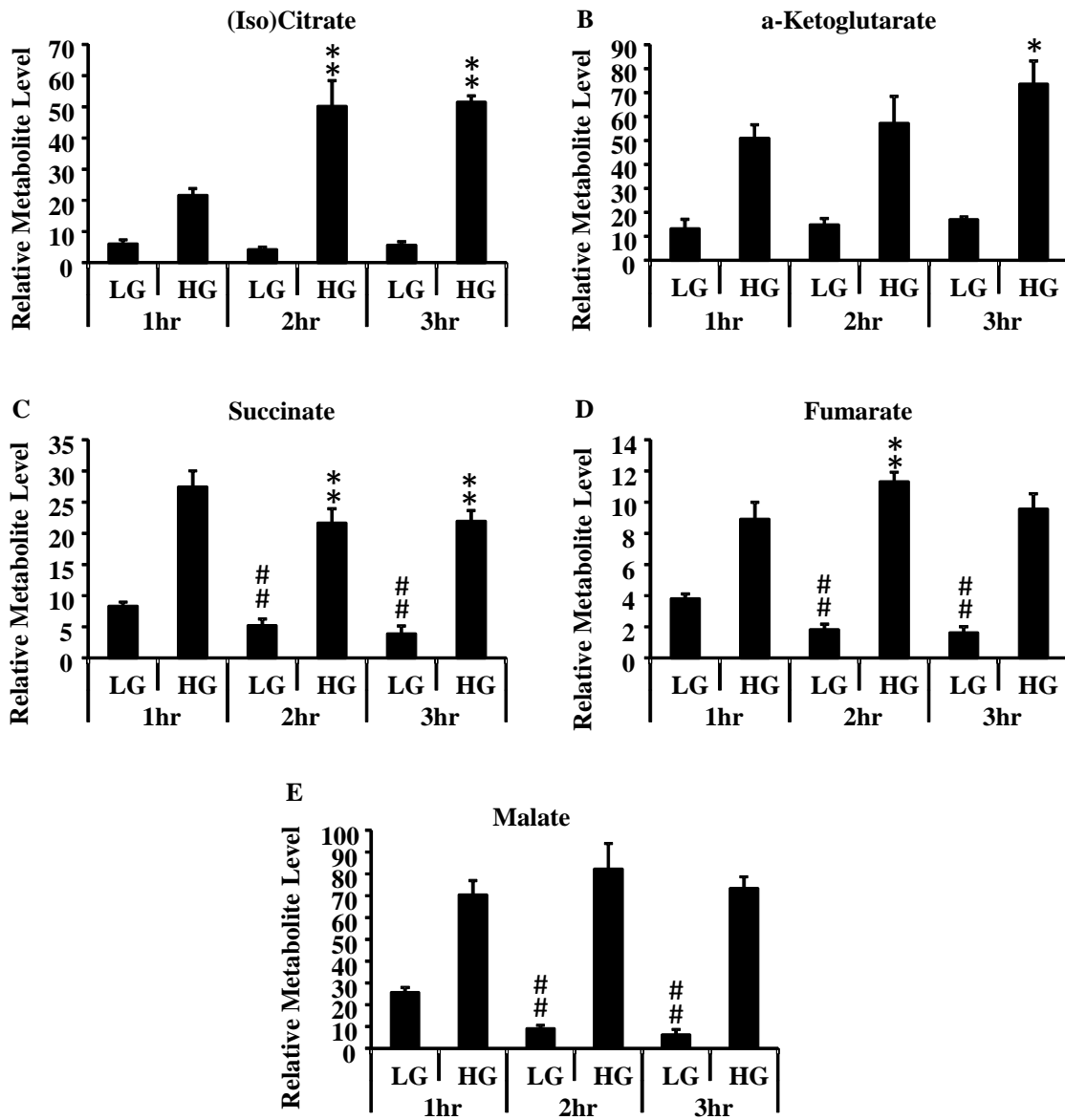


Figure 5-5 Time-dependent effects revealed by TCA intermediates

Metabolites are isolated from INS-1 832/13 beta cells, run on GC/MS and identified by searching spectra against Fiehn library. The metabolites levels are normalized by internal standards (Myristic acid D-27). A) Citrate/Isocitrate, B) alpha-Ketoglutarate, C) Succinate, D) Fumarate, E) Malate. (LG = 2 mM glucose; HG = 10 mM glucose) (n=4). 1 hr LG versus 2hr or 3hr LG #, $p < 0.05$; ##, $p < 0.01$; 1 hr HG versus 2hr or 3hr HG *, $p < 0.05$; **, $p < 0.01$

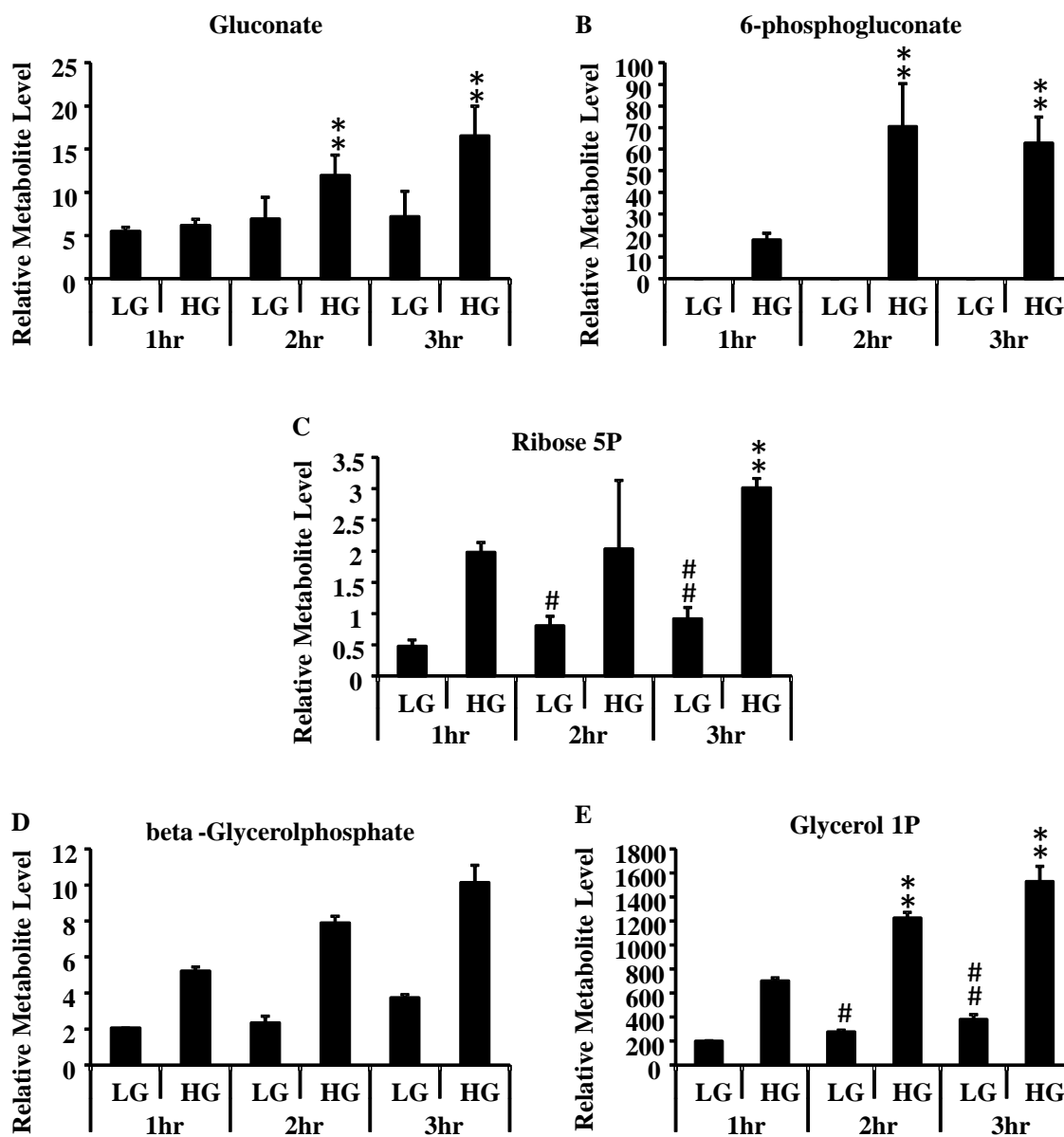


Figure 5-6 Time-dependent effects revealed by pentose phosphate pathway intermediates

Metabolites are isolated from INS-1 832/13 beta cells, run on GC/MS and identified by searching spectra against Fiehn library. The metabolites levels are normalized by internal standards (Myristic acid D-27). A) Gluconate, B) 6-phosphogluconate, C) Ribose-5-phosphate, D) beta-Glycerolphosphate, E) Glycerol-1-phosphate. (LG = 2 mM glucose; HG = 10 mM glucose) (n=4). 1 hr LG versus 2hr or 3hr LG #, $p < 0.05$; ##, $p < 0.01$; 1 hr HG versus 2hr or 3hr HG *, $p < 0.05$; **, $p < 0.01$

Alanine and hydroxy-proline both were negatively correlated with TDE, since metabolite levels decreased along pre-culture time by as much as 80 percent for alanine and 90 percent for hydroxyl-proline under either non-stimulatory or stimulatory glucose conditions. Despite their different roles in regulation of GSIS, both serine and aspartate levels under stimulation of stimulatory glucose were increased along pre-culture time.

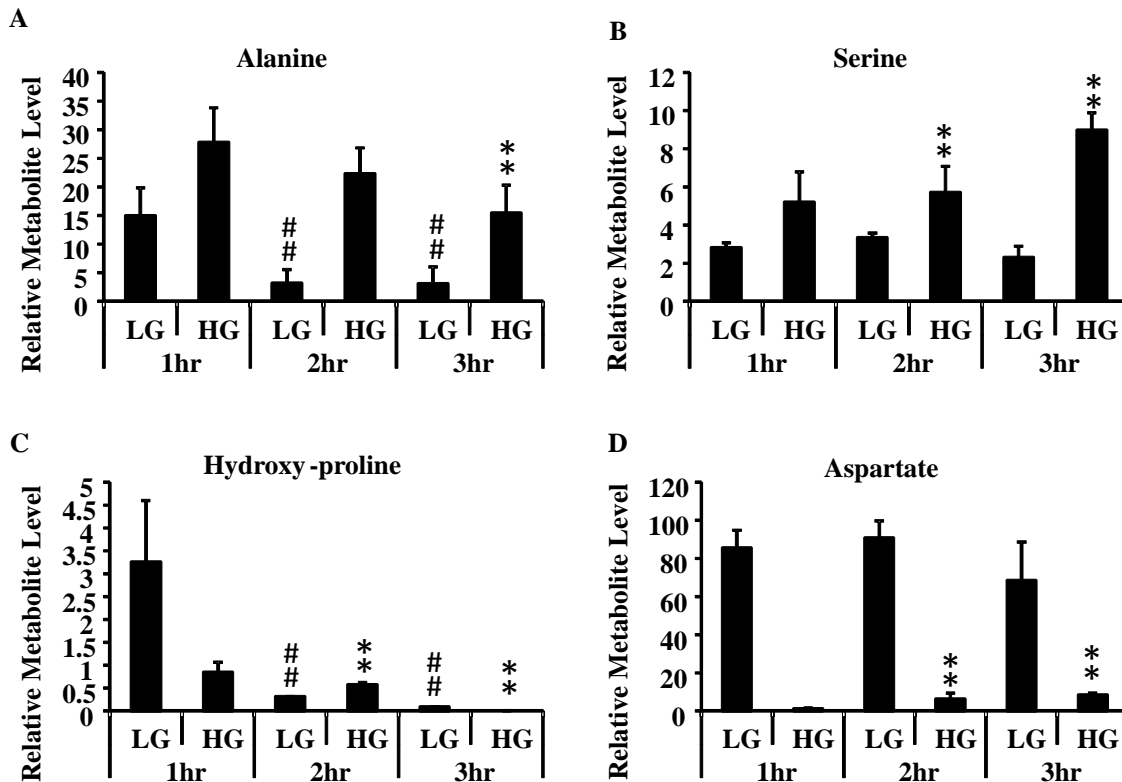


Figure 5-7 Time-dependent effects revealed by amino acids

Metabolites are isolated from INS-1 832/13 beta cells, run on GC/MS and identified by searching spectra against Fiehn library. The metabolites levels are normalized by internal standards (Myristic acid D-27). A) Alanine, B) Serine C) Hydroxy-proline, D) Aspartate. (LG = 2 mM glucose; HG = 10 mM glucose) (n=4). 1 hr LG versus 2hr or 3hr LG #, $p < 0.05$; ##, $p < 0.01$; 1 hr HG versus 2hr or 3hr HG *, $p < 0.05$; **, $p < 0.01$

5.4 Discussion

Under physiological conditions, the pancreatic beta cell is never subjected to short-lasting stimulations. At any given time, the secretory activity of pancreatic beta cells is not only influenced by the present stimuli, but is also conditioned, either positively or negatively, by the memory of past stimuli. Therefore, the study of these regulatory mechanisms is imperative when determining the molecular basis of dynamic insulin secretion.

As seen in Figure 1, when INS-1 832/13 cells were primed with 2 mM glucose for different periods of time, a TDI of insulin secretion was observed in cells treated with a non-stimulatory glucose, but not in cells treated with glucose at the stimulatory level. Cells appeared to secrete approximately the same amount of insulin, regardless of pre-culture conditions, which could be a result of either a deficiency of TDI or, alternatively, the neutralization of TDI by an opposing mechanism, e.g. TDP. In order to discriminate between these two possible mechanisms, insulin secreted within the first 10 min. of stimulatory glucose exposure was measured and exhibited a clear increasing pattern over pre-culture time. This observation suggests the existence of an opposing potentiation effect that neutralizes the TDI effect. Interestingly, this potentiation effect occurred at the same time as the peak observed in the first phase of insulin secretion.

This potentiation effect elicited by stimulatory glucose was further supported by our metabolomics data shown in Figure 5-2F. In the absence of TDI, metabolic activity should remain relatively stable even with changing pre-culture conditions. However, as seen in Figure 5-2F, many metabolite levels were distinctly up-regulated as pre-stimulatory period prolongs. Hence, we conclude that TDI is present in cells treated with both basal and stimulatory glucose. However, in the latter case, an opposing mechanism also exists which neutralizes the TDI effect making it seemingly invisible. Therefore, distinct changes in the metabolome in response to glucose could be anticipated, enabling us to develop a metabolomic analysis of pancreatic beta cells to investigate the mechanism of TDE.

Our OPLS model, as shown in Figure 5-3 not only supports the conclusion drawn from the above data, but also enables the discovery of potential coupling factors mediating TDE by effectively summarizing the data (98.7% information was reflected by new data). Among all the metabolites detected by our system, 19 well-studied metabolites were found to be strongly associated with the metabolic response of cells to either insulin secretion or TDE (Figure 5-3D).

As the coefficient plot (Figure 5-3D) shows, two glycolytic intermediates, DHAP and 3-phosphoglycerate, are identified as the most significant coupling factors involved in TDE, although

one is positively and the other is negatively correlated to TDE. DHAP, one of two products of generated by fructose 1,6-bisphosphate breakdown, is the only glycolytic metabolite that cannot be used directly and hence, needs to be converted to glyceraldehyde 3-phosphate (GADP) (the other produce generated by fructose 1,6-bisphosphate breakdown) for the further process in glycolysis. Therefore, the divergence brought in by DHAP provides a good opportunity for transmitting the message carried by glycolysis to other metabolic pathways. DHAP is also involved in a cytosolic glucose metabolism pathway, the polyol pathway, which is speculated to play a certain role in insulin secretion of primary human islets as our data shows (Figure 3-11).

The steady-state quantity of each metabolite is the net balance between its production and consumption. Hence, the observed decrease in DHAP should result from either the relative decrease of its available upstream metabolites, e.g. fructose 1,6-bisphosphate, or the relative increase in production of its down-stream metabolites, e.g. GADP, and/or alpha-glycerolphosphate (alpha-GP). Neither fructose 1,6-bisphosphate nor GADP were detected by our system. However, three other affected compounds were identified. Glucose 6-phosphate (G6P), the upstream metabolites of fructose 1,6-bisphosphate, along with the downstream intermediates of DHAP and 3-phosphoglycerate (3PG) and alpha-GP, were elevated in our study.

Both alpha-GP and DHAP are essential intermediates for the glycerol phosphate shuttle. As our data shows, despite the elevated alpha-GP level, DHAP is markedly decreased by a longer pre-culture period, and could potentially lead to a decrease of cytosolic NAD^+/NADH ratio. NADH re-oxidation is tightly regulated in pancreatic beta cells to maintain an optimal NAD^+ level such that glycolysis remains unhindered [405, 406]; hence the postulated decrease of NAD^+/NADH ratio will likely affect glycolysis. Similar to the decreased DHAP: alpha-GP ratio, malate and aspartate, two intermediates in the malate-aspartate shuttle, which is another cycle to regenerate NADH, were also reversely correlated to TDE and could cause a reduction of NAD^+/NADH ratio. Additionally, the reduced lactate output observed in samples pre-treated for a longer time also fits nicely with the above observations. The extension of pre-stimulatory period decreased lactate output (Figure 5-4E). The generation of lactate is governed by lactate dehydrogenase (LDH), which remains highly active in insulinoma-derived beta cell lines [407, 408], and leads to the re-oxidation of NADH. Hence a preliminary conclusion can be drawn that cytosolic redox state, reflected by DHAP: alpha-GP ratio, malate-aspartate shuttle activity as well as lactate output, could mediate the TDI effect.

The reduction in DHAP: alpha-GP ratio is related to the activity occurring in the glycerol phosphate shuttle. The oxidation of alpha-GP to DHAP can be achieved by two reactions: a NAD^+ -linked

cytosolic glycerol phosphate dehydrogenase and/or a mitochondrial FAD-linked glycerol phosphate dehydrogenase in the glycerol phosphate shuttle. Formation of DHAP from alpha-GP by the cytosolic glycerol phosphate dehydrogenase is an equilibrium reaction that should not alter the DHAP:alpha-GP ratio [405]. On the contrary, oxidation of newly formed alpha-GP to DHAP by the FAD-linked glycerol phosphate dehydrogenase in the mitochondrial loop of the glycerol phosphate shuttle does affect the DHAP:alpha-GP ratio [405, 406, 409, 410]. Thus, the elevation of alpha-GP and the decrease of DHAP could result from the blocking or decrease of mitochondrial FAD-linked glycerol phosphate dehydrogenase activity, suggesting that glucose mitochondrial metabolism is involved in mediating TDP.

Two potential coupling factors for TDE, 3-phosphoglycerate [97, 411] and citrate [97], were shown to couple glucose sensing to insulin exocytosis by specifically inactivating divalent-cation independent serine/threonine protein phosphatase (PPase) [97, 411, 412]. Complementary to the increased activity of protein kinases, PPase inhibition is believed to be an important mechanism also contributing to and further augmenting the event elicited by phosphorylation-stimulated pancreatic beta cell regulatory proteins [413] during stimulation of insulin exocytosis, including the hyper phosphorylation and hence activation of voltage-activated L-type Ca^{2+} channels [97, 98, 413-416]. Hence, the TDI effect was obscured in stimulatory glucose-treated beta cells probably by the activation of insulin exocytosis resulting from the elevation of 3-phosphoglycerate and citrate.

However, this counteracting mechanism neutralizes but does not overcome the naturally elicited TDI effect on insulin secretion, likely because there is not enough insulin content and succinate-mediated proinsulin biosynthesis to sustain an observable potentiation effect. Although insulinoma cell line INS-1 retains many important characteristics of primary pancreatic beta cells and sustains the responsiveness to glucose within the physiological range, the total insulin content is only 20% of that of the native cells [417]. On the other hand, the regulation of insulin secretion and proinsulin biosynthesis have been shown to be tightly coupled, so that under normal circumstances intracellular insulin stores are replenished optimally and in a timely fashion for a proper insulin secretion upon demand [418-420]. This inconsistency can be explained by the action of succinate, which is an important coupling factor for glucose-stimulated proinsulin biosynthesis in rat pancreatic islets [421-423]. Since succinate was affected by pre-stimulation, it might cause an uncoupling of insulin secretion and proinsulin synthesis, in addition to the depressed insulin content of INS-1 insulinoma cells, which might explain the difference of TDE between primary pancreatic beta cells and insulinoma cell line.

As our data suggest, the TCA cycle seems to be split into two mini-cycles based on their response to the pre-stimulatory period. With an increase in pre-culture duration, the first half cycle from citrate to alpha-ketoglutarate was up-regulated by stimulatory glucose and the second half from succinate to malate was down-regulated by non-stimulatory glucose as pre-stimulatory period persisted. This phenomenon agrees with the investigation done by Rustin and Yudkoff [424, 425], which suggests that the TCA cycle is comprised of two mini-cycles that are interconnected by the malate-aspartate shuttle [425], with one segment ranging between oxaloacetate and alpha-ketoglutarate, whereas the other segment extends from alpha-ketoglutarate to oxaloacetate [424]. This alternate conceptualization of the TCA cycle is supported by the observation that both segments can operate at different rates. As evidenced in rat brain synaptosomes, the metabolite flux between alpha-ketoglutarate and oxaloacetate was estimated to be three to five fold higher than that between oxaloacetate and 2-oxoglutarate. The branch of anaplerosis that enhances the supply and utilization of alpha-ketoglutarate in the TCA cycle also plays an essential role in the generation of TDP [403], but the mechanism and the down-stream pathways have yet to be elucidated. As seen in our unpublished data, there is evidence that it might be acting through alpha-ketoglutarate hydroxylases [95].

The role of the PPP in GSIS is still under investigation, since a number of studies in the last 30 years have produced some contradictory results [33, 77, 150, 346-348]. Based on our unpublished data in Figure 3-11D, the PPP and polypol pathway are speculated to affect TDE through a potentiating mechanism, which also contributes to the regulation of GSIS in human islets (Figure 3-11). This TDP provides a dynamic feedback mechanism and can adapt pancreatic beta cells to changes of environment, which is extremely useful for maintaining a good glucose homeostasis. The disruption of this feedback mechanism could lead to the partial functional loss of beta cells and eventually to development of type 2 diabetes.

Additional amino acids, such as alanine, glycine, and serine, are known to induce a greater enhancement of both glucagon and insulin secretion than other amino acids [371], but their exact function in pancreatic beta cells remains elusive. Metabolomics is an important tool to study insulin secretion, because it is driven by glucose metabolism. However, as shown in our study, data mining and data interpretation of such a complex data set in a systematic way still highly relies on the researchers' experience and knowledge.

Aside from a few inherent drawbacks, such as derivatization, which might introduce bias into a metabolomics analysis, GC-MS is still considered to be one of the best metabolite detection and

measurement technologies due to its good sensitivity, high resolution, decent reproducibility and nice robustness. As our study showed, untargeted metabolomics coupled with powerful chemometric analysis provides a comprehensive data set, which, when contextualized with proper and abundant knowledge of metabolic pathways and/or signaling networks, can fuel a truly mechanistic biochemical study, and can even lead to an unanticipated discovery complementary to the original topic investigated. However, as the core of a robust mechanistic study, proper verification and more strict validation are required to assist the interpretation of metabolomics data, since the cause-effect relationships cannot be revealed by metabolomics.

5.5 Conclusion

It is concluded that TDE does exist in the INS-1 832/13 cell line, and pre-culturing cells in non-stimulatory glucose does affect acute stimulation-secretion coupling in the following way: the longer the pre-culture time, the higher the acute insulin response. In fact, the acute stimulation on insulin secretion, which can be easily modified by pre-culture, likely constitutes the first phase of biphasic insulin secretion. However, regardless of the pre-culture condition, the same amount of insulin secretion was elicited by stimulatory glucose as a result of the net balance between the concurrent acute stimulation, as well as TDI and TDP for applied-stimuli lasting longer than threshold duration. As our metabolomics data suggested, TDI effect may be regulated by the redox state of pancreatic beta cells, reflected by DHAP: alpha-GP ratio, the diminished malate-aspartate shuttle activity, the lowered lactate output and the altered NAD^+/NADH ratio. Alternatively, TDP is mainly correlated to phosphorylation-mediated insulin exocytosis, which is, probably coupled to succinate-regulated pro-insulin biosynthesis. Because TDI is directly mediated by glucose metabolism and TDP is likely correlated with the proximal part of the stimulus-response coupling pathway, e.g. glucose-stimulated insulin exocytosis as well as pro-insulin biosynthesis, TDI is generated sooner than TDP as reported. In summary, our study unravels important metabolic pathways involving glycolysis and anaplerosis that differentially modulate TDI and TDP in response to previously applied glucose and hence constitute biphasic insulin secretion. Furthermore, our study proves the tremendous promise offered by the application of metabolomics in the mechanistic study of biochemical research.

Chapter 6

Hydroxylation, an Important Mechanism in Regulation of Glucose Metabolism

6.1 Overview

The metabolic pathways involved in regulating glucose stimulated insulin secretion (GSIS) remain incompletely understood. Previous studies have pointed to glucose derived anaplerotic and cataplerotic signals as part of the regulation mechanism. Of all possibilities, alpha-ketoglutarate and its relevant effectors have received the most attention. Our study demonstrates that inhibition of alpha-ketoglutarate dependent hydroxylation resulting from iron deficiency created by ethyl-3,4-dihydroxybenzoate (EDHB) has a dose-dependent effect on GSIS in both INS-1 cell lines and primary rat islets. Low dosage EDHB can promote a moderate increase of insulin secretion by enhancing beta cell oxygen consumption used for ATP generation without altering glycolytic influx. However, a high level of EDHB severely impairs pancreatic beta cell secretion competency by attenuating both cytoplasmic and mitochondrial glucose metabolism, as seen through a reduction of both glycolytic and anaplerotic metabolites. The fact that neither the expression nor the function of hypoxia-inducible factor-1alpha (HIF-1alpha) is altered indicates that short-term inhibition of hydroxylation can work through a HIF-1alpha independent mechanism. Based on these data, our study suggests iron-dependent hydroxylation is important for both cytoplasmic and mitochondrial glucose metabolism and may play a critical role in regulation of pancreatic beta cell secretion function.

6.2 Introduction

Despite decades of efforts, only one well-established glucose metabolism and insulin secretion coupling pathway is widely accepted by scientists studying insulin secretion. This pathway is initiated by an increase in the ATP/ADP ratio leading to inhibition of ATP-sensitive K^+ (K_{ATP}) channels, plasma membrane depolarization, activation of voltage-gated Ca^{2+} channels, and eventually influx of extracellular Ca^{2+} serving to activate insulin granule exocytosis [48, 50, 65, 426]. This pathway is hence referred to as the K_{ATP} channel dependent pathway or triggering pathway. However, other studies revealed that islets were still able to retain their insulin secretion function in conditions

lacking functional K_{ATP} channels [60-62, 64] or when K_{ATP} channels were held open [56, 57]. Accordingly, this unknown coupling mechanism between glucose metabolism and insulin secretion was called the K_{ATP} channel independent pathway or amplifying pathway [109]. This pathway has been suggested, by accumulating evidence, to potentially involve the activity of several other coupling factor(s) that link mitochondrial metabolism to insulin secretion, such as GTP [331, 427], glutamate [94, 339, 428, 429], malonylCoA/LC-CoA [336, 337, 430], NADPH [338, 431, 432] and pyruvate carboxylase (PC) -mediated anaplerosis [49, 76, 81, 84, 353, 433, 434].

The correlation between GSIS and pyruvate cycling has led to active investigations of glucose-derived anaplerosis and cataplerosis to elucidate the mechanism of K_{ATP} channel independent pathway in regulation of fuel-induced insulin secretion [76, 80-82, 84]. Of particular interest are the coupling factors generated by the pyruvate-isocitrate cycling pathway. In this pathway, both citrate and isocitrate leave mitochondria through the citrate-isocitrate carrier (CIC), and enter the cytoplasm where they are converted into alpha-ketoglutarate by a cytosolic NADP-dependent isocitrate dehydrogenase (ICDc) (citrate is first converted into isocitrate by cytosolic aconitase before ICDc can act on it). Alpha-ketoglutarate can flux back into TCA cycle in the mitochondria via 2-oxoglutarate carrier (OGC). The importance of this pathway has been underlined by studies showing that suppression of CIC, ICDc and OGC strikingly impaired GSIS [81, 82, 84].

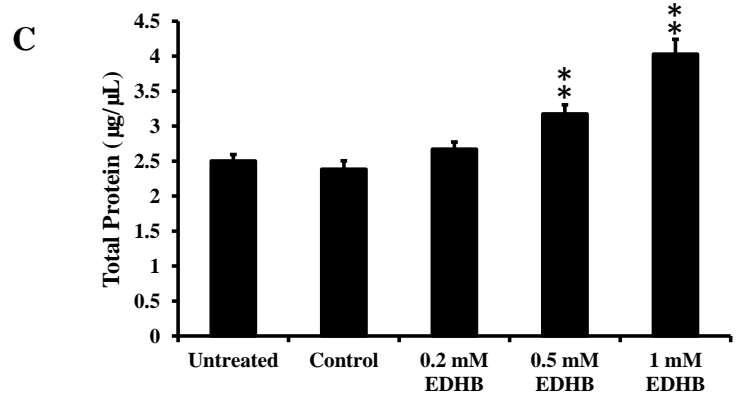
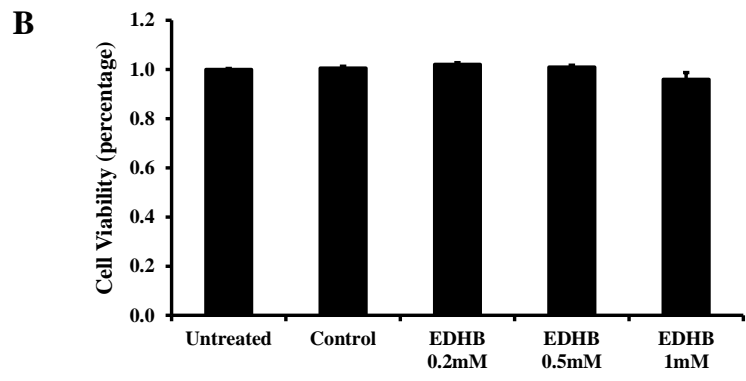
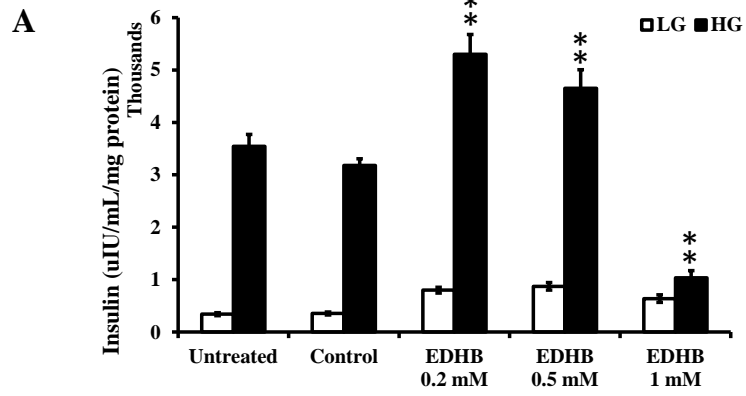
In addition to its involvement in pyruvate-isocitrate cycling, alpha-ketoglutarate has been implicated in insulin secretion by two other recent studies. First, alpha-ketoglutarate itself can act as an insulin secretagogue [435]. Second, alpha-ketoglutarate-dependent hydroxylases have been shown to participate in GSIS, either directly or indirectly [95, 96]. The Fe(II)/alpha-ketoglutarate-dependent hydroxylase superfamily serves to catalyze a variety of reactions, in which decarboxylation of alpha-ketoglutarate produces succinate and CO_2 and an active oxygen species leading to the hydroxylation of the primary substrate [390]. Inhibitors of alpha-ketoglutarate-dependent hydroxylases promptly decrease insulin secretion in rat pancreatic islets [95]. In the long term, increase of hypoxia-inducible factor-1alpha (HIF-1alpha) levels by deferoxamine (DFO) or deferasirox (DFS), which stops HIF-1alpha hydroxylation via iron chelation, enhances insulin secretion and beta cell function in mice [96]. These studies suggest that Fe(II)/alpha-ketoglutarate-dependent hydroxylases might be important effectors in defining the extramitochondrial role of alpha-ketoglutarate in insulin secretion. To explore the role of Fe(II)/alpha-ketoglutarate-dependent hydroxylases in regulation of insulin secretion, ethyl-3,4-dihydroxybenzoate (EDHB), a cell-permeable inhibitor that competitively binds to prolyl hydroxylases (PHDs) which initiates ubiquitination and proteolysis of HIF-1alpha by

hydroxylating the proline residue, was used to impair iron-dependent hydroxylation in pancreatic beta cells. Our study of the effect of EDHB on beta cell stimulus secretion provides convincing evidence that iron-dependent hydroxylation plays an important role in regulation of insulin secretion through a HIF-1alpha independent mechanism.

6.3 Results

6.3.1 EDHB affects insulin secretion in INS-1 832/13 cells

An insulin secretion assay was performed first on INS-1 832/13 cells to test the effect of EDHB on pancreatic beta cells. As Figure 6-1A shows, 0.2 mM EDHB markedly improved insulin secretion by 58 percent and 0.5 mM EDHB also had a similar effect on INS-1 832/13 cells treated with stimulatory glucose concentrations (10 mM glucose). However, high dosage EDHB (1mM) significantly decreased insulin release in static incubation studies by $70 \pm 4\%$ as compared to control cells (Figure 6-1B), without affecting cell viability. In fact, total cellular protein levels were increased $25 \pm 5\%$ by 0.5 mM EDHB and $60 \pm 8\%$ by 1 mM EDHB as shown in Figure 6-1C.



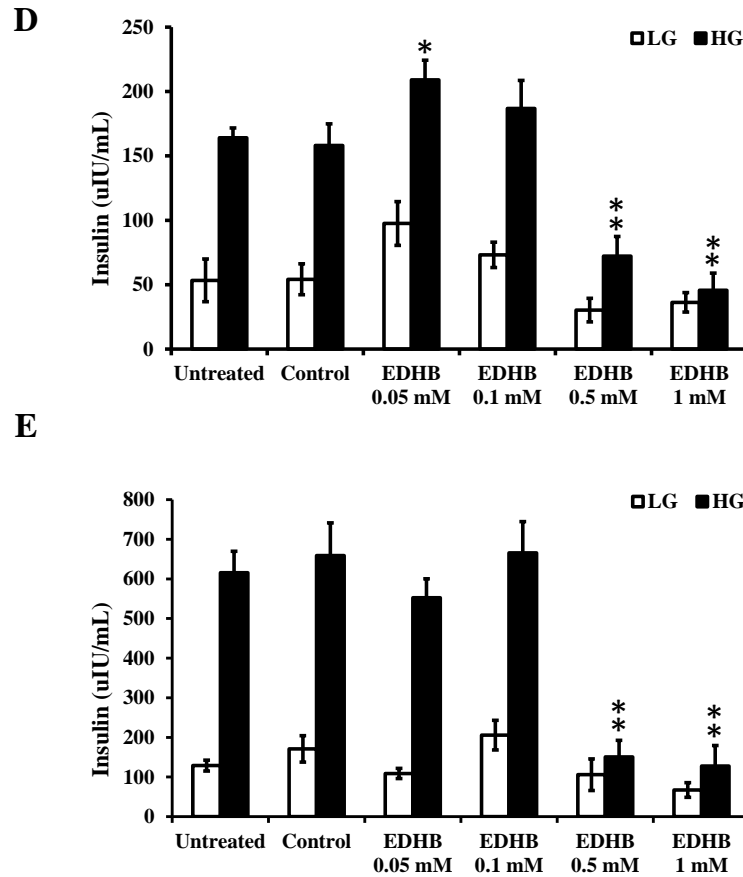


Figure 6-1 Effects of EDHB on insulin secretion and cell viability

Different dosage of EDHB was used to treat either cells or islets and then (A) insulin secretion, (B) cell viability and (C) total protein level in INS-1 832/13 cells, and insulin secretion on (D) rat islets (E) human islets were measured. Results represent mean \pm S.E. (n = 6-12 replicates incubations for each condition). LG, low glucose (2 mM); HG, high glucose (10 mM). Non-treated versus treated group, * p < 0.05; ** p < 0.01 versus same secretagogue condition without ethyl-3,4-dihydroxybenzoate (EDHB) for insulin secretion.

6.3.2 EDHB affects insulin secretion in primary rat and human islets

The effect of EDHB on insulin secretion was further investigated by running an insulin secretion assay on primary islets. Although the low dosage amounts differed from that used in INS-1 832/13 cells, the same dose-dependent reverse effect was observed on freshly isolated rat islets as shown in Figure 6-1D, in which cells treated with 0.05 mM EDHB were able to secrete 30 percent more insulin

than untreated cells. Treatment with the intermediate dose of 0.1 mM EDHB seemed to have a slight effect on enhancing insulin secretion, but was not significant. However, high dosages of EDHB, represented by 0.5 mM and 1 mM, impaired insulin release in rat islets (Figure 6-1D) to almost the same extent (by $70 \pm 8\%$) as that observed in INS-1 832/13 cells (Figure 6-1C). The insulin secretion deficiency elicited by high dosage of EDHB was even more noticeable in human islets (Figure 6-1E) compared to rat islets. The loss of insulin secretion at stimulatory glucose level was as high as 79.97 ± 8.1 percent. Similarly, a small amount of EDHB did not seem to alter secretion function in human islet.

6.3.3 EDHB affects glucose utilization and oxygen consumption

Glucose metabolism is tightly coupled to insulin secretion in pancreatic beta cells. Glucose utilization and oxygen consumption are two factors indicating the overall glucose metabolism as well as the activity of pancreatic beta cells. Hence, both glucose utilization and oxygen consumption were assessed to evaluate the effect of EDHB on glucose metabolism. As expected, stimulatory glucose (10 mM) induced a 6 fold increase (± 0.35) in glycolytic flux and 1.8 fold increase (± 0.04) in oxygen consumption from both untreated and control (treated with the same amount of ethanol used to dissolve EDHB) INS-1 832/13 cells (Figure 6-2A). 1mM EDHB treatment resulted in $40 \pm 5\%$ decline of glycolytic flux (Figure 2A), but had no obvious effect on oxygen consumption (Figure 6-2B). On the contrary, 0.2 mM EDHB caused 1.7 fold increase (± 0.18) in oxygen consumption (Figure 6-2B), but did not affect glycolytic flux (Figure 6-2A). Further analysis showed that the oxygen consumption specifically needed for ATP generation (Figure 6-2C) was raised by the same ratio as the overall oxygen consumption in 0.2 mM EDHB treated cells. On the other hand, cells treated with 1 mM EDHB used $60 \pm 5\%$ less oxygen for ATP generation, also seen in Figure 6-2C.

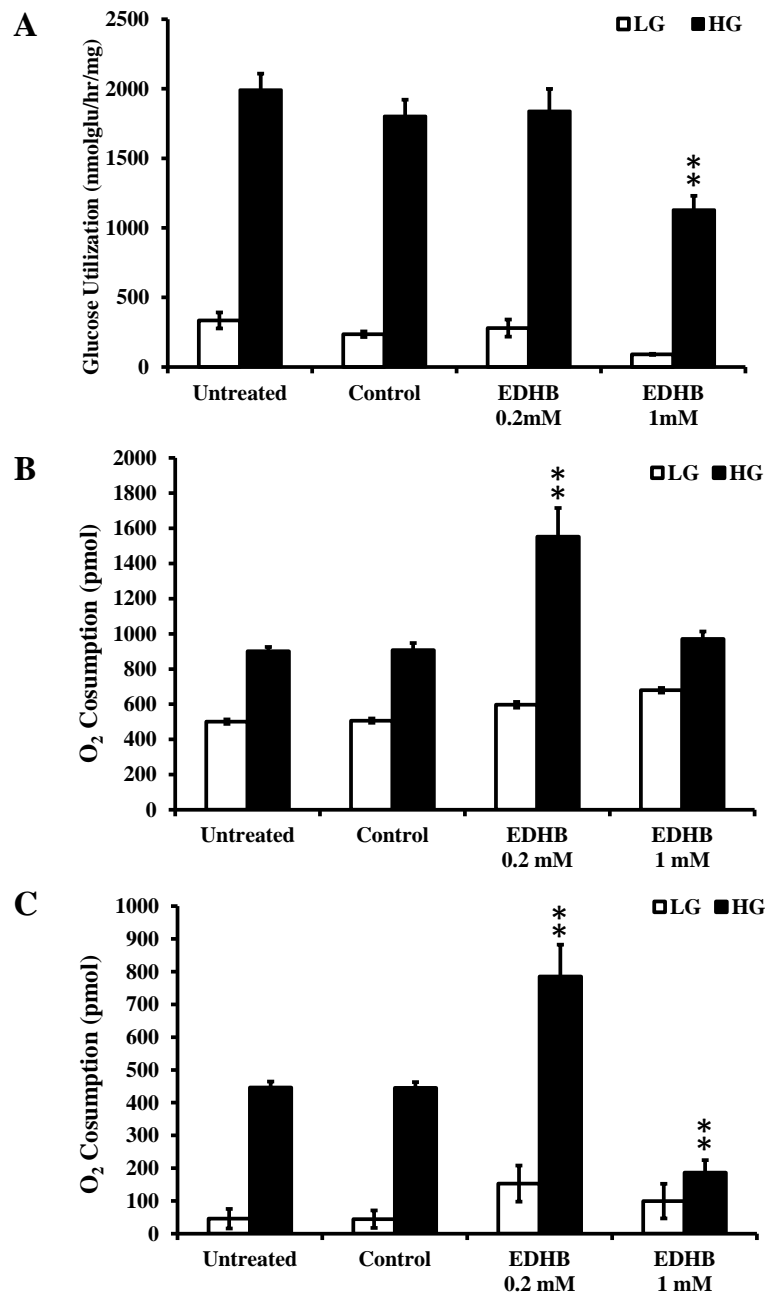


Figure 6-2 Effects of EDHB on glucose metabolism

Different dosage of EDHB was used to treat either cells or islets and then (A) glucose utilization and (B) oxygen consumption and (C) oxygen consumed for ATP generation in INS-1 832/13 cells were measured. Results represent mean \pm S.E. (n = 8~18 replicates incubations for each

condition). LG, low glucose (2 mM); HG, high glucose (10 mM). * $p < 0.05$; ** $p < 0.01$ versus same secretagogue condition without ethyl-3,4-dihydroxybenzoate (EDHB).

6.3.4 EDHB has no effects on HIF-1alpha expression or function

EDHB is a cell-permeable inhibitor that competitively binds to prolyl hydroxylases (PHDs), which initiates ubiquitination and proteolysis of HIF-1alpha by hydroxylating proline residue. Therefore, HIF-1alpha expression and transcriptional function were tested to investigate whether the effect of EDHB on insulin secretion is through the HIF-1alpha dependent mechanism.

As shown in Figure 6-3, both endogenous HIF-1alpha mRNA (Figure 6-3A) and protein (Figure 6-3B and 6-3C) level in INS-1 832/13 cells remained unchanged after one hour EDHB treatment. A real-time PCR assay revealed that mRNA levels of HIF-1alpha targeting genes (Figure 6-4), including aryl hydrocarbon receptor nuclear translocator (ARNT), glucose transporter 2 (Glut2), glucokinase (GK), glyceraldehyde 3-phosphate dehydrogenase (GAPDH), pyruvate kinase muscle isozyme 1 (PKM1), pyruvate kinase muscle isozyme 2 (PKM2), also remained unaffected even if cellular hydroxylation was inhibited by EDHB.

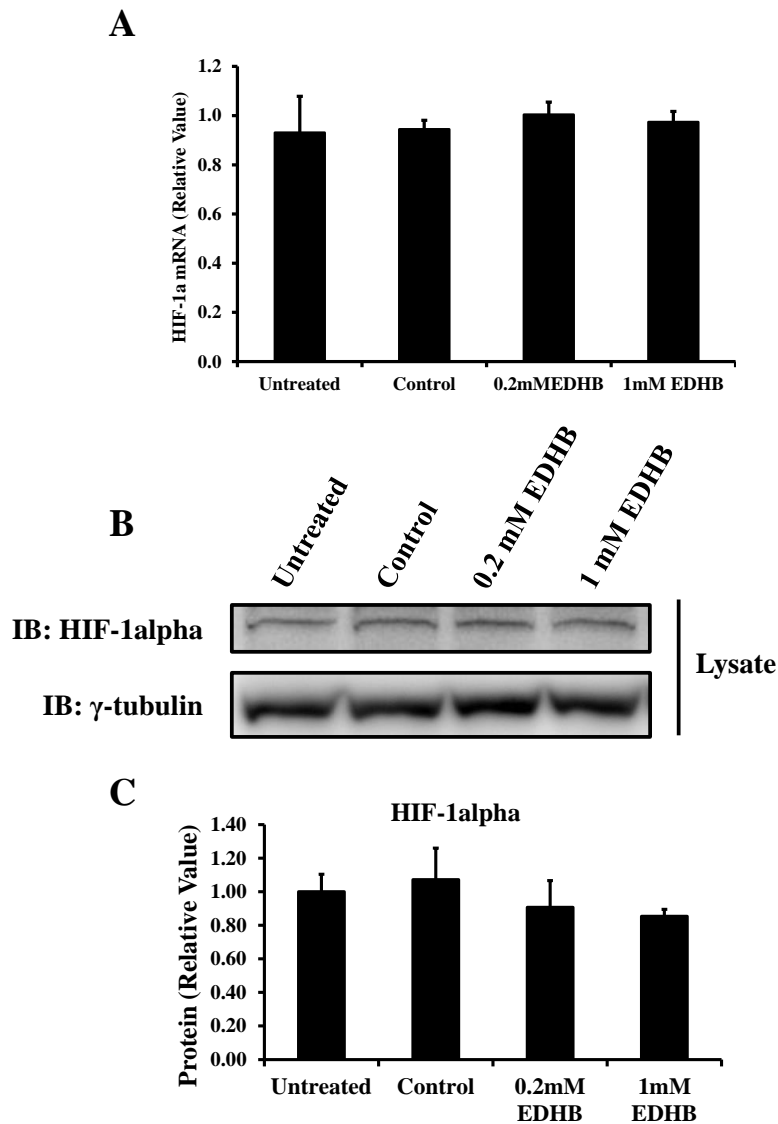


Figure 6-3 Effects of EDHB on hypoxia-inducible factor 1-alpha (HIF-1alpha) gene and protein
(A) RT-PCR analysis of HIF-1alpha mRNA **(B)** Immunoblot analysis of HIF-1alpha and γ -tubulin protein **(C)** HIF-1alpha protein level normalized by γ -tubulin. Results represent mean \pm S.E. (n = 4-9 replicates incubations for each condition. INS-1 832/13 cells were incubated with 2mM glucose for 2 hr and then treated with different levels of glucose as indicated for 1 hr before harvested for further analysis.

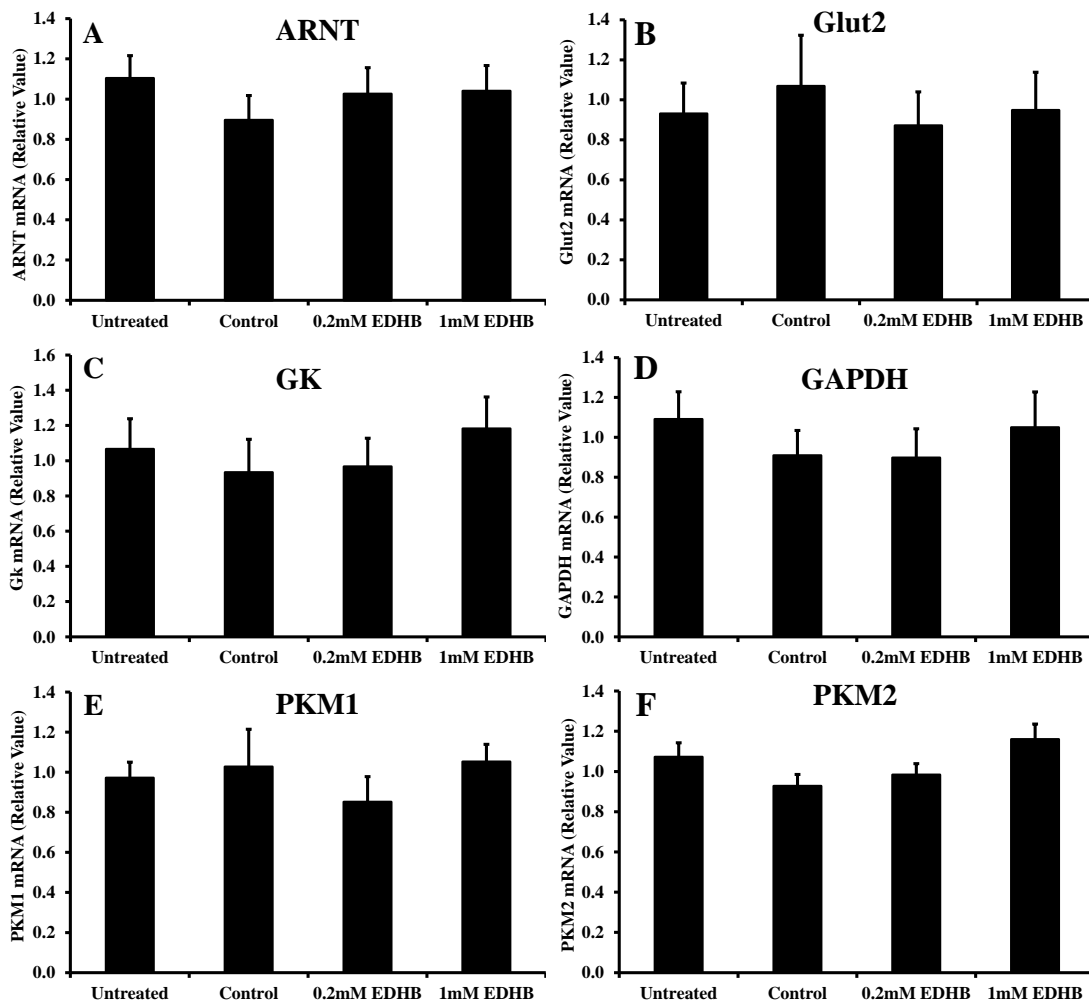


Figure 6-4 Effects of EDHB on HIF-1-alpha target genes

(a) Aryl hydrocarbon receptor nuclear translocator (ARNT) (b) glucose transporter 2 (Glut2) (c) glucokinase (GK) (d) glyceraldehyde 3-phosphate dehydrogenase (GAPDH) (e) pyruvate kinase muscle isozyme 1 (PKM1) (f) pyruvate kinase muscle isozyme (PKM2) mRNA expression in INS-1 832/13 cells. Results represent mean \pm S.E. (n = 6-8 replicates incubations for each condition).

6.3.5 Prolyl hydroxylases suppression has no effect on GSIS

For each prolyl hydroxylase (PHD1, 2 and 3), two siRNA duplexes targeting different gene regions were transfected into INS-1 832/13 cells. A previously characterized, a nonspecific siRNA sequence (siControl) was used as the control [81, 84, 319]. As shown in Figure 6-5, an 80 percent decline of

mRNA for each PHD was obtained by using both siRNA treatments; however, inhibiting individual PHD did not cause any significant effect on insulin release.

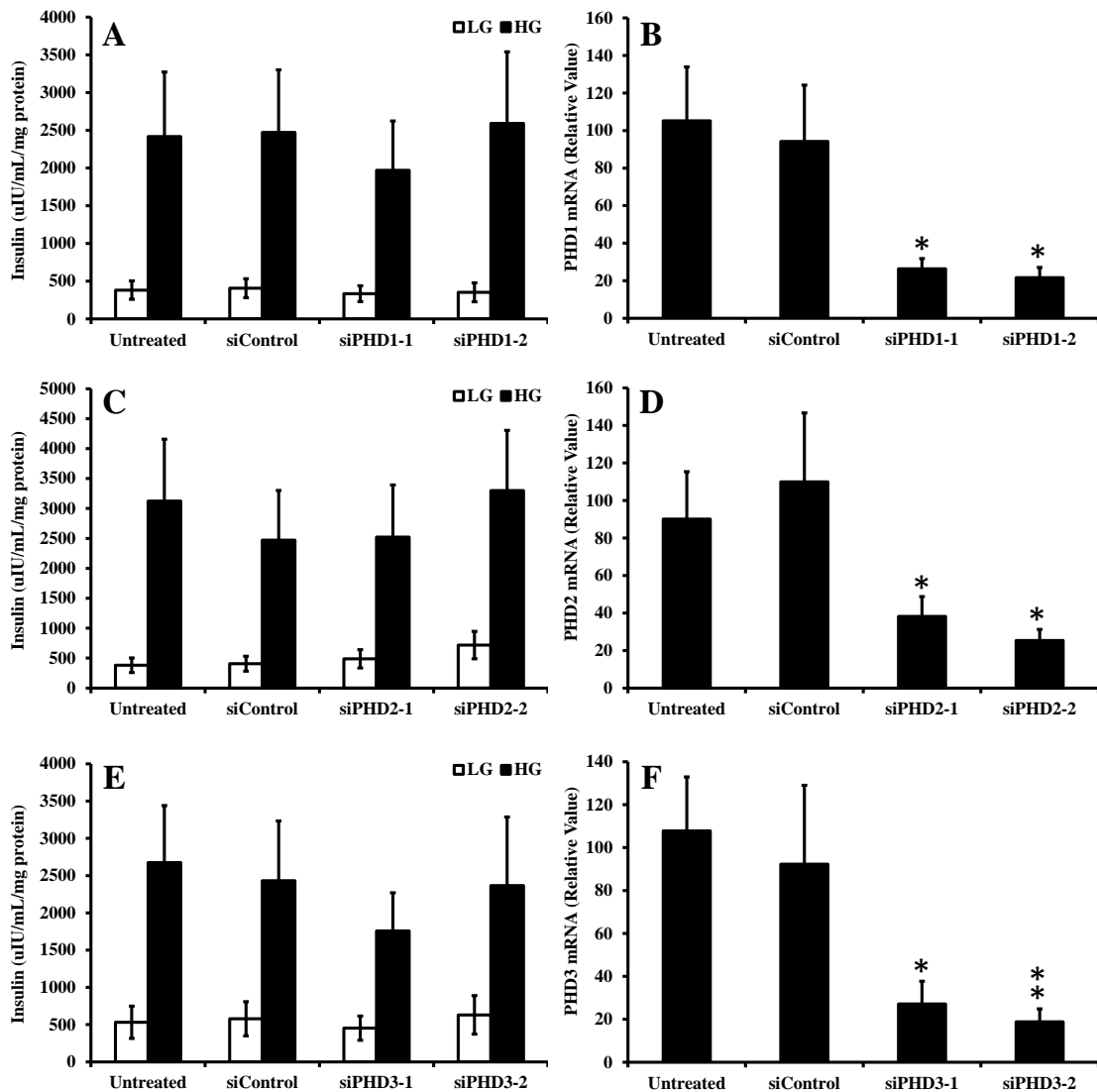


Figure 6-5 Effects of siRNA-mediated suppression of prolyl hydroxylases GSIS

Effects of two siRNA duplexes (siPHD1-1 and siPHD1-2) targeting against PHD1 on (a) GSIS and (b) PHD1 expression. Effects of two siRNA duplexes (siPHD2-1 and siPHD2-2) targeting against PHD2 on (c) GSIS and (d) PHD2 expression. Effects of two siRNA duplexes (siPHD3-1 and siPHD3-2) targeting against PHD3 on (e) GSIS and (f) PHD3 expression. siRNA duplexes were introduced into 832/13 cells at ~50% confluence. Experiments were performed 72 h after transfection. mRNA values are normalized to cyclophilin. Results represent mean \pm S.E. (n = 9-

12 replicate incubations for each condition). LG, low glucose (2 mM); HG, high glucose (10 mM). * $p < 0.05$; ** $p < 0.01$ versus same secretagogue condition without siRNA duplex.

6.3.6 High dosage of EDHB affects glucose metabolism

To further investigate the mechanism of EDHB in regulation of pancreatic beta cell secretion function, a GC-MS metabolomics approach was used to study the metabolite profiling of glycolytic and anaplerotic responses. As shown in Figure 6-6, the glycolytic intermediates, glucose 6-phosphate, 3-phosphoglycerate and pyruvate, were down-regulated by at least 75 percent after one hour treatment of 1 mM EDHB, but remained unaltered by 0.2 mM EDHB. Lactate remained unchanged in any of these conditions.

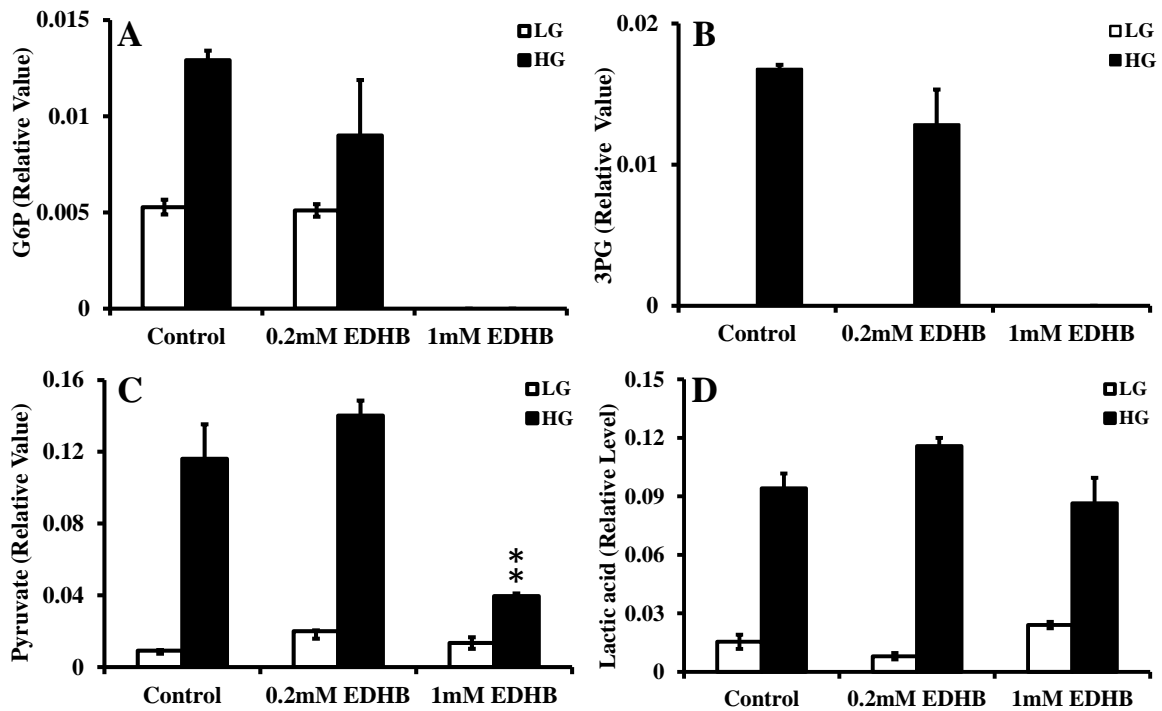


Figure 6-6 Effects of EDHB on glycolysis metabolites

Metabolites are isolated from INS-1 832/13 beta cells, run on GC/MS and identified by searching spectra against Fiehn library. The metabolites levels are normalized by internal standards (Myristic acid D-27). (A) Glucose 6-phosphate (B) 3-Phosphoglycerate (C) Pyruvate (D) Lactic Acid in INS-1 832/13 cells. Represent mean \pm S.E. (n = 6 replicates incubations for

each condition). LG, low glucose (2 mM); HG, high glucose (10 mM). **, $p < 0.01$, non-treated versus EDHB treated

All glucose-derived anaplerotic metabolites, which were detected by our mass spectrometer, exhibited the same trend as glycolytic intermediates (Figure 6-7). The levels of TCA cycle metabolites remained unchanged in cells treated with 0.2 mM EDHB, but were inhibited to the same extent as glycolytic intermediates in cells treated with 1 mM EDHB.

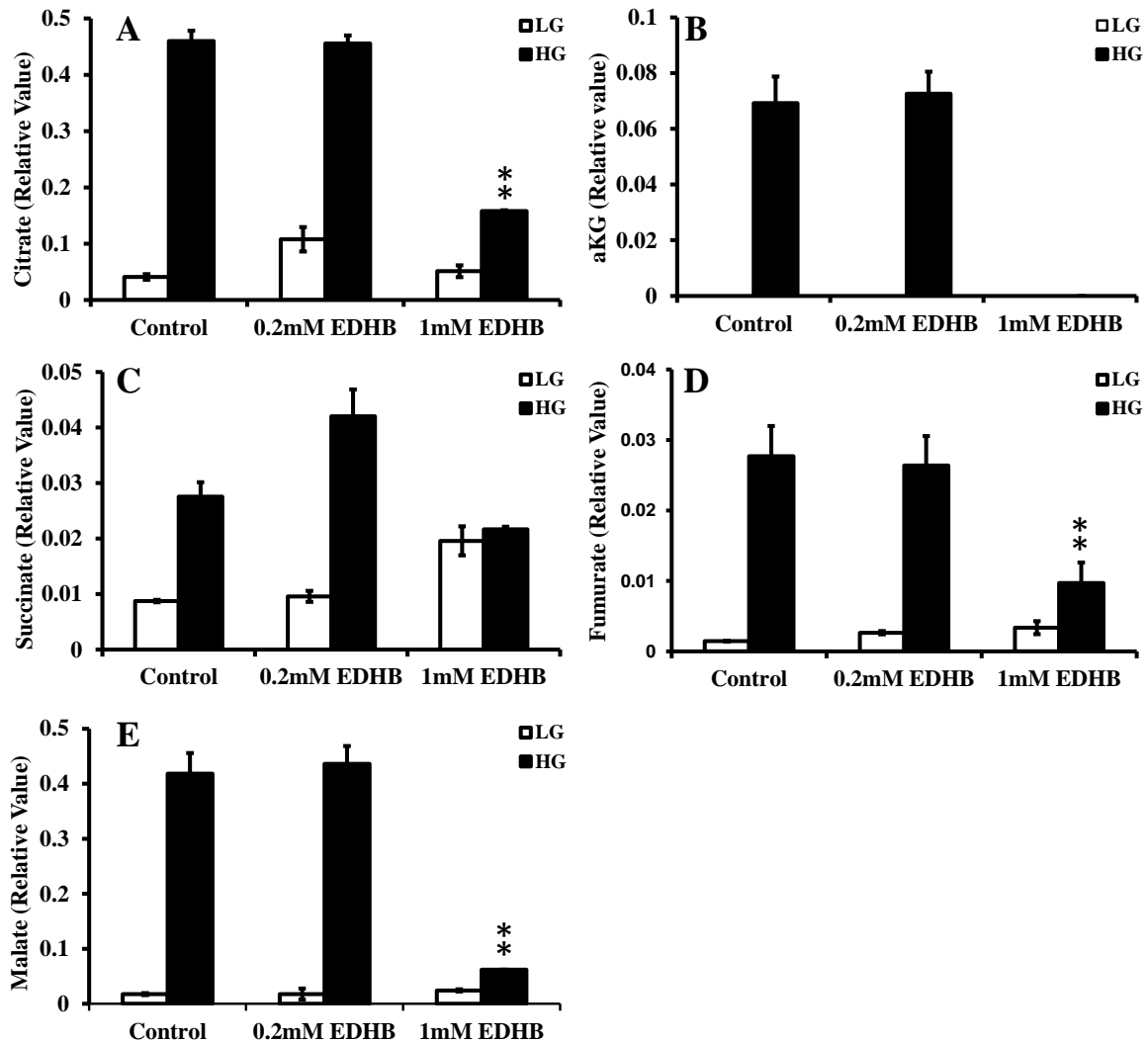


Figure 6-7 Effects of EDHB on TCA metabolites

Metabolites are isolated from INS-1 832/13 beta cells, run on GC/MS and identified by searching spectra against Fiehn library. The metabolites levels are normalized by internal standards (Myristic acid D-27). (A) Citrate (B) alpha-Ketoglutarate (C) Succinate (D)

Fumurate (E) Malate in INS-1 832/13 cells. Represent mean \pm S.E. (n = 6 replicates incubations for each condition). LG, low glucose (2 mM); HG, high glucose (10 mM). **, p<0.01, non-treated versus EDHB treated

Aspartate, which has been shown repeatedly by our previous studies to be negatively correlated to GSIS [320], was markedly impaired by 1 mM EDHB treatment (Figure 6-8).

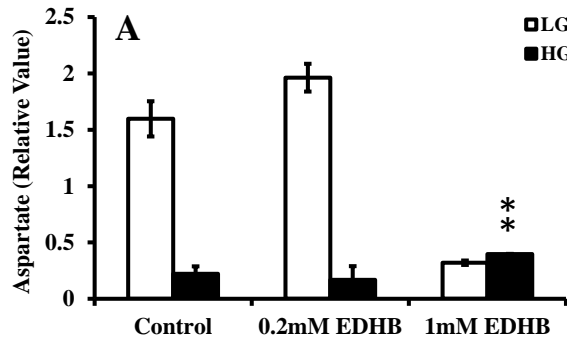


Figure 6-8 Effects of EDHB on aspartate

Metabolites are isolated from INS-1 832/13 beta cells, run on GC/MS and identified by searching spectra against Fiehn library. The metabolites levels are normalized by internal standards (Myristic acid D-27). Represent mean \pm S.E. (n = 6 replicates incubations for each condition). LG, low glucose (2 mM); HG, high glucose (10 mM). **, p<0.01, non-treated versus EDHB treated

6.4 Discussion

Insulin secretagogue carbon derived anaplerosis has been shown to play an important role in maintaining the secretion function of pancreatic beta cells. Theoretically, cataplerosis should be equally important as anaplerosis because glucose derived carbon fed into the TCA cycle through PC needs to find a way to leave mitochondria. One of the main reasons for the metabolite translocation from mitochondria to cytoplasm is to enable the signal generated in the mitochondrion, where glucose derived carbon fluxes into primary metabolism, to travel to the cytoplasm, where insulin granule exocytosis actually happens. Previous studies have brought our attention to alpha-ketoglutarate and its cofactors, among which Fe(II)/alpha-ketoglutarate dependent hydroxylases are believed to be promising candidates.

Fe(II)/alpha-ketoglutarate-dependent hydroxylase is a superfamily of enzymes consisting of more than 30 members identified from different species [390]. All members in this whole enzymes family are characterized by their ability to selectively catalyze the decomposition of alpha-ketoglutarate along with the formation of CO₂, succinate and an active oxygen species [390, 436]. Both its substrate (alpha-ketoglutarate) and product (succinate), are active members of the TCA cycle, therefore, the Fe(II)/alpha-ketoglutarate-dependent hydroxylase has received lots of attention as a highly competitive potential factor coupling glucose metabolite with insulin secretion.

In order to investigate the involvement of Fe(II)/alpha-ketoglutarate-dependent hydroxylase in GSIS, EDHB was used to create an iron-deficient condition inside pancreatic beta cells, because EDHB is capable of chelating the enzyme-bound iron [437] and effectively inhibiting the activity of enzymes. As shown in Figure 6-1, a high dosage of EDHB represented by 1mM in INS-1 cells and over 0.5 mM in rat and human pancreatic islets can significantly lower insulin release without causing any cell toxicity in a short term, a finding which is consistent with previous studies [95]. Surprisingly, insulin released by cells treated with small amounts of EDHB (0.2 mM in INS-1 832/13 cells and 0.05 mM in islets) was actually improved. This enhancement is most likely due to the stimulation of an energy relevant process rather than glucose uptake, since glucose influx did not change but oxygen consumption rose substantially. The incremental increase of total oxygen consumption was almost the same as that used for ATP generation, which suggests that hydroxylation might be involved in maintaining ATP generation. Although no gross change in total oxygen consumption occurred as a consequence of 1 mM EDHB treatment, both glucose utilization and ATP generation were impaired, indicating that some oxygen-dependent cellular activities increased in order to make up for the loss of oxygen consumption used for ATP generation.

EDHB was commonly used as a cell-permeable inhibitor for prolyl hydroxylases [438, 439]. Endogenous PHDs [440-442], one of the first Fe(II)/alpha-ketoglutarate-dependent hydroxylases identified by Hutton [441], as well as lysyl hydroxylases [440, 443-446], have been detected in INS-1 cells, rat and human pancreatic islets [95]. Prolyl hydroxylases can initiate HIF-1alpha ubiquitination and proteolysis by hydroxylation of HIF-1alpha on its proline residue [447-449]. Knowing this information, a further test was done to investigate whether the effect of EDHB on insulin secretion was through a HIF-1alpha dependent mechanism. Detection of HIF-1alpha expression revealed that neither its mRNA nor its protein level was affected by EDHB, although the total protein level was significantly altered by EDHB (Figure 6-1C). Additionally, HIF-1alpha's ability to function as a transcription cofactor remains unaffected, since the expression of its targeting genes was not altered

as shown in Figure 6-4. This suggests EDHB regulates pancreatic beta cell function through a HIF-1alpha independent mechanism, which might be relevant to hydroxylation-mediated ubiquitination and degradation, because the total protein level rose, indicating protein degradation was inhibited. Surprisingly, siRNA mediated inhibition of individual prolyl hydroxylase did not affect GSIS either, likely due to a compensation by other prolyl hydroxylase or even other groups of iron-responsive hydroxylases. The discrepancy in insulin release between EDHB-induced iron deficiency and siRNA-mediated prolyl hydroxylase inhibition along with the dose-dependent reverse effects of EDHB strongly implies the existence of a regulatory network of iron-dependent proteins, which involves, but is not limited to just prolyl hydroxylases, in pancreatic beta cells. Further work needs to be done to identify the exact target(s) of prolyl hydroxylase and/or other iron-dependent components responsive to EDHB in this whole iron-regulatory protein network.

This independency of HIF-1alpha mechanism is not only consistent with previous studies [450], but also supported by our metabolomics analysis. As shown in Figure 6-8, all glycolytic and TCA metabolites were down-regulated by 1 mM EDHB in INS-1 cells, which can explain why GSIS was extensively reduced in both INS-1 832/13 cells and islets. Metabolomics data also strongly indicates that hydroxylation is an important mechanism to globally control the glucose and TCA cycle metabolism, which will further exert their effects on insulin secretion.

6.5 Conclusion

In this study, EDHB was used to create an iron-free condition to study the role of alpha-ketoglutarate dependent hydroxylation in regulation of GSIS. It was found that EDHB had a dose-dependent effect on GSIS in both INS-1 cell lines and primary rat islets. Low dosage EDHB caused a moderate increase of insulin secretion probably by enhancing beta cell oxygen consumption used for ATP generation without altering glycolytic influx. A high level of EDHB severely impaired pancreatic beta cell secretion function and reduced both glycolytic and anaplerotic metabolites. Neither the expression nor the function of hypoxia-inducible factor-1alpha (HIF-1alpha) was altered, which indicates that hydroxylation works through a HIF-1alpha independent mechanism. Overall, our study has revealed that iron-responsive and alpha-ketoglutarate dependent hydroxylation is an important mechanism to regulate glucose metabolism and that its existence is critical to the normal function of pancreatic beta cells. These data suggest that the existence of iron-responsive and alpha-ketoglutarate dependent hydroxylation in regulation of glucose metabolism actually provides a positive feedback loop for GSIS and offers a potential for diabetes treatment.

Chapter 7
Discussion and Conclusion

7.1 Discussion

7.1.1 Technique aspects of untargeted metabolomics

In the postgenomic era, metabolomics has gained growing attention because it is capable of providing the most integrated profile of biological status. For example, the search for biomarkers, which serve as clear and strong indicators of disease progression, benefits from the progress of metabolomics. However, even with today's powerful analytical instruments and computer technology, the unambiguous and simultaneous determination of the whole set of metabolome in a biological system currently remains a great challenge. The technique bottleneck is the lack of an efficient sample preparation method for unbiased metabolite extraction due to the chemical complexity of native metabolites and wide range of metabolites concentration (over three magnitudes). Therefore, an unbiased metabolite extraction process needs to be included in metabolomics sampling approaches, from tissue isolation and homogenization to metabolites extraction and storage. Sample preparation is also considered the limiting step in metabolome analysis because it is an important source of variability in the analysis.

Our studies identified approximately 300 putative metabolites and their derivatives, which cover more than 20 chemical classes (data not shown), for example, amino acids, nucleotides, nucleosides, carboxylic acids, ketones, glycolipids, fatty acids, and sugar. This suggests that our extraction method works well. In fact, the combination of water and methanol is less comprehensive than the mixture of cold methanol/chloroform/water in terms of the coverage of metabolites polarity [194, 195, 197-201]. The latter was not used in our study because it was shown to affect the extraction of nucleotides, e.g. ATP, ADP, NADP, NADPH, which play a vital role in coupling glucose metabolism to insulin secretion. In this case, the comprehensiveness of extraction methods was sacrificed for the efficiency and effectiveness of nucleotides extraction. Although carboxylic acids themselves are not compatible with GC-MS, they were constantly and repeatedly detected in our study with little variation, which suggests that they are structurally more amenable to chemical derivatization than nucleotides.

In fact, only those volatile and less polar metabolites, which do not ionize very well by LC-MS ionization techniques, such as plant terpenes, steroids, diglycerides, mono-, di- and tri-saccharides, and sugar alcohols, are suited to GC-MS. In contrast, LC is commonly used to analyze those polar and not volatile metabolites, such as amino acids, organic acids, nucleosides, nucleotides, which actually covers a much wider range of chemical species. However, there is no publicly available MS/MS spectral library for LC-MS, like NIST for GC-MS. So the practical way to identify

metabolites based on LC-MS spectra is manual *de novo* interpretation and structure elucidation supported by MS/MS fragmentation from a high resolution mass spectrometer. Another advantage of GC over LC is the high chromatographic resolution, a benefit of long GC column (30 m GC column length vs. 0.15m LC column length), which allows a good separation of structurally similar metabolites, such as fatty acids. The last reason that GC is still a popular technique for metabolomics is that electron ionization (EI), the ionization commonly used in GC-MS, is robust and reproducible in producing MS spectra.

It is worth mentioning that metabolomics can only measure steady-state metabolite levels and is not able to determine the turnover rate of metabolites, which can be obtained by metabolic flux measurement. Some metabolites might be at high level with a low turnover rate and other metabolites turn out to be at low level but actually with high turnover rate. In practice, metabolic flux can be determined by the time-dependent measurement of steady-state distribution of isotope labelled atoms presented in growth culture media, such as ^{13}C , by NMR or MS [244]. This method is called ‘metabolic balancing’.

In some cases, although the overall concentration of metabolites is not altered by treatments, the change of relative metabolites abundance between different subcellular compartments, such as cytosol versus mitochondria, can provide further information and be used to reveal important mechanisms. To obtain such data, separation of different subcellular compartments prior to extraction of metabolites is necessary.

Overall, the sample preparation method used in our studies, including quenching and metabolites extraction, was proved to be effective, providing satisfactory comprehensiveness, reproducibility and variation.

7.1.2 Multivariate analysis in metabolomics

Metabolomic data acquisition techniques generate a large volume of data containing hundreds or even thousands of observations and variables, which are rich in information. Therefore, MVA is an essential chemometrical tool integrated into untargeted metabolomics to reveal this underlying information.

PCA has been recommended as the starting point for studies requiring MVA, because it provides a quick overview of data. Despite the many options we have, PCA is so far still the method widely used in metabolomics, and to date, majority of metabolomics publications are based on PCA. Only a few papers have tried PLS [451] or OPLS [148], even though this situation has changed in last couple of

years. As mentioned before, PCA cannot perform quantitative analysis and hence is not the right tool for biomarker discovery, for which purpose PLS or OPLS is recommended and expected to be developed to a major multivariate approach for untargeted metabolomics in the near future. The combination of several MVA methods, such as hierarchical PCA and PLS, has been tested and proved to enhance data interpretation [289, 452-456].

Both PLS and OPLS were tried in our study. As shown in chapter 3 to 6, OPLS was applied to two classes (Chapter 3) as well as dynamic studies (Chapter 4) in this thesis. Actually, OPLS was found to outweigh PLS in modeling, such as samples classification, data interpretation, and discovery of biomarkers. For example, PLS identified six new latent variables, while OPLS generated only three predictive and two orthogonal latent variables for an equally good modeling of metabolomics data designed to reveal the mechanism of TDEs in Chapter 5 (data not shown). This is mainly because orthogonal latent variables negatively affect PLS modeling and data interpretation, since they are just structure noise unrelated to Y matrix.

No matter which MVA tool is used for data analysis, we found that large datasets were more effective in building more reliable and interpretable models than datasets with a low number of replicates. However, although an appropriate MVA method is powerful enough to find the underlying correlation obscured in the original data matrix, it cannot determine the cause-and-effect relationship between two phenomena. For example, although the PPP was shown by MVA to contribute to the cluster of high glucose treated cells in Chapter 3, we don't know whether it is the elevated pentose-phosphate pathway that promotes GSIS or it is extra glucose that fluxes into the PPP and hence increases the metabolites levels. So, what is even more important is rigorous verification or validation of results from MVA on both a statistical (Q2) and biological level. As seen in Figure 3-11, both siRNA mediated knockdown and pharmaceutical inhibitors of the PPP were used to verify the discovery by MVA and to test the cause-and-effect relationship between the PPP and GSIS.

MVA is a chemometrical technique critical to reliable interpretation of metabolomics data. But it is of great importance to choose the appropriate method, to optimize different parameters and to apply strict validation as well as biologically meaningful verification.

7.1.3 Significance of untargeted metabolomics

The traditional strategy for research is generally hypothesis-driven, in which some preliminary knowledge is generally required for a formation of preconceived notions and their confirmation by some experiments designed to test the hypothesis [457, 458]. Preliminary knowledge and great

wisdom generated from experience play a considerable role in determining how valid the hypothesis is, since even data collected from well-designed experiments can agree with, be completely irrelevant to, or even contradict proposed hypothesis. That's why the traditional knowledge discovery strategy is highly risky in terms of successful confirmation of a hypothesis and low throughput.

In the post genomic era, some research intended to generate new knowledge has turned from a hypothesis-driven to data-driven stage, since scientists are capable of collecting a high amount of data simultaneously and the hypothesis or even knowledge is manifested by these observations themselves [459]. The novel knowledge discovery strategy benefiting from untargeted metabolomics doesn't require preliminary data for proposal of hypothesis, and hence is especially useful for a novel project with little a priori background. This is why untargeted metabolomics is becoming more and more interesting to scientists.

This data-driven strategy is clearly shown in Chapter 3-6. For example, in Chapter 5, if there is no untargeted metabolomics, a conclusion can be easily drawn that pre-culture condition has no effect on GSIS. However, a great discrepancy between insulin secretion competency (Figure 5-1A) and metabolic activity (Figure 5-2) was clearly revealed by untargeted metabolomics analysis, which gave a further clue about which metabolites are most likely responsible for TDE. In Chapter 6, the untargeted metabolomics data once again links the HIF-1 α independent mechanism to global regulation of glucose metabolism, thus providing a direction for further study (e.g. to investigate the hydroxylation status of enzymes involved in glycolysis and TCA cycle metabolism).

7.1.4 Insight into metabolic regulation of insulin secretion

Insulin secretion is tightly controlled by glucose metabolism. Hence, metabolite measurement is of particular importance in studies of the pancreatic beta cell secretion function. Metabolomic analysis has a distinct advantage over other classical biochemical approaches used for metabolite measurement, because metabolomics can directly determine the steady-state metabolite levels.

Whether the PPP is involved in glucose stimulus and insulin secretion coupling in pancreatic cells function has been under debate. One reason to cause this argument is probably the difference between species. The major evidence against the idea that PPP participates in GSIS is from INS-1 cells and mouse islets [33, 354]. Studies showing the involvement of PPP in GSIS were done on human islets [149]. Our data (Figure 3-7 and 3-11) also indicates that a species difference exists between human and rat islets as reported [149]. The different culture conditions are the second reason for the

contradictory results revealed by studies investigating the role of PPP in regulation of pancreatic secretion function. Experiments generating the data denying the involvement of PPP in GSIS involved static incubation, in which insulin was secreted into and stayed in medium [33, 354]. However, insulin accumulation was reported to block and obscure glucose concentration-dependent PPP activity [348], if insulin was not removed from medium. In addition, the pre-culture condition affected the activity of PPP in rat islets [77]. Our data not only reveal the possibility that PPP might be a part of the regulatory network of pancreatic beta cells secretion function (Figure 3-11), but also indicate that the PPP might be specifically active in the first phase of insulin secretion (Figure 4-5A), which agrees with other studies done by Spégl [148]. The mechanistic study has mainly focused on the role of PPP in providing NADPH for defense against oxidative stress induced in pancreatic beta cells [349]. Much less attention has been paid to investigate whether the ability of PPP to generate the precursor for pentose synthesis of aromatic amino acids, and nucleotides is dispensable to GSIS, which remains established.

TDEs were suggested to be one model to explain biphasic property of insulin secretion, because a tight correlation was discovered between the magnitude of TDP and the slope of the second phase insulin response [144]. However, our metabolomic analysis suggests that TDP is likely correlated with the proximal part of the stimulus-response coupling pathway, e.g. glucose-stimulated insulin exocytosis as well as pro-insulin biosynthesis (Chapter 5), while the alpha-ketoglutarate mediated proline hydroxylation might be central for the second phase insulin secretion (Chapter 4). Although both TDP and the second phase insulin secretion are driven by glucose-derived anaplerosis, the fact that they are governed by distinct mechanism indicates that TDP and the second phase of insulin secretion are two different characterizations of pancreatic beta-cells. Studies, which revealed that TDP can be induced by glucose in the absence of extracellular Ca^{2+} [460, 461] and was critically dependent on intracellular pH [460], also support our discovery that different mechanisms are responsible for TDP and the second phase insulin secretion.

Our data suggests that metabolomic analysis provides strong support for the mechanistic study of insulin secretion.

7.2 Conclusion

Our studies clearly showed that a feasible GC-MS untargeted metabolomics strategy, from sample preparation to data interpretation, was established and its application can successfully convert the

knowledge discovery method from hypothesis-dependent to data-driven strategy. In this dissertation, untargeted metabolomics has been applied to studies of GSIS, the mechanism of biphasic insulin secretion and TDEs, as well as the role of iron-responsive and alpha-ketoglutarate dependent hydroxylation in regulation of insulin secretion.

In addition to glycolysis, the PPP, sorbitol-aldose reductase pathway as well as aspartate are strongly suggested to be relevant to GSIS. For characterization of kinetics insulin secretion, alpha-ketoglutarate, succinate and hydroxyproline were revealed to be the metabolites strongly associated with the second phase of biphasic insulin secretion. Study of TDEs by metabolomics shows that TDI effect is mainly regulated by redox state in pancreatic beta cells, since it is correlated to the decreased DHAP: alpha-GP ratio probably as a result of the diminished malate-aspartate shuttle activity, and the lowered lactate output in beta cells. On the other hand, TDP is probably coupled with succinate-regulated pro-insulin biosynthesis. Finally, alpha-ketoglutarate dependent hydroxylation was found to be a master regulation mechanism controlling glucose metabolism, a finding which, if true, provides a positive feedback loop for GSIS in pancreatic beta cells.

7.3 Future outlook

Despite the successful application of untargeted metabolomics in our study, fully comprehensive metabolomics requires improvements in both sample preparation and metabolite measurement. Truly unbiased sample preparation should include pre-fractionation and selective enrichment for the specific chemical properties of different classes of metabolites to facilitate the detection and analysis of the structurally diverse metabolites, even though it is time-consuming. In terms of metabolite determination, both GC and LC are highly recommended to cover the whole endogenous metabolome with a wide range chemical nature. It will be exceedingly helpful if a LC-MS/MS spectral library can be established.

PCA, PLS, and OPLS are just basic algorithms for two-way X–Y data matrices, the modification of which is highly recommended. Evolvement of MVA basic algorithms leads to the development of quadratic PLS [462], batch-wise PLS (and PCA) [463], hierarchical PLS (and PCA) [289, 452-456], which are believed to have even greater promise because they can extend MVA to non-linear regression for multi-way data matrices.

As shown by our data, alpha-ketoglutarate plays an important role in coupling glucose metabolism with insulin secretion probably by hydroxylation, which could happen to all enzymes regulating

glucose metabolism or to a master protein controlling glucose metabolic pathway. No matter which protein is the substrate of hydroxylation, alpha-ketoglutarate dependent hydroxylation provides a positive feedback mechanism for glucose-stimulated insulin secretion, since alpha-ketoglutarate itself is a glucose-carbon derived molecule generated in mitochondria. So, separation of metabolites contained in different cellular compartments, such as separation of metabolites in cytoplasm from mitochondria, is expected to be included in the sample preparation process for future studies. As glucose metabolism is clearly affected by EDHB, the next question to be answered is which enzyme exactly is the substrate for hydroxylation.

Appendix A

Publications and Manuscripts in Preparation

Publications

Huang, M. and J. W. Joseph “Assessment of the metabolic pathways associated with glucose-stimulated biphasic insulin secretion” *Endocrinology* published online

Huang, M., and J.W. Joseph. (2012). Metabolomic analysis of pancreatic beta cell insulin release in response to glucose. *Islets*. 4:210-222.

Huypens, P. R., **M. Huang**, Joseph, J. W. (2012). "Overcoming the spatial barriers of the stimulus secretion cascade in pancreatic β -cells." *Islets* 4(1): 1-116.

Huypens, P., R. Pillai, T. Sheinin, S. Schaefer, **M. Huang**, M.L. Odegaard, S.M. Ronnebaum, S.D. Wettig, and J.W. Joseph. (2011) The dicarboxylate carrier plays a role in mitochondrial malate transport and in the regulation of glucose-stimulated insulin secretion from rat pancreatic beta cells. *Diabetologia*. 54:135-145.

Pillai, R., Huypens, P., **Huang, M.**, Schaefer, S., Sheinin, T., Wettig, S. D., Joseph, J. W. (2011). "Aryl hydrocarbon receptor nuclear translocator/hypoxia-inducible factor-1beta plays a critical role in maintaining glucose-stimulated anaplerosis and insulin release from pancreatic beta-cells." *J Biol Chem* 286(2): 1014-1024.

Manuscript in Preparation

Huang, M. and J. W. Joseph “Mechanistic Study of Time-Dependent Effects of Glucose on Insulin Secretion” *Manuscript in preparation*

Huang, M. and J. W. Joseph “Hydroxylation, an important mechanism in regulation of glucose metabolism” *Manuscript in preparation*

Renjitha Pillai, Kacey Prentice, Mei Huang, Eric Bombadier, Katelyn Cousteils¹ and Jamie W. Joseph, “ARNT/HIF-1 β indispensable for maintaining beta cell secretory function, but not for glucose homeostasis in mice” *Manuscript in preparation*

Bibliography

1. Guariguata, L., et al., *Global estimates of diabetes prevalence for 2013 and projections for 2035*. Diabetes Res Clin Pract, 2014. **103**(2): p. 137-49.
2. Wild, S., et al., *Global prevalence of diabetes: estimates for the year 2000 and projections for 2030*. Diabetes Care, 2004. **27**(5): p. 1047-53.
3. Alberti, K.G. and P.Z. Zimmet, *Definition, diagnosis and classification of diabetes mellitus and its complications. Part 1: diagnosis and classification of diabetes mellitus provisional report of a WHO consultation*. Diabet Med, 1998. **15**(7): p. 539-53.
4. Mitrakou, A., et al., *Role of reduced suppression of glucose production and diminished early insulin release in impaired glucose tolerance*. N Engl J Med, 1992. **326**(1): p. 22-9.
5. Meyer, C., et al., *Role of human liver, kidney, and skeletal muscle in postprandial glucose homeostasis*. Am J Physiol Endocrinol Metab, 2002. **282**(2): p. E419-27.
6. Kelley, D., et al., *Skeletal muscle glycolysis, oxidation, and storage of an oral glucose load*. J Clin Invest, 1988. **81**(5): p. 1563-71.
7. Taylor, R., et al., *Direct assessment of liver glycogen storage by ¹³C nuclear magnetic resonance spectroscopy and regulation of glucose homeostasis after a mixed meal in normal subjects*. J Clin Invest, 1996. **97**(1): p. 126-32.
8. McMahan, M., H. Marsh, and R. Rizza, *Comparison of the pattern of postprandial carbohydrate metabolism after ingestion of a glucose drink or a mixed meal*. J Clin Endocrinol Metab, 1989. **68**(3): p. 647-53.
9. Kelley, D., M. Mookan, and T. Veneman, *Impaired postprandial glucose utilization in non-insulin-dependent diabetes mellitus*. Metabolism, 1994. **43**(12): p. 1549-57.
10. In't Veld, P. and M. Marichal, *Microscopic anatomy of the human islet of Langerhans*. Adv Exp Med Biol, 2010. **654**: p. 1-19.
11. Elayat, A.A., M.M. el-Naggar, and M. Tahir, *An immunocytochemical and morphometric study of the rat pancreatic islets*. J Anat, 1995. **186 (Pt 3)**: p. 629-37.
12. Lane, M.A., *The cytological characters of the areas of langerhans*. American Journal of Anatomy, 1907. **7**(3): p. 409-422.
13. Bloom, W., *A new type of granular cell in the islets of Langerhans of man*. The Anatomical Record, 1931. **49**(4): p. 363-371.

14. Larsson, L.I., F. Sundler, and R. Hakanson, *Pancreatic polypeptide - a postulated new hormone: identification of its cellular storage site by light and electron microscopic immunocytochemistry*. *Diabetologia*, 1976. **12**(3): p. 211-26.
15. Wierup, N., et al., *The ghrelin cell: a novel developmentally regulated islet cell in the human pancreas*. *Regul Pept*, 2002. **107**(1-3): p. 63-9.
16. Stefan, Y., et al., *Quantitation of endocrine cell content in the pancreas of nondiabetic and diabetic humans*. *Diabetes*, 1982. **31**(8 Pt 1): p. 694-700.
17. Rahier, J., R.M. Goebbels, and J.C. Henquin, *Cellular composition of the human diabetic pancreas*. *Diabetologia*, 1983. **24**(5): p. 366-71.
18. Brissova, M., et al., *Assessment of human pancreatic islet architecture and composition by laser scanning confocal microscopy*. *J Histochem Cytochem*, 2005. **53**(9): p. 1087-97.
19. Cabrera, O., et al., *The unique cytoarchitecture of human pancreatic islets has implications for islet cell function*. *Proc Natl Acad Sci U S A*, 2006. **103**(7): p. 2334-9.
20. Quesada, I., et al., *Physiology of the pancreatic alpha-cell and glucagon secretion: role in glucose homeostasis and diabetes*. *J Endocrinol*, 2008. **199**(1): p. 5-19.
21. Cerasi, E. and A. Ktorza, *[Anatomical and functional plasticity of pancreatic beta-cells and type 2 diabetes]*. *Med Sci (Paris)*, 2007. **23**(10): p. 885-94.
22. Parsons, J.A., T.C. Brelje, and R.L. Sorenson, *Adaptation of islets of Langerhans to pregnancy: increased islet cell proliferation and insulin secretion correlates with the onset of placental lactogen secretion*. *Endocrinology*, 1992. **130**(3): p. 1459-66.
23. Edstrom, K., E. Cerasi, and R. Luft, *Insulin response to glucose infusion during pregnancy. A prospective study of high and low insulin responders with normal carbohydrate tolerance*. *Acta Endocrinol (Copenh)*, 1974. **75**(1): p. 87-104.
24. Gepts, W., *Pathologic anatomy of the pancreas in juvenile diabetes mellitus*. *Diabetes*, 1965. **14**(10): p. 619-33.
25. Pipeleers, D. and Z. Ling, *Pancreatic beta cells in insulin-dependent diabetes*. *Diabetes Metab Rev*, 1992. **8**(3): p. 209-27.
26. Roep, B.O., *The role of T-cells in the pathogenesis of Type 1 diabetes: from cause to cure*. *Diabetologia*, 2003. **46**(3): p. 305-21.
27. Butler, P.C., et al., *Effects of meal ingestion on plasma amylin concentration in NIDDM and nondiabetic humans*. *Diabetes*, 1990. **39**(6): p. 752-6.

28. Sanke, T., et al., *Plasma islet amyloid polypeptide (Amylin) levels and their responses to oral glucose in type 2 (non-insulin-dependent) diabetic patients*. *Diabetologia*, 1991. **34**(2): p. 129-32.
29. Ripsin, C.M., H. Kang, and R.J. Urban, *Management of blood glucose in type 2 diabetes mellitus*. *Am Fam Physician*, 2009. **79**(1): p. 29-36.
30. De Vos, A., et al., *Human and rat beta cells differ in glucose transporter but not in glucokinase gene expression*. *J Clin Invest*, 1995. **96**(5): p. 2489-95.
31. Thorens, B. and M. Mueckler, *Glucose transporters in the 21st Century*. *Am J Physiol Endocrinol Metab*, 2010. **298**(2): p. E141-5.
32. Matschinsky, F.M., *Banting Lecture 1995. A lesson in metabolic regulation inspired by the glucokinase glucose sensor paradigm*. *Diabetes*, 1996. **45**(2): p. 223-41.
33. Schuit, F., et al., *Metabolic fate of glucose in purified islet cells. Glucose-regulated anaplerosis in beta cells*. *J Biol Chem*, 1997. **272**(30): p. 18572-9.
34. Meglasson, M.D. and F.M. Matschinsky, *New perspectives on pancreatic islet glucokinase*. *Am J Physiol*, 1984. **246**(1 Pt 1): p. E1-13.
35. Huypens, P.R., M. Huang, and J.W. Joseph, *Overcoming the spatial barriers of the stimulus secretion cascade in pancreatic beta-cells*. *Islets*, 2012. **4**(1).
36. Wang, H. and P.B. Iynedjian, *Modulation of glucose responsiveness of insulinoma beta-cells by graded overexpression of glucokinase*. *Proc Natl Acad Sci U S A*, 1997. **94**(9): p. 4372-7.
37. Rorsman, P., *The pancreatic beta-cell as a fuel sensor: an electrophysiologist's viewpoint*. *Diabetologia*, 1997. **40**(5): p. 487-95.
38. Ashcroft, F.M. and F.M. Gribble, *ATP-sensitive K⁺ channels and insulin secretion: their role in health and disease*. *Diabetologia*, 1999. **42**(8): p. 903-19.
39. Seino, S., et al., *Diverse roles of K(ATP) channels learned from Kir6.2 genetically engineered mice*. *Diabetes*, 2000. **49**(3): p. 311-8.
40. Shyng, S. and C.G. Nichols, *Octameric stoichiometry of the KATP channel complex*. *J Gen Physiol*, 1997. **110**(6): p. 655-64.
41. Clement, J.P.t., et al., *Association and stoichiometry of K(ATP) channel subunits*. *Neuron*, 1997. **18**(5): p. 827-38.
42. Aguilar-Bryan, L. and J. Bryan, *Molecular biology of adenosine triphosphate-sensitive potassium channels*. *Endocr Rev*, 1999. **20**(2): p. 101-35.

43. Seino, S., *ATP-sensitive potassium channels: a model of heteromultimeric potassium channel/receptor assemblies*. *Annu Rev Physiol*, 1999. **61**: p. 337-62.
44. Tucker, S.J., et al., *Truncation of Kir6.2 produces ATP-sensitive K⁺ channels in the absence of the sulphonylurea receptor*. *Nature*, 1997. **387**(6629): p. 179-83.
45. Ashcroft, F.M., D.E. Harrison, and S.J. Ashcroft, *Glucose induces closure of single potassium channels in isolated rat pancreatic beta-cells*. *Nature*, 1984. **312**(5993): p. 446-8.
46. Cook, D.L. and C.N. Hales, *Intracellular ATP directly blocks K⁺ channels in pancreatic B-cells*. *Nature*, 1984. **311**(5983): p. 271-3.
47. Ashcroft, F.M., *The Walter B. Cannon Physiology in Perspective Lecture, 2007. ATP-sensitive K⁺ channels and disease: from molecule to malady*. *Am J Physiol Endocrinol Metab*, 2007. **293**(4): p. E880-9.
48. Pfeifer, M.A., J.B. Halter, and D. Porte, Jr., *Insulin secretion in diabetes mellitus*. *Am J Med*, 1981. **70**(3): p. 579-88.
49. Jensen, M.V., et al., *Metabolic cycling in control of glucose-stimulated insulin secretion*. *Am J Physiol Endocrinol Metab*, 2008. **295**(6): p. E1287-97.
50. Bryan, J., et al., *Insulin secretagogues, sulphonylurea receptors and K(ATP) channels*. *Curr Pharm Des*, 2005. **11**(21): p. 2699-716.
51. Gilon, P. and J.C. Henquin, *Influence of membrane potential changes on cytoplasmic Ca²⁺ concentration in an electrically excitable cell, the insulin-secreting pancreatic B-cell*. *J Biol Chem*, 1992. **267**(29): p. 20713-20.
52. Henquin, J.C. and H.P. Meissner, *Opposite effects of tolbutamide and diazoxide on 86Rb⁺ fluxes and membrane potential in pancreatic B cells*. *Biochem Pharmacol*, 1982. **31**(7): p. 1407-15.
53. Proks, P., et al., *Sulphonylurea stimulation of insulin secretion*. *Diabetes*, 2002. **51 Suppl 3**: p. S368-76.
54. Schwanstecher, M., K. Manner, and U. Panten, *Inhibition of K⁺ channels and stimulation of insulin secretion by the sulphonylurea, glimepiride, in relation to its membrane binding in pancreatic islets*. *Pharmacology*, 1994. **49**(2): p. 105-11.
55. Garrino, M.G., et al., *Mechanism of the stimulation of insulin release in vitro by HB 699, a benzoic acid derivative similar to the non-sulphonylurea moiety of glibenclamide*. *Diabetologia*, 1985. **28**(9): p. 697-703.

56. Gembal, M., P. Gilon, and J.C. Henquin, *Evidence that glucose can control insulin release independently from its action on ATP-sensitive K⁺ channels in mouse B cells*. J Clin Invest, 1992. **89**(4): p. 1288-95.
57. Komatsu, M., et al., *Augmentation of Ca²⁺-stimulated insulin release by glucose and long-chain fatty acids in rat pancreatic islets: free fatty acids mimic ATP-sensitive K⁺ channel-independent insulinotropic action of glucose*. Diabetes, 1999. **48**(8): p. 1543-9.
58. Ravier, M.A., et al., *Glucose controls cytosolic Ca²⁺ and insulin secretion in mouse islets lacking adenosine triphosphate-sensitive K⁺ channels owing to a knockout of the pore-forming subunit Kir6.2*. Endocrinology, 2009. **150**(1): p. 33-45.
59. Szollosi, A., M. Nenquin, and J.C. Henquin, *Overnight culture unmasks glucose-induced insulin secretion in mouse islets lacking ATP-sensitive K⁺ channels by improving the triggering Ca²⁺ signal*. J Biol Chem, 2007. **282**(20): p. 14768-76.
60. Nenquin, M., et al., *Both triggering and amplifying pathways contribute to fuel-induced insulin secretion in the absence of sulfonylurea receptor-1 in pancreatic beta-cells*. J Biol Chem, 2004. **279**(31): p. 32316-24.
61. Szollosi, A., et al., *Glucose stimulates Ca²⁺ influx and insulin secretion in 2-week-old beta-cells lacking ATP-sensitive K⁺ channels*. J Biol Chem, 2007. **282**(3): p. 1747-56.
62. Remedi, M.S., et al., *Hyperinsulinism in mice with heterozygous loss of K(ATP) channels*. Diabetologia, 2006. **49**(10): p. 2368-78.
63. Doliba, N.M., et al., *Restitution of defective glucose-stimulated insulin release of sulfonylurea type 1 receptor knockout mice by acetylcholine*. Am J Physiol Endocrinol Metab, 2004. **286**(5): p. E834-43.
64. Shiota, C., et al., *Sulfonylurea receptor type 1 knock-out mice have intact feeding-stimulated insulin secretion despite marked impairment in their response to glucose*. J Biol Chem, 2002. **277**(40): p. 37176-83.
65. Henquin, J.C., et al., *Hierarchy of the beta-cell signals controlling insulin secretion*. Eur J Clin Invest, 2003. **33**(9): p. 742-50.
66. Prentki, M., *New insights into pancreatic beta-cell metabolic signaling in insulin secretion*. Eur J Endocrinol, 1996. **134**(3): p. 272-86.
67. MacDonald, M.J., *Feasibility of a mitochondrial pyruvate malate shuttle in pancreatic islets. Further implication of cytosolic NADPH in insulin secretion*. J Biol Chem, 1995. **270**(34): p. 20051-8.

68. Cline, G.W., et al., *¹³C NMR isotopomer analysis of anaplerotic pathways in INS-1 cells*. J Biol Chem, 2004. **279**(43): p. 44370-5.
69. Farfari, S., et al., *Glucose-regulated anaplerosis and cataplerosis in pancreatic beta-cells: possible implication of a pyruvate/citrate shuttle in insulin secretion*. Diabetes, 2000. **49**(5): p. 718-26.
70. Hasan, N.M., et al., *Impaired anaplerosis and insulin secretion in insulinoma cells caused by small interfering RNA-mediated suppression of pyruvate carboxylase*. J Biol Chem, 2008. **283**(42): p. 28048-59.
71. Xu, J., et al., *The role of pyruvate carboxylase in insulin secretion and proliferation in rat pancreatic beta cells*. Diabetologia, 2008. **51**(11): p. 2022-30.
72. MacDonald, M.J., et al., *Decreased levels of metabolic enzymes in pancreatic islets of patients with type 2 diabetes*. Diabetologia, 2009. **52**(6): p. 1087-91.
73. Han, J. and Y.Q. Liu, *Reduction of islet pyruvate carboxylase activity might be related to the development of type 2 diabetes mellitus in Agouti-K mice*. J Endocrinol, 2010. **204**(2): p. 143-52.
74. MacDonald, M.J., *Glucose enters mitochondrial metabolism via both carboxylation and decarboxylation of pyruvate in pancreatic islets*. Metabolism, 1993. **42**(10): p. 1229-1231.
75. Khan, A., Z.C. Ling, and B.R. Landau, *Quantifying the carboxylation of pyruvate in pancreatic islets*. J Biol Chem, 1996. **271**(5): p. 2539-42.
76. Lu, D., et al., *¹³C NMR isotopomer analysis reveals a connection between pyruvate cycling and glucose-stimulated insulin secretion (GSIS)*. Proc Natl Acad Sci U S A, 2002. **99**(5): p. 2708-13.
77. MacDonald, M.J., *Estimates of glycolysis, pyruvate (de)carboxylation, pentose phosphate pathway, and methyl succinate metabolism in incapacitated pancreatic islets*. Arch Biochem Biophys, 1993. **305**(2): p. 205-14.
78. Flamez, D., et al., *Critical role for cataplerosis via citrate in glucose-regulated insulin release*. Diabetes, 2002. **51**(7): p. 2018-24.
79. Jitrapakdee, S., et al., *Regulation of insulin secretion: role of mitochondrial signalling*. Diabetologia, 2010. **53**(6): p. 1019-32.
80. Huypens, P., et al., *The dicarboxylate carrier plays a role in mitochondrial malate transport and in the regulation of glucose-stimulated insulin secretion from rat pancreatic beta cells*. Diabetologia, 2011. **54**(1): p. 135-45.

81. Joseph, J.W., et al., *The mitochondrial citrate/isocitrate carrier plays a regulatory role in glucose-stimulated insulin secretion.* J Biol Chem, 2006. **281**(47): p. 35624-32.
82. Odegaard, M.L., et al., *The mitochondrial 2-oxoglutarate carrier is part of a metabolic pathway that mediates glucose- and glutamine-stimulated insulin secretion.* J Biol Chem, 2010. **285**(22): p. 16530-7.
83. Stark, R., et al., *Phosphoenolpyruvate cycling via mitochondrial phosphoenolpyruvate carboxykinase links anaplerosis and mitochondrial GTP with insulin secretion.* J Biol Chem, 2009. **284**(39): p. 26578-90.
84. Ronnebaum, S.M., et al., *A pyruvate cycling pathway involving cytosolic NADP-dependent isocitrate dehydrogenase regulates glucose-stimulated insulin secretion.* J Biol Chem, 2006. **281**(41): p. 30593-602.
85. Pralong, W.F., C. Bartley, and C.B. Wollheim, *Single islet beta-cell stimulation by nutrients: relationship between pyridine nucleotides, cytosolic Ca²⁺ and secretion.* EMBO J, 1990. **9**(1): p. 53-60.
86. Heart, E., et al., *Ca²⁺, NAD(P)H and membrane potential changes in pancreatic beta-cells by methyl succinate: comparison with glucose.* Biochem J, 2007. **403**(1): p. 197-205.
87. Prentki, M., F.M. Matschinsky, and S.R. Madiraju, *Metabolic signaling in fuel-induced insulin secretion.* Cell Metab, 2013. **18**(2): p. 162-85.
88. Scott, I., *Regulation of cellular homeostasis by reversible lysine acetylation.* Essays Biochem, 2012. **52**: p. 13-22.
89. Wang, Q., et al., *Acetylation of metabolic enzymes coordinates carbon source utilization and metabolic flux.* Science, 2010. **327**(5968): p. 1004-7.
90. Herrero, L., et al., *Alteration of the malonyl-CoA/carnitine palmitoyltransferase I interaction in the beta-cell impairs glucose-induced insulin secretion.* Diabetes, 2005. **54**(2): p. 462-71.
91. Chen, S., et al., *More direct evidence for a malonyl-CoA-carnitine palmitoyltransferase I interaction as a key event in pancreatic beta-cell signaling.* Diabetes, 1994. **43**(7): p. 878-83.
92. Stanley, C.A., *Regulation of glutamate metabolism and insulin secretion by glutamate dehydrogenase in hypoglycemic children.* Am J Clin Nutr, 2009. **90**(3): p. 862S-866S.
93. Kelly, A., et al., *Glutaminolysis and insulin secretion: from bedside to bench and back.* Diabetes, 2002. **51 Suppl 3**: p. S421-6.

94. Bertrand, G., et al., *The elevation of glutamate content and the amplification of insulin secretion in glucose-stimulated pancreatic islets are not causally related.* J Biol Chem, 2002. **277**(36): p. 32883-91.
95. Fallon, M.J. and M.J. MacDonald, *Beta-cell alpha-ketoglutarate hydroxylases may acutely participate in insulin secretion.* Metabolism, 2008. **57**(8): p. 1148-54.
96. Cheng, K., et al., *Hypoxia-inducible factor-1alpha regulates beta cell function in mouse and human islets.* J Clin Invest, 2010. **120**(6): p. 2171-83.
97. Sjöholm, A., et al., *Glucose metabolites inhibit protein phosphatases and directly promote insulin exocytosis in pancreatic beta-cells.* Endocrinology, 2002. **143**(12): p. 4592-8.
98. Haby, C., et al., *Inhibition of serine/threonine protein phosphatases promotes opening of voltage-activated L-type Ca²⁺ channels in insulin-secreting cells.* Biochem. J., 1994. **298**(2): p. 341-0.
99. Li, C., et al., *Elimination of KATP channels in mouse islets results in elevated [U-¹³C]glucose metabolism, glutaminolysis, and pyruvate cycling but a decreased gamma-aminobutyric acid shunt.* J Biol Chem, 2008. **283**(25): p. 17238-49.
100. Pizarro-Delgado, J., et al., *Glucose promotion of GABA metabolism contributes to the stimulation of insulin secretion in beta-cells.* Biochem J, 2010. **431**(3): p. 381-9.
101. Braun, M., R. Ramracheya, and P. Rorsman, *Autocrine regulation of insulin secretion.* Diabetes Obes Metab, 2012. **14 Suppl 3**: p. 143-51.
102. Xu, E., et al., *Intra-islet insulin suppresses glucagon release via GABA-GABAA receptor system.* Cell Metab, 2006. **3**(1): p. 47-58.
103. Li, C., et al., *Regulation of glucagon secretion in normal and diabetic human islets by gamma-hydroxybutyrate and glycine.* J Biol Chem, 2013. **288**(6): p. 3938-51.
104. Curry, D.L., L.L. Bennett, and G.M. Grodsky, *Dynamics of insulin secretion by the perfused rat pancreas.* Endocrinology, 1968. **83**(3): p. 572-84.
105. Grodsky, G.M., et al., *[Further studies on the dynamic aspects of insulin release in vitro with evidence for a two-compartmental storage system].* Acta Diabetol Lat, 1969. **6 Suppl 1**: p. 554-78.
106. O'Connor, M.D., H. Landahl, and G.M. Grodsky, *Comparison of storage- and signal-limited models of pancreatic insulin secretion.* Am J Physiol, 1980. **238**(5): p. R378-89.
107. Cerasi, E. and R. Luft, *Plasma-Insulin Response to Sustained Hyperglycemia Induced by Glucose Infusion in Human Subjects.* Lancet, 1963. **2**(7322): p. 1359-61.

108. Henquin, J.C., et al., *Signals and pools underlying biphasic insulin secretion*. Diabetes, 2002. **51 Suppl 1**: p. S60-7.
109. Henquin, J.C., *Regulation of insulin secretion: a matter of phase control and amplitude modulation*. Diabetologia, 2009. **52**(5): p. 739-51.
110. Luzi, L. and R.A. DeFronzo, *Effect of loss of first-phase insulin secretion on hepatic glucose production and tissue glucose disposal in humans*. Am J Physiol, 1989. **257**(2 Pt 1): p. E241-6.
111. Nesher, R. and E. Cerasi, *Modeling phasic insulin release: immediate and time-dependent effects of glucose*. Diabetes, 2002. **51 Suppl 1**: p. S53-9.
112. Nunemaker, C.S., et al., *Insulin secretion in the conscious mouse is biphasic and pulsatile*. Am J Physiol Endocrinol Metab, 2006. **290**(3): p. E523-9.
113. Henquin, J.C., et al., *In vivo and in vitro glucose-induced biphasic insulin secretion in the mouse: pattern and role of cytoplasmic Ca²⁺ and amplification signals in beta-cells*. Diabetes, 2006. **55**(2): p. 441-51.
114. Zawalich, W.S. and K.C. Zawalich, *Species differences in the induction of time-dependent potentiation of insulin secretion*. Endocrinology, 1996. **137**(5): p. 1664-9.
115. Zawalich, W.S., et al., *Insulin secretion and IP levels in two distant lineages of the genus Mus: comparisons with rat islets*. Am J Physiol Endocrinol Metab, 2001. **280**(5): p. E720-8.
116. Lenzen, S., *Insulin secretion by isolated perfused rat and mouse pancreas*. Am J Physiol, 1979. **236**(4): p. E391-400.
117. Berglund, O., *Different dynamics of insulin secretion in the perfused pancreas of mouse and rat*. Acta Endocrinol (Copenh), 1980. **93**(1): p. 54-60.
118. Sato, Y. and J.C. Henquin, *The K⁺-ATP channel-independent pathway of regulation of insulin secretion by glucose: in search of the underlying mechanism*. Diabetes, 1998. **47**(11): p. 1713-21.
119. Efendic, S., P.E. Lins, and E. Cerasi, *Potentiation and inhibition of insulin release in man following priming with glucose and with arginine--effect of somatostatin*. Acta Endocrinol (Copenh), 1979. **90**(2): p. 259-71.
120. Nesher, R., E. Abramovitch, and E. Cerasi, *Correction of diabetic pattern of insulin release from islets of the spiny mouse (Acomys cahirinus) by glucose priming in vitro*. Diabetologia, 1985. **28**(4): p. 233-6.

121. Zawalich, W.S. and K.C. Zawalich, *Regulation of insulin secretion by phospholipase C*. Am J Physiol, 1996. **271**(3 Pt 1): p. E409-16.
122. Ma, Y.H., et al., *Differences in insulin secretion between the rat and mouse: role of cAMP*. Eur J Endocrinol, 1995. **132**(3): p. 370-6.
123. Zawalich, W.S., H. Yamazaki, and K.C. Zawalich, *Biphasic insulin secretion from freshly isolated or cultured, perfused rodent islets: comparative studies with rats and mice*. Metabolism, 2008. **57**(1): p. 30-9.
124. Caumo, A. and L. Luzi, *First-phase insulin secretion: does it exist in real life? Considerations on shape and function*. Am J Physiol Endocrinol Metab, 2004. **287**(3): p. E371-85.
125. Steiner, K.E., et al., *The relative importance of first- and second-phase insulin secretion in countering the action of glucagon on glucose turnover in the conscious dog*. Diabetes, 1982. **31**(11): p. 964-72.
126. Steiner, K.E., et al., *Relative importance of first- and second-phase insulin secretion in glucose homeostasis in conscious dog. II. Effects on gluconeogenesis*. Diabetes, 1986. **35**(7): p. 776-84.
127. Del Prato, S., P. Marchetti, and R.C. Bonadonna, *Phasic insulin release and metabolic regulation in type 2 diabetes*. Diabetes, 2002. **51 Suppl 1**: p. S109-16.
128. Cerasi, E., R. Luft, and S. Efendic, *Decreased sensitivity of the pancreatic beta cells to glucose in prediabetic and diabetic subjects. A glucose dose-response study*. Diabetes, 1972. **21**(4): p. 224-34.
129. van Haeften, T.W., et al., *Disturbances in beta-cell function in impaired fasting glycemia*. Diabetes, 2002. **51 Suppl 1**: p. S265-70.
130. Haffner, S.M., et al., *Decreased insulin action and insulin secretion predict the development of impaired glucose tolerance*. Diabetologia, 1996. **39**(10): p. 1201-7.
131. Grodsky, G.M., *A threshold distribution hypothesis for packet storage of insulin and its mathematical modeling*. J Clin Invest, 1972. **51**(8): p. 2047-59.
132. Cerasi, E., *An analogue computer model for the insulin response to glucose infusion*. Acta Endocrinol (Copenh), 1967. **55**(1): p. 163-83.
133. Straub, S.G. and G.W. Sharp, *Glucose-stimulated signaling pathways in biphasic insulin secretion*. Diabetes Metab Res Rev, 2002. **18**(6): p. 451-63.

134. Barg, S., et al., *Delay between fusion pore opening and peptide release from large dense-core vesicles in neuroendocrine cells*. Neuron, 2002. **33**(2): p. 287-99.
135. Ohara-Imaizumi, M., et al., *Imaging analysis reveals mechanistic differences between first- and second-phase insulin exocytosis*. J Cell Biol, 2007. **177**(4): p. 695-705.
136. Rorsman, P. and E. Renstrom, *Insulin granule dynamics in pancreatic beta cells*. Diabetologia, 2003. **46**(8): p. 1029-45.
137. Varadi, A., et al., *Involvement of conventional kinesin in glucose-stimulated secretory granule movements and exocytosis in clonal pancreatic beta-cells*. J Cell Sci, 2002. **115**(Pt 21): p. 4177-89.
138. Komatsu, M., et al., *KATP channel-independent glucose action: an elusive pathway in stimulus-secretion coupling of pancreatic beta-cell*. Endocr J, 2001. **48**(3): p. 275-88.
139. Cerasi, E., *Feed-back inhibition of insulin secretion in subjects with high and low insulin response to glucose*. Diabete Metab, 1975. **1**(2): p. 73-6.
140. Cerasi, E., *Potentiation of insulin release by glucose in man. I. Quantitative analysis of the enhancement of glucose-induced insulin secretion by pretreatment with glucose in normal subjects*. Acta Endocrinol (Copenh), 1975. **79**(3): p. 483-501.
141. Cerasi, E., *Potentiation of insulin release by glucose in man. II. Role of the insulin response, and enhancement of stimuli other than glucose*. Acta Endocrinol (Copenh), 1975. **79**(3): p. 502-10.
142. Cerasi, E., *Potentiation of insulin release by glucose in man*. Acta Endocrinol (Copenh), 1975. **79**(3): p. 511-34.
143. Cerasi, E., G. Fick, and M. Rudemo, *A mathematical model for the glucose induced insulin release in man*. Eur J Clin Invest, 1974. **4**(4): p. 267-78.
144. Cerasi, E., *Differential actions of glucose on insulin release: reevaluation of a mathematical model*, in *Carbohydrate metabolism : quantitative physiology and mathematical modelling*, C. Cobelli and R.N. Bergman, Editors. 1981, Wiley: Chichester [West Sussex] ; New York :. p. 3.
145. Grill, V., U. Adamson, and E. Cerasi, *Immediate and time-dependent effects of glucose on insulin release from rat pancreatic tissue. Evidence for different mechanisms of action*. J Clin Invest, 1978. **61**(4): p. 1034-43.
146. Ashby, J.P. and D. Shirling, *Evidence for priming and inhibitory effects of glucose on insulin secretion from isolated islets of Langerhans*. Diabetologia, 1980. **18**(5): p. 417-21.

147. Nesher, R. and E. Cerasi, *Biphasic insulin release as the expression of combined inhibitory and potentiating effects of glucose*. *Endocrinology*, 1987. **121**(3): p. 1017-24.
148. Spegel, P., et al., *Time-resolved metabolomics analysis of beta-cells implicates the pentose phosphate pathway in the control of insulin release*. *Biochem J*, 2013. **450**(3): p. 595-605.
149. Ammon, H.P., et al., *Pentose phosphate shunt, pyridine nucleotides, glutathione, and insulin secretion of fetal islets*. *Am J Physiol*, 1983. **244**(4): p. E354-60.
150. Ammon, H.P., T.N. Patel, and J. Steinke, *The role of the pentose phosphate shunt in glucose induced insulin release: in vitro studies with 6-aminonicotinamide, methylene blue, NAD + , NADH, NADP + , NADPH and nicotinamide on isolated pancreatic rat islets*. *Biochim Biophys Acta*, 1973. **297**(2): p. 352-67.
151. Brown, L.J., et al., *Chronic reduction of the cytosolic or mitochondrial NAD(P)-malic enzyme does not affect insulin secretion in a rat insulinoma cell line*. *J Biol Chem*, 2009. **284**(51): p. 35359-67.
152. Guay, C., et al., *A role for ATP-citrate lyase, malic enzyme, and pyruvate/citrate cycling in glucose-induced insulin secretion*. *J Biol Chem*, 2007. **282**(49): p. 35657-65.
153. Heart, E., et al., *Role for malic enzyme, pyruvate carboxylation, and mitochondrial malate import in glucose-stimulated insulin secretion*. *Am J Physiol Endocrinol Metab*, 2009. **296**(6): p. E1354-62.
154. MacDonald, M.J., *Differences between mouse and rat pancreatic islets: succinate responsiveness, malic enzyme, and anaplerosis*. *Am J Physiol Endocrinol Metab*, 2002. **283**(2): p. E302-310.
155. MacDonald, M.J., M.J. Longacre, and M.A. Kendrick, *Mitochondrial malic enzyme (ME2) in pancreatic islets of the human, rat and mouse and clonal insulinoma cells*. *Arch Biochem Biophys*, 2009. **488**(2): p. 100-4.
156. Pongratz, R.L., et al., *Cytosolic and mitochondrial malic enzyme isoforms differentially control insulin secretion*. *J Biol Chem*, 2007. **282**(1): p. 200-7.
157. Ronnebaum, S.M., et al., *Silencing of cytosolic or mitochondrial isoforms of malic enzyme has no effect on glucose-stimulated insulin secretion from rodent islets*. *J Biol Chem*, 2008. **283**(43): p. 28909-17.
158. Xu, J., et al., *Malic enzyme is present in mouse islets and modulates insulin secretion*. *Diabetologia*, 2008. **51**(12): p. 2281-9.

159. Lee, C.Y., et al., *Identification and biochemical analysis of mouse mutants deficient in cytoplasmic malic enzyme*. *Biochemistry*, 1980. **19**(22): p. 5098-103.
160. Roduit, R., et al., *A role for the malonyl-CoA/long-chain acyl-CoA pathway of lipid signaling in the regulation of insulin secretion in response to both fuel and nonfuel stimuli*. *Diabetes*, 2004. **53**(4): p. 1007-19.
161. Mulder, H., et al., *Overexpression of a modified human malonyl-CoA decarboxylase blocks the glucose-induced increase in malonyl-CoA level but has no impact on insulin secretion in INS-1-derived (832/13) beta-cells*. *J Biol Chem*, 2001. **276**(9): p. 6479-84.
162. Oliver, S.G., et al., *Systematic functional analysis of the yeast genome*. *Trends Biotechnol*, 1998. **16**(9): p. 373-8.
163. Fiehn, O., *Metabolomics--the link between genotypes and phenotypes*. *Plant Mol Biol*, 2002. **48**(1-2): p. 155-71.
164. Wishart, D.S., et al., *HMDB 3.0--The Human Metabolome Database in 2013*. *Nucleic Acids Res*, 2013. **41**(Database issue): p. D801-7.
165. Villas-Boas, S.G., et al., *Metabolome Analysis: An Introduction* 2007: Wiley.
166. Viant, M.R., E.S. Rosenblum, and R.S. Tiederema, *NMR-based metabolomics: a powerful approach for characterizing the effects of environmental stressors on organism health*. *Environ Sci Technol*, 2003. **37**(21): p. 4982-9.
167. Nicholson, J.K., J.C. Lindon, and E. Holmes, *'Metabonomics': understanding the metabolic responses of living systems to pathophysiological stimuli via multivariate statistical analysis of biological NMR spectroscopic data*. *Xenobiotica*, 1999. **29**(11): p. 1181-9.
168. Griffiths, J.R. and M. Stubbs, *Opportunities for studying cancer by metabolomics: preliminary observations on tumors deficient in hypoxia-inducible factor 1*. *Adv Enzyme Regul*, 2003. **43**: p. 67-76.
169. Bain, J.R., et al., *Metabolomics applied to diabetes research: moving from information to knowledge*. *Diabetes*, 2009. **58**(11): p. 2429-43.
170. Watkins, S.M. and J.B. German, *Metabolomics and biochemical profiling in drug discovery and development*. *Curr Opin Mol Ther*, 2002. **4**(3): p. 224-8.
171. German, J.B., et al., *Metabolomics and individual metabolic assessment: the next great challenge for nutrition*. *J Nutr*, 2002. **132**(9): p. 2486-7.

172. German, J.B., M.-A. Roberts, and S.M. Watkins, *Genomics and Metabolomics as Markers for the Interaction of Diet and Health: Lessons from Lipids*. The Journal of Nutrition, 2003. **133**(6): p. 2078S-2083S.
173. Watkins, S.M., et al., *Individual metabolism should guide agriculture toward foods for improved health and nutrition*. The American Journal of Clinical Nutrition, 2001. **74**(3): p. 283-286.
174. Watkins, S.M. and J.B. German, *Toward the implementation of metabolomic assessments of human health and nutrition*. Current Opinion in Biotechnology, 2002. **13**(5): p. 512-516.
175. D'Alessandro, A., et al., *Clinical metabolomics: the next stage of clinical biochemistry*. Blood Transfus, 2012. **10 Suppl 2**: p. s19-24.
176. Collino, S., F.P. Martin, and S. Rezzi, *Clinical metabolomics paves the way towards future healthcare strategies*. Br J Clin Pharmacol, 2013. **75**(3): p. 619-29.
177. Gowda, G.A., et al., *Metabolomics-based methods for early disease diagnostics*. Expert Rev Mol Diagn, 2008. **8**(5): p. 617-33.
178. Nielsen, J. and S. Oliver, *The next wave in metabolome analysis*. Trends Biotechnol, 2005. **23**(11): p. 544-6.
179. de Koning, W. and K. van Dam, *A method for the determination of changes of glycolytic metabolites in yeast on a subsecond time scale using extraction at neutral pH*. Anal Biochem, 1992. **204**(1): p. 118-23.
180. Rizzi, M., et al., *In vivo analysis of metabolic dynamics in Saccharomyces cerevisiae: II. Mathematical model*. Biotechnol Bioeng, 1997. **55**(4): p. 592-608.
181. Marshall, S., O. Nadeau, and K. Yamasaki, *Dynamic actions of glucose and glucosamine on hexosamine biosynthesis in isolated adipocytes: differential effects on glucosamine 6-phosphate, UDP-N-acetylglucosamine, and ATP levels*. J Biol Chem, 2004. **279**(34): p. 35313-9.
182. Shryock, J.C., R. Rubio, and R.M. Berne, *Extraction of adenine nucleotides from cultured endothelial cells*. Anal Biochem, 1986. **159**(1): p. 73-81.
183. Kopka, J., J.B. Ohlrogge, and J.G. Jaworski, *Analysis of in vivo levels of acyl-thioesters with gas chromatography/mass spectrometry of the butylamide derivative*. Anal Biochem, 1995. **224**(1): p. 51-60.

184. Hajjaj, H., et al., *Sampling techniques and comparative extraction procedures for quantitative determination of intra- and extracellular metabolites in filamentous fungi*. FEMS Microbiology Letters, 1998. **164**(1): p. 195-200.
185. Buziol, S., et al., *New bioreactor-coupled rapid stopped-flow sampling technique for measurements of metabolite dynamics on a subsecond time scale*. Biotechnology and Bioengineering, 2002. **80**(6): p. 632-636.
186. Villas-Bôas, S.G., et al., *Global metabolite analysis of yeast: evaluation of sample preparation methods*. Yeast, 2005. **22**(14): p. 1155-1169.
187. Sargenti, S.R. and W. Vichnewski, *Sonication and liquid chromatography as a rapid technique for extraction and fractionation of plant material*. Phytochemical Analysis, 2000. **11**(2): p. 69-73.
188. Pernet, F. and R. Tremblay, *Effect of ultrasonication and grinding on the determination of lipid class content of microalgae harvested on filters*. Lipids, 2003. **38**(11): p. 1191-1195.
189. Waksmundzka-Hajnos, M., et al., *Effect of extraction method on the yield of furanocoumarins from fruits of Archangelica officinalis Hoffm*. Phytochemical Analysis, 2004. **15**(5): p. 313-319.
190. Smedsgaard, J., *Micro-scale extraction procedure for standardized screening of fungal metabolite production in cultures*. Journal of Chromatography A, 1997. **760**(2): p. 264-270.
191. Stout, S.J., et al., *Microwave-Assisted Extraction Coupled with Liquid Chromatography/Electrospray Ionization Mass Spectrometry for the Simplified Determination of Imidazolinone Herbicides and Their Metabolites in Plant Tissue*. Journal of Agricultural and Food Chemistry, 1996. **44**(11): p. 3548-3553.
192. Michalke, B., H. Witte, and P. Schramel, *Effect of different extraction procedures on the yield and pattern of Se-species in bacterial samples*. Analytical and Bioanalytical Chemistry, 2002. **372**(3): p. 444-447.
193. Tondo, E.C., et al., *High biodegradation levels of 4,5,6-trichloroguaiacol by Bacillus sp. isolated from cellulose pulp mill effluent*. Revista de Microbiologia, 1998. **29**: p. 265-270.
194. Maharjan, R.P. and T. Ferenci, *Global metabolite analysis: the influence of extraction methodology on metabolome profiles of Escherichia coli*. Anal Biochem, 2003. **313**(1): p. 145-54.
195. Villas-Boas, S.G., et al., *Global metabolite analysis of yeast: evaluation of sample preparation methods*. Yeast, 2005. **22**(14): p. 1155-69.

196. Wu, H., et al., *High-throughput tissue extraction protocol for NMR- and MS-based metabolomics*. Anal Biochem, 2008. **372**(2): p. 204-12.
197. Smits, H.P., et al., *Cleanup and analysis of sugar phosphates in biological extracts by using solid-phase extraction and anion-exchange chromatography with pulsed amperometric detection*. Anal Biochem, 1998. **261**(1): p. 36-42.
198. Jensen, N.B., K.V. Jokumsen, and J. Villadsen, *Determination of the phosphorylated sugars of the Embden-Meyerhoff-Parnas pathway in Lactococcus lactis using a fast sampling technique and solid phase extraction*. Biotechnol Bioeng, 1999. **63**(3): p. 356-62.
199. Belle, J.E.L., et al., *A comparison of cell and tissue extraction techniques using high-resolution 1H-NMR spectroscopy*. NMR in Biomedicine, 2002. **15**(1): p. 37-44.
200. Cremin, P., et al., *Liquid chromatographic-thermospray mass spectrometric analysis of sesquiterpenes of Armillaria (Eumycota: Basidiomycotina) species*. Journal of Chromatography A, 1995. **710**(2): p. 273-285.
201. Koning, W.d. and K.v. Dam, *A method for the determination of changes of glycolytic metabolites in yeast on a subsecond time scale using extraction at neutral pH*. Analytical Biochemistry, 1992. **204**(1): p. 118-123.
202. Villas-Bôas, S.G., et al., *High-throughput metabolic state analysis: the missing link in integrated functional genomics of yeasts*. Biochem. J., 2005. **388**(2): p. 669-677.
203. Roessner, U., et al., *Technical advance: simultaneous analysis of metabolites in potato tuber by gas chromatography-mass spectrometry*. Plant J, 2000. **23**(1): p. 131-42.
204. Roessner-Tunali, U., et al., *Metabolic profiling of transgenic tomato plants overexpressing hexokinase reveals that the influence of hexose phosphorylation diminishes during fruit development*. Plant Physiol, 2003. **133**(1): p. 84-99.
205. Provencher, S.W., *Estimation of metabolite concentrations from localized in vivo proton NMR spectra*. Magn Reson Med, 1993. **30**(6): p. 672-9.
206. Bennett, B.D., et al., *Absolute metabolite concentrations and implied enzyme active site occupancy in Escherichia coli*. Nat Chem Biol, 2009. **5**(8): p. 593-9.
207. Fraser, P.D., et al., *Technical advance: application of high-performance liquid chromatography with photodiode array detection to the metabolic profiling of plant isoprenoids*. Plant J, 2000. **24**(4): p. 551-8.

208. Johnson, H.E., et al., *High-throughput metabolic fingerprinting of legume silage fermentations via Fourier transform infrared spectroscopy and chemometrics*. Appl Environ Microbiol, 2004. **70**(3): p. 1583-92.
209. Gidman, E., et al., *Investigating plant-plant interference by metabolic fingerprinting*. Phytochemistry, 2003. **63**(6): p. 705-10.
210. Thomas, N., et al., *Fourier transform infrared spectroscopy of follicular fluids from large and small antral follicles*. Hum Reprod, 2000. **15**(8): p. 1667-71.
211. Rashed, M.S., *Clinical applications of tandem mass spectrometry: ten years of diagnosis and screening for inherited metabolic diseases*. J Chromatogr B Biomed Sci Appl, 2001. **758**(1): p. 27-48.
212. Fiehn, O., et al., *Metabolite profiling for plant functional genomics*. Nat Biotechnol, 2000. **18**(11): p. 1157-61.
213. Raamsdonk, L.M., et al., *A functional genomics strategy that uses metabolome data to reveal the phenotype of silent mutations*. Nat Biotechnol, 2001. **19**(1): p. 45-50.
214. Serkova, N.J. and C.U. Niemann, *Pattern recognition and biomarker validation using quantitative 1H-NMR-based metabolomics*. Expert Rev Mol Diagn, 2006. **6**(5): p. 717-31.
215. Keun, H.C. and T.J. Athersuch, *Nuclear magnetic resonance (NMR)-based metabolomics*. Methods Mol Biol, 2011. **708**: p. 321-34.
216. Kim, H.K., Y.H. Choi, and R. Verpoorte, *NMR-based plant metabolomics: where do we stand, where do we go?* Trends Biotechnol, 2011. **29**(6): p. 267-75.
217. Salek, R., K.K. Cheng, and J. Griffin, *The study of mammalian metabolism through NMR-based metabolomics*. Methods Enzymol, 2011. **500**: p. 337-51.
218. Choi, B.K., D.M. Hercules, and A.I. Gusev, *Effect of liquid chromatography separation of complex matrices on liquid chromatography-tandem mass spectrometry signal suppression*. J Chromatogr A, 2001. **907**(1-2): p. 337-42.
219. Hakansson, K., et al., *Low-mass ions observed in plasma desorption mass spectrometry of high explosives*. J Mass Spectrom, 2000. **35**(3): p. 337-46.
220. Gates, S.C., N. Dendramis, and C.C. Sweeley, *Automated metabolic profiling of organic acids in human urine. I. Description of methods*. Clin Chem, 1978. **24**(10): p. 1674-9.
221. Gates, S.C., et al., *Automated metabolic profiling of organic acids in human urine. II. Analysis of urine samples from "healthy" adults, sick children, and children with neuroblastoma*. Clin Chem, 1978. **24**(10): p. 1680-9.

222. Gates, S.C. and C.C. Sweeley, *Quantitative metabolic profiling based on gas chromatography*. Clin Chem, 1978. **24**(10): p. 1663-73.
223. Halket, J.M., et al., *Chemical derivatization and mass spectral libraries in metabolic profiling by GC/MS and LC/MS/MS*. J Exp Bot, 2005. **56**(410): p. 219-43.
224. Little, J.L., *Artifacts in trimethylsilyl derivatization reactions and ways to avoid them*. J Chromatogr A, 1999. **844**(1-2): p. 1-22.
225. Stein, S.E., *An integrated method for spectrum extraction and compound identification from gas chromatography/mass spectrometry data*. Journal of the American Society for Mass Spectrometry, 1999. **10**(8): p. 770-781.
226. Veriotti, T. and R. Sacks, *High-Speed GC and GC/Time-of-Flight MS of Lemon and Lime Oil Samples*. Analytical Chemistry, 2001. **73**(18): p. 4395-4402.
227. Kind, T., et al., *FiehnLib: mass spectral and retention index libraries for metabolomics based on quadrupole and time-of-flight gas chromatography/mass spectrometry*. Anal Chem, 2009. **81**(24): p. 10038-48.
228. Maurer, H.H., *Liquid chromatography-mass spectrometry in forensic and clinical toxicology*. J Chromatogr B Biomed Sci Appl, 1998. **713**(1): p. 3-25.
229. Bendahl, L., et al., *Hyphenation of ultra performance liquid chromatography (UPLC) with inductively coupled plasma mass spectrometry (ICP-MS) for fast analysis of bromine containing preservatives*. J Pharm Biomed Anal, 2006. **40**(3): p. 648-52.
230. Churchwell, M.I., et al., *Improving LC-MS sensitivity through increases in chromatographic performance: comparisons of UPLC-ES/MS/MS to HPLC-ES/MS/MS*. J Chromatogr B Analyt Technol Biomed Life Sci, 2005. **825**(2): p. 134-43.
231. Tolstikov, V.V. and O. Fiehn, *Analysis of highly polar compounds of plant origin: combination of hydrophilic interaction chromatography and electrospray ion trap mass spectrometry*. Anal Biochem, 2002. **301**(2): p. 298-307.
232. Want, E.J., et al., *Global metabolic profiling procedures for urine using UPLC-MS*. Nat Protoc, 2010. **5**(6): p. 1005-18.
233. Castro-Perez, J., et al., *Increasing throughput and information content for in vitro drug metabolism experiments using ultra-performance liquid chromatography coupled to a quadrupole time-of-flight mass spectrometer*. Rapid Commun Mass Spectrom, 2005. **19**(6): p. 843-8.

234. Leandro, C.C., et al., *Comparison of ultra-performance liquid chromatography and high-performance liquid chromatography for the determination of priority pesticides in baby foods by tandem quadrupole mass spectrometry*. J Chromatogr A, 2006. **1103**(1): p. 94-101.
235. O'Connor, D., et al., *Ultra-performance liquid chromatography coupled to time-of-flight mass spectrometry for robust, high-throughput quantitative analysis of an automated metabolic stability assay, with simultaneous determination of metabolic data*. Rapid Commun Mass Spectrom, 2006. **20**(5): p. 851-7.
236. Perrett, D. and G. Ross, *Capillary electrophoresis: A powerful tool for biomedical analysis and research?* TrAC Trends in Analytical Chemistry, 1992. **11**(4): p. 156-163.
237. Jia, L. and S. Terabe, *Capillary Electrophoresis and Its Application in Metabolome Analysis*, in *Metabolome Analyses: Strategies for Systems Biology*, S. Vaidyanathan, G. Harrigan, and R. Goodacre, Editors. 2005, Springer US. p. 83-101.
238. Perrett, D., et al., *Capillary electrophoresis for small molecules and metabolites*. Biochem Soc Trans, 1997. **25**(1): p. 273-8.
239. Wang, X., et al., *Capillary electrophoresis-mass spectrometry in metabolomics: the potential for driving drug discovery and development*. Curr Drug Metab, 2013. **14**(7): p. 807-13.
240. Kami, K., et al., *Metabolomic profiling of lung and prostate tumor tissues by capillary electrophoresis time-of-flight mass spectrometry*. Metabolomics, 2013. **9**(2): p. 444-453.
241. Kleparnik, K., *Recent advances in the combination of capillary electrophoresis with mass spectrometry: from element to single-cell analysis*. Electrophoresis, 2013. **34**(1): p. 70-85.
242. Ferruzzi, M.G., et al., *Analysis of lycopene geometrical isomers in biological microsamples by liquid chromatography with coulometric array detection*. J Chromatogr B Biomed Sci Appl, 2001. **760**(2): p. 289-99.
243. Lindon, J.C., E. Holmes, and J.K. Nicholson, *So what's the deal with metabolomics?* Anal Chem, 2003. **75**(17): p. 384A-391A.
244. Szyperski, T., *¹³C-NMR, MS and metabolic flux balancing in biotechnology research*. Q Rev Biophys, 1998. **31**(1): p. 41-106.
245. Wiechert, W. and A.A. de Graaf, *Bidirectional reaction steps in metabolic networks: I. Modeling and simulation of carbon isotope labeling experiments*. Biotechnology and Bioengineering, 1997. **55**(1): p. 101-117.
246. Pan, Z. and D. Raftery, *Comparing and combining NMR spectroscopy and mass spectrometry in metabolomics*. Anal Bioanal Chem, 2007. **387**(2): p. 525-7.

247. Keun, H.C., et al., *Cryogenic probe ¹³C NMR spectroscopy of urine for metabonomic studies*. Anal Chem, 2002. **74**(17): p. 4588-93.
248. Lindon, J.C., J.K. Nicholson, and E. Holmes, *The Handbook of Metabonomics and Metabolomics* 2011: Elsevier Science.
249. Garrod, S., et al., *High-resolution magic angle spinning ¹H NMR spectroscopic studies on intact rat renal cortex and medulla*. Magn Reson Med, 1999. **41**(6): p. 1108-18.
250. Cheng, L.L., et al., *Correlation of high-resolution magic angle spinning proton magnetic resonance spectroscopy with histopathology of intact human brain tumor specimens*. Cancer Res, 1998. **58**(9): p. 1825-32.
251. Wishart, D.S., et al., *HMDB: a knowledgebase for the human metabolome*. Nucleic Acids Res, 2009. **37**(Database issue): p. D603-10.
252. Wishart, D.S., et al., *HMDB: the Human Metabolome Database*. Nucleic Acids Res, 2007. **35**(Database issue): p. D521-6.
253. Kopka, J., et al., *GMD@CSB.DB: the Golm Metabolome Database*. Bioinformatics, 2005. **21**(8): p. 1635-8.
254. Zhu, Z.J., et al., *Liquid chromatography quadrupole time-of-flight mass spectrometry characterization of metabolites guided by the METLIN database*. Nat Protoc, 2013. **8**(3): p. 451-60.
255. Smith, C.A., et al., *METLIN: a metabolite mass spectral database*. Ther Drug Monit, 2005. **27**(6): p. 747-51.
256. Tautenhahn, R., et al., *An accelerated workflow for untargeted metabolomics using the METLIN database*. Nat Biotechnol, 2012. **30**(9): p. 826-8.
257. Eisen, M.B., et al., *Cluster analysis and display of genome-wide expression patterns*. Proc Natl Acad Sci U S A, 1998. **95**(25): p. 14863-8.
258. Jonsson, P., et al., *Predictive metabolite profiling applying hierarchical multivariate curve resolution to GC-MS data--a potential tool for multi-parametric diagnosis*. J Proteome Res, 2006. **5**(6): p. 1407-14.
259. De Souza, D.P., et al., *Progressive peak clustering in GC-MS Metabolomic experiments applied to Leishmania parasites*. Bioinformatics, 2006. **22**(11): p. 1391-6.
260. Tikunov, Y., et al., *A novel approach for nontargeted data analysis for metabolomics. Large-scale profiling of tomato fruit volatiles*. Plant Physiol, 2005. **139**(3): p. 1125-37.

261. Alter, O., P.O. Brown, and D. Botstein, *Singular value decomposition for genome-wide expression data processing and modeling*. Proc Natl Acad Sci U S A, 2000. **97**(18): p. 10101-6.
262. Tamayo, P., et al., *Interpreting patterns of gene expression with self-organizing maps: methods and application to hematopoietic differentiation*. Proc Natl Acad Sci U S A, 1999. **96**(6): p. 2907-12.
263. Scholz, M., et al., *Metabolite fingerprinting: detecting biological features by independent component analysis*. Bioinformatics, 2004. **20**(15): p. 2447-54.
264. Goodacre, R., et al., *Metabolomics by numbers: acquiring and understanding global metabolite data*. Trends Biotechnol, 2004. **22**(5): p. 245-52.
265. Manly, B.F.J., *Multivariate Statistical Methods: A Primer, Second Edition* 1994: Taylor & Francis.
266. Martens, H. and T. Naes, *Multivariate Calibration* 1991: Wiley.
267. Wold, S., et al., *The Collinearity Problem in Linear Regression. The Partial Least Squares (PLS) Approach to Generalized Inverses*. SIAM Journal on Scientific and Statistical Computing, 1984. **5**(3): p. 735-743.
268. Lundstedt, T., et al., *Experimental design and optimization*. Chemometrics and Intelligent Laboratory Systems, 1998. **42**(1-2): p. 3-40.
269. Wold, S., et al., *Multivariate Data Analysis in Chemistry*, in *Chemometrics*, B. Kowalski, Editor 1984, Springer Netherlands. p. 17-95.
270. Rumelhart, D.E., G.E. Hinton, and R.J. Williams, *Learning representations by back-propagating errors*. Nature, 1986. **323**(6088): p. 533-536.
271. Harrington, P.B., *Fuzzy multivariate rule-building expert systems: Minimal neural networks*. Journal of Chemometrics, 1991. **5**(5): p. 467-486.
272. Quinlan, J.R., *C4.5: Programs for Machine Learning* 1993: MORGAN KAUFMAN PUBL Incorporated.
273. Muggleton, S., *Inductive Logic Programming: Issues, results and the challenge of Learning Language in Logic*. Artificial Intelligence, 1999. **114**(1-2): p. 283-296.
274. Baeck, T., D.B. Fogel, and Z. Michalewicz, *Handbook of Evolutionary Computation* 1997: Taylor & Francis.
275. Kell, D.B., R.M. Darby, and J. Draper, *Genomic computing. Explanatory analysis of plant expression profiling data using machine learning*. Plant Physiol, 2001. **126**(3): p. 943-51.

276. Dieterle, F., et al., *Metabolite projection analysis for fast identification of metabolites in metabonomics. Application in an amiodarone study*. Anal Chem, 2006. **78**(11): p. 3551-61.
277. Yin, P., et al., *Metabonomics study of intestinal fistulas based on ultraperformance liquid chromatography coupled with Q-TOF mass spectrometry (UPLC/Q-TOF MS)*. J Proteome Res, 2006. **5**(9): p. 2135-43.
278. Ramadan, Z., et al., *Metabolic profiling using principal component analysis, discriminant partial least squares, and genetic algorithms*. Talanta, 2006. **68**(5): p. 1683-91.
279. Constantinou, M.A., et al., *¹H NMR-based metabonomics for the diagnosis of inborn errors of metabolism in urine*. Analytica Chimica Acta, 2005. **542**(2): p. 169-177.
280. Yang, J., et al., *High Performance Liquid Chromatography–Mass Spectrometry for Metabonomics: Potential Biomarkers for Acute Deterioration of Liver Function in Chronic Hepatitis B*. Journal of Proteome Research, 2006. **5**(3): p. 554-561.
281. Stella, C., et al., *Susceptibility of human metabolic phenotypes to dietary modulation*. J Proteome Res, 2006. **5**(10): p. 2780-8.
282. Trygg, J. and S. Wold, *Orthogonal projections to latent structures (O-PLS)*. Journal of Chemometrics, 2002. **16**(3): p. 119-128.
283. Bylesjö, M., et al., *OPLS discriminant analysis: combining the strengths of PLS-DA and SIMCA classification*. Journal of Chemometrics, 2006. **20**(8-10): p. 341-351.
284. Weckwerth, W. and O. Fiehn, *Can we discover novel pathways using metabolomic analysis?* Curr Opin Biotechnol, 2002. **13**(2): p. 156-60.
285. Kvalheim, O.M., *The latent variable*. Chemometrics and Intelligent Laboratory Systems, 1992. **14**(1–3): p. 1-3.
286. Trygg, J., E. Holmes, and T. Lundstedt, *Chemometrics in metabonomics*. J Proteome Res, 2007. **6**(2): p. 469-79.
287. Hotelling, H., *The Generalization of Student's Ratio*. The Annals of Mathematical Statistics, 1931. **2**(3): p. 360-378.
288. Eriksson, L. and U. AB., *Multi- and Megavariate Data Analysis*2006: Umetrics AB.
289. Eriksson, L., et al., *Multi- and Megavariate Data Analysis: Principles and Applications*2001: Umetrics Academy.
290. Shen, H., et al., *Automated curve resolution applied to data from multi-detection instruments*. Analytica Chimica Acta, 2001. **446**(1–2): p. 311-326.

291. Halket, J.M., et al., *Deconvolution gas chromatography/mass spectrometry of urinary organic acids--potential for pattern recognition and automated identification of metabolic disorders*. Rapid Commun Mass Spectrom, 1999. **13**(4): p. 279-84.
292. Jonsson, P., et al., *Extraction, interpretation and validation of information for comparing samples in metabolic LC/MS data sets*. Analyst, 2005. **130**(5): p. 701-7.
293. Jonsson, P., et al., *A strategy for identifying differences in large series of metabolomic samples analyzed by GC/MS*. Anal Chem, 2004. **76**(6): p. 1738-45.
294. Almstetter, M.F., et al., *Integrative normalization and comparative analysis for metabolic fingerprinting by comprehensive two-dimensional gas chromatography-time-of-flight mass spectrometry*. Anal Chem, 2009. **81**(14): p. 5731-9.
295. Vogels, J.T.W.E., et al., *A new method for classification of wines based on proton and carbon-13 NMR spectroscopy in combination with pattern recognition techniques*. Chemometrics and Intelligent Laboratory Systems, 1993. **21**(2-3): p. 249-258.
296. Torgrip, R.J.O., et al., *Peak alignment using reduced set mapping*. Journal of Chemometrics, 2003. **17**(11): p. 573-582.
297. Pluskal, T., et al., *MZmine 2: modular framework for processing, visualizing, and analyzing mass spectrometry-based molecular profile data*. BMC Bioinformatics, 2010. **11**: p. 395.
298. Katajamaa, M., J. Miettinen, and M. Oresic, *MZmine: toolbox for processing and visualization of mass spectrometry based molecular profile data*. Bioinformatics, 2006. **22**(5): p. 634-6.
299. Lommen, A. and H.J. Kools, *MetAlign 3.0: performance enhancement by efficient use of advances in computer hardware*. Metabolomics, 2012. **8**(4): p. 719-726.
300. Lommen, A., *MetAlign: interface-driven, versatile metabolomics tool for hyphenated full-scan mass spectrometry data preprocessing*. Anal Chem, 2009. **81**(8): p. 3079-86.
301. Baran, R., et al., *MathDAMP: a package for differential analysis of metabolite profiles*. BMC Bioinformatics, 2006. **7**: p. 530.
302. Smith, C.A., et al., *XCMS: processing mass spectrometry data for metabolite profiling using nonlinear peak alignment, matching, and identification*. Anal Chem, 2006. **78**(3): p. 779-87.
303. Benton, H.P., et al., *XCMS2: processing tandem mass spectrometry data for metabolite identification and structural characterization*. Anal Chem, 2008. **80**(16): p. 6382-9.
304. Patti, G.J., R. Tautenhahn, and G. Siuzdak, *Meta-analysis of untargeted metabolomic data from multiple profiling experiments*. Nat Protoc, 2012. **7**(3): p. 508-16.

305. Tautenhahn, R., et al., *metaXCMS: second-order analysis of untargeted metabolomics data*. Anal Chem, 2011. **83**(3): p. 696-700.
306. Patti, G.J., et al., *A View from Above: Cloud Plots to Visualize Global Metabolomic Data*. Analytical Chemistry, 2012. **85**(2): p. 798-804.
307. Tautenhahn, R., et al., *XCMS Online: a web-based platform to process untargeted metabolomic data*. Anal Chem, 2012. **84**(11): p. 5035-9.
308. Choe, S., et al., *Development of a target component extraction method from GC-MS data with an in-house program for metabolite profiling*. Anal Biochem, 2012. **426**(2): p. 94-102.
309. Evans, C.R. and J.W. Jorgenson, *Multidimensional LC-LC and LC-CE for high-resolution separations of biological molecules*. Anal Bioanal Chem, 2004. **378**(8): p. 1952-61.
310. Kammerer, B., et al., *Achiral-chiral LC/LC-MS/MS coupling for determination of chiral discrimination effects in phenprocoumon metabolism*. Anal Biochem, 2005. **339**(2): p. 297-309.
311. Mondello, L., et al., *Silver-ion reversed-phase comprehensive two-dimensional liquid chromatography combined with mass spectrometric detection in lipidic food analysis*. J Chromatogr A, 2005. **1086**(1-2): p. 91-8.
312. Sheldon, E.M., *Development of a LC-LC-MS complete heart-cut approach for the characterization of pharmaceutical compounds using standard instrumentation*. J Pharm Biomed Anal, 2003. **31**(6): p. 1153-66.
313. Stroink, T., et al., *On-line multidimensional liquid chromatography and capillary electrophoresis systems for peptides and proteins*. J Chromatogr B Analyt Technol Biomed Life Sci, 2005. **817**(1): p. 49-66.
314. Jenkins, H., et al., *A proposed framework for the description of plant metabolomics experiments and their results*. Nat Biotechnol, 2004. **22**(12): p. 1601-6.
315. Bino, R.J., et al., *Potential of metabolomics as a functional genomics tool*. Trends Plant Sci, 2004. **9**(9): p. 418-25.
316. Lindon, J.C., et al., *Summary recommendations for standardization and reporting of metabolic analyses*. Nat Biotechnol, 2005. **23**(7): p. 833-8.
317. Castle, A.L., et al., *Metabolomics Standards Workshop and the development of international standards for reporting metabolomics experimental results*. Brief Bioinform, 2006. **7**(2): p. 159-65.

318. Hohmeier, H.E., et al., *Isolation of INS-1-derived cell lines with robust ATP-sensitive K⁺ channel-dependent and -independent glucose-stimulated insulin secretion*. *Diabetes*, 2000. **49**(3): p. 424-30.
319. Pillai, R., et al., *Aryl hydrocarbon receptor nuclear translocator/hypoxia-inducible factor-1{beta} plays a critical role in maintaining glucose-stimulated anaplerosis and insulin release from pancreatic {beta}-cells*. *J Biol Chem*, 2011. **286**(2): p. 1014-24.
320. Huang, M. and J.W. Joseph, *Metabolomic analysis of pancreatic beta-cell insulin release in response to glucose*. *Islets*, 2012. **4**(3): p. 210-22.
321. Joseph, J.W., et al., *Normal flux through ATP-citrate lyase or fatty acid synthase is not required for glucose-stimulated insulin secretion*. *J Biol Chem*, 2007. **282**(43): p. 31592-600.
322. Joseph, J.W., et al., *Free fatty acid-induced beta-cell defects are dependent on uncoupling protein 2 expression*. *J Biol Chem*, 2004. **279**(49): p. 51049-56.
323. Zhang, C.Y., et al., *Uncoupling protein-2 negatively regulates insulin secretion and is a major link between obesity, beta cell dysfunction, and type 2 diabetes*. *Cell*, 2001. **105**(6): p. 745-55.
324. Lacy, P.E. and M. Kostianovsky, *Method for the isolation of intact islets of Langerhans from the rat pancreas*. *Diabetes*, 1967. **16**(1): p. 35-9.
325. Hughes, S.D., et al., *Transfection of AtT-20ins cells with GLUT-2 but not GLUT-1 confers glucose-stimulated insulin secretion. Relationship to glucose metabolism*. *J Biol Chem*, 1993. **268**(20): p. 15205-12.
326. Wu, M., et al., *Multiparameter metabolic analysis reveals a close link between attenuated mitochondrial bioenergetic function and enhanced glycolysis dependency in human tumor cells*. *Am J Physiol Cell Physiol*, 2007. **292**(1): p. C125-36.
327. Wikstrom, J.D., et al., *A novel high-throughput assay for islet respiration reveals uncoupling of rodent and human islets*. *PLoS One*, 2012. **7**(5): p. e33023.
328. Kahn, S.E., R.L. Hull, and K.M. Utzschneider, *Mechanisms linking obesity to insulin resistance and type 2 diabetes*. *Nature*, 2006. **444**(7121): p. 840-6.
329. Marx, J., *Unraveling the causes of diabetes*. *Science*, 2002. **296**(5568): p. 686-9.
330. Henquin, J.C., et al., *Shortcomings of current models of glucose-induced insulin secretion*. *Diabetes Obes Metab*, 2009. **11 Suppl 4**: p. 168-79.

331. Detimary, P., G. Van den Berghe, and J.C. Henquin, *Concentration dependence and time course of the effects of glucose on adenine and guanine nucleotides in mouse pancreatic islets*. J Biol Chem, 1996. **271**(34): p. 20559-65.
332. Kibbey, R.G., et al., *Mitochondrial GTP regulates glucose-stimulated insulin secretion*. Cell Metab, 2007. **5**(4): p. 253-64.
333. Spegel, P., et al., *Metabolomic analyses reveal profound differences in glycolytic and tricarboxylic acid cycle metabolism in glucose-responsive and -unresponsive clonal beta-cell lines*. Biochem J, 2011. **435**(1): p. 277-84.
334. Maechler, P. and C.B. Wollheim, *Mitochondrial glutamate acts as a messenger in glucose-induced insulin exocytosis*. Nature, 1999. **402**(6762): p. 685-689.
335. Maechler, P., A. Gjinovci, and C.B. Wollheim, *Implication of glutamate in the kinetics of insulin secretion in rat and mouse perfused pancreas*. Diabetes, 2002. **51 Suppl 1**: p. S99-102.
336. Corkey, B.E., et al., *A role for malonyl-CoA in glucose-stimulated insulin secretion from clonal pancreatic beta-cells*. J Biol Chem, 1989. **264**(36): p. 21608-12.
337. Prentki, M., et al., *Malonyl-CoA and long chain acyl-CoA esters as metabolic coupling factors in nutrient-induced insulin secretion*. J Biol Chem, 1992. **267**(9): p. 5802-10.
338. Ivarsson, R., et al., *Redox control of exocytosis: regulatory role of NADPH, thioredoxin, and glutaredoxin*. Diabetes, 2005. **54**(7): p. 2132-42.
339. MacDonald, M.J. and L.A. Fahien, *Glutamate is not a messenger in insulin secretion*. J Biol Chem, 2000. **275**(44): p. 34025-7.
340. Scalbert, A., et al., *Mass-spectrometry-based metabolomics: limitations and recommendations for future progress with particular focus on nutrition research*. Metabolomics, 2009. **5**(4): p. 435-458.
341. Szpunar, J., *Advances in analytical methodology for bioinorganic speciation analysis: metallomics, metalloproteomics and heteroatom-tagged proteomics and metabolomics*. Analyst, 2005. **130**(4): p. 442-65.
342. Dettmer, K., P.A. Aronov, and B.D. Hammock, *Mass spectrometry-based metabolomics*. Mass Spectrom Rev, 2007. **26**(1): p. 51-78.
343. Fernandez, C., et al., *Metabolomic and proteomic analysis of a clonal insulin-producing beta-cell line (INS-1 832/13)*. J Proteome Res, 2008. **7**(1): p. 400-11.

344. Katajamaa, M. and M. Oresic, *Data processing for mass spectrometry-based metabolomics*. J Chromatogr A, 2007. **1158**(1-2): p. 318-28.
345. Ohtsubo, K., et al., *Dietary and genetic control of glucose transporter 2 glycosylation promotes insulin secretion in suppressing diabetes*. Cell, 2005. **123**(7): p. 1307-21.
346. Giroix, M.H., A. Sener, and W.J. Malaisse, *Pentose cycle pathway in normal and tumoral islet cells*. FEBS Lett, 1985. **185**(1): p. 1-3.
347. Oliveira, H.R., R. Curi, and A.R. Carpinelli, *Glucose induces an acute increase of superoxide dismutase activity in incubated rat pancreatic islets*. Am J Physiol, 1999. **276**(2 Pt 1): p. C507-10.
348. Verspohl, E.J., M. Handel, and H.P. Ammon, *Pentosephosphate shunt activity of rat pancreatic islets: its dependence on glucose concentration*. Endocrinology, 1979. **105**(5): p. 1269-74.
349. Zhang, Z., et al., *High glucose inhibits glucose-6-phosphate dehydrogenase, leading to increased oxidative stress and beta-cell apoptosis*. FASEB J, 2010. **24**(5): p. 1497-505.
350. Lange, K. and E.R. Proft, *Inhibition of the 6-phosphogluconate dehydrogenase in the rat kidney by 6-aminonicotinamide*. Naunyn Schmiedebergs Arch Pharmakol, 1970. **267**(2): p. 177-80.
351. Krus, U., et al., *Pyruvate dehydrogenase kinase 1 controls mitochondrial metabolism and insulin secretion in INS-1 832/13 clonal beta-cells*. Biochem J, 2010. **429**(1): p. 205-13.
352. Newsholme, P., et al., *Amino acid metabolism, insulin secretion and diabetes*. Biochem Soc Trans, 2007. **35**(Pt 5): p. 1180-6.
353. MacDonald, P.E., J.W. Joseph, and P. Rorsman, *Glucose-sensing mechanisms in pancreatic beta-cells*. Philos Trans R Soc Lond B Biol Sci, 2005. **360**(1464): p. 2211-25.
354. Hedekov, C.J. and K. Capito, *The pentose cycle and insulin release in isolated mouse pancreatic islets during starvation*. Biochem J, 1975. **152**(3): p. 571-6.
355. Ashcroft, S.J. and P.J. Randle, *Enzymes of glucose metabolism in normal mouse pancreatic islets*. Biochem J, 1970. **119**(1): p. 5-15.
356. Monte Alegre, S., et al., *Insulin secretion in patients deficient in glucose-6-phosphate dehydrogenase*. Horm Metab Res, 1991. **23**(4): p. 171-3.
357. Moonsammy, G.I. and M.A. Stewart, *Purification and properties of brain aldose reductase and L-hexonate dehydrogenase*. J Neurochem, 1967. **14**(12): p. 1187-93.

358. Clements, R.S., Jr. and A.I. Winegrad, *Modulation of mammalian polyol: NADP oxidoreductase activity by ADP and ATP*. Biochem Biophys Res Commun, 1969. **36**(6): p. 1006-12.
359. Jeffery, J. and H. Jornvall, *Enzyme relationships in a sorbitol pathway that bypasses glycolysis and pentose phosphates in glucose metabolism*. Proc Natl Acad Sci U S A, 1983. **80**(4): p. 901-5.
360. Gabbay, K.H. and W.J. Tze, *Inhibition of glucose-induced release of insulin by aldose reductase inhibitors*. Proc Natl Acad Sci U S A, 1972. **69**(6): p. 1435-9.
361. Laclau, M., F. Lu, and M.J. MacDonald, *Enzymes in pancreatic islets that use NADP(H) as a cofactor including evidence for a plasma membrane aldehyde reductase*. Mol Cell Biochem, 2001. **225**(1-): p. 151-60.
362. Malaisse, W.J., A. Sener, and M. Mahy, *The Stimulus-Secretion Coupling of Glucose-Induced Insulin Release*. European Journal of Biochemistry, 1974. **47**(2): p. 365-370.
363. Hamaoka, R., et al., *Overexpression of the aldose reductase gene induces apoptosis in pancreatic beta-cells by causing a redox imbalance*. J Biochem, 1999. **126**(1): p. 41-7.
364. MacDonald, M.J., et al., *The role of rapid lipogenesis in insulin secretion: Insulin secretagogues acutely alter lipid composition of INS-1 832/13 cells*. Arch Biochem Biophys, 2008. **470**(2): p. 153-62.
365. Nolan, C.J. and M. Prentki, *The islet beta-cell: fuel responsive and vulnerable*. Trends Endocrinol Metab, 2008. **19**(8): p. 285-91.
366. Nolan, C.J., et al., *Fatty acid signaling in the beta-cell and insulin secretion*. Diabetes, 2006. **55 Suppl 2**: p. S16-23.
367. Macdonald, M.J., N.M. Hasan, and M.J. Longacre, *Studies with leucine, beta-hydroxybutyrate and ATP citrate lyase-deficient beta cells support the acetoacetate pathway of insulin secretion*. Biochim Biophys Acta, 2008. **1780**(7-8): p. 966-72.
368. MacDonald, M.J., et al., *Feasibility of pathways for transfer of acyl groups from mitochondria to the cytosol to form short chain acyl-CoAs in the pancreatic beta cell*. J Biol Chem, 2007. **282**(42): p. 30596-606.
369. Fahien, L.A. and M.J. MacDonald, *The Complex Mechanism of Glutamate Dehydrogenase in Insulin Secretion*. Diabetes, 2011. **60**(10): p. 2450-2454.

370. Carobbio, S., et al., *Deletion of glutamate dehydrogenase in beta-cells abolishes part of the insulin secretory response not required for glucose homeostasis*. J Biol Chem, 2009. **284**(2): p. 921-9.
371. Kuhara, T., et al., *Effects of intravenous infusion of 17 amino acids on the secretion of GH, glucagon, and insulin in sheep*. Am J Physiol, 1991. **260**(1 Pt 1): p. E21-6.
372. MacDonald, M.J., *The export of metabolites from mitochondria and anaplerosis in insulin secretion*. Biochim Biophys Acta, 2003. **1619**(1): p. 77-88.
373. Gerich, J.E., *Is reduced first-phase insulin release the earliest detectable abnormality in individuals destined to develop type 2 diabetes?* Diabetes, 2002. **51 Suppl 1**: p. S117-21.
374. Cerasi, E., *Mechanisms of glucose stimulated insulin secretion in health and in diabetes: some re-evaluations and proposals*. Diabetologia, 1975. **11**(1): p. 1-13.
375. Fritsche, A., et al., *A novel hyperglycaemic clamp for characterization of islet function in humans: assessment of three different secretagogues, maximal insulin response and reproducibility*. Eur J Clin Invest, 2000. **30**(5): p. 411-8.
376. Ricordi, C., et al., *Automated method for isolation of human pancreatic islets*. Diabetes, 1988. **37**(4): p. 413-20.
377. Takei, S., et al., *Isolation and function of human and pig islets*. Pancreas, 1994. **9**(2): p. 150-6.
378. Bertuzzi, F., et al., *Long-term in vitro exposure to high glucose increases proinsulin-like-molecules release by isolated human islets*. J Endocrinol, 1998. **158**(2): p. 205-11.
379. Prentki, M. and F.M. Matschinsky, *Ca²⁺, cAMP, and phospholipid-derived messengers in coupling mechanisms of insulin secretion*. Physiol Rev, 1987. **67**(4): p. 1185-248.
380. Ashcroft, F.M. and P. Rorsman, *Electrophysiology of the pancreatic beta-cell*. Prog Biophys Mol Biol, 1989. **54**(2): p. 87-143.
381. Deeney, J.T., M. Prentki, and B.E. Corkey, *Metabolic control of beta-cell function*. Semin Cell Dev Biol, 2000. **11**(4): p. 267-75.
382. Lorenz, M.A., et al., *Metabolome Response to Glucose in the beta-Cell Line INS-1 832/13*. J Biol Chem, 2013. **288**(15): p. 10923-35.
383. Zawalich, W.S., M. Bonnet-Eymard, and K.C. Zawalich, *Insulin secretion, inositol phosphate levels, and phospholipase C isozymes in rodent pancreatic islets*. Metabolism, 2000. **49**(9): p. 1156-63.

384. Neshler, R., et al., *Beta-cell protein kinases and the dynamics of the insulin response to glucose*. Diabetes, 2002. **51 Suppl 1**: p. S68-73.
385. Ganesan, S., et al., *Glucose-induced translocation of protein kinase C in rat pancreatic islets*. Proc Natl Acad Sci U S A, 1990. **87**(24): p. 9893-7.
386. Zawalich, W.S., K.C. Zawalich, and G.G. Kelley, *Regulation of insulin release by phospholipase C activation in mouse islets: differential effects of glucose and neurohumoral stimulation*. Endocrinology, 1995. **136**(11): p. 4903-9.
387. Malaisse, W.J., et al., *Synergistic effect of a tumor-promoting phorbol ester and a hypoglycemic sulfonylurea upon insulin release*. Endocrinology, 1983. **113**(5): p. 1870-7.
388. Zawalich, W.S., et al., *Effects of the phorbol ester phorbol 12-myristate 13-acetate (PMA) on islet-cell responsiveness*. Biochem J, 1991. **278 (Pt 1)**: p. 49-56.
389. Halestrap, A.P., *The mechanism of the inhibition of the mitochondrial pyruvate transportater by alpha-cyanocinnamate derivatives*. Biochem J, 1976. **156**(1): p. 181-3.
390. Hausinger, R.P., *FelII/alpha-ketoglutarate-dependent hydroxylases and related enzymes*. Crit Rev Biochem Mol Biol, 2004. **39**(1): p. 21-68.
391. Zraika, S., et al., *The hexosamine biosynthesis pathway regulates insulin secretion via protein glycosylation in mouse islets*. Arch Biochem Biophys, 2002. **405**(2): p. 275-9.
392. Takagi, H., *Proline as a stress protectant in yeast: physiological functions, metabolic regulations, and biotechnological applications*. Appl Microbiol Biotechnol, 2008. **81**(2): p. 211-23.
393. Krishnan, N., M.B. Dickman, and D.F. Becker, *Proline modulates the intracellular redox environment and protects mammalian cells against oxidative stress*. Free Radic Biol Med, 2008. **44**(4): p. 671-81.
394. Donald, S.P., et al., *Proline oxidase, encoded by p53-induced gene-6, catalyzes the generation of proline-dependent reactive oxygen species*. Cancer Res, 2001. **61**(5): p. 1810-5.
395. Liu, Y., et al., *Proline oxidase activates both intrinsic and extrinsic pathways for apoptosis: the role of ROS//superoxides, NFAT and MEK//ERK signaling*. Oncogene, 2006. **25**(41): p. 5640-5647.
396. Tiedge, M., et al., *Relation between antioxidant enzyme gene expression and antioxidative defense status of insulin-producing cells*. Diabetes, 1997. **46**(11): p. 1733-42.
397. Lenzen, S., *Oxidative stress: the vulnerable beta-cell*. Biochem Soc Trans, 2008. **36**(Pt 3): p. 343-7.

398. Fridlyand, L.E. and L.H. Philipson, *Does the glucose-dependent insulin secretion mechanism itself cause oxidative stress in pancreatic beta-cells?* Diabetes, 2004. **53**(8): p. 1942-8.
399. Pipeleers, D.G., M.A. Pipeleers-Marichal, and D.M. Kipnis, *Regulation of tubulin synthesis in islets of Langerhans.* Proc Natl Acad Sci U S A, 1976. **73**(9): p. 3188-91.
400. Montague, W., S.L. Howell, and I.C. Green, *Insulin release and the microtubular system of the islets of Langerhans: effects of insulin secretagogues on microtubule subunit pool size.* Horm Metab Res, 1976. **8**(3): p. 166-9.
401. Nesher, R., M. Praiss, and E. Cerasi, *Immediate and time-dependent effects of glucose on insulin release: differential calcium requirements.* Acta Endocrinol (Copenh), 1988. **117**(3): p. 409-16.
402. Nesher, R., et al., *Beta-cell memory to insulin secretagogues: characterization of the time-dependent inhibitory control system in the isolated rat pancreas.* Endocrinology, 1989. **124**(1): p. 142-8.
403. Gunawardana, S.C., et al., *Anaplerotic input is sufficient to induce time-dependent potentiation of insulin release in rat pancreatic islets.* Am J Physiol Endocrinol Metab, 2004. **287**(5): p. E828-833.
404. Gunawardana, S.C., et al., *Mechanisms of time-dependent potentiation of insulin release: involvement of nitric oxide synthase.* Diabetes, 2006. **55**(4): p. 1029-33.
405. Ishihara, H., et al., *Effect of mitochondrial and/or cytosolic glycerol 3-phosphate dehydrogenase overexpression on glucose-stimulated insulin secretion from MIN6 and HIT cells.* Diabetes, 1996. **45**(9): p. 1238-44.
406. Ishihara, H. and C.B. Wollheim, *What couples glycolysis to mitochondrial signal generation in glucose-stimulated insulin secretion?* IUBMB Life, 2000. **49**(5): p. 391-5.
407. Tamarit-Rodriguez, J., et al., *Lactate production in pancreatic islets.* Diabetes, 1998. **47**(8): p. 1219-23.
408. Ishihara, H., et al., *Overexpression of monocarboxylate transporter and lactate dehydrogenase alters insulin secretory responses to pyruvate and lactate in beta cells.* J Clin Invest, 1999. **104**(11): p. 1621-9.
409. Noel, R.J., et al., *Engineering of glycerol-stimulated insulin secretion in islet beta cells. Differential metabolic fates of glucose and glycerol provide insight into mechanisms of stimulus-secretion coupling.* J Biol Chem, 1997. **272**(30): p. 18621-7.

410. Newgard, C.B. and J.D. McGarry, *Metabolic coupling factors in pancreatic beta-cell signal transduction*. *Annu Rev Biochem*, 1995. **64**: p. 689-719.
411. Pek, S.B., et al., *Protein phosphorylation in pancreatic islets induced by 3-phosphoglycerate and 2-phosphoglycerate*. *Proc Natl Acad Sci U S A*, 1990. **87**(11): p. 4294-8.
412. Ueda, T. and D.G. Plagens, *3-Phosphoglycerate-dependent protein phosphorylation*. *Proc Natl Acad Sci U S A*, 1987. **84**(5): p. 1229-33.
413. Sjöholm, A., R.E. Honkanen, and P.O. Berggren, *Inhibition of serine/threonine protein phosphatases by secretagogues in insulin-secreting cells*. *Endocrinology*, 1995. **136**(8): p. 3391-7.
414. Ammala, C., et al., *Activation of protein kinases and inhibition of protein phosphatases play a central role in the regulation of exocytosis in mouse pancreatic beta cells*. *Proc Natl Acad Sci U S A*, 1994. **91**(10): p. 4343-7.
415. Hisatomi, M., H. Hidaka, and I. Niki, *Ca²⁺/calmodulin and cyclic 3,5' adenosine monophosphate control movement of secretory granules through protein phosphorylation/dephosphorylation in the pancreatic beta-cell*. *Endocrinology*, 1996. **137**(11): p. 4644-9.
416. Larsson, O., et al., *Inhibition of phosphatases and increased Ca²⁺ channel activity by inositol hexakisphosphate*. *Science*, 1997. **278**(5337): p. 471-4.
417. Asfari, M., et al., *Establishment of 2-mercaptoethanol-dependent differentiated insulin-secreting cell lines*. *Endocrinology*, 1992. **130**(1): p. 167-78.
418. Ashcroft, S.J., *Glucoreceptor mechanisms and the control of insulin release and biosynthesis*. *Diabetologia*, 1980. **18**(1): p. 5-15.
419. Orci, L., *The insulin factory: a tour of the plant surroundings and a visit to the assembly line. The Minkowski lecture 1973 revisited*. *Diabetologia*, 1985. **28**(8): p. 528-46.
420. Skelly, R.H., et al., *Glycerol-stimulated proinsulin biosynthesis in isolated pancreatic rat islets via adenoviral-induced expression of glycerol kinase is mediated via mitochondrial metabolism*. *Diabetes*, 2001. **50**(8): p. 1791-8.
421. Attali, V., et al., *Regulation of insulin secretion and proinsulin biosynthesis by succinate*. *Endocrinology*, 2006. **147**(11): p. 5110-8.
422. Alarcon, C., et al., *Succinate Is a Preferential Metabolic Stimulus-Coupling Signal for Glucose-Induced Proinsulin Biosynthesis Translation*. *Diabetes*, 2002. **51**(8): p. 2496-2504.

423. Leibowitz, G., et al., *Mitochondrial regulation of insulin production in rat pancreatic islets*. Diabetologia, 2005. **48**(8): p. 1549-59.
424. Yudkoff, M., et al., *Tricarboxylic acid cycle in rat brain synaptosomes. Fluxes and interactions with aspartate aminotransferase and malate/aspartate shuttle*. J Biol Chem, 1994. **269**(44): p. 27414-20.
425. Rustin, P., et al., *Inborn errors of the Krebs cycle: a group of unusual mitochondrial diseases in human*. Biochim Biophys Acta, 1997. **1361**(2): p. 185-97.
426. Meglasson, M.D. and F.M. Matschinsky, *Pancreatic islet glucose metabolism and regulation of insulin secretion*. Diabetes Metab Rev, 1986. **2**(3-4): p. 163-214.
427. Meredith, M., M.E. Rabaglia, and S.A. Metz, *Evidence of a role for GTP in the potentiation of Ca(2+)-induced insulin secretion by glucose in intact rat islets*. J Clin Invest, 1995. **96**(2): p. 811-21.
428. Maechler, P. and C.B. Wollheim, *Mitochondrial glutamate acts as a messenger in glucose-induced insulin exocytosis*. Nature, 1999. **402**(6762): p. 685-9.
429. Bertrand, G., et al., *Glutamate stimulates insulin secretion and improves glucose tolerance in rats*. Am J Physiol, 1995. **269**(3 Pt 1): p. E551-6.
430. Liang, Y. and F.M. Matschinsky, *Content of CoA-esters in perfused rat islets stimulated by glucose and other fuels*. Diabetes, 1991. **40**(3): p. 327-33.
431. Merglen, A., et al., *Glucose sensitivity and metabolism-secretion coupling studied during two-year continuous culture in INS-1E insulinoma cells*. Endocrinology, 2004. **145**(2): p. 667-78.
432. Hedekov, C.J., K. Capito, and P. Thams, *Cytosolic ratios of free [NADPH]/[NADP+] and [NADH]/[NAD+] in mouse pancreatic islets, and nutrient-induced insulin secretion*. Biochem J, 1987. **241**(1): p. 161-7.
433. Jensen, M.V., et al., *Compensatory responses to pyruvate carboxylase suppression in islet beta-cells. Preservation of glucose-stimulated insulin secretion*. J Biol Chem, 2006. **281**(31): p. 22342-51.
434. Huypens, P., et al., *The dicarboxylate carrier plays a role in mitochondrial malate transport and in the regulation of glucose-stimulated insulin secretion from rat pancreatic beta cells*. Diabetologia, 2010.
435. Rabaglia, M.E., et al., *Alpha-Ketoisocaproate-induced hypersecretion of insulin by islets from diabetes-susceptible mice*. Am J Physiol Endocrinol Metab, 2005. **289**(2): p. E218-24.

436. Hanauske-Abel, H.M. and V. Gunzler, *A stereochemical concept for the catalytic mechanism of prolylhydroxylase: applicability to classification and design of inhibitors*. J Theor Biol, 1982. **94**(2): p. 421-55.
437. Wang, J., et al., *The prolyl 4-hydroxylase inhibitor ethyl-3,4-dihydroxybenzoate generates effective iron deficiency in cultured cells*. FEBS Lett, 2002. **529**(2-3): p. 309-12.
438. Sasaki, T., K. Majamaa, and J. Uitto, *Reduction of collagen production in keloid fibroblast cultures by ethyl-3,4-dihydroxybenzoate. Inhibition of prolyl hydroxylase activity as a mechanism of action*. J Biol Chem, 1987. **262**(19): p. 9397-403.
439. Majamaa, K., et al., *Partial identity of the 2-oxoglutarate and ascorbate binding sites of prolyl 4-hydroxylase*. J Biol Chem, 1986. **261**(17): p. 7819-23.
440. Kivirikko, K.I. and T. Pihlajaniemi, *Collagen hydroxylases and the protein disulfide isomerase subunit of prolyl 4-hydroxylases*. Adv Enzymol Relat Areas Mol Biol, 1998. **72**: p. 325-98.
441. Hutton, J.J., Jr., A.L. Trappel, and S. Udenfriend, *Requirements for alpha-ketoglutarate, ferrous ion and ascorbate by collagen proline hydroxylase*. Biochem Biophys Res Commun, 1966. **24**(2): p. 179-84.
442. Helaakoski, T., et al., *Molecular cloning of the alpha-subunit of human prolyl 4-hydroxylase: the complete cDNA-derived amino acid sequence and evidence for alternative splicing of RNA transcripts*. Proc Natl Acad Sci U S A, 1989. **86**(12): p. 4392-6.
443. Hautala, T., et al., *Cloning of human lysyl hydroxylase: complete cDNA-derived amino acid sequence and assignment of the gene (PLOD) to chromosome 1p36.3---p36.2*. Genomics, 1992. **13**(1): p. 62-9.
444. Passoja, K., et al., *Cloning and characterization of a third human lysyl hydroxylase isoform*. Proc Natl Acad Sci U S A, 1998. **95**(18): p. 10482-6.
445. Valtavaara, M., et al., *Cloning and characterization of a novel human lysyl hydroxylase isoform highly expressed in pancreas and muscle*. J Biol Chem, 1997. **272**(11): p. 6831-4.
446. Valtavaara, M., et al., *Primary structure, tissue distribution, and chromosomal localization of a novel isoform of lysyl hydroxylase (lysyl hydroxylase 3)*. J Biol Chem, 1998. **273**(21): p. 12881-6.
447. Bunn, H.F. and R.O. Poyton, *Oxygen sensing and molecular adaptation to hypoxia*. Physiol Rev, 1996. **76**(3): p. 839-85.

448. Huang, L.E., et al., *Regulation of hypoxia-inducible factor 1alpha is mediated by an O2-dependent degradation domain via the ubiquitin-proteasome pathway*. Proc Natl Acad Sci U S A, 1998. **95**(14): p. 7987-92.
449. Salceda, S. and J. Caro, *Hypoxia-inducible factor 1alpha (HIF-1alpha) protein is rapidly degraded by the ubiquitin-proteasome system under normoxic conditions. Its stabilization by hypoxia depends on redox-induced changes*. J Biol Chem, 1997. **272**(36): p. 22642-7.
450. Li, B., et al., *A prolyl-hydroxylase inhibitor, ethyl-3,4-dihydroxybenzoate, induces haem oxygenase-1 expression in human cells through a mechanism independent of hypoxia-inducible factor-1alpha*. J Biochem, 2008. **144**(5): p. 643-54.
451. Zhang, A.-h., et al., *Metabolomics study of type 2 diabetes using ultra-performance LC-ESI/quadrupole-TOF high-definition MS coupled with pattern recognition methods*. Journal of Physiology and Biochemistry, 2013: p. 1-12.
452. Berglund, A., M. Rosa, and S. Wold, *Alignment of flexible molecules at their receptor site using 3D descriptors and Hi-PCA*. Journal of Computer-Aided Molecular Design, 1997. **11**(6): p. 601-612.
453. Westerhuis, J.A., T. Kourti, and J.F. MacGregor, *Analysis of multiblock and hierarchical PCA and PLS models*. Journal of Chemometrics, 1998. **12**(5): p. 301-321.
454. Wold, S., N. Kettaneh, and K. Tjessem, *Hierarchical multiblock PLS and PC models for easier model interpretation and as an alternative to variable selection*. Journal of Chemometrics, 1996. **10**(5-6): p. 463-482.
455. Janné K., et al., *Hierarchical principal component analysis (PCA) and projection to latent structure (PLS) technique on spectroscopic data as a data pretreatment for calibration*. Journal of Chemometrics, 2001. **15**(4): p. 203-213.
456. Eriksson, L., et al., *Megavariate analysis of hierarchical QSAR data*. Journal of Computer-Aided Molecular Design, 2002. **16**(10): p. 711-726.
457. Kell, D.B. and S.G. Oliver, *Here is the evidence, now what is the hypothesis? The complementary roles of inductive and hypothesis-driven science in the post-genomic era*. Bioessays, 2004. **26**(1): p. 99-105.
458. Kell, D.B., *Genotype phenotype mapping: genes as computer programs*. Trends in genetics : TIG, 2002. **18**(11): p. 555-559.
459. Brent, R., *Genomic biology*. Cell, 2000. **100**(1): p. 169-83.

460. Gunawardana, S.C. and G.W. Sharp, *Intracellular pH plays a critical role in glucose-induced time-dependent potentiation of insulin release in rat islets*. *Diabetes*, 2002. **51**(1): p. 105-13.
461. Yamada, S., et al., *Time-dependent potentiation of the beta-cell is a Ca²⁺-independent phenomenon*. *J Endocrinol*, 2002. **172**(2): p. 345-54.
462. Wold, S., N. Kettaneh-Wold, and B. Skagerberg, *Nonlinear PLS modeling*. *Chemometrics and Intelligent Laboratory Systems*, 1989. **7**(1-2): p. 53-65.
463. Wold, S., et al., *Modelling and diagnostics of batch processes and analogous kinetic experiments*. *Chemometrics and Intelligent Laboratory Systems*, 1998. **44**(1-2): p. 331-340.